Metabolic signalling in pancreatic beta cells

UCL

Kaisa Piipari

Department of Medicine

University College London

A thesis submitted for the degree of

Doctor of Philosophy

December, 2010

I dedicate this thesis to Matias

Acknowledgements

I, Kaisa Piipari, declare that the work presented in this thesis is my own and any collaboration or assistance is specifically indicated in the text.

Abstract

The main function of pancreatic beta cells is to maintain correct glucose homeostasis within the body by secretion of insulin in response to increased blood glucose concentration. Beta cell dysfunction contributes to the pathogenesis of diabetes. Using transgenic mouse models, the work described in this thesis has investigated the role of AMP-activated protein kinase (AMPK) and phosphatidylinositol 3-kinase (PI3K) in beta cell function and their role in the regulation of glucose-stimulated insulin secretion (GSIS). AMPK is activated by low cellular energy levels. Once activated it acts as a cellular fuel gauge to restore energy levels back to normal. An anti-diabetic drug metformin is thought to achieve its blood glucose lowering effect by activation of AMPK in liver and skeletal muscle. However, the role of AMPK in pancreatic beta cells has remained uncertain and controversial. This thesis shows that transgenic mice, which lack functional AMPK in beta cells are glucose intolerant caused by impaired GSIS. Investigation of islet function *in vitro* revealed that lack of AMPK in beta cells alters glucose sensing and insulin secretory behaviour, which is associated with down-regulation of mitochondrial uncoupling protein 2.

PI3K functions as a lipid kinase downstream of receptor tyrosine kinases such as insulin receptor. Previous studies have shown that it has an important role in the regulation of energy metabolism, but no studies to date have investigated the specific role of PI3K in beta cells using mouse knockout models. The study in this thesis demonstrates that transgenic mice that lack functional PI3K catalytic subunits p110α and p110β in beta cells develop marked glucose intolerance and impaired GSIS. Together these two studies demonstrate that

AMPK and PI3K signalling in beta cells is essential for the regulation of whole-body glucose homeostasis and insulin secretion.

Contents

List of Figures

List of Tables

Chapter 1

Introduction

1.1 Diabetes – a global problem

Diabetes has become a major burden for health care systems throughout the
world. For example in United Kingdom approximately 10 % of NHS resources are
used in the management of diabetes (Gloyn, 2003). Currently, diabetes affects over
180 million people worldwide. Of all the individuals with diabetes, 90% have type
2 diabetes mellitus (T2DM), the non-insulin dependent form of diabetes (WHO,
2006). It has been predicted that by 2030 over 377 million people will suffer from
T2DM worldwide (Albright, 2008). Alarmingly, a significant number of new cases
of T2DM will be diagnosed among children and adolescent (Gloyn, 2003). T2DM
is defined as a systemic disorder of glucose homeostasis. It is characterised in terms
of hyperglycaemia, peripheral tissue insulin resistance, abnormal splanchic (liver
and gut) glucose uptake, impaired insulin secretion, and is also associated with
hyperlipidaemia (DeFronzo, 2004). A fasting blood glucose level of > 7 mmol/L,
and/or > 11 mmol/L glucose two hours after an oral glucose load are the bench
marks of T2DM (Kuzuya et al., 2002). T2DM is associated with a variety of other
diseases including microvascular diseases (such as neuropathy, nephropathy and
retinopathy) and macrovascular diseases (such as atherosclerosis and coronary
artery disease) (Milicevic et al., 2008; Reasner, 2008; Soldatos and Cooper, 2008).

1.1.1   Genome-wide association studies

Type 2 diabetes is a polygenic, multifactorial disease that can arise due to polymorphisms in multiple genes. However, environmental factors such as diet and physical activity can also have a major influence on disease prevalence and severity (Ridderstråle and Groop, 2009). At least eighteen genes associated with TD2M have recently been identified by the whole genome-wide association studies (GWAS) (McCarthy and Zeggini, 2009; Ridderstråle and Groop, 2009). Most of the recognised genes are involved in beta cell function, suggesting that beta cell dysfunction plays a key role in the pathogenesis of the disease. A study using a cohort of non-diabetic Finnish men found that 8 of the previously identified loci are significantly (*TCF7L2*, *SLC30A8*, *HHEX*, *CDKN2B*, *CDKAL1* and *MTNR1B*), or nominally (*KCNJ11* and *IGF2BP2*) associated with a decreased early-phase insulin secretion. *TCF7L2*, *SLC30A8*, *HHEX*, and *CDKAL1* could also be associated with impaired conversion of proinsulin to insulin (Sladek et al., 2007; Stancáková et al., 2009). However, each loci only a have modest risk effect on the development of T2DM (Rung et al., 2009). Candidate gene studies have identified a Pro12Ala variant in a transcription factor peroxisome proliferator-activator receptor γ (*PPARG*) gene that is associated with T2DM (Gloyn, 2003). Another new risk locus near *IRS-1* has been identified, which is associated with insulin resistance and hyperinsulinaemia (Rung et al., 2009). Defect in glucose- and tolbutamide stimulated insulin secretion was observed in beta cells that contained a similar polymorphisms in *IRS-1* (Aspinwall et al., 2000). In order to understand the cellular and molecular mechanisms responsible for T2DM, it is necessary to conceptualise the framework within which glycaemia is controlled, and this is discussed further below.

1.2   Glycaemic control

Glucose is an important source of energy for all tissue types of the body, especially to the brain that is acutely dependent on energy provided by glucose (Marty et al., 2007). It is essential to maintain the blood glucose concentration within the healthy limits of 4-7 mmol/L. This involves a balance between hepatic glu-

coneogenesis and uptake of glucose by tissues including the gut, skeletal muscle and adipose tissue, although most (80-85 %) of peripheral glucose uptake occurs in muscle (DeFronzo, 2004) (Figure 1.1). Two primary hormones involved in regulating these processes are insulin and glucagon, both secreted by the endocrine pancreas.

1.3 Endocrine pancreas

Beta cells are a central part of the pancreatic endocrine system. They are clustered together with other endocrine cells such as alpha cells (glucagon secretion), delta cells (somatostatin secretion) and PP cells (pancreatic polypeptide secretion) to form the islets of Langerhans. Beta cells constitute more than 70 % of the islet cells mass followed by alpha cells which make up 10 % of total islet cell mass (Cabrera et al., 2006). Regulation of pancreatic beta cell mass is achieved by balanced action between beta cell proliferation, regulation of cell size and cell death, as well as beta cell neogenesis (Leibiger and Berggren, 2008). However, maintenance of beta cell mass is largely achieved by proliferation of existing beta cells, a process which is controlled by the interplay of various proteins of the cell cycle machinery (Chang-Chen et al., 2008).

1.4 Insulin secretion by pancreatic beta cells – a two phase process

The main function of pancreatic beta cells is to maintain correct glucose homeostasis within the body by secretion of insulin in response to increased blood glucose concentration. Other nutrients such as some amino acids (leucine, glutamine and arginine), fatty acids, neurotransmitters (e.g. acetylcholine) and incretins (gut-derived hormones) such as gastric inhibitory polypeptide (GIP) and glucagon-like peptide-1 (GLP-1) also exhibit an insulinotropic effect on the pancreatic beta cells (DeFronzo, 2004; Leclerc and Rutter, 2004; Maechler and Wollheim, 2001; Tarasov et al., 2004; Thorens, 2008; Wollheim and Maechler, 2002). Classically, insulin secretion can be divided into two phases, which are described
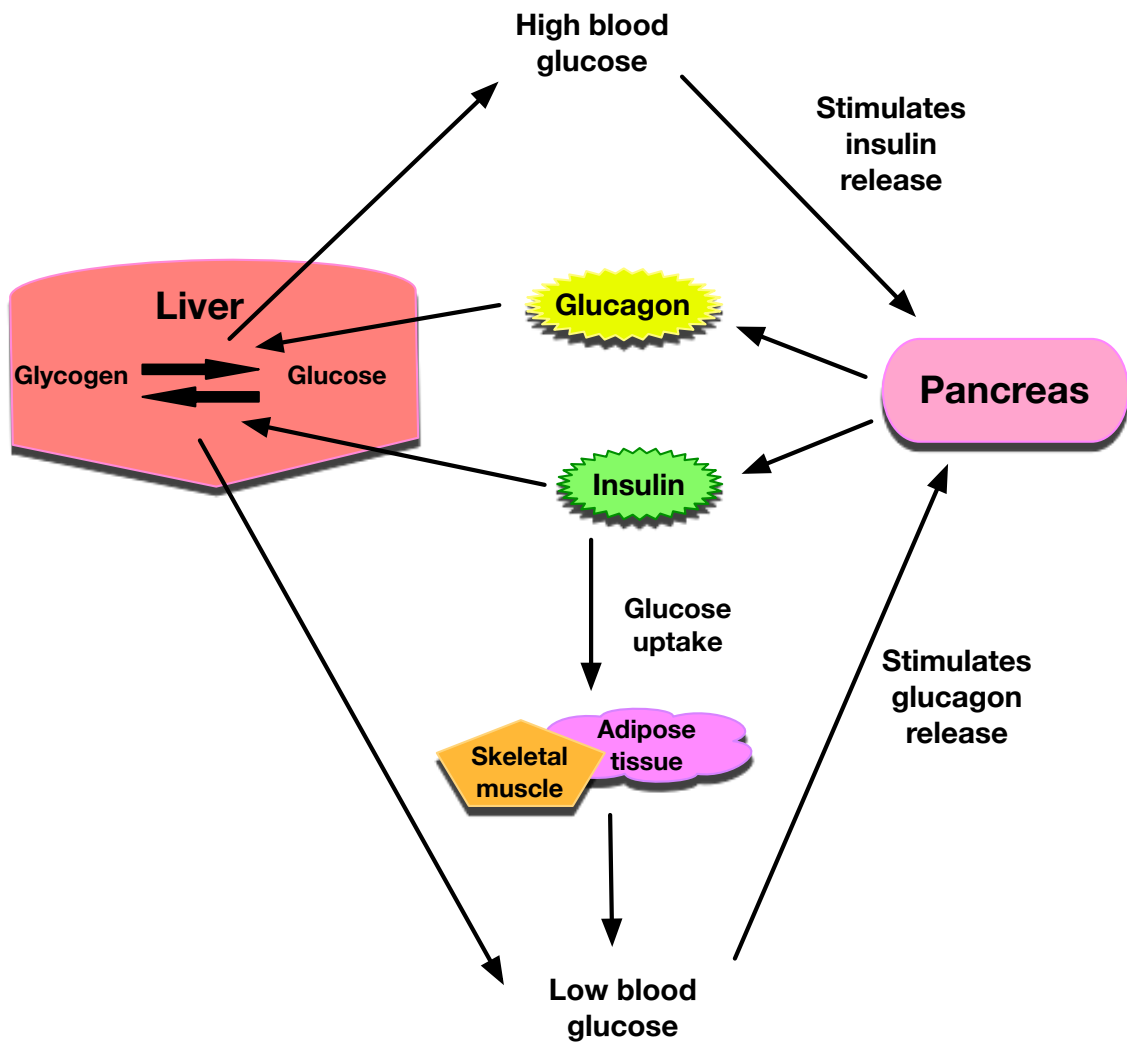
Figure 1.1: Insulin action and control of glucose homeostasis. Raised blood glucose stimulates insulin release from pancreatic beta cells. Insulin stimulates glucose uptake and glycogen and lipid synthesis in skeletal muscle and adipose tissue. In liver, insulin stimulates glycogen synthesis and inhibits gluconeogenesis and glycogenolysis. Thus, insulin action on peripheral tissues leads to reduction in blood glucose levels. Opposing the insulin action, glucagon, secreted from pancreatic alpha cells in response to hypoglycaemia, stimulates liver gluconeogenesis and raises blood glucose levels.

further below.

1.4.1 The first phase of insulin release – the K_{ATP}-channel dependent insulin secretion

Glucose is taken up into beta cells via a glucose transporter GLUT2 (in mice) and GLUT1 (in humans) (Hiriart and Aguilar-Bryan, 2008; Vos et al., 1995). Glucose is then metabolised by glycolysis and the tricarboxylic acid (TCA) cycle (Herman and Kahn, 2006). Both pathways provide substrates (NADH and $FADH_2$) for the respiratory chain within mitochondria to produce ATP (Duchen, 2004). ATP is transported into the cytoplasm, where it binds to the Kir6.2 subunit of the K_{ATP}-channel (Ashcroft, 2005; Klingenberg, 2008). The binding of ATP causes channel closure, resulting in the depolarisation of the plasma membrane. The depolarisation triggers the opening of the L-type voltage-gated calcium channels, which leads to the influx of Ca^{2+}-ions. Calcium triggers the exocytosis of insulin secretory vesicles and results in the release of insulin from beta cells (Straub and Sharp, 2002). As calcium uptake and insulin release are dependent on potassium channel closure by ATP, this pathway is called the K_{ATP}-channel dependent insulin secretion pathway. See Figure 1.2 for a graphical representation of the first-phase insulin release in beta cells.

1.4.2 The second phase of insulin release – the K_{ATP}-channel independent insulin secretion

The sustained second phase of insulin secretion is called K_{ATP}-channel independent insulin secretion, as insulin secretion occurs despite the potassium channel being open or otherwise dysfunctional (Tengholm and Gylfe, 2009). The second phase involves augmented insulin release in response to elevated intracellular calcium levels. The mechanisms for this are still unknown but are thought to involve changes in concentrations and actions of cAMP, phospholipase C and plasma membrane phosphoinositides (Straub and Sharp, 2002; Tengholm and Gylfe, 2009). Poorly defined metabolic coupling pathways such as generation of mitochondrial NADH, malonyl-CoA and cytosolic long chain-CoA esters are also

required (Prentki, 1996; Prentki et al., 1997). I will now discuss in further details about different steps involved in the glucose-stimulated insulin secretory pathway including glucose sensing and glucose metabolism coupled beta cell electrical activity.
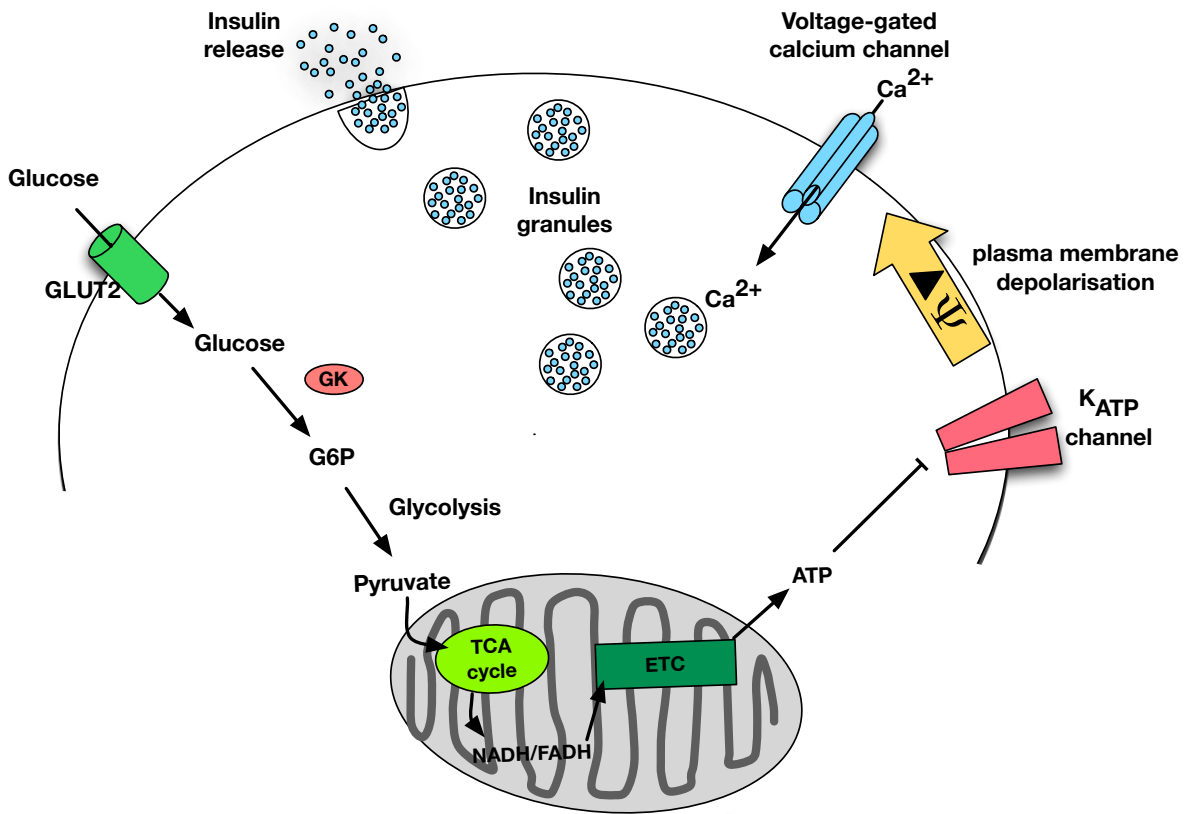
Figure 1.2: A simplified model of beta cell function. Glucose is taken up into the cells via GLUT2 (mouse)/GLUT1(human) glucose transporters. Glucose is then metabolised in the cytosol and mitochondria to yield ATP. ATP closes the K_{ATP} -channels on the plasma membrane, which leads to membrane depolarisation. This triggers the opening of L-type voltage-gated calcium channels and calcium influx into the cytosol stimulates insulin granule exocytosis. G6P = glucose-6-phosphate, TCA = tricarboxylic acid, ETC = electron transport chain

1.5   Glucose sensing by beta cells

Two high Km enzymes, glucose transporter GLUT2 and glucokinase (GK) are responsible for glucose sensing and initiation of glucose-stimulated insulin secretion pathway in pancreatic beta cells. GLUT2 is an integral membrane protein that facilitates glucose transport across the plasma membrane, thus regulating beta cell glucose uptake (Herman and Kahn, 2006; Hiriart and Aguilar-Bryan, 2008). GLUT2 has a low affinity for glucose and has a Km of $\approx$ 20-66 mM, meaning that increases in blood glucose concentration over a range of physiological glucose concentrations are met by increased capacity to transport glucose across the membrane (Kahn, 1992; Shepherd and Kahn, 2000). It has been shown repeatedly that GLUT2 is important for beta cell glucose-stimulated insulin secretion. Glucose stimulated, but not arginine stimulated insulin secretion is reduced in islets obtained from type 2 diabetic patients. In these islets, *GLUT2* mRNA expression is decreased over 40 % (Guerra et al., 2005). Similar results have been obtained from mouse islets that are deficient in GLUT2. The GLUT2 deficient mice are hyperglycaemic and hypoinsulinaemic, and investigation of *in vitro* glucose-stimulated insulin secretion in GLUT2 deficient islet showed a loss of first-phase insulin secretion, and reduced second-phase insulin secretion indicating the importance of GLUT2 in the regulation of GSIS (Thorens, 2001).

The rate of glucose uptake by GLUT2 usually exceeds the rate of glucose phosphorylation by glucokinase (GK) i.e. hexokinase IV, which is a rate-limiting enzyme of glucose metabolism, and is the primary glucose sensor in beta cells (Herman and Kahn, 2006; Thorens, 2001). Expression of high-affinity hexokinases (hexokinase I, II and III) in beta cells is very low. This means that when glucose concentration is low (<2.5 mmol/L), phosphorylation of glucose to glucose-6-phosphate is kept at minimum, resulting in low glycolytic flux and low ATP levels, consequently keeping insulin release at basal level (Schuit et al., 2001). When glucose concentration increases (>2.5 mmol/L), the low-affinity GK phosphorylates glucose and increases glycolytic flux, which eventually leads to increased cellular ATP/ADP levels and stimulation of insulin secretion from beta cells (Schuit et al., 2001). GK has a Km of 10 mM for glucose and enzyme kinetics have shown that there is a sigmoidal relationship between glucokinase activity and glucose

concentration (Matschinsky et al., 1993; Thorens, 2008). Because GK is not negatively inhibited by glucose-6-phosphate, unlike the high affinity hexokinases I, II and III, glycolytic flux remains high as long as the glucose concentration remains elevated.

Mice lacking GK in pancreatic beta cells develop perinatal diabetes and die a few days after birth (Remedi and Nichols, 2009). Over 200 mutations (overactivating and inactivating) have been identified along the *GK* gene (Gloyn et al., 2008). Inactivating mutations generally result in decreased insulin secretion and T2DM (Beall et al., 2010). *GK* was also the first gene to be found to cause maturity onset diabetes of young (MODY), and over 140 mutations have been identified along the *GK* gene that cause MODY2, characterised by mild hyperglycaemia and progressive beta cell failure over time (Gloyn, 2003; Gloyn et al., 2008). Overactivating mutations in *GK* result in increased insulin secretion and hypoglycaemia, as seen in persistent hyperinsulinaemic hypoglycaemia of infancy (PHHI) (Gloyn et al., 2008). Hence it is easy to understand why GK has a key role as a primary cellular glucose sensor.

1.6 Glucose metabolism

Once glucose has been transported into the beta cells it enters glycolysis in the cytoplasm where it is metabolised to pyruvate (Herman and Kahn, 2006). Pyruvate enters mitochondrial matrix where it acts as a substrate for pyruvate carboxylase, which converts pyruvate to oxaloacetate, and for pyruvate dehydrogenase, which converts it to acetyl-CoA (Herman and Kahn, 2006). Both oxaloacetate and acetyl-CoA are substrates for the TCA cycle that provides NADH and $FADH_2$ for the mitochondrial respiratory chain (Wollheim and Maechler, 2002).

1.7 Mitochondrial function in beta cells

The mitochondrial respiratory chain is located on the inner mitochondrial membrane. Briefly, its function is to transfer electrons from NADH (complex I) and $FADH_2$ (complex II) along the complexes on the inner membrane to complex IV

where electrons are used to reduce molecular oxygen to H_2O. Transfer of electrons is coupled to pumping of protons through complex I, III and IV into the inner membrane space, creating a membrane potential (proton gradient) across the inner mitochondrial membrane. When protons move down the proton gradient back to the matrix through ATP synthase (complex V), it is able to use the proton motive force, created by the proton gradient, to phosphorylate ADP to produce ATP (Duchen, 2004). ATP is then transported back to the cytoplasm by adenine nucleotide transferase (ANT) where it is used as an energy source, and more importantly in beta cells, used as a signalling molecule to stimulate insulin secretion (Maechler and Wollheim, 2001).

1.7.1 Mitochondrial ROS production and beta cell insulin secretion

Mitochondrial dysfunction has been shown to contribute to the development of type 2 diabetes (Molina et al., 2009). As described above, mitochondria function as cellular energy factors that couple metabolism of glucose and other nutrients to the production of ATP. Most of the cellular production of reactive oxygen species (ROS) occurs in mitochondria when reduction of molecular oxygen is incomplete (Maechler and Wollheim, 2001). ROS are chemically unstable and highly reactive species that contain oxygen (D'Autréaux and Toledano, 2007). Superoxide anion is the most reactive form of ROS and is quickly converted to H_2O_2 by superoxide dismutase (SOD). Increased glycolytic flux, decreased ADP levels and increased intracellular Ca^{2+} can lead to considerable increase in the production of superoxide anion, mainly at complex I and between ubiquinone and complex III (Pi et al., 2010). By its chemical virtues (small, uncharged) and cellular functions, H_2O_2 can be considered as an intracellular messenger. Its cellular downstream targets include protein tyrosine phosphatases, tumour suppressor phosphatase PTEN, c-Jun N-terminal kinase, NF-κB, SIRT1 deacetylase and voltage-gated K^+ channels (Pi et al., 2010). It has been brought into focus that production of ROS from glucose metabolism, such as H_2O_2 and superoxide anion, might serve as a signal for glucose-stimulated insulin secretion in beta cells (Pi et al., 2007b, 2010). In general, it has been shown that, stimulation of cellular H_2O_2 levels

enhance insulin secretion, and antioxidants and other agents that act to reverse oxidative stress, inhibit insulin secretion (Pi et al., 2010). Acute treatment of rat islets with ROS generators alloxan and xanthine oxidase leads to short-term increased insulin release (Ebelt et al., 2000). Increasing H_2O_2 levels in INS-1 cells and mouse islets also increased insulin secretion, whereas exogenous antioxidants inhibited insulin secretion (Pi et al., 2010). However, stimulation of insulin secretion is still dependent on ATP generation, as inhibitors of ATP production (e.g. oligomycin) that also increase ROS production, cannot stimulate insulin secretion (Pi et al., 2010).

1.7.2 UCP2 in beta cells

Uncoupling protein 2 (UCP2) is located on the inner mitochondrial membrane where it acts to dissipate the proton gradient created by the respiratory chain across the mitochondrial inner membrane. Uncoupling of the respiratory chain causes a mild depolarisation of the mitochondrial membrane potential and diminished ATP production (Duchen, 2004). It has also been suggested that mild uncoupling can protect against ROS generation is some cases as there is less electron leakage and increased rate of respiration that leads to the reduction of oxygen to water (Duchen, 2004).

Polymorphism in the UCP2 promoter (-866G/A), which leads to increased UCP2 expression, has been associated with beta cell dysfunction, decreased insulin secretion and T2DM (Chan and Kashemsant, 2006; Sesti et al., 2003). The polymorphism has also been shown to be a predictor of development of T2DM (Chan and Kashemsant, 2006). UCP2 protein and mRNA levels are increased in the islets of obese *ob/ob* mice, and mice fed with high fat diet, and this has been shown to cause beta cell dysfunction (Zhang et al., 2001). In *ob/ob* islets, UCP2 levels were increased before progression of hyperglycaemia and diabetes in these animals, suggesting that upregulation of UCP2 protein expression may have a causal effect on the obesity associated development of T2DM (Chan and Kashemsant, 2006; Zhang et al., 2001). In general, overexpression of UCP2 in beta cells leads to decreased insulin secretion as production of ATP is attenuated (Maechler and Wollheim, 2001). However, another study failed to reproduce these results, leav-

ing some discrepancies between the effects of UCP2 overexpression on beta cell insulin secretion (Produit-Zengaffinen et al., 2007). On the other hand, UCP2 deficient mice have higher islet ATP content and increased GSIS *in vitro* (Zhang et al., 2001). They also have increased fasted and fed plasma insulin levels and improved glucose tolerance (Affourtit and Brand, 2008). Similarly, treating islets with genipin, an active compound of *Gardenia* fruit extract, is thought to inhibit UCP2 mediated proton leak, increase ATP levels and enhance GSIS *in vitro* (Zhang et al., 2006). UCP2 deficient *ob/ob* mice also showed improved glucose tolerance and GSIS, and treatment of *ob/ob* islets with genipin caused an acute improvement in GSIS (Zhang et al., 2006). Overall, it has been shown that UCP2 is involved in the regulation of GSIS in beta cells, possibly by regulation of mitochondrial ROS production (Affourtit and Brand, 2008).

1.7.3 K_{ATP}-channels

ATP-sensitive K^+-channels (i.e. K_{ATP}-channels) in beta cells consist of four inwardly rectifying pore-forming K^+ channel subunits (Kir6.2) that are surrounded by four sulphonylurea receptor subunits (SUR1) (Henquin et al., 2003; McTaggart et al., 2010). K_{ATP}-channels have an important role in beta cells in coupling glucose metabolism to cell excitability, which eventually leads to stimulation of insulin secretion. At basal glucose concentration (<5 mmol/L), glucose metabolism and cellular ATP/ADP ratio are low, plasma membrane K_{ATP}-channels remain open and active and beta cells are electrically silent (Rorsman, 1997). Active K_{ATP}-channels mediate K^+-ion outflux that keeps the resting membrane potential near -70 mV (near the K^+ equilibrium potential) (Macdonald et al., 2005). When glucose concentration rises above 5 mmol/L, glucose metabolism increases, which leads to a rise in cellular ATP/ADP ratio (Rorsman, 1997). ATP binds to the Kir6.2 subunits of the K_{ATP}-channel, which leads to channel closure. This causes plasma membrane depolarisation, as the inside of the beta cell becomes more positive due to accumulation of potassium ions inside the cell.

Loss of functional K_{ATP}-channels or mutations in Kir6.2 or SUR1 subunits, lead to increased electrical activity and insulin secretion at low glucose (Ashcroft, 2005; Miki et al., 1998; Seghers et al., 2000). Over 150 mutations have been found in

11

SUR1 encoding gene (*ABCC8*) and 24 in Kir6.2 gene (*KCNJ11*). These mutations cause congenital hyperinsulinism (HI), which is characterised by very high levels of insulin secretion, even at low glucose levels (McTaggart et al., 2010). It appears that the beta cells in HI individuals are permanently depolarised, which leads to a constant calcium influx and stimulation of insulin secretion.

Gain-of-function mutations in Kir6.2 and SUR1 subunits cause neonatal diabetes (ND). In general, these mutations prevent ATP from channel closure, which leads to a constant hyperpolarisation of the plasma membrane, even at high glucose concentrations, and suppression of insulin secretion, causing diabetes (McTaggart et al., 2010). A common polymorphism in Kir6.2 (E23K) has been associated with T2DM, but the mechanisms underlying this association are as yet unknown (McTaggart et al., 2010).

1.7.4 L-type Ca^{2+}-channels

As mentioned above, beta cells become electrically active when K$_{ATP}$-channel closure causes depolarisation of the plasma membrane. This opens L-type voltage-gated calcium channels, which leads to calcium influx in to the cell, an increase in intracellular free calcium concentration and triggering of insulin granule exocytosis (Henquin, 2009, 2000). The opening of calcium channels occurs in a pulsatile manner. Initial membrane depolarisation results in the opening of few calcium channels, which upon opening, trigger further depolarisation of the plasma membrane and opening of the remaining, closed L-type channels (Rorsman, 1997). Hence, firing of calcium potentials are observed as membrane depolarisation, which are separated by brief electrically silent periods when the membrane repolarises (Rorsman and Renström, 2003).

1.7.5 Insulin granule exocytosis

A single beta cell contains over 10,000 insulin secretory granules, in which insulin is associated with zinc (Rorsman and Renström, 2003). Insulin secretory granules are divided into different cellular pools of granules that differ in terms of their cellular location and in their releasability status (Macdonald et al., 2005). At least three different type of pools exist: an intracellular reserve pool (accounts

for 90 % of all the granules), a morphologically docked pool ($\approx$ 10 %) and a readily releasable pool, primed for release ($\approx$ 0.3-2.2 %). Insulin granules are likely to move along microtubules, powered by the ATP-dependent motor activity of the conventional kinesin KIF5B in the cytoplasm and along cortical actin network near the plasma membrane by the ATP-dependent myosin (Macdonald et al., 2005). Insulin granule fusion to the plasma membrane is mediated by SNARE proteins that include the vesicular protein VAMP and Syntaxin and SNAP-25 on the plasma membrane (Macdonald et al., 2005).

1.7.6   cAMP

Cyclic AMP (cAMP) is an important cellular second messenger that can stimulate beta cell insulin secretion, independently from glucose and K_{ATP}-channels. It is formed from ATP by adenylyl cyclase, which is activated by G-protein coupled receptors (GPCR) such as GLP-1 (glucagon-like peptide 1) receptor at the plasma membrane (Maechler and Wollheim, 2001). Thus incretins such as GLP-1 and GIP (gastric inhibitory polypeptide) and other agonists of the GPCRs are thought to stimulate insulin secretion by generation of cAMP. Cyclic AMP can stimulate and amplify insulin secretion via activation of several, distinct cellular processes, for example inhibition of K_{ATP}-channel activity, stimulation of L-type Ca^{2+}-channels and stimulation of calcium release from intracellular calcium stores, either by activation of protein kinase A (PKA) or independently of PKA (Eliasson, 2003; Maechler and Wollheim, 2001).

1.8   The pathophysiology of T2DM

Insulin resistance is in general the earliest pathophysiological sign in the development of T2DM. However, while pancreatic beta cells are able to compensate for the increased insulin demand via insulin hypersecretion, thus maintaining blood glucose within reasonable limits, once relative beta cell failure occurs, T2DM becomes manifest (Figure 1.3). It is therefore key to understand the mechanisms of beta cell failure in T2DM.
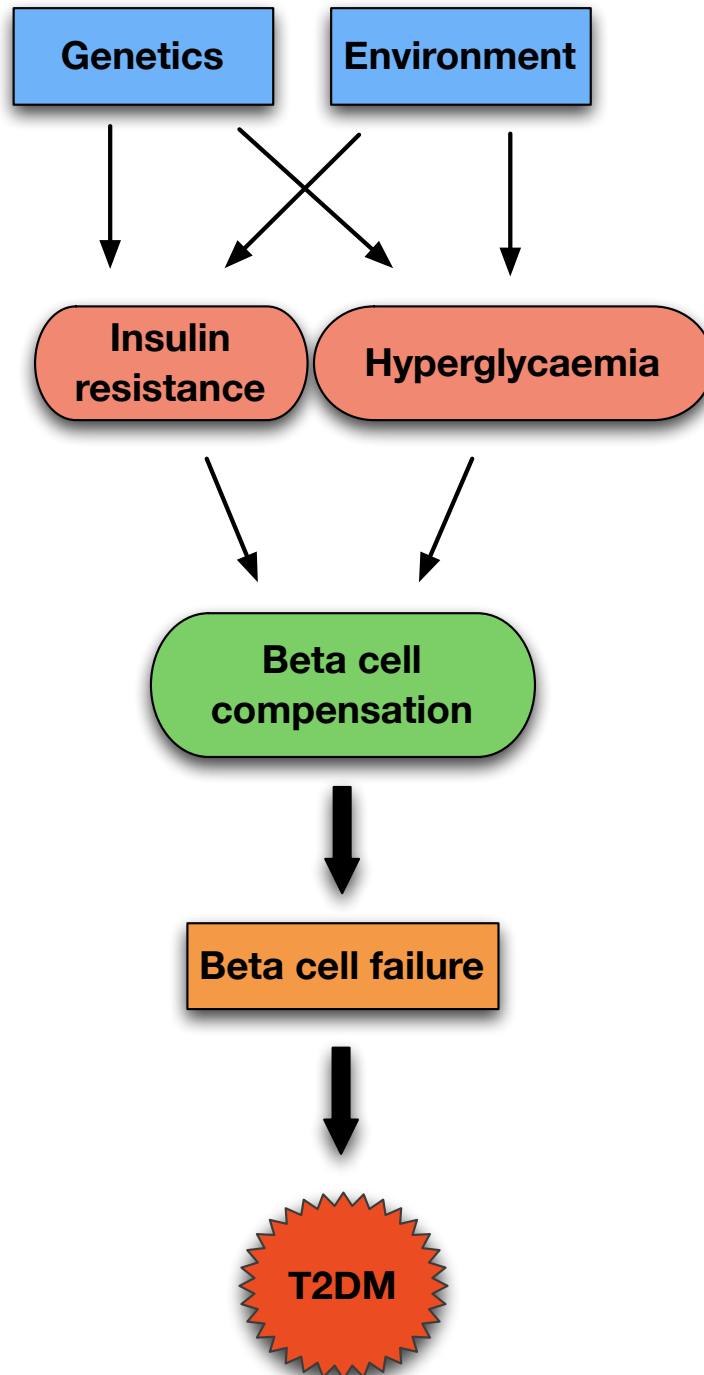
Figure 1.3: The pathogenesis of T2DM. Genetics and environmental factors affect the insulin sensitivity of peripheral tissues that can lead to insulin resistance and hyperglycaemia. Increased insulin demand is compensated by insulin hypersecretion from the pancreatic beta cells, thus maintaining blood glucose within reasonable limits. However, once relative beta cell failure occurs, T2DM becomes manifest.

1.8.1 Insulin resistance

Insulin resistance in liver and skeletal muscle is often present in individuals with T2DM. Overall about 25 % of the adult population are insulin resistant, but in most individuals, pancreatic beta cells are able to compensate for the increased insulin demand by increasing their insulin secretion (DeFronzo, 2004). The characteristics of insulin resistance are increased hepatic glucose output and decreased muscle glucose uptake that often leads to fasting hyperglycaemia and glucose intolerance (DeFronzo, 2004). Decreased insulin receptor tyrosine kinase activity, reduced IRS-1 phosphorylation, and reduced PI3K activity in muscle are often found in insulin resistant subjects and in individuals with T2DM (DeFronzo, 2004). Gly-972-Arg mutation in the *IRS-1* gene has been associated with T2DM and insulin resistance, although the physiological consequences of this mutation is still unknown (DeFronzo, 2004). *Prkaa2* gene (encoding AMPKα2) has been found to be located at the Japanese T2DM loci. Hence, *AMPKα2* is another candidate gene for insulin resistance and T2DM diabetes, at least in Japanese population (Horikoshi et al., 2006). I will discuss AMPK in more detail further in this chapter.

1.8.2 Beta cell dysfunction

Insulin resistance is usually compensated by insulin hypersecretion from beta cells and enhanced insulin secretion in response to acute glucose challenge. This is usually seen as an increase in beta cell mass or insulin production from individual beta cells (Chang-Chen et al., 2008). Expansion of beta cell mass is achieved mainly by increased beta cell proliferation but also by beta cell hypertrophy, often found in humans and rodent models of insulin resistance (Weir and Bonner-Weir, 2004). However, if T2D ensues despite the beta cell compensatory effect, a significant reduction in beta cell mass can be detected, and this is thought to be due to increased beta cell apoptosis (Butler et al., 2003; de Koning et al., 2008). Apoptosis is only one disorder that contributes to beta cell dysfunction. Loss of first phase insulin secretion and reduced and delayed second phase, decreased insulin gene expression and beta cell insulin content are also associated with beta cell dysfunction in T2DM (de Koning et al., 2008; DeFronzo, 2004; Robertson

and Harmon, 2006; Zhang et al., 2001). The cause for the loss of the first phase insulin secretion is not well understood, but it is thought to involve dysregulation of gene expression needed in the first phase, and can possibly be caused by glucotoxicity (Weir and Bonner-Weir, 2004).

Beta cell dysfunction is also accompanied by general changes in gene expression profile in the beta cells, involving both upregulation and downregulation of genes. For example, *glucose-6-phosphatase*, *lactate dehydrogenase*, antioxidants and apoptotic and proapoptotic genes are found to be upregulated (Weir and Bonner-Weir, 2004). Even though an acute increase in plasma glucose levels stimulates *insulin* gene expression and insulin release from beta cells, chronic exposure to elevated glucose concentration and fatty acids has the opposite effect on beta cell function. Increased levels of oxidative stress are associated with chronic hyperglycaemia and are often recorded in diabetic patients (Robertson and Harmon, 2006). These can be termed as gluco- and lipotoxicity of the beta cells (Robertson et al., 2004). Chronic elevation of glucose concentration results in increased glucose oxidation that in turn causes mitochondrial dysfunction and increased production of reactive oxygen species (ROS) (Chang-Chen et al., 2008; Robertson et al., 2004). It also increases cytosolic calcium levels that can have a pro-apoptotic effect in beta cells and induces endoplasmic reticulum (ER) stress (Chang-Chen et al., 2008; Eizirik et al., 2008).

In conclusion, insulin resistance is the first step in the development of T2DM, compensated by increased beta cell mass and insulin secretion. However, chronic hyperglycaemia can cause mitochondrial dysfunction, increased oxidative stress and activation of apoptotic pathways that leads to beta cell dysfunction. Beta cell dysfunction progressively leads to beta cell failure, which means that beta cells are unable to meet the increased insulin demand and T2DM manifests (See Figure 1.4).
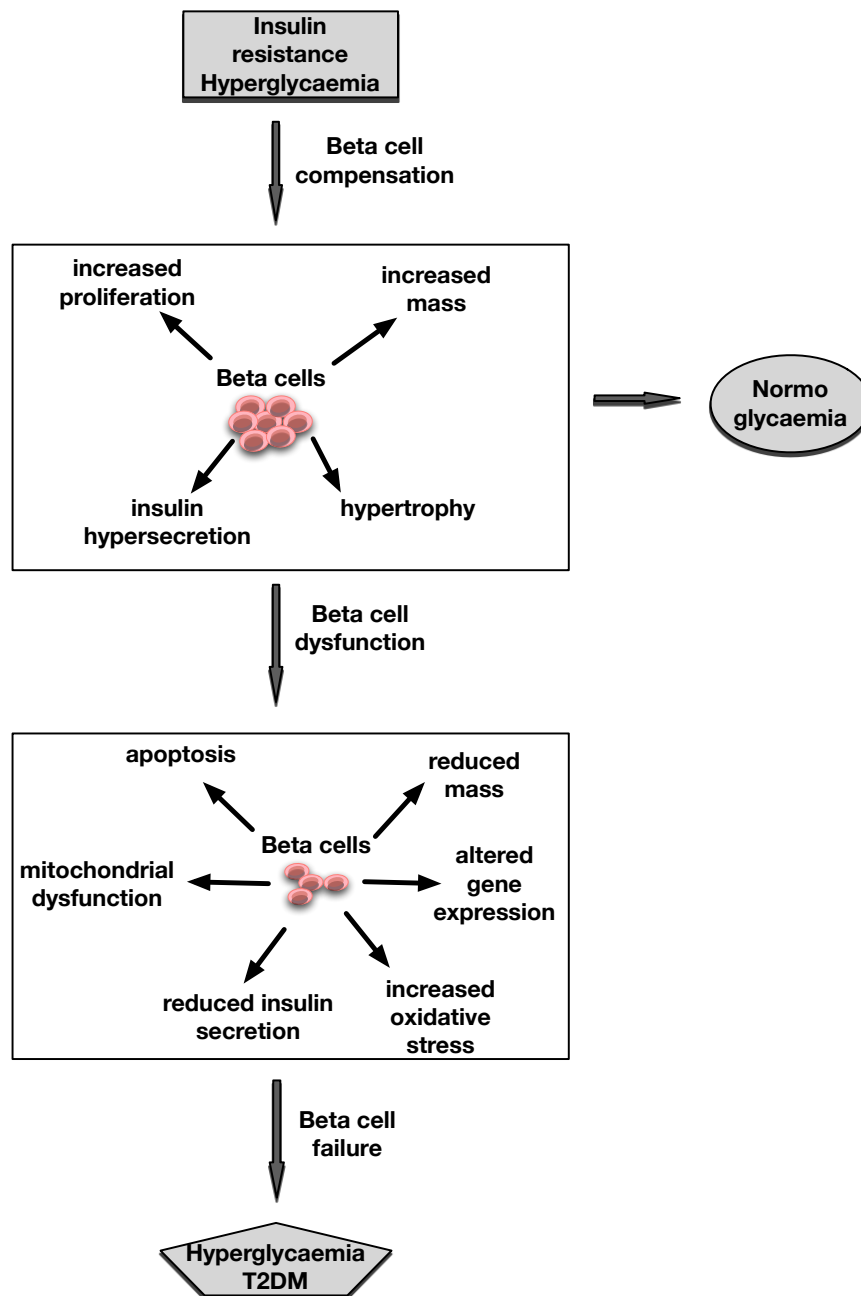
Figure 1.4: Beta cell dysfunction and development of T2DM. Insulin resistance and hyperglycaemia lead to increase in insulin demand from pancreatic beta cells. Beta cells compensate by increased proliferation, increased mass and insulin hypersecretion. However, if normoglycaemia cannot be achieved, chronic hyperglycaemia and constant insulin hypersecretion eventually lead to beta cell dysfunction, characterised by increased apoptosis and oxidative stress, mitochondrial dysfunction, altered gene expression and reduced beta cell mass and insulin secretion. Ultimately beta cell failure occurs, which leads to development of T2DM.

1.9 Regulation of energy homeostasis by the central nervous system (CNS)

Yet, the beta cells are not the only important regulators of glucose homeostasis. The central nervous system (CNS) also participates in the regulation of energy- and glucose homeostasis. It is also thought that altered neuronal pathways can possibly contribute to the development of metabolic diseases such as obesity and T2DM. Therefore, understanding how the CNS participates in the regulation of whole-body glucose and energy homeostasis is important.

Glucose is the primary fuel source for the brain. Hence it is essential that the brain glucose levels are kept within a narrow range, regulated by the central nervous system (CNS) (Marty et al., 2007). The CNS receives hormonal and nutritional status of the body that translates to changes in neuronal activity in the brain stem and hypothalamus (Seeley and Tschop, 2006). Autonomic nervous system also signals additional information in response to nutrients such as amino acids, glucose and lipids (Marty et al., 2007). For example, the CNS controls peripheral glucose homeostasis, including hepatic glucose production by the hepatic portal vein that acts as a glucose sensor, which then projects to the different parts of the hypothalamus such as the paraventricular hypothalamus and the arcuate nucleus (ARC) (Marty et al., 2007). A subset of neurons located in the arcuate nucleus of the hypothalamus have a central role in the regulation of energy homeostasis (Elmquist et al., 2005). Neuronal populations that co-express the orexigenic neuropeptide Y (NPY) and agouti-related peptide (AgRP), inhibited by insulin and leptin, regulate energy homeostasis by stimulating feeding and decreasing energy expenditure (Seo et al., 2008; Woods et al., 2006). Another neuronal population that acts in the opposite direction by stimulating food intake and energy expenditure, activated by insulin and leptin, co-express the pro-opiomelanocortin (POMC) and cocaine-amphetamine-regulated-transcript (CART) neuropeptides (Seo et al., 2008; Woods et al., 2006).

One of the most essential roles for the CNS in regulation of glucose homeostasis is hypoglycaemic sensing. Failure to respond to hypoglycaemia can lead to reduced neuronal activity and in severe cases to complete neuronal damage (Mobbs et al., 2001). Several brain regions including the ventromedial and paraventricu-

lar hypothalamus and arcuate nucleus participate in the hypoglycaemic sensing (Donovan and Bohland, 2009). Specialised glucose sensing neurons respond to changes in extracellular glucose levels in the brain and change their electrical activity accordingly. These neurons are divided into two types according to their activity in response to extracellular glucose levels. Glucose excited neurons become activated by increase in extracellular glucose (Marty et al., 2007). Most of the glucose excited neurons are thought to work similarly to the pancreatic beta cells. This means that they are dependent on GLUT2 and glucokinase as glucose sensors, and production of ATP from glucose metabolism to inhibit K_{ATP}-channel activity, which leads to depolarisation of the plasma membrane (Burdakov et al., 2005). For example POMC neurons are glucose excited neurons that are located in the hypothalamic arcuate nucleus. Transgenic mice with a disruption of K_{ATP}-channel activity in POMC neurons developed impaired whole-body glucose homeostasis, and glucose sensing in the mutated POMC neurons was blunted (Parton et al., 2007). Less is known about the mechanisms of glucose inhibited neurons that become electrically silent in response to increase in glucose levels. It is thought that inhibition of these neurons involves activation of Cl^- currents and reduced Na^+/K^+ pump activity (Burdakov et al., 2005). One key enzyme regulating brain hypoglycaemic sensing and whole-body energy homeostasis is AMP-activated protein kinase (AMPK). AMPK is regarded as a cellular energy gauge that is activated by decreased energy levels in order to restore energy levels back to normal. In the hypothalamus, AMPK activity is increased upon fasting, which leads to increased food intake and body weight. *Vice versa*, feeding inhibits hypothalamic AMPK activity, which leads to a reduction in food intake and loss in body weight (Xue and Kahn, 2006). Both insulin and leptin, the key signalling molecules involved in the hypothalamus in the regulation of energy homeostasis, suppress hypothalamic AMPK activity (Kim and Lee, 2005). For example inhibition of AMPK activity by leptin, secreted from adipocytes in proportion to fat mass, leads to reduction in food intake (Bjørbaek and Kahn, 2004; Obici, 2009; Okamoto et al., 2008).

In conclusion, the CNS regulation of hypoglycaemia and whole-body energy homeostasis is essential. Food intake, body weight and energy storage and expenditure are regulated by a complex signalling network within the CNS. In addition,

peripheral glucose homeostasis such as production of hepatic glucose as well as insulin secretion from the pancreatic beta cells can also be controlled by the CNS. Therefore, in order to understand diseases such as obesity and T2DM, it is important to understand the complexity involved in the regulation of whole-body glucose- and energy homeostasis.

1.10 AMP-activated protein kinase

Beta cell energetics, mitochondrial function and generation of ATP are essential for proper beta cell function and insulin secretion. Dysfunction in these mechanisms can lead to impaired beta cell function and development of diabetes. Therefore, understanding the pathways that regulate beta cell energy homeostasis is important. One key enzyme whose main function is to regulate cellular energy levels is AMP-activated protein kinase (AMPK).

AMP-activated protein kinase (AMPK) is a serine/threonine protein kinase that phosphorylates proteins with a specific sequence motif $\Phi(X,\beta)XX(S/T)XXX\Phi$, where Φ is a bulky hydrophobic residue, and β is a basic residue (Corton et al., 1995). AMPK functions as a regulator of cellular and whole-body energy homeostasis, and as the name suggests, it is activated by low energy levels associated with a rise in the cellular AMP/ATP ratio (Corton et al., 1994). In general any environmental stress that causes depletion of cellular ATP, such as hypoxia, heat shock, starvation or prolonged exercise leads to the activation of AMPK (Corton et al., 1995; Viollet et al., 2009). Human tumour suppressor liver kinase B1 (LKB1) is a direct upstream kinase of AMPK that activates AMPK by phosphorylating threonine 172, located in the activation loop of the catalytic subunit (Shackelford and Shaw, 2009). Another AMPK upstream kinase that phosphorylates and activates AMPK is a Ca^{2+}/calmodulin-dependent protein kinase kinase (CaMKK)α/β, which is activated by increased intracellular Ca^{2+}. However, the activity of CaMKKs is mainly restricted to the brain, whereas LKB1 is ubiquitously expressed (Carling et al., 2008; Kola, 2008; Xue and Kahn, 2006). Active AMPK switches on ATP-producing, catabolic processes that aid in restoring the depleted energy levels. These include glucose transport, glycolysis, mitochondrial biogenesis and fatty acid oxidation (Kurth-Kraczek et al., 1999; Merrill

et al., 1997; Reznick et al., 2007). AMPK also switches off ATP-consuming, anabolic processes such as protein translation, fatty acid and cholesterol synthesis (Hardie and Carling, 1997), as well as gluconeogenesis in the liver (Lochhead et al., 2000). AMPK therefore acts as a fuel gauge, restoring cellular energy balance short-term directly by phosphorylation of key enzymes, and long-term via regulation of gene expression (Holmes et al., 1999; Kurth-Kraczek et al., 1999; Zheng et al., 2001) (See Figure 1.5).

1.10.1   Heterotrimeric AMPK

AMPK is an evolutionary conserved protein kinase and its gene homologues are expressed in almost all eukaryotes from fruit fly (*Drosophila melanogaster*) (Corton et al., 1995; Pan and Hardie, 2002) and yeast (*Saccharomyces cerevisae*) to rodents and humans (Richter and Ruderman, 2009). In mammals, AMPK consists of a complex of three subunits, each encoded by a different gene, and each subunit is expressed as at least two different isoforms.

AMPK catalytic subunits, AMPKα1 (*Prkaa1*) and AMPKα2 (*Prkaa2*) contain a serine/threonine kinase domain in the N-terminus, a phosphorylation site at Thr172 (Hawley et al., 1996), immediately followed by an inhibitory domain between residues 312-392. In addition, $\approx$150 amino acid residues at the C-terminus are needed for association with the two regulatory subunits β and γ (Crute et al., 1998).

The regulatory subunit β (1 and 2) act as a scaffolding subunit for the other two subunits and also contains a glycogen binding domain (Woods et al., 1996). The γ subunit (1, 2 and 3) contains a regulatory subunit that consists of four cystathione -synthase (CBS) domains that function in pairs to bind adenosine nucleotides (AMP, ATP and ADP) (Cheung et al., 2000). AMPK activity is thought to be regulated allosterically by the binding of AMP to the CBS domains in the γ subunit, and by reversible phosphorylation of the Thr172, essential for activation, by the upstream kinases (Xavier et al., 2003). The allosteric activation promotes Thr172 phosphorylation and prevents dephosphorylation by protein phosphatases (Carling, 2004; Xiao et al., 2007).
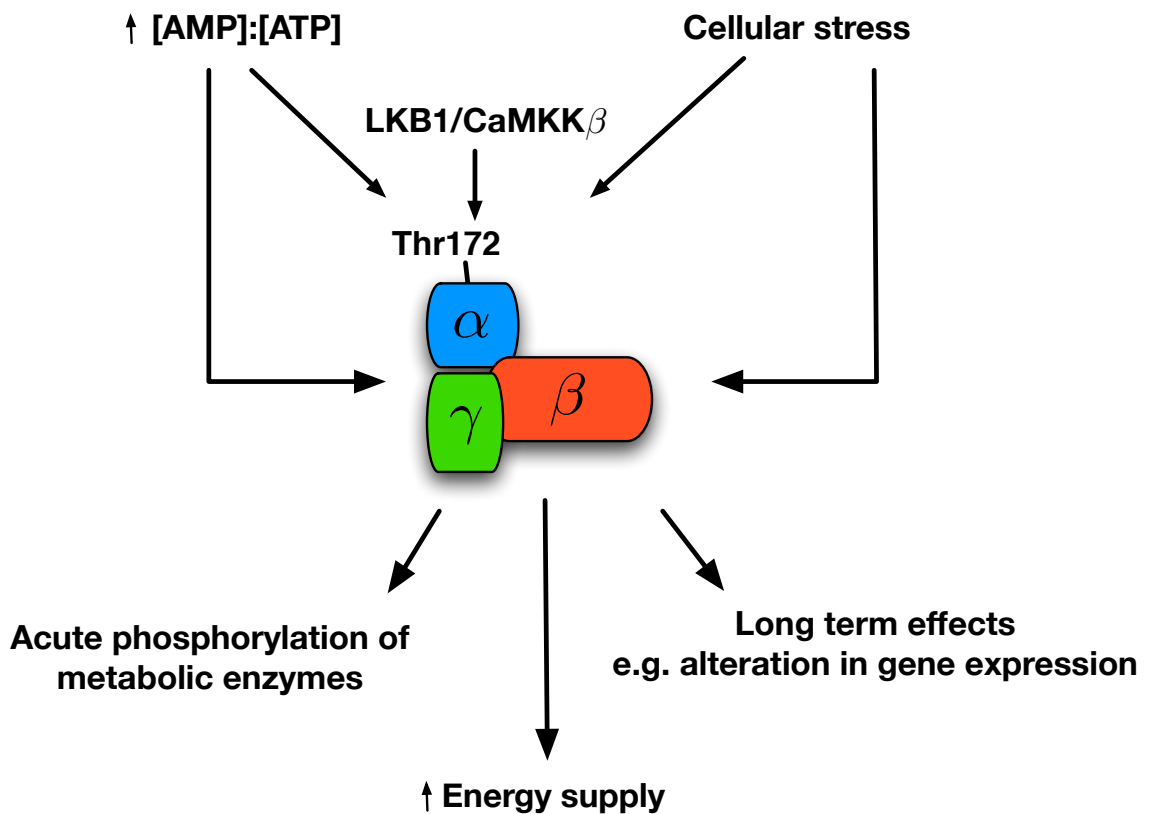
Figure 1.5: Evolutionary conserved AMPK acts as a cellular fuel gauge. AMPK is a heterotrimeric serine/threonine protein kinase that consists of catalytic subunit α and two regulatory subunits β and γ. AMPK is activated by a change in cellular AMP/ATP ratio and cellular stress, but the main activator is phosphorylation of the catalytic subunit alpha by upstream kinases such as LKB1. Active AMPK switches on catabolic ATP-producing processes and switches off ATP-consuming processes through acute phosphorylation of metabolic enzymes and long term by alteration in gene expression, thus restoring energy levels back to normal. AMPK was initially recognised as a regulator of cellular energy status but now it is well known that it has a key role in the regulation whole-body energy homeostasis. Adapted from Carling (2004).

1.10.2 The role of AMPK in the beta cells

Islet beta cells use ATP as an energy source, but ATP is also a key signalling molecule for insulin secretion. Glucose metabolism is tightly coupled to production of ATP, and small changes in glucose concentrations are met with adjustments in cellular ATP/ADP and ATP/AMP ratios that are kept within narrow limits. As AMPK functions as a cellular energy regulator and its activity is linked to changes in cellular ATP/AMP ratio, it seems obvious that it could have a key role in the regulation of beta cell function and insulin secretion (See Figure 1.6). The role of AMPK in pancreatic beta cells has been of great interest for several years. However, despite the numerous studies conducted over the years, no clear conclusion has been made yet, and discrepancies between studies exists, especially about the role of AMPK in the regulation of insulin secretion.

Most of the studies that have investigated the role of AMPK in beta cells have been carried out on imperfect beta cell models (such as INS-1 and MIN6), which are immortalised insulinoma cell lines (Hohmeier and Newgard, 2004). Secondly, manipulation of AMPK has involved the overexpression of constitutively active (AMPK CA) or dominant negative (AMPK DN) constructs of AMPK, or use of pharmacological agents to activate (AICAR, metformin) or inhibit AMPK (Compound C). The problem in using pharmacological agents in the activation and inhibition of AMPK is that the drugs are not very specific. For example AICAR (5-aminoimidazole-4-carboxamide ribonucleoside) has been long used as an activator of AMPK and many AMPK studies have been based on AICAR activated AMPK (Corton et al., 1995).

AICAR is metabolised in the cell, which leads to accumulation of 5-aminoimidazole-4-carboxamide ribonucleoside (ZMP), a mimic of AMP, without changing the cellular ATP/ADP or ATP/AMP ratio. ZMP is then thought to act similarly to AMP in activating AMPK (Corton et al., 1995). However, ZMP can also activate other enzymes within the cell such as a glycolytic enzyme fructose-1,6-bisphosphatase, which is also regulated by AMP (Iancu et al., 2005). Hence the current approaches to determine the function of AMPK in beta cells have their drawbacks and it is unclear whether the observed results are attributable to AMPK activation or inhibition.

Adipose tissue

Fatty acid synthesis
Lipolysis

Skeletal muscle

Glucose uptake
Glycolysis
Fatty acid oxidation

Brain

Food intake
Fatty acid oxidation
Hypoglycaemic sensing

AMPK

Pancreas

?

Insulin secretion
Glucose sensing

Liver

Gluconeogensis
Fatty acid and cholesterol
synthesis
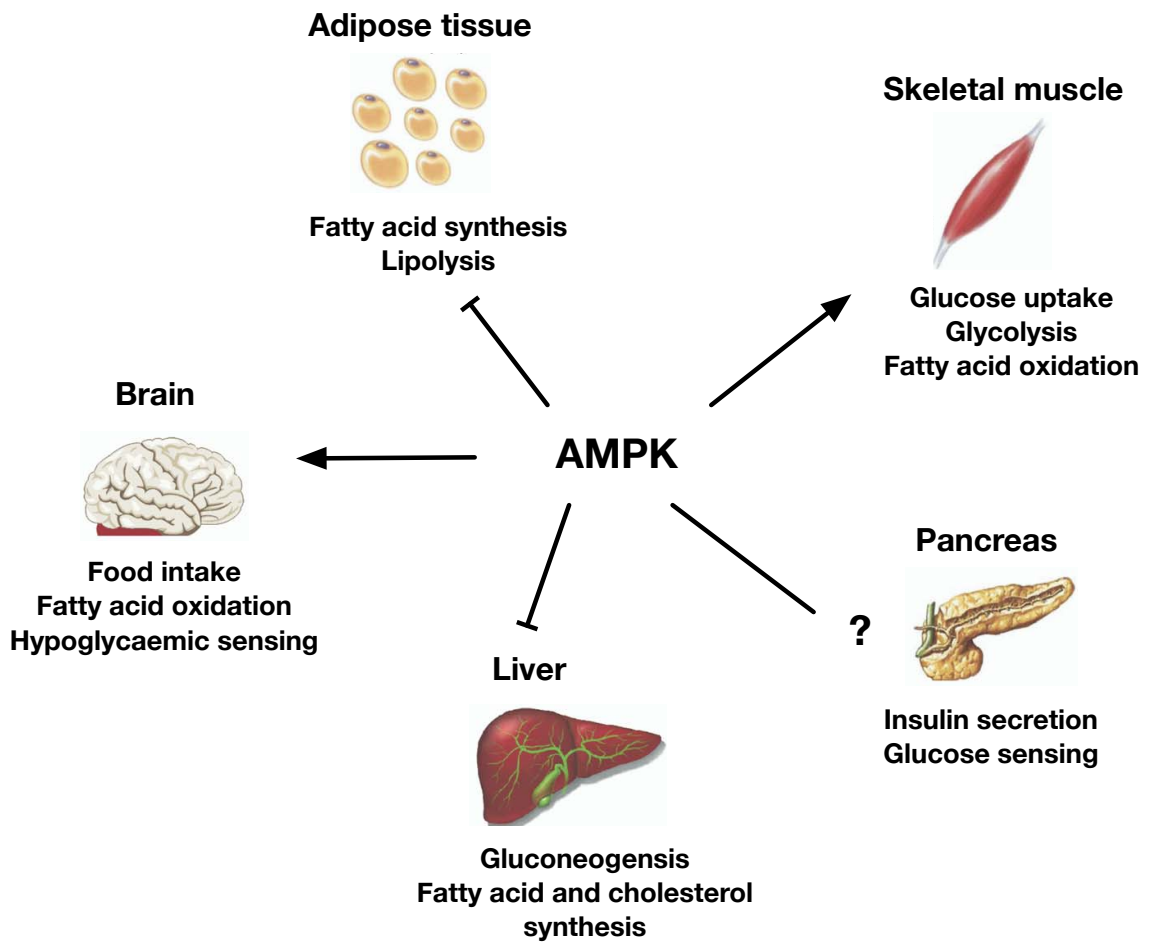
Figure 1.6: AMPK is involved in the regulation of whole-body energy homeostasis. Changes in AMPK activity lead to changes in energy expenditure and feeding. AMPK regulates lipid metabolism in skeletal muscle, liver, adipose tissue and hypothalamus by inhibition of fatty acid synthesis and stimulation of fatty acid oxidation. AMPK is also thought to stimulate lipolysis by phosphorylation of hormone sensitive lipase. In skeletal muscle, AMPK also stimulates glucose uptake and glycolysis. In liver, one of the main functions for AMPK is inhibition of gluconeogenesis. In hypothalamus, AMPK activation, in addition to activation of fatty acid oxidation, stimulates food intake and increases body weight gain. It has also been shown that AMPK activation in several hypothalamic nuclei seems to have a role in hypoglycaemic sensing. Adapted from Kahn et al. (2005).

1.10.3 AMPK regulated expression of key beta cell genes

AMPK is reported to play an important role in beta cell gene regulation. For example, one such gene, which is regulated by AMPK, is the *hepatic nuclear factor-4* (HNF4), a transcription factor that regulates gene expression in liver, intestine and pancreas. Mutations in *HNF4* cause maturity-onset diabetes of the young 1 (MODY1), an autosomal-dominant form of T2DM (Yamagata et al., 1996). Genes regulated by HNF4 in beta cells include *GLUT2*, *L-PK* (liver type pyruvate kinase) and *aldolase B* (Leclerc et al., 2001). HNF4 is thought to be a direct target for AMPK phosphorylation. This results in the reduction of HNF4 protein levels, which then leads to a significant reduction in mRNA levels of HNF4 regulated genes (Leclerc et al., 2001). Other genes reported to have an altered expression in islets overexpressing AMPK are *peroxisome proliferator activated receptor* (*PPAR*) (Ravnskjaer et al., 2006) and *pre-proinsulin* (*PPI*) (da Silva Xavier et al., 2000), both of whose gene expression were downregulated by AMPK. Activation of AMPK by AICAR has also been reported to suppress expression of the *preproinsulin* gene by decreasing the expression of transcription factor *BETA2*, which regulates *insulin* gene transcription (Kim et al., 2008). AMPK phosphorylates transcriptional coactivator p300 at serine-89 *in vivo* and *in vitro*, which inhibits the interaction between p300 and transcription factors PPARγ, thyroid-, retinoic acid- and retinoid X receptors (Yang et al., 2001b). However, the physiological role of the p300 phosphorylation by AMPK is yet unknown.

1.10.4 Role of AMPK in beta cell apoptosis

Chronic exposure of beta cells to elevated glucose concentrations leads to beta cell apoptosis. Culturing MIN6 cells in low glucose or with AICAR resulted in mitochondrial dysfunction and increased production of ROS, which led to initiation of mitochondrial apoptotic pathway, suggesting that activation of AMPK might contribute to beta cell apoptosis (Cai et al., 2007). Similarly, overexpression of constitutively active AMPK construct (AMPK-CA) in MIN6 beta cells and CD1 mouse islets, or exposure of MIN6 cells to cytokines (TNF-α, interleuking-1β, interferon-γ) induced beta cell apoptosis (Riboulet-Chavey et al., 2008; Xavier et al., 2003). However, the cytokine induced apoptosis was prevented by over-

expression of dominant negative form of AMPK (AMPK-DN) (Riboulet-Chavey et al., 2008). AMPK probably induces apoptosis via activation of JNK that leads to caspase-3 release and DNA fragmentation as a JNK inhibitor prevented AICAR induced apoptosis (Kefas et al., 2003, 2004). However it seems that a short term activation of AMPK might protect cells agains apoptosis, but a long term activation might lead to increased apoptosis (Hinke et al., 2007). On the other hand, Jambal et al. (2003) and Inoki et al. (2003) showed that inhibition of PKB and mTOR by AMPK leads to inhibition of an anti-apoptotic pathway (Riboulet-Chavey et al., 2008). Hence, discrepancies exist about the role of AMPK in regulation of apoptosis and more research is needed to properly assess the role of AMPK on cell survival and apoptosis.

1.10.5 The controversial role of AMPK in beta cell insulin secretion

The role of AMPK in insulin secretion has remained controversial and unclear. In general, some studies have shown that activation of AMPK (expression of constitutively active (CA) AMPK construct, AICAR, metformin, alpha-lipoic acid) decrease glucose-stimulated insulin secretion, whereas others have shown the opposite. On the other hand, similar discrepancies have been shown upon inhibition of AMPK activity (expression of dominant negative (DN) AMPK construct, amino acids, compound C). The factors that most likely affect the inconsistencies between the different studies are the cell/islet types used, experimental set up and normalisation of data. Also, the concentration of AICAR that is used to activate AMPK varies between 200 and 1000 μM, which can possibly affect the specificity of AICAR acting on AMPK.

The effect of AMPK on insulin secretion also seems to vary depending on glucose concentration (low vs. high). As AMPK is mainly activated when the cellular ATP/AMP ratio is low, one would assume that AMPK is in an inactive state when glucose concentration is high and insulin secretion is elevated. Indeed, Leclerc et al. (2004) have shown that high glucose concentration and amino acids such as leucine, arginine and glycine reduce AMPK activity markedly and that insulin secretion and AMPK activity are inversely correlated with each other (Leclerc

et al., 2004). The higher the AMPK activity, the lower the insulin secretion and *vice versa* (Leclerc and Rutter, 2004). Therefore, overexpression of CA AMPK for instance, does not necessarily provide any useful information about AMPK in relation to insulin secretion in high glucose concentration, as in normal situation AMPK would not be activated. The results of the studies that have looked at the role of AMPK in insulin secretion have been summarised in Table 1.1.

Table 1.1: Summary of studies investigating AMPK regulated insulin secretion. The table summarises different studies that have investigated the role of AMPK in insulin secretion at low and high glucose concentrations. The studies have either activated or inhibited AMPK in MIN6 cells or mouse, rat or human islets. Treatments that have been used to activate AMPK include different concentrations of AICAR, alpha-lipoic acid, metformin, phenformin, rosiglitazone and expression of constitutively activated AMPK. Amino acids, glucose, compound C, expression of dominant negative form of AMPK and deletion of AMPK catalytic subunits have been used to inhibit AMPK activity.

Cell type	Treatment	AMPK activity	Insulin secretion at low glucose (in comparison to control)	Insulin secretion at high glucose (in comparison to control)	References
MIN6/rat islet	AICAR (200uM)	increased	normal (3mM G)	decreased (30mM G)	DaSilvaXavier et al. Biochem J 2003
MIN6/rat islet	CA AMPK	increased	normal (3mM G)	decreased (30mM G)	
MIN6/rat islet	DN AMPK	decreased	increased (3mM G)	normal (30mM G)	
Mouse/rat islet	CA AMPK	Increased	normal (3mM G)	decreased (17mM G)	Richards et al. J Endocrinol 2005
Mouse islet	DN AMPK	decreased	normal (3mM G)	normal (17mM G)	
Rat islet	AICAR (1000 uM)	increased	normal (2.8M G)	decreased (16.7mM G)	Targonsky et al. Diabetologia 2006
Rat islet	alpha-lipoic acid (2mM)	increased	normal (2.8M G)	decreased (16.7mM G)	
MIN6	AICAR (1000 uM)	increased	normal (0M G)	decreased (15mM G)	
MIN6	alpha-lipoic acid (2mM)	increased	decreased (0M G)	decreased (15mM G)	
MIN6	Metformin (1mM)	increased	normal (0M G)	decreased (15mM G)	
Human islet	CA AMPK	increased	n/a	decreased (17mM G)	Leclerc et al. Am J Physiol Endocrinol Metab 2004
Human islet	DN AMPK	decreased	n/a	increased (17mM G)	
MIN6	Metformin (1mM)	increased	normal (3mM G)	decreased (17mM G)	
Human islet	Metformin (1mM)	increased	normal (3mM G)	decreased (17mM G)	
MIN6	Rosiglitazone (4.5uM)	Increased	increased (3mM G)	increaseaad (16.7mM G)	Chang et al. Diabetologia 2009
MIN6	AICAR (50uM)	increased	increased (3mM G)	increaseaad (16.7mM G)	
Mouse islet	AICAR (300uM)	Increased	increased (5mM G)	Increased (8mM and 14mM G)	Wang et al. Biochem Biophys Res Commun 2005
MIN6	Leu, Gln, Arg	decreased	increased (n/a)	n/a	Leclerc et al. Diabetes 2004
MIN6	Glucose	decreased	n/a	increased (17mM G)	
MIN6	AICAR (1000 uM)	increased	normal (3mM G)	Increased (30mM G)	Gleason et al. J Biol Chem 2007
MIN6	Phenformin (10mM)	increased	increased (3mM G)	Increased (30mM G)	
Rat islet	AICAR (1mM)	increased	increased (5.5mM G)	Increased (8.3nM G)	
Mouse islet	AMPKα1,α2KO	decreased	normal (3mM G)	increased (16.7mM G)	Sun et al. Diabetologia 2010
Mouse islet	AMPKα1,α2KO + AICAR (400 uM)	decreased/ increased		decreased (16.7mM G)	
Mouse islet	CA AMPK	increased	increased (3mM G)	decreased (16.7mM G)	
Mouse islet	DN AMPK	decreased	normal (3mM G)	increaseaad (16.7mM G)	
Rat islet	AICAR (500 uM)	increased	decreased (0M G)	decreased (11mM G)	Lim et al. Diabetes 2009
Rat islet	Compund C (10 uM)	decreased	increased (0M G)	increased (11mM G)	

1.10.6 Knowledge from transgenic AMPK animals

Transgenic mouse models of the AMPK pathway have provided some new information about the role of this pathway in beta cells, but even these studies have been inconclusive and controversial. *AMPKα2*-global-null mice were not reported to have any intrinsic beta cell defect, even though they showed impaired glucose homeostasis and reduced glucose-stimulated insulin secretion *in vivo*. Deletion of the AMPK upstream kinase, LKB1, in beta cells (*RIPCreLKB1KO, Pdx-CreLKB1KO*) leads to enhanced insulin secretion and improved glucose tolerance *in vivo* (Granot et al., 2009; Sun et al., 2010b). *In vitro* GSIS was normal in the LKB1 KO islets but beta cell mass, and islet- and beta cell size were increased and islet architecture altered (Sun et al., 2010b; Xue and Kahn, 2006). The general consensus is that AMPK does have a pivotal role in beta cells. Based on the knowledge from cell culture studies its role includes regulation of gene expression, beta cell survival and insulin secretion.

1.10.7 AMPK in peripheral tissues

Activation of AMPK in peripheral tissues leads to regulation of metabolic processes that improve cellular and whole-body glucose- and lipid homeostasis. Exercise also induces AMPK activation in these tissues (See Figure 1.6). For example, IL-6, which is produced and released from contracting skeletal muscle, activates AMPK by raising intracellular cAMP levels and secondly the AMP/ATP ratio (Kelly et al., 2009). Peripheral AMPK is also activated by two adipocyte derived hormones, leptin and adiponectin, highlighting a role for AMPK in the regulation of whole-body energy homeostasis (Cool et al., 2006b). The most commonly used oral anti-diabetic drug metformin is thought improve blood glucose levels by activation of AMPK in peripheral tissues such as muscle, liver and adipocytes.

1.10.7.1 Skeletal muscle

Muscle glucose uptake constitutes about 80-85 % of the peripheral blood glucose uptake (DeFronzo, 2004). Insulin receptor signalling stimulates glucose uptake in the muscle. However, as muscle insulin resistance is often manifest in pre-

diabetic and diabetic individuals, activation of AMPK in skeletal muscle provides an alternative way to stimulate glucose uptake into the muscle (Holmes et al., 1999). This is thought to be achieved by AMPK mediated upregulation of *GLUT4* gene expression and GLUT4 translocation to the plasma membrane (Kurth-Kraczek et al., 1999; Zheng et al., 2001).

AMPK activity also enhances muscle fatty acid oxidation, directly by phosphorylation and inhibition of acetyl-CoA carboxylase (ACC) that catalyses the conversion of acetyl-CoA to malonyl-CoA (Merrill et al., 1997). Inhibition of ACC results in the reduction in malonyl-CoA, which inhibits the entry of fatty acids into the mitochondria, facilitated by carnitine:palmitoyl-CoA acyltranserase (CPT I). Hence, the reduction in malonyl-CoA levels results in the entry of fatty acid into the mitochondria for β-oxidation (Hardie and Carling, 1997). AMPK also stimulates muscle β-oxidation indirectly by increasing the mRNA expression of *peroxisome proliferator-activated receptor-α* (PPARα) and transcription regulator *peroxisome proliferator-activated receptor-γ coactivator 1α* (PGC-1α), which activates expression of genes involved mitochondrial biogenesis such as β-oxidation (Lee et al., 2006).

AMPK is involved in the regulation of mitochondrial biogenesis but the exact mechanisms have remained unclear. However, it has been thought to involve direct phosphorylation or increased expression of the transcription regulator *PGC-1α*, which induces the expression of genes involved in mitochondrial and lipid metabolism (Cantó et al., 2009). Activation of PGC-1α involves its deacetylation, a process mediated by AMPK and NAD^+-dependent type III deacetylase (SIRT1). AMPK induces mitochondrial β-oxidation that leads to increased mitochondrial NAD^+ levels and increased NAD^+/NADH ratio, thus inducing SIRT1 activity and deacetylation of PGC-1α (Cantó et al., 2009). It is also possible that AMPK- and SIRT1-dependent deacetylation is one mechanism to activate another transcription regulator FoxO that is also involved in the transcriptional regulation of energy expenditure (Cantó et al., 2009). Muscle protein and glycogen synthesis are also inhibited by AMPK. AMPK acts as a negative regulator of mTOR signalling in skeletal muscle by activation of TSC2, which inhibits mTOR activity and leads to decreased protein synthesis (Deshmukh et al., 2008; Gleason et al., 2007). AMPK also directly phosphorylates glycogen synthase (GS) that

leads to the inactivation of GS (Jørgensen et al., 2004; Lage et al., 2008).

1.10.7.2 Liver

The main role for liver in glucose homeostasis is the regulation of hepatic gluconeogenesis. Insulin receptor signalling inhibits the gluconeogenic pathway, but again in insulin resistant state, this is blunted. This usually leads to increased hepatic glucose output and further increase in blood glucose levels. Activation of AMPK in liver inhibits gluconeogenesis, independently from insulin, by phosphorylation of transducer of regulated CREB (cyclic AMP response element binding protein) activity 2 (TORC2) (Andreelli et al., 2006). Phosphorylation of TORC2 prevents its translocation from the cytoplasm to the nucleus where TORC2 mediates the transcription of gluconeogenic genes *phosphoenolpyruvate carboxykinase* (PEPCK) and *glucose-6-phosphatase* (G6Pase) (Xue and Kahn, 2006). Hence, activation of AMPK also leads to the inhibition of gluconeogenesis in liver by downregulating the expression of two gluconeogenic enzymes PEPCK and glucose-6-phosphatase (Cool et al., 2006b).

Transgenic mouse models of AMPK have also demonstrated the importance of hepatic AMPK in the regulation of glucose homeostasis. For example, liver specific AMPKα2KO mice displayed fasted hyperglycaemia and glucose intolerance and endogenous glucose production in these mice was increased by 50 % (Andreelli et al., 2006). On the other hand, short term overexpression of *AMPKα2* in mouse liver leads to mild hypoglycaemia in wt mice, and improves blood glucose levels in streptozotocin-induced and *ob/ob* diabetic mice due to enhanced suppression of gluconeogenesis (Foretz et al., 2005).

1.10.8 AMPK in the hypothalamus

AMPK has become one of the key regulators of whole-body energy homeostasis. As mentioned earlier, the adipokines leptin and adiponectin that regulate whole-body energy homeostasis in the hypothalamus, activate AMPK in peripheral tissues. However, in the hypothalamus, leptin inhibits AMPK activity (Bjørbaek and Kahn, 2004; Okamoto et al., 2008). Leptin is produced and secreted from adipocytes in proportion to adipocyte mass and is a key signalling

molecule in the hypothalamus in the regulation of energy storage and expenditure and food intake (Obici, 2009). AMPK activity is increased upon fasting in the hypothalamus, which leads to increased food intake and body weight. *Vice versa*, feeding inhibits hypothalamic AMPK activity, leading to a reduction in food intake and loss in body weight (Xue and Kahn, 2006).

1.10.9 AMPK in the regulation of whole-body energy homeostasis

AMPKα1-global-null and *AMPKα2*-global-null mice were created to study the role of the AMPK catalytic subunits isoforms in whole-body physiology (Viollet et al., 2003a). Glucose homeostasis was normal in *AMPKα1*-global-null mice, and no other obvious phenotype was observed in these mice. In contrast, *AMPKα2*-global-null mice displayed abnormal glucose homeostasis. In the fed state the *AMPKα2*-global-null mice were hyperglycaemic and hypoinsulinaemic. A glucose tolerance test showed that the mice were glucose intolerant and glucose-stimulated insulin secretion (GSIS) was impaired (Viollet et al., 2003a). However, isolated islets from the *AMPKα2*-global-null mice did not show any intrinsic beta cell defect in glucose- or arginine-stimulated insulin secretion. Additionally, insulin sensitivity and muscle glycogen synthesis were both reduced, and free fatty acids were elevated in the *AMPKα2*-global-null mice. Urine catecholamine levels in these mice were increased, which suggested that alterations in the autonomic nervous system accounts for the defects in glucose handling, insulin sensitivity and insulin secretion exhibited by these animals (Viollet et al., 2003a,b).

The role of AMPKα2 in hypothalamic AgRP and POMC neurons of the arcuate nucleus was studied by specific deletion of *AMPKα2* in these neurons by cre-loxP system. *AgRPα2KO* mice developed an age-dependent lean phenotype, whereas *POMCα2KO* mice were obese due to decreased energy expenditure and increased food intake. Both the *AgRPα2KO* and *POMCα2KO* neurons were unable to respond to changes in extracellular glucose; lack of AMPKα2 prevented hyperpolarisation in response to reduced glucose concentration. These findings suggest a key role for AMPK in hypothalamic function and glucose sensing (Claret et al., 2007) (Figure 1.6).

1.10.10 AMPK as a drug target

Metformin (N,N-dimethylbiguanide) is a commonly used oral drug that is used in the treatment of T2DM (Cantó et al., 2009; Hinke et al., 2007; Rutter and Leclerc, 2008). It mainly works by inhibiting hepatic gluconeogenesis (Hinke et al., 2007; Viollet et al., 2009). It is thought that many of the beneficial effects of metformin are achieved in part by activation of AMPK in peripheral tissues (Hinke et al., 2007). However, early this year Foretz et al. (2010) reported that metformin inhibits gluconeogenesis independently of LKB1/AMPK pathway. Another oral T2DM drug rosiglitazone (thiazolidinedione) is an insulin sensitiser that improves peripheral glucose uptake and has been thought to act partially via activation of AMPK (Viollet et al., 2009). However, due to increased risk of cardiovascular complications, rosiglitazone has been withdrawn from the clinical use (Agency, 2010). Yet both metformin and rosiglitazone have also been shown to activate AMPK in MIN6 beta cells and human or rat islets respectively (Chang et al., 2009; Viollet et al., 2009). However, whereas activation of AMPK by metformin inhibited glucose-stimulated insulin secretion, rosiglitazone activated AMPK was linked to stimulation of insulin secretion (Leclerc et al., 2004). Therefore, it is unclear whether cellular AMPK activation is actually involved in the treatment of T2DM. In addition, whether activation of AMPK by the current anti-diabetic drugs, or potential new drugs that might activate AMPK, are beneficial for beta cells is still unknown.

1.11 Insulin signaling in pancreatic beta cells

All insulin target tissues contain insulin receptors that initiate insulin receptor signalling cascades inside the cell, which lead to regulation of multiple cellular processes from cell growth and survival to cell metabolism. The insulin receptor signalling pathway has been originally described in traditional insulin target tissues such as liver, muscle and fat. However, insulin also possess an autocrine effect on beta cells and there is clear evidence that insulin and insulin-like growth factor pathways regulate beta cell function. I will now describe insulin receptor signalling and its downstream pathways. I will also talk about how insulin

receptor pathways regulates beta cell function.

1.11.1   Insulin action on insulin secretion

Studies about the role of insulin autocrine effect on beta cells have shown that insulin modulates insulin gene transcription via insulin receptor-A. However, controversies exist whether insulin negatively or positively regulates insulin secretion from beta cells (Khan et al., 2001). It has been shown that insulin activates K_{ATP}-channels in rat hypothalamic neurons, single mouse pancreatic beta cells and islets. This then leads to hyperpolarisation of the plasma membrane, and in case of beta cells, reduces calcium oscillations, thus inhibiting insulin secretion (Khan et al., 2001). In both cases, non-selective phosphoinositide 3-kinase (PI3K) inhibitors wortmannin and LY-294002 prevented insulin induced K_{ATP}-channel activation. Hence, these studies suggested that insulin might have a negative impact on islet physiology and it is possible that insulin achieves this through PI3K-dependent pathway (Khan et al., 2001). In contrast, another study has shown that insulin positively stimulates beta cell insulin secretion by stimulation of calcium release from intracellular ER calcium stores. Increase in intracellular calcium stimulates insulin granule exocytosis. It has been shown previously that IRS-1 is required for insulin stimulated increase in intracellular calcium levels and subsequent insulin exocytosis (Aspinwall et al., 2000). PI3K was shown to have a similar role in promoting calcium release from calcium stores and insulin secretion. Beta cells treated with the PI3K inhibitor wortmannin, failed to increase intracellular calcium levels and insulin exocytosis (Khan et al., 2001). Hence these results suggest that insulin mediates a positive feedback loop to stimulate intracellular calcium release and insulin exocytosis. This effect seems to be dependent on IRS-1 and PI3K. However, production of PIP_3 by PI3K and possible activation of PLC-γ that can stimulate opening of IP3-sensitive calcium store, are not involved (Aspinwall et al., 2000). Therefore, discrepancies about the role of insulin autocrine effect remain to be solved. However, it is clear that insulin signalling in pancreatic beta cells is important for functional cells.

1.11.2   The role of insulin receptor in beta cells

Insulin receptor-global-null mice die within days after birth due to ketoacidosis associated with severe diabetes, thus demonstrating the importance of insulin receptors in the regulation of whole-body glucose homeostasis (Accili et al., 1996; Joshi et al., 1996). In contrast, mice that lack insulin or IGF-1 receptor specifically in pancreatic beta cells (*RIPCreIRKO* and *RIPCreIGF1KO*) are viable, but develop progressive impaired glucose tolerance due to a loss of first-phase insulin secretion in response to glucose (Kulkarni, 2002). These mice demonstrate the importance of IR and IGF-1 receptor signalling in the regulation of beta cell glucose homeostasis and insulin secretion. The results also suggest that insulin resistance within beta cells might lead to the loss of glucose-stimulated insulin secretion from beta cells (Kulkarni et al., 1999). Studies using the *RIPCreIRKO* islet also demonstrated that insulin receptor, not IGF-1 receptor is responsible for high glucose or insulin induced upregulation of endogenous insulin gene transcription (Leibiger and Berggren, 2008). This insulin stimulated insulin gene expression is dependent on PI3K and its downstream target p70S6K (Leibiger et al., 2002). Using a beta cell line, obtained from *RIPCreIRKO* mice, it has been possible to show that glucose is unable to activate PI3K and Akt, and stimulation of mTOR is reduced in insulin receptor lacking beta cells. Furthermore, glucose induced anti-apoptotic property is lost in insulin receptor KO beta cells and glucose and insulin induced *GLUT2* expression is diminished (Assmann et al., 2009).

1.11.3   The role of insulin receptor substrates in beta cells

IRS-1-global-null mice showed growth retardation and are insulin resistant. However, due to increased insulin secretion and expansion of beta cell mass, these mice do not progress to develop diabetes (Araki et al., 1994; Tamemoto et al., 1994). In contrast, *IRS-2*-global-null mice displayed marked glucose intolerance, peripheral insulin resistance and reduced beta cell mass, which eventually led to the development of severe diabetes (Withers et al., 1998). Mice with a deletion of *IRS-2* in pancreatic beta cells show impaired glucose tolerance and reduced beta cell mass Cantley et al. (2007); Choudhury et al. (2005). While *RIPCreIrs2KO* mice also show reduced fasted blood glucose levels and increased fasted insulin levels,

PdxCreIrs2KO mice have normal fasted glucose and insulin levels, but display increased fed glucose levels (Cantley et al., 2007). Interestingly, *RIPCreIrs2KO* mice also had a significant hypothalamic phenotype (increased leptin levels, body weight, food intake) due to a deletion of *IRS-2* in insulin expressing hypothalamic neurons. Hypothalamic phenotype might also explain why the *RIPCreIrs2KO* mice were insulin resistance, as altered CNS function can affect whole-body insulin sensitivity Choudhury et al. (2005). Hence, *PdxCreIrs2KO* mice can be considered to be a better mouse model for the study of IRS-2 function specifically in beta cells as PdxCre only deletes in the pancreas. These mice had normal insulin sensitivity and did not display any hypothalamic phenotype. As mentioned above, these mice were glucose intolerant due to a significant reduction in glucose-stimulated insulin secretion observed *in vivo* and *in vitro*. Loss of *IRS-2* in beta and alpha cells also resulted in reduced beta cell mass, reduced pancreatic insulin content and reduced *insulin* mRNA expression, and beta cell proliferation was reduced over 50 %. *GLUT2* and *FoxO1* mRNA expression was also decreased and *IRS-2* KO beta cells displayed reduced glucose-stimulated increase in calcium uptake. Hence these results suggested that IRS-2 signalling has an essential role in the maintenance of beta cell mass and regulation of glucose-stimulated insulin secretion (Cantley et al., 2007).

1.11.4   The role of PI3K in beta cells

Numerous studies have demonstrated the importance of insulin receptor signalling pathway for functional beta cells. Phosphoinositide 3-kinases (PI3K) are lipid kinases that generate lipid second messengers called phosphatidylinositols (PtdIns), located on the plasma membrane. Upstream and downstream signalling molecules of PI3K have been shown to be important in beta cells, especially for the maintenance of beta cell mass, which involves regulation of cell proliferation, size and apoptosis. Most of the upstream and downstream molecules of PI3K pathway have been subjected to targeted gene deletion, and further studies using siRNA technique in beta cell lines have provided important insight to the function of these proteins. Stimulation of pancreatic beta cells with glucose leads to increased insulin secretion, which subsequently leads to activation of beta cell

insulin receptor signalling pathway, including PI3K (Barker et al., 2002). Glucose stimulates activation of PI3K, Akt and mTOR in beta cells. Glucose, together with insulin also stimulates expression of *GLUT2* in beta cells. All these actions of glucose have been suggested to be dependent on PI3K signalling, as PI3K inhibitor LY-294002, prevented them.

The exact role for PI3K in beta cells is however not well understood. As the *p110α*-global-null and *p110β*-global-null mice were not viable, and single or double heterozygous *p110α*-global-null and *p110β*-global-null mice did not show any obvious phenotype, genetic targeting of PI3K catalytic subunits p110α and p110β have not provided us any clues about the role of these isoforms in beta cells. Because both the upstream and downstream effectors of the PI3K pathway have shown to be important for beta cells, one would expect that the p110α and p110β isoforms also have important role in this regulation.

Using relatively non-selective PI3K inhibitors wortmannin and LY-294002 that do not target specific PI3K catalytic isoforms in inhibiting PI3K in beta cells have suggested that PI3K has a role in stimulating insulin secretion by regulation of intracellular calcium levels and insulin exocytosis. However, as these inhibitors also inhibit other kinases downstream of PI3K such as mTOR, the specificity of the inhibitors towards PI3K in these studies has remained unclear (Al-Qassab et al., 2009). Therefore, studies that have employed the use of PI3K inhibitors should be regarded with caution.

The studies employing inhibitors have shown for example that a novel thiazolidinedione, BLX-1002, potentiated insulin secretion at high glucose concentration, but this effect was blocked by treatment with PI3K inhibitors wortmannin and LY-294002 (Zhang et al., 2009). Another thiazolidinedione, rosiglitazone (RSG), enhanced insulin secretion and stimulated first- and second phase of glucose-stimulated insulin secretion, but again this effect was blocked by LY294002, which prevented stimulation of insulin secretion (Yang et al., 2001a).

Glucagon-like peptide-1 (GLP-1) is an insulinotropic agent that is secreted from the gut cells. It can stimulate beta cell insulin secretion by binding to the GLP-1 receptors on the surface of beta cells. It also inhibits apoptosis by upregulating the expression of anti-apoptotic proteins such as Bcl-2 and Bcl-xL. The anti-apoptotic property of GLP-1 is thought to be achieved via PI3K as treatment

with the PI3K inhibitor LY-294002, prevented GLP-1 protecting MIN6 cells from H_2O_2 induced apoptosis (Hui et al., 2003).

1.11.5   The role of Pdk1 in beta cells

Phosphatidylinositol dependent kinase 1 (Pdk1) is a serine/threonine protein kinase that binds to PIP_3 and phosphorylates Akt, thus mediating signals downstream from insulin receptor and PI3K. Deletion of Pdk1 in mouse pancreatic beta cells leads to a progressive hyperglycaemia and reduced plasma insulin levels and finally to death between the ages of 12-24 weeks due to uncontrollable diabetes (Hashimoto et al., 2006). This is due to reduced beta cell number and size, as well as reduced islet density. FoxO1 haploinsufficiency helped to restore the blood glucose levels to normal by increasing islet density and beta cell number, but not the size, by increasing the proliferation of beta cells (Hashimoto et al., 2006).

1.11.6   The role of Akt in beta cells

Protein kinase B, also known as Akt, is a serine/threonine protein kinase that is a member of the AGC protein family. Three Akt isoforms exist, each encoded by a different gene (Elghazi et al., 2007). Akt2 is the main isoform involved in the regulation of glucose homeostasis (Hirsch et al., 2007). In resting cells, Akt is mainly cytosolic, but upon stimulation and generation of PIP_3, Akt is recruited to the plasma membrane via its interaction with PIP_3 where it becomes activated upon phosphorylation of Thr308 by Pdk1, and on Ser473, probably by TORC2. Activated Akt is then able to translocate to the nucleus where it phosphorylate its various downstream targets (Elghazi et al., 2007; Hirsch et al., 2007).
Akt regulates a wide variety of cellular processes and has a critical role in mediating signals downstream from insulin receptor via PI3K and Pdk1. For example, it inactivates glycogen synthase kinase-3 (GSK3) by phosphorylation, which relieves the inhibition on glycogen synthase (GS) and leads to increased glycogen synthesis (Taniguchi et al., 2006). It stimulates glucose uptake by phosphorylation and inhibition of the Rab-GTPase-activating protein (AS160), which then activates Rab-GTPases that stimulates translocation of GLUT2 to the plasma membrane

(Taniguchi et al., 2006). Akt also stimulates protein synthesis by phosphorylation and inhibition of tuberous sclerosis complex-2 (TSC2), which then leads to activation of mTOR pathway that results in phosphorylation of p70 ribosomal protein S6 kinase (p70 S6K) and eukaryotic translation initiation factor 4E binding protein-1 (4EBP1) (Taniguchi et al., 2006). Akt has also been shown to possess anti-apoptotic properties by modulation of FoxO1 and GSK3β activity, and direct phosphorylation and inhibition of pro-apoptotic enzymes Bad and Caspase 9 (Elghazi and Bernal-Mizrachi, 2009; Molina et al., 2009).

Mice deficient in Akt2 develop glucose intolerance and insulin resistance, and some progress to develop diabetes. Mice overexpressing a kinase-dead Akt in beta cells (*RIP-KdAkt*) have a defective insulin secretion due to defective exocytosis but surprisingly, the islet morphology and beta cell mass were unchanged (Elghazi and Bernal-Mizrachi, 2009). On the other hand, transgenic mice that express a constitutively active Akt in beta cells have increased beta cell mass, cell proliferation and size, and increased neogenesis (Bernal-Mizrachi et al., 2004; Tuttle et al., 2001). One might assume that the kinase-dead Akt mice would have decreased beta cell mass, as expression of constitutively active Akt resulted in increased beta cell mass. The discrepancies could be caused by difference in genetic background in mice. However, overexpression of kinase-dead Akt was detected in 80 % of mouse beta cells (Tuttle et al., 2001). Therefore it is also possible that 20 % of the beta cells with residual Akt expression are able to maintain the beta cell mass within normal limits.

1.11.7 The role of FoxO1 in beta cells

Forkhead trasnscription factor member FoxO regulates transcription of genes involved in cell proliferation, apoptosis, differentiation and metabolism and is negatively regulated by Akt (Accili and Arden, 2004). Akt phosphorylates FoxO, which leads to the translocation of FoxO from the nucleus to the cytoplasm where it is inactivated and labelled for protein degradation (Elghazi and Bernal-Mizrachi, 2009). In murine islets and cultured beta cells, FoxO1 is the main form of FoxOs expressed (Kitamura et al., 2002). FoxO1 haploinsufficiency rescues *IRS-2*-global-null mice from diabetes and restores beta cell area to about 80 % of

normal wt levels by increasing beta cell proliferation via increased Pdx1 expression (Kitamura et al., 2002). Phosphorylation of FoxO1 is regulated by glucose, but is dependent on plasma membrane depolarization, calcium influx and autocrine effect of insulin receptor signalling through PI3K. Glucose starvation of MIN6 insulinoma cells results in FoxO1 dephosphorylation and translocation to the nucleus. Glucose treatment of starved cells leads to rapid phosphorylation and nuclear exclusion of FoxO1 (Martinez et al., 2006).

1.12 Phosphoinositide 3-kinase

Earlier I discussed the importance of insulin signalling pathway in beta cells. In the following section, I will give a more general overview of PI3K as it is a topic of the study described in Chapter 4. Phosphoinositide 3-kinases (PI3K) are lipid kinases that phosphorylate the position D3 hydroxyl on the inositol ring of the phosphatidylinositols (PtdIns) (See Figure 1.7). PtdIns consist of a glycerol that has two fatty acid chains attached at positions one and two, and an inositol 1-phosphate group at position three (Vanhaesebroeck and Alessi, 2000). Phosphorylated PtdIns are lipid second messengers that amplify signals downstream from the cell surface. This leads to triggering of intracellular processes such as regulation of cell proliferation, survival and growth, membrane trafficking, cell migration and metabolism (Hirsch et al., 2007). PI3Ks are divided into three classes (PI3K Class I, II and III) depending on the mechanism they are activated and which PtdIns they phosphorylate. Of the three classes, only class IA and class II are activated by insulin (Creveaux et al., 2010). The class I PI3Ks are the best characterised of the three classes. Therefore, I will only concentrate on the description of the class I PI3K from now on as these are thought to be the most critical mediators of insulin signalling (See Figure 1.8).

1.12.1 Class IA PI3K

Class I PI3Ks are responsible for the formation of PtdIns 3,4,5-trisphosphate ($PI(3,4,5)P_3$) by phosphorylation of PtdIns 3,4-bisphosphate ($PI(3,4)P_2$). They are heterodimers that consist of a catalytic and a regulatory/adaptor subunit.
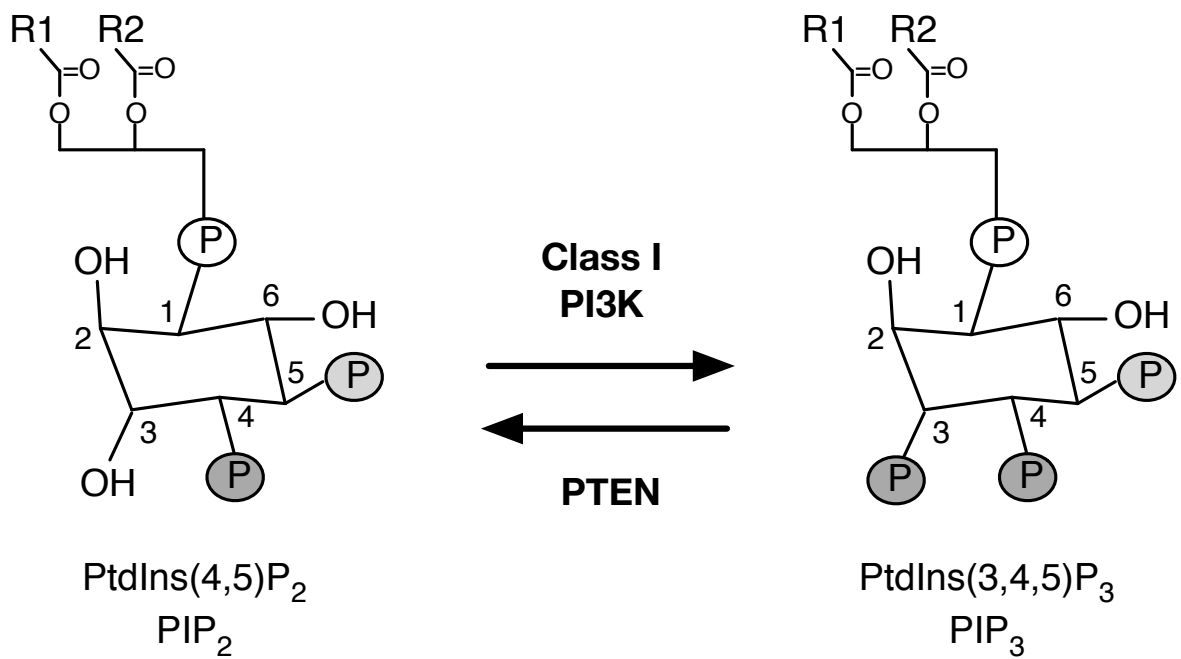
Figure 1.7: Structure of PtdIns(4,5)P_2 and PtdIns(3,4,5)P_3. Class I PI3Ks phosphorylate position 3 hydroxyl on the inositol ring of PIP$_2$ to generate PIP$_3$. Protein phosphatase PTEN can remove the position 3 phosphate from PIP$_3$. Thus PTEN functions as a negative regulator of PI3K by generation of PIP$_2$ from PIP$_3$. Adapted from Hirsch et al. (2007).
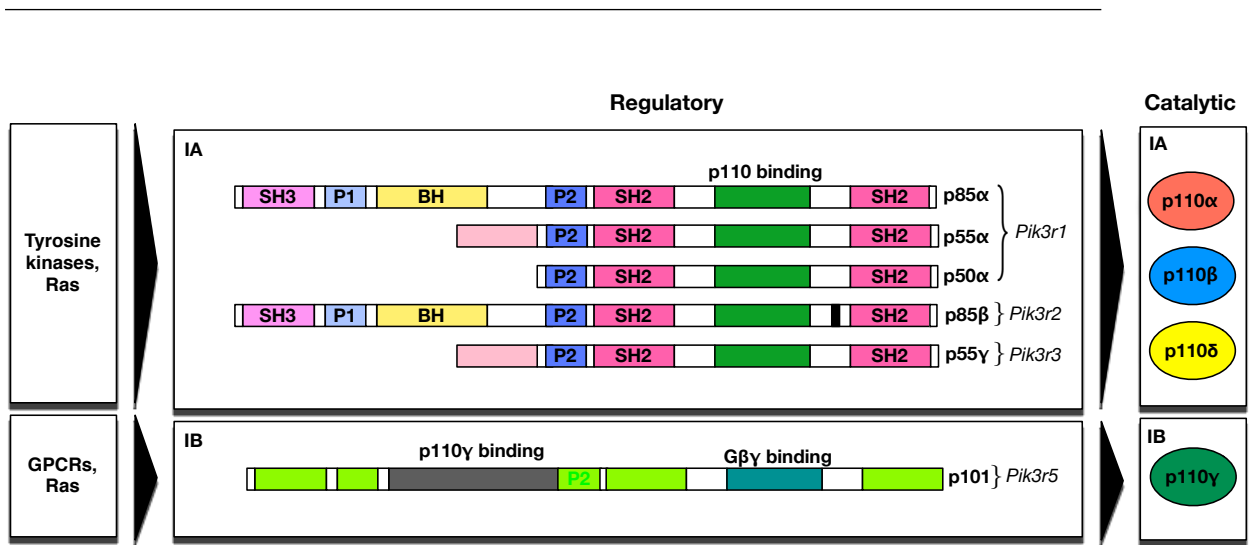
Figure 1.8: Class I PI3K subunit composition. Adapted from Vanhaesebroeck et al. (2005).

Mammals express four class I PI3K catalytic subunit genes: *Pik3ca*, *Pik3cb*, *Pik3cg* and *Pik3cd*, although they are generally termed as PI3Kα, β, γ and δ. *Pik3ca* and *Pik3cb* are ubiquitously expressed whereas *Pik3cg* and *Pik3cd* are mainly expressed in leukocytes (Hirsch et al., 2007; Taniguchi et al., 2006). The catalytic subunits are highly homologous and their molecular mass is approximately 110 kDa, hence they are usually called p110 catalytic subunits. They all contain a C-terminal kinase domain, and a Ras and a p85 binding domains towards the N-terminus (Shepherd et al., 1998). The class I PI3Ks are further divided into two sub-categories: IA and IB. The sub-categories are defined in terms of different adaptor/regulatory subunits that are associated with the catalytic subunits.

The class IA PI3Ks are activated by tyrosine kinase receptors and Ras, and consists of PI3Kα, β and δ (Hirsch et al., 2007). They bind to highly homologous p85 family of regulatory subunits that consists of three genes *Pik3r1*, *Pik3r2* and *Pik3r3*. Due to alternative splicing, *Pik3r1* gene encodes for p85α, p55α and p50α. *Pik3r2* encodes for p85β and *Pik3r3* for p55γ. p85α and p85β are ubiquitously expressed whereas p55α and p50α are expressed in fat, muscle, liver and brain. p55γ is mainly present in the brain (Hirsch et al., 2007). The PI3K adapter/regulatory proteins all consist of two Src-homology-2 (SH2)-domains, a P2-domain and a p110-binding domain. The SH2-domains facilitate the binding

to phosphorylated tyrosine residues in the YXXM motif of the tyrosine receptor, or receptor associated adaptor proteins such as insulin receptor (IR) and insulin receptor substrate (IRS) (Hirsch et al., 2007).

1.12.2   Class IB PI3K

PI3Kγ is the only member of the class IB PI3K family. Whereas the class IA PI3Ks are activated by tyrosine kinase receptors, PI3Kγ is activated when both the catalytic subunit and the adapter subunit p101 bind to the $\beta\gamma$ subunit of heterotrimeric G protein-coupled receptors (GPCR) (Shepherd et al., 1998). The adaptor/regulatory proteins p101 and p84/87 also assist in the activation of PI3Kγ by docking it to the plasma membrane (Hirsch et al., 2007).

1.12.3   PI3K in insulin signalling

Activation of the insulin receptor and subsequent phosphorylation of tyrosine residues of the insulin receptor substrates (IRS) leads to activation of the class IA PI3Ks. The p85 adapter/regulatory proteins of PI3K bind to phospho-tyrosine motifs on IRS proteins via two SH2 domains (Taniguchi et al., 2006). This recruits the p110 catalytic subunits to close proximity to the plasma membrane where activated PI3K phosphorylates $PI(3,4)P_2$, which leads to the formation of a lipid second messenger $PI(3,4,5)P_3$ i.e. PIP_3. Various proteins, such as the serine/threonine kinases of the AGC protein family (Pdk1, PKB/Akt, PKC, p70S6K and SgK) are recruited and docked to the plasma membrane by binding to PIP_3 via plextrin homology (PH) domain, which then leads to their activation (Taniguchi et al., 2006). Thus formation of PIP_3 leads to activation of numerous downstream effectors that participate in the regulation of various metabolic processes such as stimulation of glucose uptake, glycogen and protein synthesis, and inhibition of gluconeogenesis and lipolysis (Hirsch et al., 2007).

PI3K activity is negatively regulated by two protein phosphatases. Phosphatase and tensin homologue (PTEN) and SH2-domain containing tyrosine phosphatase-2 (SHIP2) are protein phosphatases that dephosphorylate PIP_3. PTEN removes phosphates from the 3-position and SHIP2 from the 5-position hydroxyl of the phosphoinositides, thus leading to inactivation of PIP_3 and generation of PIP_2

(Taniguchi et al., 2006).

1.12.4 Transgenic mouse models of PI3K

In order to understand and determine the role of class IA PI3Ks in cellular and whole-animal physiology, various approaches ranging from PI3Ks inhibitors, microinjection of antibodies targeting specific subunits of PI3Ks and transgenic animal models have been used (Foukas and Okkenhaug, 2003). Each of the class I PI3Ks catalytic subunits and regulatory subunits p85α and p85β have been subjected to inactivation by gene targeting in transgenic mouse models (Vanhaesebroeck et al., 2005). Surprisingly, most of the transgenic mouse models of PI3K with a total or tissue specific loss of PI3K subunits have revealed changes in expression levels and activities in non-targeted subunits in addition to the targeted one, hence complicating the conclusion that can be drawn from these studies (Vanhaesebroeck et al., 2005).

It has been shown that p85 adaptor/regulatory subunits are in abundance over p110 catalytic subunits, and that there might be a cellular pool of free p85 subunits available that compete with p85-p110 complexes over the phospho-tyrosine binding sites. Adaptor/regulatory subunits also have an inhibitory role over p110 catalytic subunits which is relieved upon p85 binding to phospho-tyrosines (Geering et al., 2007).

1.12.4.1 Targeting of regulatory subunits

Four class I PI3K knock-out mouse models exist that are targeted against the p85 regulatory subunits. The metabolic phenotypes reported are summarised in Table 1.2. In general, *pan-p85α*-global-null mice (disrupted expression of *Pik3r1* gene products; p85α, p55α and p50α) show perinatal lethality and are hypoglycaemic and hypoinsulinaemic. They also have reduced p110α and p110β expression levels, and elevated p85β expression levels (Vanhaesebroeck et al., 2005). Heterozygous *pan-p85α*-global-null mice are viable and display increased glucose tolerance and increased insulin sensitivity. Mouse embryonic fibroblasts (MEFs) from these mice have increased PIP$_3$ levels upon IGF-1 stimulation (Vanhaesebroeck et al., 2005). The other transgenic knock-out mice with a disruption of one of the reg-

ulatory subunits p85α, p85β or p55α and p50α are also viable (Vanhaesebroeck et al., 2005). In general, these transgenic mice show increased insulin sensitivity, hypoglycaemia, increased glucose transport in adipocytes and skeletal muscle and increased insulin induced PIP$_3$ generation (Affourtit and Brand, 2008; Terauchi et al., 1999). Liver specific p85α KO mice have improved peripheral insulin sensitivity, which is probably due to increased PIP$_3$ levels and increased insulin-stimulated Akt phosphorylation, even though PI3K activity is reduced. Reduced PTEN activity in these mice, probably explains why the PIP$_3$ levels were increased. Hence, p85α functions not only as a regulatory subunit for PI3Ks but also as a regulator of PTEN activity (Vanhaesebroeck et al., 2005).

Table 1.2: Transgenic mouse models of PI3K regulatory subunits. Adapted from Vanhaesebroeck et al. (2005). MEF = mouse embryonic fibroblast, ES cells = embryonic stem cells.

Target subunit		Viability	Metabolic phenotype	Biochemical features of insulin-sensitive cells		References
				PI3K subunit expression	Phosphorylation of Akt/PKB (Ser473) upon stimulus	
pan-p85α (p85α, p55α,p50α)	Homozygous	Perinatal lethality	Hypoinsulinaemia Hypoglycaemia	↑p85β,↓p110α, ↓p110β	MEFs:↓upon insulin and↓upon IGF-1 ES cells:↓upon IGF-1	Fruman et al. Nat. Genet. 2000
pan-p85α (p85α, p55α,p50α)	Heterozygous	Viable	↑Glucose tolerance ↑Insulin sensitivity	↑p85β	Liver and skeletal muscle:↑upon intravenous insulin MEFs:↑upon IGF-1	Frumn et al. Nat. Genet. 2000
p85α-only (still express p55α and p50α)		Viable	↑Insulin sensitivity, Hypoglycaemia	↑p55α,↑p50α in muscle and fat cells	Not reported	Terauchi et al. Nat. Genet. 1999
p55α and p50α (still express p85α)		Viable	↑Insulin sensitivity	↓p85α in muscle	Skeletal muscle:↑upon insulin stimulation	Chen et al. Mol Cell. Biol. 2004
p85β		Viable	↑Insulin sensitivity, Hypoinsulinaemia, Hypoglycaemia	Not reported	Skeletal muscle:↑upon insulin stimulation	Ueki et al. Proc. Natl. Acad. Sci. 2002

1.12.4.2 Targeting of catalytic subunits

p110α-global-null or *p110β*-global-null mice die at embryonic stage E10.5 and E3.5 respectively (Vanhaesebroeck et al., 2005). Interestingly, heterozygous *p110α*-global and/or *p110β*-global knockin (KI) mice were viable (Foukas and Okkenhaug, 2003). Mice heterozygous for a *p110α*-global knockin (KI) mutation (D933A) that disrupts the kinase activity are insulin resistant and glucose intolerant. They are also smaller in size and are hyperleptinaemic and hyperphagic (Foukas et al., 2006). Mice expressing kinase dead *p110β* become insulin resistance and glucose intolerant at 6-months of age which might be linked to changes in Akt phosphorylation (Ciraolo et al., 2008).

p110δ-global-null mice are viable and do not display any metabolic phenotype, but display a complicated immunological phenotype. Similar phenotype is seen in *p110δ* kinase-dead animals (Vanhaesebroeck et al., 2005). Deletion of *p110γ* results in decreased glucose-stimulated insulin secretion but increased pancreatic beta cell mass and increased insulin tolerance (MacDonald et al., 2004). These mice also display altered immunological phenotype.

Inactivation of p110α in mouse endothelial cells leads to embryonic lethality due to defects in the development of vasculature. In contrast, mice with a deficiency of *p110β* or *p110δ* were viable and fertile, and did not display any vascular abnormalities (Graupera et al., 2008).

Conditional knockout of *p110β* in mouse liver caused impaired glucose homeostasis and decreased insulin sensitivity. However, phosphorylation of Akt in response to insulin and epidermal growth factor (EGF) was almost unchanged, but cell proliferation was slowed down, implicating that p110β possesses a kinase-independent role upon insulin stimulus that is involved in cell proliferation (Jia et al., 2008). The metabolic phenotypes reported are summarised in Table 1.3.

Table 1.3: Transgenic mouse models of PI3K catalytic subunits. Adapted from Vanhaesebroeck et al. (2005).

Target subunit	Viability	Metabolic phenotype	References
p110α	KO	Embryonic lethal (E10.5)	Not applicable	Bi et al. J. Biol. Chem. 1999
p110α	Heterozygous	Viable	Normal	Bi et al. J. Biol. Chem. 1999
p110α	Homozygous KI Heterozygous KI	Embryonic lethal Viable	Hyperinsulinaemia, glucose intolerance, insulin resistance hyperphagia, increased adiposity, reduced somatic growth	Foukas et al. Nature. 2006
p110β	KO	Embryonic lethal (E3.5)	Not applicable	Bi et al. Mamm. Genome. 2002
p110β	Heterozygous	Viable	Normal	Bi et al. Mamm. Genome. 2002
p110β	KI	Viable	Age-dependent insulin resitance, hyperglycaemia, hyperinsulinaemia, reduced somatic growth	Ciraolo et al. Sci Signal. 2009
p110δ	KO	Viable	Not reported	Vanhaesebroeck et al. Trend Biochem. Sci. 2005
p110δ	KI	Viable	Not reported	Vanhaesebroeck et al. Trend Biochem. Sci. 2005
p110γ	KO	Viable	↕Glucose-stimulated insulin secretion, ↑pancreatic beta cell mass, ↑insulin tolerance	MacDonald et al. Endocrinol. 2004
p110γ	KI	Viable	Not reported	MacDonald et al. Endocrinol. 2004

1.12.5 Isoform specific differences in insulin receptor signalling in different tissues

Several studies have looked at the isoform specific roles for the class IA PI3K catalytic isoforms in tyrosine kinase receptor signalling and shown that in most tissues, p110α is the dominant PI3K isoform and p110β is the main PI3K isoform in inducing signals downstream of GPCR. It has also been shown that p110α is the main PI3K isoform that is recruited to insulin stimulated IRS-1/2 complexes, and that p110β lipid kinase activity is not present in these complexes (Foukas et al., 2006; Guillermet-Guibert et al., 2008; Hooshmand-Rad et al., 2000). For example, in endothelial cells, p110α is the main PI3K isoform in mediating signals downstream from tyrosine kinase receptors such as vascular endothelial growth factor (VEGF) whereas p110β activity is concentrated on GPCR (Graupera et al., 2008). Inhibition of p110β and p110γ in bone marrow derived macrophages (BMMs) did not prevent tyrosine kinase induced phosphorylation of Akt and Erk. However, the GPCR agonist complement 5a (C5a) stimulated Akt phosphorylation was abolished upon p110β or p110γ inhibition. These results further confirm that p110β and p110γ isoforms are not the main signalling molecules downstream form tyrosine kinase receptors, but are coupled to the GPCR (Guillermet-Guibert et al., 2008).

Studies that have used isoform specific inhibitors of p110α (PIK-75, PIK-90), p110β (TGX-115, TGX-286) and p110γ (IC87114, PIK-23), have also shown that p110α is the predominant PI3K isoform in two insulin responsive cell types, 3T3-L1 adipocytes and L6 myotubes (Knight et al., 2006). Insulin stimulated glucose uptake and phosphorylation of Akt, p70S6K and rpS6 were blocked by p110α inhibitors, but not with p110β or p110γ inhibitors. Insulin stimulated decline in blood glucose levels *in vivo* was also prevented by p110α inhibitors, as assessed by an insulin tolerance test in mice. No effect on blood glucose levels was observed in mice treated with p110β inhibitors (Knight et al., 2006).

On the contrary, we have previously shown in mouse POMC and AgRP neurons that in the arcuate nucleus, p110β isoform has a more dominant role over p110α in the regulation of energy homeostasis. Mice with an inactivation of p110β in POMC neurons were hyperphagic, hyperleptineamic and had increased adi-

posity on normal chow and increased sensitivity to high-fat feeding (Al-Qassab et al., 2009). Electrical activity in response to insulin or leptin was blunted in *POMCp110βKO* neurons. In contrast, *POMCp110αKO* mice had a relatively normal body weight phenotype during chow diet, but did display hyperleptinaemia and increased adiposity on a HFD. However, insulin stimulated hyperpolarisation of POMC neurons was also prevented in p110α deficient neurons (Al-Qassab et al., 2009). Mice with an inactivation of p110β in AgRP neurons developed an age-dependent lean phenotype and were resistant to obesity induced by hight-fat feeding (Al-Qassab et al., 2009). Overall, it seems that in hypothalamic insulin signalling, p110β is the dominant PI3K isoform and in peripheral tissues p110α is responsible for mediating insulin receptor signalling.

1.13 General insulin receptor signalling

1.13.1 Insulin receptor

All insulin target tissues contain insulin receptors that initiate insulin signalling cascades inside the cell, which lead to regulation of multiple cellular processes from cell growth and survival to cell metabolism (See Figure 1.9). There are two types of insulin receptors: insulin receptor type A (IR-A) and insulin receptor type B (IR-B). At high concentrations, insulin also binds to insulin-like growth factor-1 receptor (IGF-1) (Taniguchi et al., 2006). In order to function, insulin receptors form dimers with each others and as each receptor can function as homoreceptors (IR-A, IR-B and IGF-1) and hybrid-receptors (IR-A/IR-B, IR-A/IGF-1, IR-B/IGF-1), the insulin receptors can form six different type of combinations of functional receptor pairs (Leibiger and Berggren, 2008). Insulin receptors are tetrameric proteins that contain two extracellular, insulin binding α-subunits and two intracellular β-subunits that are linked together by disulphide-bonds (DeFronzo, 2004). Insulin binds to insulin and IGF-1 receptors (IR) and stimulates intrinsic tyrosine kinase function that leads to autophosphorylation of tyrosine residues within the receptor (Taniguchi et al., 2006). Receptor associated adapter proteins, such as insulin receptor substrates (IRS), Gab-1 and Shc, bind to phosphorylated tyrosine residues on the receptors, and are subsequently

tyrosine phosphorylated by the receptors (Leibiger and Berggren, 2008). Phosphorylated adapter proteins then facilitate downstream signalling cascade from the receptor, leading to activation of PI3K/AKt and MAPK pathways (DeFronzo, 2004; Morris et al., 2009).

1.13.2 Insulin receptor substrates

There are six insulin receptor substrate (IRS) isoforms, termed IRS-1 to 6 (Taniguchi et al., 2006). IRS-1 and IRS-2 are the most widely expressed, including the insulin target tissues. The N-terminus of IRS proteins contains both plextrin homology (PH) domain and phosphotyrosine-binding (PTB) domain that are needed for the high affinity association with the insulin receptor (Taniguchi et al., 2006). Multiple tyrosine phosphorylation sites are located in the middle and C-terminus of the proteins that are phosphorylated by the receptor, and can be bound by Src-homology-2-domain (SH2) containing proteins such as p85-regulatory protein of phosphoinositide 3-kinase (PI3K) and son-of-sevenless (SOS) associated adaptor protein Grb2 that leads to the activation of PI3K and Ras-MAPK pathways respectively (Taniguchi et al., 2006).

1.13.3 Insulin signalling via MAPK pathway

Mitogen-activated protein kinase (MAPK) signals downstream of insulin receptors. Two receptor associated adaptor proteins Grb2 and Shc bind to tyrosine-phosphorylated IRS-1 and IRS-2 molecules that are associated with insulin activated receptor. This signalling cascade leads to activation of MAPK-pathway, which stimulates gene expression of a range of transcription factors that stimulate cell growth, differentiation and proliferation (DeFronzo, 2004).

1.14 Summary and aims of investigation

1.14.1 Rationale for study: AMPK

Understanding the mechanisms regulating whole-body glucose homeostasis is important in order to understand what happens in a disease state such as T2DM.
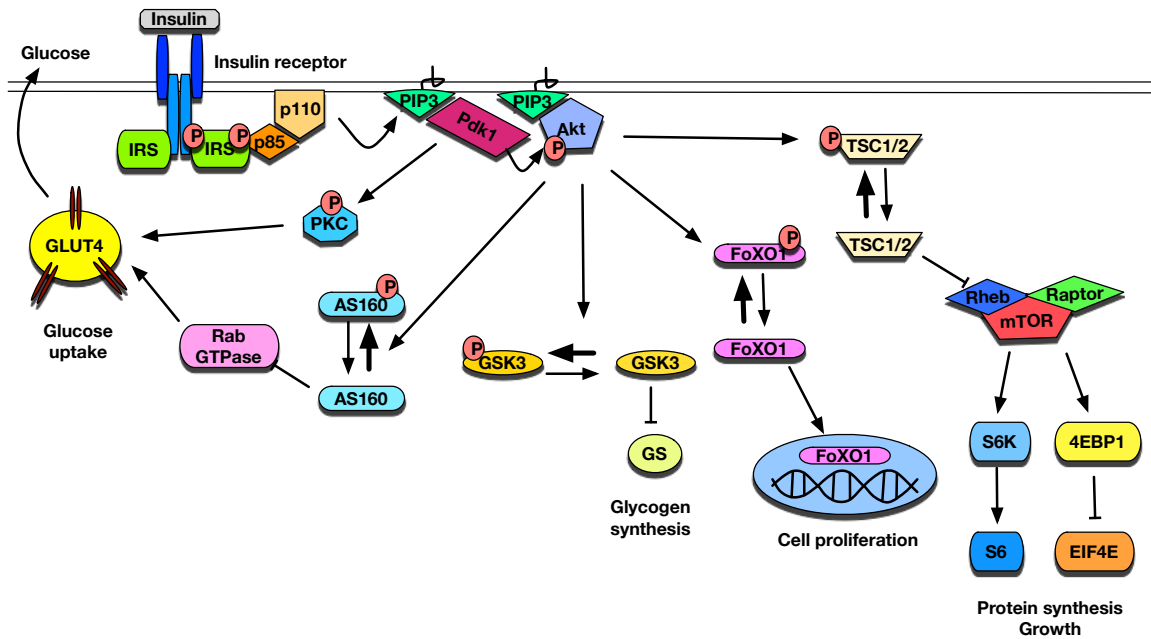
Figure 1.9: Insulin receptor signalling network. Insulin binding to insulin receptor activates the receptor, which leads to recruitment of an insulin receptor substrate (IRS) docking protein to the receptor and phosphorylation of IRS. Phosphorylated IRS recruits regulatory protein p85 subunit and catalytic p110 subunit of PI3K near the plasma membrane and activation of the PI3K pathway. PI3K stimulates production of PtdIns(3,4,5)P$_3$ (PIP$_3$). Serine/threonine kinases of the AGC protein family such as Pdk1, Akt, and PKC are recruited and docked to the plasma membrane by binding to PIP$_3$ via plextrin homology (PH) domain, which then leads to their activation. Activation of Akt by phosphorylation by Pdk1 leads to regulation and activation of multiple cellular processes such as protein and glycogen synthesis, cell proliferation, growth and metabolism. Activation of Akt as well as PKC also leads to stimulation of glucose uptake. Adapted from Hirsch et al. (2007) and Taniguchi et al. (2006).

Pancreatic beta cells play a central part in the regulation of glucose homeostasis. It is eventually the beta cell dysfunction and subsequent failure that leads to the development of type 2 diabetes. Tight control of beta cell metabolic coupling and production of ATP, as well as insulin receptor signalling pathway are all essential for functional beta cells and regulation of glucose-stimulated insulin secretion. AMPK functions as a cellular energy regulator and its activity is linked to changes in cellular ATP/AMP ratio. Therefore, it seems obvious that it could have a key role in the regulation of beta cell function and insulin secretion. The role of AMPK in pancreatic beta cells has been of great interest for several years. However, despite the numerous studies conducted over the years, no clear conclusion has been made yet, and discrepancies between studies exists, especially about the role of AMPK in the regulation of insulin secretion. Anti-diabetic drugs metformin and rosiglitazone are thought to activate AMPK in peripheral tissues that leads to a reduction in blood glucose levels. Whether activation of AMPK in beta cells by these or new drugs is beneficial is still unclear. Because AMPK is a known drug target for the treatment of T2DM, it is important to understand the cellular function of AMPK in beta cells and how this translates to the regulation of whole-body glucose homeostasis. This could also aid in the development of a new generation of drugs that are more specific and with less side-effects. Even though the *AMPKα2*-global-null mice had impaired glucose homeostasis and reduced *in vivo* GSIS, surprisingly no intrinsic beta cell defect was found and defective GSIS was argued to be caused by increased catecholamine levels. No other transgenic mouse model exists that would have studied the *in vivo* role of AMPK in beta cells. Thus it would be of great benefit to conduct an extensive study about the role of AMPK in the beta cell by means of a transgenic approach.

1.14.2 Hypothesis and experimental plan

Bases on previous studies, I propose the following hypothesis: AMPK in pancreatic beta cells is central for the maintenance of normal whole-body glucose homeostasis by regulation of insulin secretion from the beta cells. To determine the specific role of AMPK in beta cell function, transgenic mice will be generated, employing the cre-loxP system. Firstly, to study the role of AMPKα2 in

beta cells, *RIPCreα2KO* mice are created, in which floxed *AMPKα2* catalytic subunit (*Prkaa2*) is deleted by recombination with Cre-recombinase, expressed from rat insulin promoter (RIP). Expression of cre from rat insulin promoter occurs only in pancreatic beta cells and in a population of hypothalamic neurons. To combine the deletion of *AMPKα2* with a deletion of *AMPKα1* (*Prkaa1*) in beta cells, *RIPCreα2KO* mice are crossed with *AMPKα1*-global-null mice to create *α1KORIPCreα2KO* mice.

1.14.3 Rationale for study: PI3K

Class I PI3Ks have been shown to have a central role in insulin receptor signalling. All viable transgenic mouse models of class IA PI3K regulatory or catalytic subunits have highlighted an important role for PI3K in the regulation of glucose homeostasis. Recent studies have implicated differential roles for class IA catalytic subunit isoforms p110α and p110β. In peripheral tissues, p110α has been shown to be the dominant isoform in insulin receptor signalling (Foukas et al., 2006). On the other hand, we have shown previously that p110β has a more important role in regulation of whole-body energy homeostasis in POMC and AgRP neurons and insulin- and leptin receptor signalling (Al-Qassab et al., 2009). All viable transgenic mouse models of class IA PI3K regulatory or catalytic subunits have highlighted an important role for PI3K in the regulation of glucose homeostasis. However, no previous studies exist that have directly studied the catalytic subunits of class IA PI3K isoforms specifically in pancreatic beta cells. Current studies have involved using relatively non-selective inhibitors such as wortmannin and LY-294002. Results from these studies have provided indications that inhibition of PI3K in beta cells results in alterations in glucose-stimulated insulin secretion, K$_{ATP}$-channel activity and intracellular calcium signalling (Aspinwall et al., 2000; Khan et al., 2001). However, the results have been controversial and inconclusive. Beta cell specific roles of upstream and downstream molecules of the PI3K pathway, such as insulin receptor, IRS, Pdk1 and Akt have provided invaluable information about the role of the insulin receptor signalling pathway in the regulation of beta cell function. In general, these studies have shown that loss of these molecules leads to a diabetes-like phenotype at the whole-animal

level, which usually results in reduced beta cell mass, change in islet morphology or alteration in glucose sensing and stimulation of glucose uptake and metabolism (Bernal-Mizrachi et al., 2004; Cantley et al., 2007; Hashimoto et al., 2006; Tuttle et al., 2001). However, the role of PI3K catalytic isoforms in beta cells remains unknown. In the light of the previous studies, it would be likely to expect a significant role for the PI3K in the regulation of glucose homeostasis and insulin secretion.

1.14.4   Hypothesis and experimental plan

Bases on previous studies, I propose the following hypothesis: PI3K in pancreatic beta cells and insulin expressing hypothalamic neurons is essential for the maintenance of normal whole-body energy- and glucose homeostasis. To determine the specific role of PI3K in beta cells and RIPCre expressing neurons, transgenic mice will be generated by the cre-loxP system. *RIPCrep110αβKO* mice are created, in which floxed *p110α* and floxed *p110β* catalytic subunits are both deleted by recombination with cre-recombinase, expressed from rat insulin promoter (RIP). Expression from rat insulin promoter occurs only in pancreatic beta cells and in a population of hypothalamic neurons.

Chapter 2

Materials and Methods

2.1 Animals

All animal procedures were approved by the British Home Office Animals Scientific Procedures Act 1986 (Project License no. 0971) and UCL Animal Users Ethics Committee. Animals were maintained at 20-23°C with 12 hour light-dark cycle, with *ad libitum* access to standard mouse chow (RM1 diet SDS UK Ltd) and water. Mice had free access to water during all the studies. Animals were tail tipped for genotyping purpose at 15 days of age using ethyl chloride as local anaesthesia. At 21 days of age mice were weaned and housed with the same sex with a maximum of 8 mice per cage.

2.1.1 *RIPCre* mice

The *RIPCre* mice, which express cre-recombinase driven by the Rat Insulin 2 promoter (Postic et al., 1999) were obtained from the Jackson laboratory (http://www.jax.org/).
RIPCre specific expression occurs in pancreatic beta cells and in RIPCre expressing population of hypothalamic neurons.

2.1.2 *AMPKα2flox* mice

AMPKα2flox were obtained from Dr. Benoit Viollet (Institut Cochin, Université René Descartes, Paris) and were generated using conditional gene targetting of *Prkaa2* gene (Jørgensen et al., 2004). These mice were maintained on a mixed 129Sv x C57BL/6 genetic background.

2.1.3 *AMPKα1*-global-null mice

AMPKα1-global-null mice (*Prkaa1*) were obtained from Dr. Benoit Viollet (Institut Cochin, Université René Descartes, Paris) and were generated using conditional gene targetting (Jørgensen et al., 2004). These mice were maintained on a mixed 129Sv x C57BL/6 genetic background.

2.1.4 Generation of *RIPCreα2KO* and *α1KORIPCreα2KO* mice

RIPCreAMPKα2KO mice were generated, named as *RIPCreα2KO*, to study the role of AMPKα2 specifically in pancreatic beta cells, and also in RIP expressing neurons. Briefly, RIPCre transgenic mice were crossed with the *AMPKα2flox* mice to generate heterozygous *RIPCreα2flox* mice. The heterozygous mice (Cre^+ $flox^{+/-}$) were intercrossed to generate *RIPCreα2KO* (Cre^+ $flox^{+/+}$) and relevant control mice of all genotypic combinations. The same breeding cycle was performed to obtain *α1KORIPCreAMPKα2KO* mice, named as *α1KORIPCreα2KO*, by starting with homozygous mice for *RIPCreα2flox* crossed with *AMPKα1*-global-null mice. Hence, two transgenic AMPK KO mouse lines were generated: *RIPCreα2KO*, lacking *AMPKα2* in RIPCre expressing cells (beta cells and a population of hypothalamic neurons) and *α1KORIPCreα2KO*, lacking AMPKα1 globally and AMPKα2 in RIP Cre expressing cells.

The official gene names for *AMPKα1* and *AMPKα2* are *Prkaa1* and *Prkaa2* respectively. However, *AMPKα1* and *AMPKα2* are commonly used instead of the official gene names. Therefore, I will be using *AMPKα1* and *AMPKα2* through out in this thesis.

2.1.5 *P110αflox* mice

P110αflox mice were generated in the laboratory of Professor Vanhaesebroeck (Institute of Cancer, Queen Mary, University of London) using conditional gene targeting of the *Pik3ca* gene (Graupera et al., 2008). Cre-mediated recombination of floxed *p110α* results in a kinase-dead p110α protein without changing the stoichiometry of PI3Kp110α and p85 signalling complexes (Al-Qassab et al., 2009). The mice were maintained on a mixed 129Sv x C57BL/6 genetic background.

2.1.6 *P110βflox* mice

P110βflox mice were generated in the laboratory of Professor Vanhaesebroeck (Institute of Cancer, Queen Mary, University of London) using conditional gene targeting of the *Pik3cb* gene (Guillermet-Guibert et al., 2008). Cre-mediated recombination of floxed *p110β* results in a kinase-dead p110β protein without changing the stoichiometry of PI3Kp110β and p85 signalling complexes (Al-Qassab et al., 2009). The mice were maintained on a mixed 129Sv x C57BL/6 genetic background.

2.1.7 Generation of *RIPCrep110αβKO* mice

RIPCrep110αβKO mice were generated to study the role of PI3K signalling specifically in pancreatic beta cells and RIP expressing neurons. Briefly, mice homozygous for *p110αflox* and mice homozygous for *p110βflox* were crossed together to generate mice heterozygous for *loxP* sites at both alleles. These *p110αflox$^{+/-}$ p110βflox$^{+/-}$* mice were crossed with *RIPCre* transgenic mice. The resulting *RIPCrep110αflox$^{+/-}$ p110βflox$^{+/-}$* offspring were subsequently mated with *p110αflox$^{+/-}$ p110βflox$^{+/-}$* mice to generate *RIPCrep110αβKO* mice and relevant control mice of all genotypic combinations.

The official gene names for *p110α* and *p110β* are *Pik3ca* and *Pik3cb* respectively. However, *p110α* and *p110β* are commonly used instead of the official gene names. Therefore, I will be using *p110α* and *p110β* through out in this thesis.

2.2 Genotyping of mice

2.2.1 DNA extraction

Animals were tail tipped for genotyping purpose at 15 days of age using ethyl chloride as local anaesthesia, and DNA extracted from these tail tips. Each tail tip was put in a 1.5 ml eppendorf tube and boiled in 600 μl of 0.1 mol/L NaOH for 10 minutes and allowed to cool down for 10 minutes at room temperature. 100 μl of 1 mol/L Tris (pH 6.8) was then added to each tail sample.

2.2.2 Determination of genotype using PCR

For the determination of mouse genotype 1-3 μl of DNA extract, depending on the gene of interest, was used per polymerase chain reaction (PCR) in a 96-well plate. Two types of PCR master mix was used, depending on PCR cycle: 1X Reddy Mix (Thermo Scientific # AB-00575/LD/B) and 2X Goldstar Red Master Mix (Eurogentec # PK-0064-02R). All primers are oligo primers from Eurogentec. PCR products were resolved with 2-3 % agarose gel electrophoresis in TAE buffer (See Appendix A - Solutions), and visualised by UV excited fluorescence of ethidium bromide stained DNA (1 in 50,000 dilution).

2.2.3 *RIPCre* genotyping

RIPCre genotyping was performed to determine whether the mice were expressing Cre by using a set of four primers. One pair was used to amplify a promoter specific 550 bp sequence (Cre present): RIPCre Forward (RIP3) 5′ CTC TGG CCA TCT GCT GAT CC 3′ and RIPCre Reverse (Cre 102) 5′ CGC CGC ATA ACC AGT GAA AC 3′. The second pair was used to amplify the interleukin-2 (*IL2*) gene 100 bp sequence, as an internal control: IL2 Forward 5′ CTA GGC CAC AGA ATT GAA AGA TCT 3′ and IL2 Reverse 5′ GTA GGT GGA AAT TCT AGC ATC ATC C 3′. See Figure 2.1 for *RIPCre* PCR cycle and reaction.
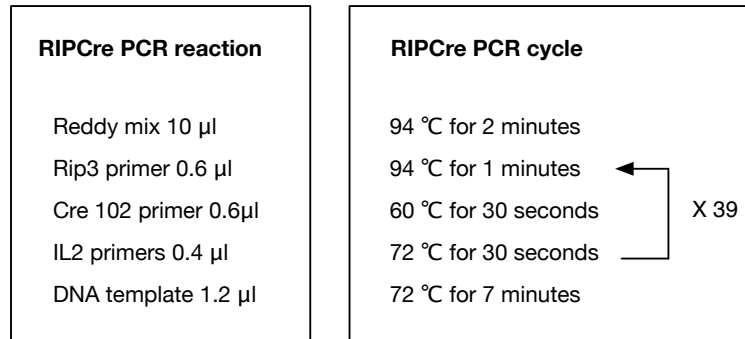
Figure 2.1: *RIPCre* PCR reaction

2.2.4 *AMPKα2flox* genotyping

AMPKα2 genotyping was performed to determine whether the mice were wild type, heterozygous or homozygous for the targeted allele. Genotyping was performed using the following two primers α2flox-F 5′ GCT TAG CAC GTT ACC CTG GAT GG 3′ and α2flox-R 5′ GTT ATC AGC CCA ACT AAT TAC AC 3′. A 250 bp homozygous band is amplified if the locus is targeted with loxP sites and a 200 bp wild type band if untargeted. If a mouse is a heterozygous for the floxed *AMPKα2* both a 250 bp and a 200 bp bands are detected. See Figure 2.2 for *AMPKα2* PCR cycle and reaction.
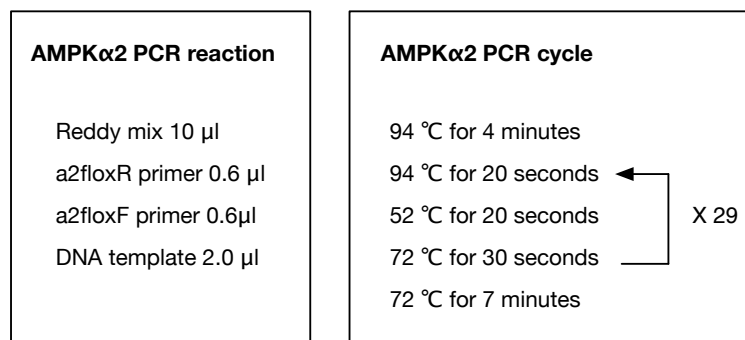
Figure 2.2: *AMPKα2* PCR reaction

2.2.5 *AMPKα1* genotyping

Two individual PCR reactions were required to determine if mice were wild type, heterozygous or homozygous for global deletion of *AMPKα1*.

To detect the presence of a wild type *AMPKα1* allele, the following primers were used: AMPKα1wtF 5′ A GCC GAC TTT GGT AAG GAT 3′ and AMPKα1wtR 5′ CC CAC TTT CCA TTT TCT CCA 3′. The generation of a 500bp indicated the presence of a wild type allele.

To detect the deletion of an *AMPKα1* allele, the following primers were used: AMPKα1IRESFa 5′ GGG CTG CAG GAA TTC GAT ACA AGC 3′ and AMPKα13.0Ra 5′ CC TTC CTG AAA TGA CTT CTG TGC 3′. The amplification of a 300bp indicated deletion of *AMPKα1* allele. If a mouse is a heterozygous for the *AMPKα1* both a 300 bp and a 500 bp bands are detected. See Figure 2.3 for *AMPKα1* PCR cycle and reaction.

AMPKα1 wt PCR reaction

Gold mix (2X) 12.5 µl

ddH₂O 7.5 µl

MgCl₂ (25 mmol/l) 1.5 µl

AMPKa1wtF primers 0.75 µl

AMPKa1wtR primers 0.75 µl

DNA template 2.5 µl

AMPKα1 wt PCR cycle

94 ℃ for 4 minutes

94 ℃ for 30 seconds

58 ℃ for 40 seconds   X 30

72 ℃ for 90 seconds

72 ℃ for 7 minute

AMPKα1 null PCR reaction

Gold mix (2X) 12.5 µl

ddH₂O 7.5 µl

MgCl₂ (25 mmol/l) 1.5 µl

AMPKa1ResFa primers 0.75 µl

AMPKa13.0Ra primers 0.75 µl

DNA template 2.5 µl

AMPKα1 null PCR cycle

94 ℃ for 4 minutes

94 ℃ for 30 seconds

58 ℃ for 40 seconds   X 30

72 ℃ for 90 seconds

72 ℃ for 7 minute

Figure 2.3: *AMPKα1* PCR reaction

2.2.6 *P110αflox* genotyping

P110αflox genotyping was performed to determine whether the mice were wild type, heterozygous or homozygous for the targeted allele. Genotyping was performed using the following two primers: FE1 5′ GGA TGC GGT CTT TAT TGT C 3′ and FE5 5′ GCA TGC TGC CGA ATT 3′. This resulted in a 718 bp product for the wild-type allele and/or a 782 bp product for the *p110αflox* allele. See Figure 2.4 for *P110αflox* PCR cycle and reaction.

P110αflox PCR reaction	P110αflox PCR cycle
Gold mix (2X) 12.5 µl	94 ℃ for 3 minutes
ddH$_2$O 7.5 µl	94 ℃ for 30 seconds
MgCl$_2$ (25 mmol/l) 1.5 µl	59 ℃ for 30 seconds X 30
FE1 primers 0.75 µl	72 ℃ for 1 minute
FE1 primers 0.75 µl	72 ℃ for 1 minute
DNA template 2.5 µl	
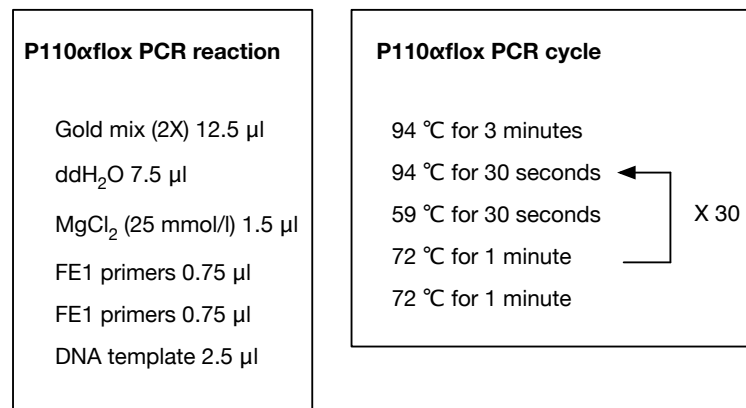
Figure 2.4: *P110αflox* PCR reaction

2.2.7 *P110βflox* genotyping

P110βflox genotyping was performed to determine whether the mice were wild type, heterozygous or homozygous for the targeted allele. Genotyping was performed using the following two primers: B3 5′ AGT GAA CGC TAT GCA TCA CAC CAG C 3′ and B98 5′ AAG TAC AAA CAT CCA AGC AA 3′. This resulted in a 304 bp product for the wild-type allele and/or a 372 bp product for the *p110βflox* allele. See Figure 2.5 for *P110βflox* PCR cycle and reaction.
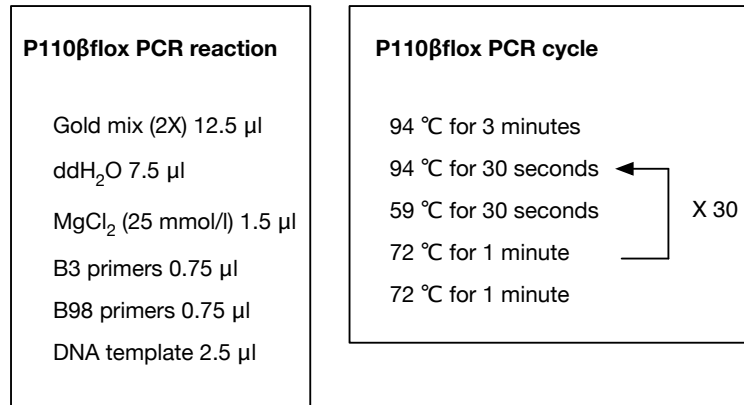
Figure 2.5: *P110βflox* PCR reaction

2.3 Analysis of tissue specific gene deletion by PCR

To confirm the tissue specificity of the cre recombinase and to ensure that the recombination of floxed alleles occurs in the correct tissues, a tissue specific gene deletion by PCR was performed. Briefly, DNA was extracted from islets, hypothalamus, cortex, liver, muscle and fat and PCR performed using a set of primers that amplify a region of DNA when two loxP sites are joined together after a recombination event catalysed by Cre recombinase.

2.3.1 DNA extraction of tissues

A snap frozen tissue weighing approximately 100 mg was homogenized with a motorised probe in a 2 ml sterilin tube with 500 μl of tissue extraction buffer (See Appendix A - Solutions). The homogenate was removed to a 1.5 ml eppendorf tube and 700 μl of chloroform:isoamylalcohol (24:1) added. The sample was allowed to mix for 2 hours at 4 °C by shaking, after which it was centrifuged at 10,000 RPM for 10 minutes at 4 °C. The upper aqueous layer was removed to a new 1.5 ml eppendorf tube and 700 μl of isopropanol added and the sample mixed by gently inverting the tube. DNA was pelleted by centrifugation at 10,000 RPM

for 10 minutes at 4 °C. The pellet was washed with 300 μl of 70 % ethanol, air dried and resuspended in 50 μl of nuclease-free H$_2$O overnight at 4 °C.

Islet DNA extraction was performed by re-suspending a snap frozen islet pellet in 150 μl of 0.1 mol/L NaOH and boiling the sample for 10 min at 100 °C. The sample was then cooled down for 10 minutes at room temperature and 25 μl of 1 mol/L Tris (pH 6.8) added.

2.3.2 Detection of *AMPKα2* deletion

AMPKα2 deletion was identified using the following primers: AMPKfloxF1 5′ GCT TAG CAC GTT ACC CTG GAT GG 3′ and AMPKneoR 5′ GCA TTG AAC CAC AGT CCT TCC TC 3′. The amplification of a 974 bp band indicated that recombination had occurred between the loxP sites, resulting in tissue specific inactivation of *AMPKα2*. See Figure 2.6 for *AMPKα2* deletion PCR cycle and reaction.

<table>
<tr>
<td>

**AMPKα2 deletion
PCR reaction**

Reddy mix 10 µl

a2delR primer 0.75 µl

a2delF primer 0.75µl

IL2 primers 0.25µl

DNA template 2.0 µl

</td>
<td>

**AMPKα2 deletion
PCR cycle**

94 ℃ for 4 minutes

94 ℃ for 30 seconds ◄

56 ℃ for 40 seconds   X 40

72 ℃ for 50 seconds

72 ℃ for 7 minutes

</td>
</tr>
</table>
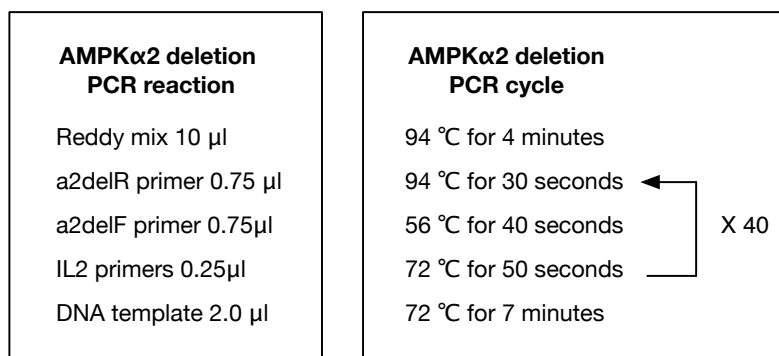
Figure 2.6: *AMPKα2* deletion PCR reaction

2.4 *In vivo* physiological studies

2.4.1 Determination of body weights

Mice body weights were measured with Sartorius BP60 balance during early light phase between 9 am and 11 am.

2.4.2 Determination of body length

Post-mortem body lengths (naso-anal) were measured in cm with a standard ruler.

2.4.3 Determination of body composition

Dual-energy X-ray absorptiometry (DEXA) scanning was used to determine the body composition of mice studied. Mice were culled using a CO_2 chamber and their body composition determined using a PIXImus DEXA scanner (Lunar, GE Healthcare, USA), designed for scanning small rodents. A mouse is placed on a luminescent panel and exposed to high and low energy X-rays and radiation hitting the luminescent panel is measured with a CCD (charged coupled device) camera. Bone mineral density (g/cm^2), bone mineral content (g), lean tissue mass (g), fat tissue mass (g) and body fat (%) are then determined depending on the ability of different tissue types to absorb and reflect X-rays.

2.4.4 Feeding studies

2.4.5 Analysis of food intake

Mice were singly caged and allowed to acclimatise for a week before starting the food intake experiment. A pre-weighed amount of standard chow (≈ 100 g) was given to each mouse and *ad libitum* feeding allowed. Food intake and body weights were measured daily during early light phase (9 am-11 am) for a duration of seven days using a Sartorius BP60 balance.

2.4.6 Response to fasting

Singly caged mice were fasted overnight for 16-hrs with free access to water. Next morning a pre-weighed amount of chow (≈100 g) was given to each mouse during early light phase (≈ 9 am). Food was then measured 1 hr, 2 hrs, 4 hrs, 8 hrs and 24 hrs after re-feeding using a Sartorius BP60 balance.

2.4.7 Response to peripheral MT-II treatment

Mice were singly caged for two weeks before starting the study. They were sham injected with 100 μl of saline each morning at 9 am for a week before the study. Food was removed from the cages and mice were fasted overnight for 16-hr the night before starting the study. Next morning mice were given an i.p. injection of either 100 μl of vehicle (saline) or 100 μl of MT-II (Bachem, # H-3902) (0.5 μg/μl in PBS) and then a pre-weighed amount of food was given to each mouse. Food was then measured 1 hr, 2 hr, 4 hr, 8 hr and 24 hr post-injection using a Sartorius BP60 balance. After a week of recovery the study was repeated in a cross-over fashion i.e. the mice that were given MT-II injection on the first week were now given vehicle injection and *vice versa*.

2.4.8 Response to peripheral leptin treatment

Mice were singly caged before starting the study. They were sham injected daily with 100 μl of saline at around 6 pm for three days before the start of the study. To check that mice were not stressed and were eating normally, daily food intake and body weight were measured at the same time with sham injections. Leptin (recombinant mouse leptin 5mg, R&D Systems, # 498-OB) was reconstituted in HCL/NaOH (See Appendix A - Solutions) as 1.85 mg/ml. Leptin concentration used for i.p. injection was 5 μg/g ($\approx$100 μl volume). Vehicle (saline) was injected in 100 μl volume (i.p.).

The study was carried out as follows. Animals were weighed and controls and KOs were randomly divided into two treatment groups (vehicle and leptin). Mice were injected with leptin or vehicle at 6 pm (late light phase) and a pre-weighed amount of food ($\approx$ 50 g) was added to each cage. The following day, food and body weight were measured at 9 am, and the mice were injected with leptin or vehicle (as before) at 6 pm. The following day, food and body weight were again measured at 9 am, and mice received their final injection of leptin or vehicle (as before) at 6 pm. On the final day, food and body weight were measured at 9 am.

This study was done using a cross-over design, meaning that both control and KO groups were divided into two groups: one group to receive leptin and one to receive vehicle (saline) injections. Animals were allowed to recover for a week

after finishing the study, after which treatment groups were changed over.

2.5   *In vivo* metabolic studies

For experiments requiring execution under fasted conditions (GTT, fasting blood-/insulin/leptin levels, GSIS) mice were fasted for 24 hrs (*RIPCreα2KO* and *α1KORIPCreα2KO*) or over night for a duration of 16 hours (*RIPCrep110αβKO*).

2.5.1   Determination of fasting blood glucose levels

Mice were fasted and blood glucose levels were measured with a Glucometer Elite (Bayer) via tail bleed.

2.5.2   Determination of fasting serum insulin levels

Mice were fasted and blood samples were collected via tail bleed using capillary blood collection tubes (Sarstedt Microvette 300). Blood samples were kept on ice and then centrifuged for 20 min at 2,000 RPM. Serum supernatant was removed to a fresh 0.5 ml eppendorf tube and stored at -80 °C. Serum insulin levels were measure with a Rat/Mouse Insulin ELISA kit (Millipore, # EZRMI-13K).

2.5.3   Determination of fasting serum leptin levels

Mice were fasted and blood samples were collected via tail bleed using capillary blood collection tubes (Sarstedt Microvette 300). Blood samples were kept on ice and then centrifuged for 20 min at 2,000 RPM. Serum supernatant was removed to a fresh 0.5 ml eppendorf tubes and stored at -80 °C. Serum leptin levels were measure with a Rat/Mouse Leptin ELISA kit (Millipore, # EZML-82K).

2.5.4   Glucose tolerance test (GTT)

Mice were fasted and fasting blood glucose levels measured as described above. Mice were then injected intraperitoneally (i.p.) with 2g/kg of 20 % D-glucose and blood glucose levels measured at 15, 30, 60, 90 and 120 minutes after injection.

2.5.5 Insulin tolerance test (ITT)

Mice were studied in the middle of the light phase with free access to food and water prior start of the study. During the study, food was not available but free access to water was provided. Blood glucose levels were measured as described earlier prior to injection with insulin. Mice were then i.p. injected with 0.75 mU of insulin/kg. Blood glucose levels were measured at 15, 30, 60, 90 and 120 minutes after injection.

2.5.6 *In vivo* glucose-stimulated insulin secretion (GSIS)

Mice were fasted and fasting blood glucose levels measured and blood samples were collected using capillary blood collection tubes (Sarstedt Microvette 300) prior to injection with glucose. Mice were injected i.p. with 2g/kg of 20 % D-glucose and blood glucose levels measured and blood samples collected at 3, 15 and 30 minutes or 3, 7 and 20 minutes after injection. Blood samples were kept on ice and after finishing the study, samples were centrifuged for 20 min at 2,000 RPM. Serum supernatants were removed to fresh 0.5 ml eppendorf tubes and stored at -80 °C. Serum insulin levels were measure with a Rat/Mouse Insulin ELISA kit (Millipore, # EZRMI-13K).

2.5.7 Determination of basal metabolic rate (BMR)

Basal metabolic rate was measured in male mice at 22 °C during light phase by indirect calorimetry using an OXYMAX system (Columbus Instruments Inc.) as previously described (Al-Qassab et al., 2009). The average of the lowest 3 consecutive measurements (heat as kcal/hr) were used as an estimate for BMR.

2.6 Islet isolation and primary culture

2.6.1 Islet isolation

Mice were killed by cervical dislocation and a laparotomy was performed. The bile duct and hepatic portal vein were clamped adjacent to liver. A 25 G needle

was inserted into the bile duct immediately before the junction of duodenum/-bile duct. The pancreas was perfused with 2 ml of ice-cold pancreatic digestion solution (See Appendix A - Solutions) and immediately dissected out and placed in a 15 ml falcon tube containing 2.5 ml of ice-cold pancreatic digestion solution. The pancreas was then incubated at 37 °C water bath for 11 minutes. After incubation the sample was placed on ice and 20 ml of ice-cold quenching buffer (See Appendix A - Solutions) was added and the tube was shaken vigorously to dissociate exocrine tissue from the islets. The digest was poured through a mesh well into a 50 ml falcon tube. The tissue digest was centrifuged at 1,000 RPM for 1 minute at 4 °C. The supernatant was discarded and the pellet was resuspended in 20 ml of quenching buffer. The centrifugation step was repeated two more times but after the last spin the pellet was resuspended in 15 ml of Ficoll-Paque PLUS (GE Healthcare #17-1440-02) and the sample vortexed. Another 15 ml of Ficoll was added carefully along the side of the tube. 10 ml of ice-cold quenching buffer was carefully added along the side of the tube and the sample centrifuged at 2510 RPM for 22 minutes at 10 °C. After the centrifugation step islets were floating between the Ficoll and quenching buffer layers. Using a 25 ml serological pipette the supernatant along with the islets was collected and passed though a 70 μm cell strainer (BD Falcon #734-0003) that was place upside down on top of a conical flask. Islets stayed on top of the cell strainer and they were washed 3 times with 20 ml of quenching buffer. After washing, the cell strainer was put on a petri dish, islet side facing the bottom of the dish and washed on to dish with 15 ml of quenching buffer. The islets were then picked to a fresh petri dish from where they were collected for tissue culture or frozen down for other assays.

2.6.2 Islet picking

If islets were to be used for DNA/RNA or protein extraction, quenching buffer with 0.5 % BSA was used. Islets were picked keeping the islets cold at all times, washed once in BSA free KRB (1X), pelleted and snap frozen and stored at -80 °C.

If islets were to be used for primary culture, quenching buffer with 10 % NCS (new-born calf serum) was used. Islets were picked on to a petri dish and

incubated in overnight culture medium (See Appendix A - Solutions) at 37 °C with 21 % O_2, 5 % CO_2 and high humidity for 24 to 48 hours before study.

2.7 *In vitro* glucose-stimulated insulin secretion (static incubation)

Islets were isolated and cultured for 24 to 48 hours in overnight culture medium as described above.

Islets were picked to a fresh petri dish and incubated in quenching buffer (See Appendix A - Solutions) supplemented with 0.5 % BSA (2 mmol/l D-glucose) at 37 °C for 1 hour before the start of the experiment. Batches of 5 size-matched islets were picked in a volume of 5 μl and plated into a v-shaped bottom 96-well plate. From each mouse different islet batches were used for incubation in either 2 mmol/L glucose or 20 mmol/L glucose. Six replicates of 5 islet batches were used per given glucose concentration. Once all the islets were picked for each condition, 125 μl of secretion buffer (with appropriate glucose concentration) was added with a multichannel pipette. Islets were incubated for 1 hour at 37 °C with 21 % O_2, 5 % CO_2. After the incubation the plate was swirled gently and centrifuged at 1,000 RPM for 1 minutes to ensure that the islet were all settled down at the bottom of the wells. 100 μl of secretate was removed with a multichannel pipette to a fresh 96-well plate and the samples immediately frozen at -80 °C. The insulin concentration in each sample was measured with Rat/Mouse Insulin ELISA kit (Millipore, # EZRMI-13K). The samples from 2 mmol/L glucose conditions were diluted 1/2 with assay buffer (from the Elisa kit) and the samples from 20 mmol/L glucose condition were diluted 1/10.

2.8 Pancreatic immunocytochemistry and morphometric analysis

2.8.1 Preparation of pancreata and Bouin's fixation

Mice were killed by cervical dislocation and laparotomy performed. The pancreas were quickly dissected out, rinsed in phosphate buffered saline (PBS) solution, blotted dry with tissue and weighed with a fine balance. The pancreas were spread on to histology cassettes and fixed in Bouin's fixative (See Appendix A - Solutions) for 3 hours at room temperature. After 3 hours the samples were rinsed in 70 % ethanol and then left in 70 % ethanol for overnight (16 hours).

2.8.2 Tissue processing for paraffin embedding

Tissues were processed as described below. Steps 1 to 6 were performed at room temperature and 7-8 at 60 °C. After processing the tissues were embedded in paraffin and cooled on ice.

1. 90 % ethanol, 1 hour

2. 95 % ethanol, 1 hour

3. 100 % ethanol, 1 hour

4. 100 % ethanol, 2 hours

5. Histoclear I, 1 hour

6. Histoclear II, 2 hours

7. Paraffin wax I, overnight

8. Paraffin wax II, 2 hours

2.8.3 Immunostaining for fluorescent detection

Paraffin embedded tissues were sliced with a microtome to obtain 5 μm sections. The sections were float mounted on to a poly-lysine coated cover slides and dried at 37 °C overnight. De-paraffinisation of the sections was performed as described below.

- Histoclear I, 5 minutes

- Histoclear II, 1 minute

- 100 % ethanol, 30 seconds

- 90 % ethanol, 30 seconds

- 70 % ethanol, 30 seconds

- ddH$_2$O, 5 minutes

- PBS, 5 minutes

- PBS + 0.05 % Tween20, 5 minutes

- PBS + 1 % Triton X-100, 5 minutes

- PBS + 0.05 % Tween20, 3 X 5 minutes

Following deparaffinisation, sections were incubated at room temperature for 30 min with blocking solution (See Appendix A - Solutions). Blocking solution was removed and the sections were placed in a hydration chamber and incubated overnight at 4 °C in blocking solution containing primary antibody (See Table 2.1 for a complete list of primary and secondary antibodies used). Next day the sections were washed three times for 5 min with PBS + 0.05 % Tween20. The sections were incubated at room temperature in darkness for 1 hour with PBS + 2 % BSA + secondary antibody, and then washed three times for 5 min with PBS + 0.05 % Tween20. Lastly, the sections were mounted with DAPI mounting media.

2.9 Pancreatic morphometry

Images for measurement of pancreatic beta cell area were captured using an Olympus fluorescent microscope and either a 10X or 20 X objective lens. Fluorescent filter channels DAPI, FITC (for Alexa fluor 488 nm) and TRITC (for Alexa fluor 594 nm) were used. Images of whole pancreas sections with a calibration slide were captured with a Sony Cyber-shot DSC-W30 digital camera, which was mounted to a dissection microscope (Nikon SMZ645). Simple PCI software (C Imaging) was used to measure beta cell area (stained with insulin) and exocrine area (whole pancreas section) from each pancreas section (4 sections per mouse). Relative beta cell volume was calculated by dividing the total beta cell area of each section with the corresponding exocrine area. The average of the four sections was then calculated. Beta cell mass (mg) was calculated by multiplying the average relative beta cell volume by pancreas weight.

2.9.1 Immunofluorescence imaging

A Zeiss LSM700 inverted confocal microscope with 20X air objective or 40X oil objective was used to capture fluorescent images of immunostained pancreas sections. Alexa fluor 594 nm conjugated secondary antibody (against insulin) was excited at 594 nm and light emitted above 617 nm was collected. Alexa fluor 488

nm conjugated secondary antibody (against glucagon) was excited at 488 nm and light emitted between 500 and 540 nm was collected. The DAPI nuclear stain was excited at 405 nm and light emitted between 420 and 480 nm was collected.

Table 2.1: Table of primary and secondary antibodies used for immunofluorescence imaging.

Primary antibody	Anti Insulin	Anti Glucagon	DAPI
Animal source	Mouse monoclonal	Rabbit polyclonal	n/a
Supplier	Sigma I-2018	Abcam Ab9379	Vector laboratories
Concentration	1:1000	1:200	Neat solution
Secondary	**Anti-mouse IgG**	**Anti-rabbit IgG**	n/a
Animal source	Chicken	Chicken	n/a
Supplier	Molecular Probes (# A-21201)	Molecular Probes (# A-21441)	
Concentration	1:400	1:400	n/a
Fluorescent conjugate	Alexa fluor 594 nm	Alexa fluor 488 nm	n/a

2.10 Western blotting

2.10.1 Tissue lysis

Islets were isolated and snap frozen as a pellet as described earlier. Islet pellet was resuspended in 40 μl of RIPA lysis buffer (Sigma, # R0278) (See Appendix A - Solutions). Islets were lysed by vortexing and carefully passing the islet suspension through an insulin syringe 15 times avoiding air bubbles. The lysate was left on ice for one hour, centrifuged at 12,000 RPM for 5 minutes and the protein concentration measured by Bradford assay (Bio-Rad 1998).

2.10.2 Immunoblotting

35 μg of islet protein was resuspended in 2 x Laemmli buffer (See Appendix A - Solutions) (Laemmli, 1970), boiled for ten minutes, cooled on ice and pulse spun. 75 μl of protein suspension was loaded onto a 12 % SDS-polyacrylamide gel (See Appendix A - Solutions) and run at 120 volts for one and half hours at room temperature with a Tris-glycine-SDS running buffer (See Appendix A - Solutions). Proteins were transferred to 0.2 μm nitrocellulose membrane (Invitrogen # LC2000) using a Tris-glycine transfer buffer (See Appendix A - Solutions).

The membrane was blocked for 30 minutes shaking at room temperature with blocking solution and then incubated overnight at 4 °C in blocking solution (See Appendix A - Solutions) with primary antibody. After this incubation with the primary antibody, the membrane was washed 3 times for 5 minutes with washing buffer and then incubated with a horseradish peroxidase (HRP) conjugated secondary antibody at room temperature for 1 hour. After the incubation, the membrane was washed 5 times for 10 minutes with washing buffer and the secondary antibody was detected using an ECL plus detection system (Amersham).

When a membrane was used for detection of multiple proteins it was stripped of antibodies by incubating the membrane for 15 min at 37 °C shaking using stripping buffer (Thermo Scientific #21059). The membrane was then washed once with 1X TBST and then blocked for 30 min with blocking solution (See Table 2.2 for a complete list of primary and secondary antibodies used).

Table 2.2: Table of primary and secondary antibodies used for Western blotting.

Primary antibody	AMPKα2	ATP5b synthase	Beta actin
Animal source	sheep	rabbit	rabbit
Supplier	David Carling	Abcam	Cell Signaling (#4967)
Concentration	1:2000	1:5000	1:1000
Secondary	Anti-sheep	Anti-rabbit	Anti-rabbit
Animal source	Rabbit	Goat	Goat
Supplier	Dako (# P0163)	Thermo Scientific (#31463)	Thermo Scientific (#31463)
Concentration	1:10 000	1:4000	1 4000

2.11 Gene expression studies

2.11.1 Reverse transcription

RNA was extracted as described below depending on the tissue source (islet or hypothalamus). Once extracted, mRNA was quantified using a NanoDrop (ThermoScientific) and reverse transcribed using the TaqMan Retrotranscription Kit (Applied Biosystems # N808-0234) in order to generate complementary DNA (cDNA) templates for RT-PCR quantification. Briefly, each sample contained 2.5 μl of RT Buffer (10X), 5.5 μl of MgCl2, 5 μl of dNTPs, 1.25 μl of oligo-DT, 0.5 μl of RNAse inhibitor and 0.5 μl of reverse transcriptase with 1 μg of RNA used as a template. Each reaction was set-up in 0.2 ml reaction tubes (BioRad) and the total volume in each tube made up to 25 μl with nuclease free water. Samples were incubated at 37 °C for 60 minutes, and the reverse transcriptase subsequently inactivated by heating the samples to 95 °C for 5 minutes. The resulting cDNA was then stored at -20 °C until PCR analysis.

2.11.2 Quantitative PCR cycling conditions

A pool of cDNA was prepared from control samples and a standard curve (arbitary) prepared from the pool of cDNA by serial dilution (usually six points, the first being undiluted). A separate standard curve was prepared for each probe (gene of interest) used. cDNA from each sample was diluted 1/2 with nuclease free water. A separate mastermix for each probe was prepared (See Table 2.3 for the TaqMan probes used).

Each sample was run in duplicate, in 10 μl volume, using TaqMan Gene Expression Master Mix (Applied Biosystems # 4369016) on a MicroAmp Optical 384-well reactive plate (Applied Biosystems # 4309849). An ABI Prism 7900 HT thermocycler (Applied Biosystems) sequence detection system with integrated 488 nm argon laser with SDS2.1 software was used (See Figure 2.7 for the qPCR programme).

2.11.3 Islet gene expression analysis

Islets were isolated as described above. RNA was extracted immediately after the islet isolation using an RNeasy Micro Kit (Qiagen # 74004). 0.5-1 μg of islet RNA was reverse transcribed into cDNA as described above. Quantitative PCR was performed as described above using fluorescent FAM/TAMRA probes from Applied Biosciences. *Glyceraldehyde-3-phosphate dehydrogenase* (GAPDH) was used as an internal control and mRNA levels were normalised to *GAPDH* levels.

2.11.4 Hypothalamic gene expression analysis

Hypothalami were dissected and immediately frozen in flat-bottomed 5 ml sterilin tubes in liquid nitrogen. RNA was extracted by homogenising each hypothalamus on ice in a 5 ml sterilin tube with 0.5 ml of cold phenol-guanidine isothiocyanate solution according to the manufacturers instructions (TRIzol Reagent, Invitrogen #15596-018). The precipitated RNA was dissolved in 40 μl of nuclease-free water. 1 μg of hypothalamic RNA was reverse transcribed into cDNA as described above. Quantitative PCR was performed as described above using fluorescent FAM/TAMRA probes from Applied Biosciences. *Hypoxanthine-guanine phosphoribosyltransferase* (HPRT) (Mm99999915_g1) was used as an internal control and mRNA levels were normalised to *HPRT* levels.
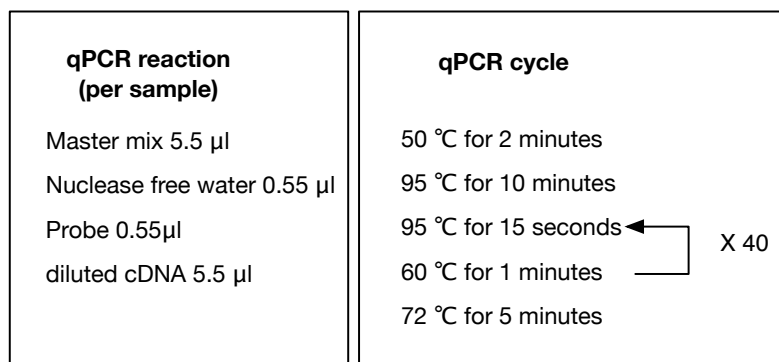
Figure 2.7: qPCR reaction and cycle

A Ct-value for each sample was obtained from the SDS2.1 software. A standard curve was plotted for each gene: arbitary cDNA concentrations were plotted

on a logarithmic scale against the Ct-values. The unknown sample values (average Ct-value) were extrapolated from the standard curve and anti-log calculated. Relative expression (arbitary concentration) to the housekeeping gene was calculated for each sample for the gene of interest. Relative mRNA expression in KO samples was calculated as a % of control expression.

Table 2.3: Table of TaqMan probes.

Gene name/symbol	Gene symbol	Primer product name
Agouti-related protein	AgRP	Mm00475829_g1
AMP-activated protein kinase, alpha 1 catalytic subunit	AMPKα1	Mm01296695_m1
AMP-activated protein kinase, alpha 2 catalytic subunit	AMPKα2	Mm01264786_g1
Forkhead box O1	Foxo1	Mm00490672_m1
Glucokinase	GK	Mm00439129_m1
Glutathione peroxidase 4	GPX4	Mm00515041_m1
Glyceraldehyde-3-phosphate dehydrogenase	GAPDH	Mm99999915_g1
Heme oxygenase (decycling) 1	HMOX1	Mm00516004_m1
Hexokinase 1	HK1	Mm01145241_m1
Hexokinase 2	HK2	Mm00443395_m1
Hexokinase 3	HK3	Mm01341937_m1
Hypoxanthine guanine phosphoribosyl transferase	HPRT	Mm00446968_m1
Insulin II	Ins2	Mm00731595_gH
Insulin receptor substrate 1	IRS-1	Mm01278327_m1
Neuropeptide Y	NPY	Mm00445771_m1
Nuclear respiratory factor 1	Nrf1	Mm00447996_m1
Peroxisome proliferator-activated receptor, gamma, coactivator 1 alpha	PGC-1α	Mm00731216_s1
Phosphatase and tensin homolog	PTEN	Mm00477210_m1
Phosphatidylinositol 3-kinase catalytic subunit p110α	p110α	Mm00435669_m1
Phosphatidylinositol 3-kinase catalytic subunit p110β	p110β	Mm00659576_m1
Phosphatidylinositol 3-kinase regulatory subunit p85	p85	Mm01282780_m1
Pro-opiomelanocortin	POMC	Mm00435874_m1
Protein kinase B	Akt	Mm01331624_m1
Pyruvate dehydrogenase kinase, isoenzyme 1	PDK1	Mm00554306_m1
Solute carrier family 2 (facilitated glucose transporter) member 2 (GLUT2)	Slc2a2	Mm11446224_m1
Sulfonylurea receptor 1	SUR1	Mm00803450_m1
Superoxide dismutase 2, mitochondrial	SOD2	Mm00449726_m1
Transcription factor A, mitochondrial	Tfam	Mm00447485_m1
Uncoupling protein 2	UCP2	Mm00627598_m1

2.12 Measurement of islet reactive oxygen species (ROS) generation

Islets were isolated as described earlier and incubated overnight in overnight culture media at 37 °C. Next day, islets were picked into a 2 ml petri dish and incubated for 1 hr at 37 °C in 1X KRB with 2 mmol/L D-glucose and 0.5 % BSA. After 1 hr islets were picked again to a new 2 ml petri dish and incubated for 30 min in 1X KRB with either 2 mmol/L or 20 mmol/L D-glucose and 1 μmol/L CM-H$_2$DCFDA (5-(and 6)-chloromethyl-2,7-dicholorodihydrofluorescein diacetate, acetyl ester) (Molecular Probes, UK # 6827). After incubation, media was removed and replaced with 1X KRB with either 2 mmol/L or 20 mmol/L

81

D-glucose and islets incubated for 15 min at 37 °C. After 15 min islets were placed on ice and H_2O_2 derived CM-H_2DCFDA fluorescence was measured with Olympus fluorescent microscope with Simple PCI software (C Imaging) and 10X objective lens.

2.13 Statistical analysis of data

Data are presented as mean values with standard error of the mean (SEM) unless otherwise indicated. n = indicates sample size and is represented as control vs KO in figure text. Unpaired two-tailed Student's t-tests were used on all statistical analysis except analysis of glucose- and insulin tolerance test and *in vivo* GSIS that were analysed with 2-way ANOVA with Bonferroni post-test. P values <0.05 (*), <0.01 (**) and <0.001 (***) were recorded as significant. Raw data were collected in Microsoft Excel and calculations of mean and SEM values, statistical analysis and graphical representation were done using GraphPad Prism 5 (GraphPad software).

Chapter 3

Physiological characterisation of *RIPCreα2KO* and *α1KORIPCreα2KO* mice

3.1 Introduction

[1]AMPK has been shown to be important in the regulation of glucose homeostasis, but as described in Chapter 1, controversies remain about its role in beta cell function. Understanding the role of AMPK in beta cells is important as a commonly used oral T2DM drug metformin is thought to achieve its blood sugar lowering effect via activation of AMPK in peripheral tissues. Activation of AMPK in liver and skeletal muscle improves glucose uptake and metabolism and inhibits hepatic gluconeogenesis (Fryer et al., 2002). However, it is unclear whether metformin possess a beneficial effect for beta cells in terms of AMPK activation, specifically because the role of AMPK in beta cells has yet to be fully determined.

AMPKα2-global-null and *AMPKα1*-global-null mice did not show that AMPK deficiency caused any intrinsic beta cell defect, even though the *AMPKα2*-global-null mice demonstrated impaired glucose homeostasis. At the time when this re-

---

[1]This chapter, and the following Chapter 4, were published in Biochemical Journal (Beall et al., 2010) where the author of this PhD thesis (KP) and C. Beall share the first authorship. See Appendix C - Publications.

search project was started, no other studies existed that would have employed transgenic mouse models in the assessment of the role of AMPK specifically in the beta cells.

In order to fully understand the role of AMPK in beta cell function, the following transgenic mouse models were generated: *RIPCreα2KO* and *α1KORIPCreα2KO*. *RIPCreα2KO* mouse lacks functional AMPKα2 specifically in the pancreatic beta cells and in a population of hypothalamic RIPCre expressing neurons. Because there was a concern about potential upregulation of *AMPKα1* we combined the deletion of *AMPKα2* in beta cells with a global deletion of *AMPKα1*, which previously has not been shown to have an effect on whole-body glucose homeostasis, hence creating *α1KORIPCreα2KO* mouse, which does not have any functional AMPK catalytic subunits expressed in the beta cells. I hypothesise that deletion of AMPK in beta cells will affect the whole-body glucose homeostasis and glucose-stimulated insulin secretion in the *RIPCreα2KO* and *α1KORIPCreα2KO* transgenic mice.

The results in this chapter confirm the specificity and efficacy of *AMPKα2* deletion in order to establish the suitability of *RIPCreα2KO* and *α1KORIPCreα2KO* mouse models for studying the role of AMPK in beta cells. Secondly hypothalamic function, whole-body glucose homeostasis and glucose-stimulated insulin secretion are examined in both mouse models.

3.2   Analysis of deletion

The following experiments were performed in order to confirm the specificity and efficacy of RIPCre-mediated deletion of *AMPKα2* in pancreatic beta cells and RIPCre expressing neurons of the hypothalamus.

3.2.1   Specificity of *AMPKα2* deletion

RIPCre has been reported to delete genes in the pancreatic beta cells and also in a small population of hypothalamic neurons (Choudhury et al., 2005). To test for the specificity of *AMPKα2* gene deletion, recombination of floxed alleles was assessed (Figure 3.1). DNA was isolated from islets, hypothalamus, and insulin

target tissues of *RIPCreα2KO* and control mice and amplified with PCR. Islets and hypothalamus from *RIPCreα2KO* mice showed a 750 bp band indicating a recombination of two loxP sites flanking a part of the *AMPKα2* catalytic subunit gene, thus indicating the deletion of *AMPKα2* catalytic subunit. No recombination could be detected in other tissue of *RIPCreα2KO* or control mice.
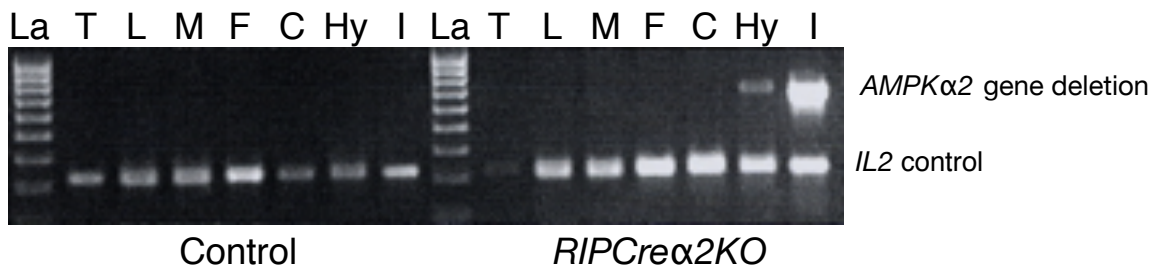
Figure 3.1: Tissue specific deletion of *AMPKα2* using RIPCre. DNA was extracted from different tissues (T, tail; L, liver; M, skeletal muscle; F, fat; C, cerebral cortex; H, hypothalamus; I, islet of Langerhans) and recombination of the floxed *AMPKα2* allele detected by PCR. The presence of the 750 bp band indicates a deletion of *AMPKα2*. Recombination was only detected in the islets of Langerhans and hypothalamus of *RIPCreα2KO* mice. A PCR reaction with *IL2* as internal control shows the presence of DNA template in all the samples. La, denotes DNA ladder.

3.2.2   Efficacy of *AMPKα2* deletion

To determine whether deletion of *AMPKα2* resulted in the anticipated reduction in mRNA level, real time quantitative PCR (qRT-PCR) was performed (Figure 3.2). RNA isolated from islets and hypothalamus of *RIPCreα2KO* and control mice was reverse transcribed to cDNA, which was then amplified with RT-PCR.

A 50 % reduction in islet, and a 20 % reduction in hypothalamic *AMPKα2* mRNA expression was detected in *RIPCreα2KO* mice in comparison to controls. In mice, beta cells only represent ≈70 % of the cell types present in islets, therefore the islets also consist of other cell types, such as alpha cells, in which

the deletion of *AMPKα2* does not occur. Therefore a 50 % reduction in the total islet *AMPKα2* mRNA levels is consistent with the deletion event driven by the RIPCre-recombinase. As with the islets, only a small population of neurons within the hypothalamus are RIPCre expressing neurons, therefore only a 20 % reduction (not significant, P = 0.1705) in total hypothalamic *AMPKα2* mRNA was detected.
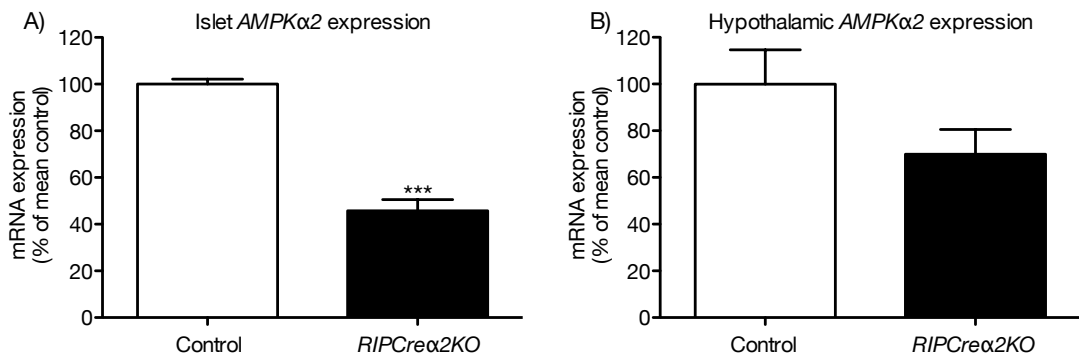
Figure 3.2: Efficiency of deletion of *AMPKα2* in islets (A) and hypothalamus (B). Quantitative RT-PCR was performed to analyse the expression of *AMPKα2* mRNA extracted from islets and hypothalamus of *RIPCreα2KO* and control mice (n = 6). Data shown is mean ± SEM, ***P<0.001.

To confirm that deletion of *AMPKα2* results in reduced AMPKα2 protein levels, Western blotting against AMPKα2 was performed (Figure 3.3). Western blot for AMPKα2 from *RIPCreα2KO* and control islets showed a clear reduction in AMPKα2 protein levels confirming a loss of AMPKα2 protein expression in *RIPCreα2KO* islets.

In summary it can be concluded that recombination of floxed *AMPKα2* catalytic subunit occurs only in pancreatic beta cells and in a population of hypothalamic neurons when cre-recombinase is expressed from the rat insulin promoter. A significant reduction ($\approx$ 50 %) in *AMPKα2* mRNA levels, as well as a clear reduction in AMPKα2 protein levels is detected in *RIPCreα2KO* islets.
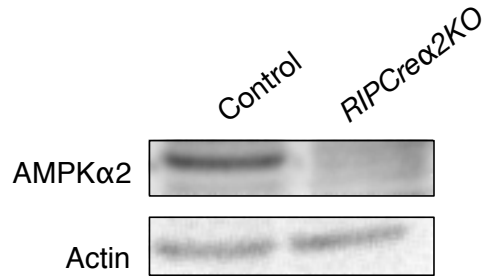
Figure 3.3: Analysis of AMPKα2 protein levels in *RIPCreα2KO* and control islets. Islet lysates were run on SDS-PAGE and western blotted against a sheep anti-AMPKα2 antibody.

3.3 Metabolic studies in *RIPCreα2KO* mice

As described before, the RIPCre transgene deletes in a small population of hypothalamic neurons. Therefore to exclude for the fact that the *RIPCreα2KO* mice do not have a hypothalamic phenotype due to a deletion of *AMPKα2* in RIPCre neurons, body weight and food intake were measured. *RIPCreα2KO* mice exhibited normal body weight in comparison to control littermates at young and old age (Figure 3.4). 24-hr food intake analysis showed that *RIPCreα2KO* mice have a normal feeding behaviour (Figure 3.5). Normal body weight and food intake suggest that the deletion of *AMPKα2* in RIPCre neurons does not affect the hypothalamic function in *RIPCreα2KO* mice, which could otherwise have an effect on whole-body glucose homeostasis.

In conclusion, the data indicates that deletion of *AMPKα2* in beta cells and in RIPCre expressing hypothalamic neurons does not lead to a major central nervous system phenotype such as altered feeding behaviour and body weight (Heinrichs, 2001).

3.4 Glucose homeostasis in *RIPCreα2KO* mice

Blood glucose concentrations of fasted, random fed and post-glucose injected *RIPCreα2KO* and control mice were measured to investigate glucose handling in these animals. Insulin sensitivity of peripheral tissues was investigated in order to
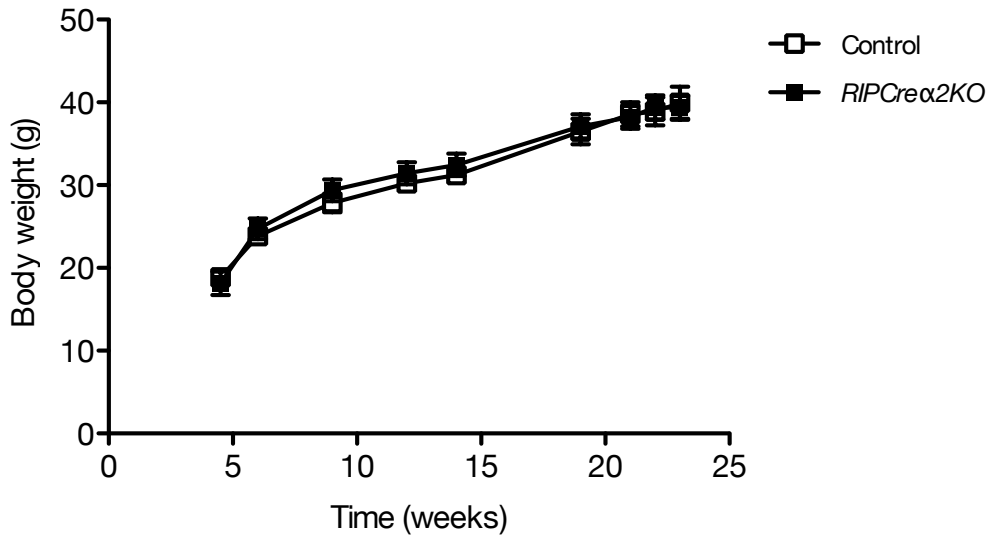
Figure 3.4: Body weight curve for male *RIPCreα2KO* and control mice. Data shown are mean ± SEM (n = 5 vs 8).
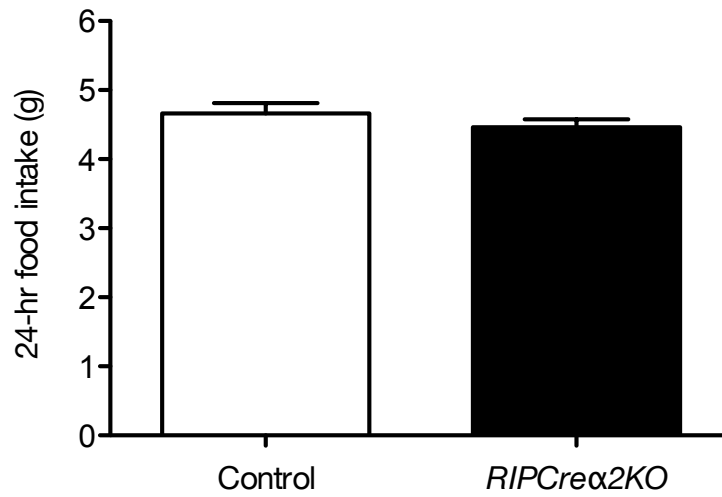
Figure 3.5: 24-hr food intake in *RIPCreα2KO* and control mice. 8-months old male mice were used (n = 7 vs 9). Data shown are mean ± SEM.

determine whether *RIPCreα2KO* mice were to suffer from insulin resistance, and fasted and fed plasma insulin levels measured to see whether the *RIPCreα2KO* beta cells were hypo/hyper-secreting insulin. *In vivo* glucose-stimulated insulin secretion was performed to assess insulin secretory function of pancreatic beta cells.

3.4.1   Fasting/fed blood glucose

Fasted and fed blood glucose levels in male *RIPCreα2KO* mice were normal in comparison to control mice at 12- and 20-weeks of age on a chow diet (Figure 3.6).

Figure 3.6: Fasted and fed blood glucose levels in *RIPCreα2KO* and control mice. (A) Blood glucose levels after a 24-hr fast in 12-week old (n = 13 vs 14), and (B) random fed blood glucose levels in 20-week old male mice (n = 9 vs 7). Bloods were collected from tail bleeds. Data shown are mean $\pm$ SEM.

3.4.2   Glucose tolerance

Glucose tolerance testing was performed on male *RIPCreα2KO* mice and their littermate controls (Figure 3.7). At 14-weeks of age *RIPCreα2KO* mice display mild glucose intolerance, especially from 30 minutes post-injection onwards.
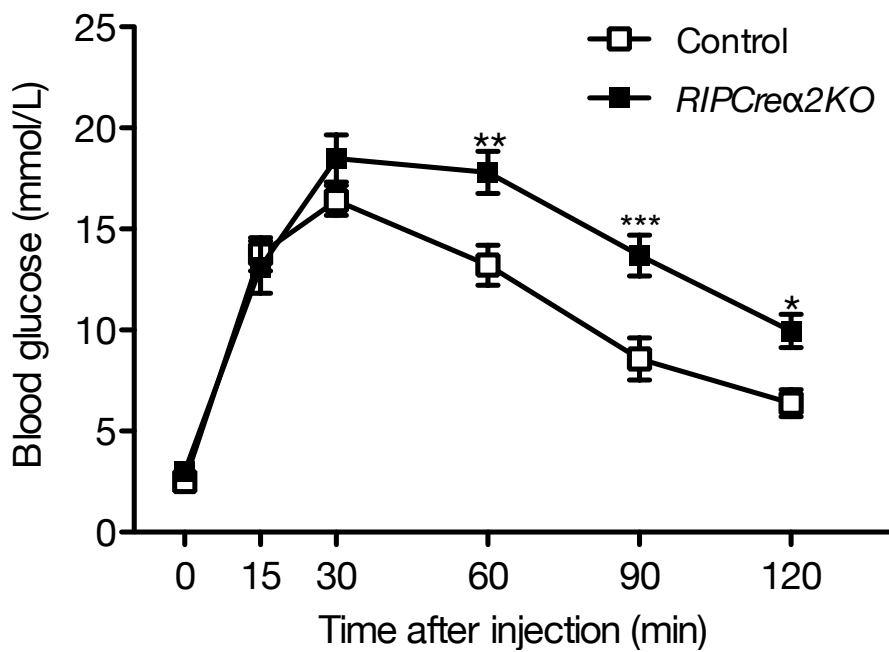
Figure 3.7: Glucose tolerance in *RIPCreα2KO* and control mice. Blood glucose concentrations were measured from tail bleeds at indicated times after an i.p. injection of 20 % D-glucose (2 g/kg). 14-week old male mice (n= 8 vs 8) were used. Data shown are mean ± SEM, *P<0.05, **P<0.01 and ***P<0.001

3.4.3 Insulin sensitivity

Insulin sensitivity was assessed in *RIPCreα2KO* and control mice. Fasted insulin levels were measured to establish whether *RIPCreα2KO* mice are hypo/hyper-secreting insulin (Figure 3.8). The fasted insulin levels were found to be normal. Next an insulin tolerance test was performed to measure insulin sensitivity of insulin target tissues, and to establish that the mice are not suffering from insulin resistance. If the mice were to suffer from insulin resistance, injection of insulin would not lead to a reduction in blood glucose levels. Glucose clearance in response to insulin was equivalent in *RIPCreα2KO*s compared to control animals (Figure 5.6). Together these results indicated normal insulin sensitivity for *RIPCreα2KO* mice.

Figure 3.8: Fasted plasma insulin levels in *RIPCreα2KO* and control mice. Plasma insulin levels after a 24-hr fast in 10-week old mice (n = 7 vs 7). Bloods were collected from tail bleeds and plasma insulin levels were measured with a Rat/Mouse Insulin Elisa Kit. Data shown are mean ± SEM.

Figure 3.9: Insulin sensitivity in *RIPCreα2KO* and control mice. Blood glucose concentrations were measured from tail bleeds at indicated times after an i.p. injection of insulin (0.75 mU/kg). Random fed, 20-week old male mice were used (n = 7 vs 7). Data shown are mean ± SEM.

3.4.4 Glucose-stimulated insulin secretion *in vivo*

To detect any insulin secretory defects in *RIPCreα2KO* mice, a glucose-stimulated insulin secretion test was performed. This revealed that even though fasted insulin levels were equivalent to those measured in control mice, *RIPCreα2KO* mice had significantly impaired insulin secretory function in response to a glucose challenge (Figure 3.10). GSIS performed for a cohort of 10-week old male *RIPCreα2KO* and control mice showed a significant difference in insulin secretion between the control and KO groups in response to glucose injection.

Figure 3.10: *In vivo* glucose-stimulated insulin secretion (GSIS) in *RIPCreα2KO* and control mice. Bloods were collected from tail bleeds at indicated times after an i.p. injection of 20 % D-glucose (2 g/kg) and plasma insulin levels were measured with a Rat/Mouse Insulin Elisa Kit. 10-week old male mice were used (n= 6 vs 7). Data shown are mean $\pm$ SEM, **P<0.01.

Taken together, the data from the glucose tolerance test and from the *in vivo* GSIS indicates that the *RIPCreα2KO* mice are more glucose intolerant in

comparison to their control littermates, with a concomitant defect in glucose-stimulated insulin secretion.

3.5 Metabolic studies in $\alpha1KORIPCre\alpha2KO$ mice

It has been reported that in some tissues, deletion of $AMPK\alpha2$ is compensated for by increased $AMPK\alpha1$ expression (Jørgensen et al., 2004). Hence we combined the deletion of $AMPK\alpha2$ with a global deletion of $AMPK\alpha1$ to create $\alpha1KORIPCre\alpha2KO$ mice that do not express any functional $AMPK\alpha1$ or $AMPK\alpha2$ subunits in islet beta cells. $AMPK\alpha1$-global-null mice were used because $AMPK\alpha1$ floxed mice were not available at the time of these studies, and because the $AMPK\alpha1$-global-null mice are reported not to have a metabolic phenotype (Viollet et al., 2003a).
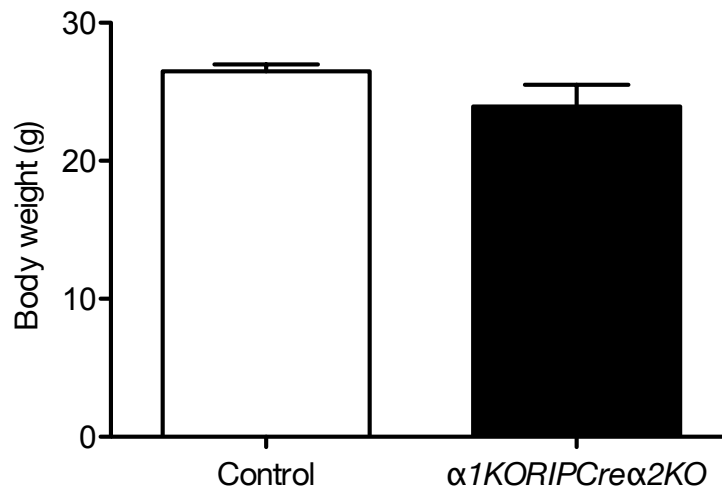
Figure 3.11: Body weight in $\alpha1KORIPCre\alpha2KO$ and control mice. 8-week old male mice were used (n = 6 vs 6). Data shown are mean $\pm$ SEM.

To confirm that $\alpha1KORIPCre\alpha2KO$ mice do not have a hypothalamic phenotype due to the deletion of $AMPK\alpha2$ in RIPCre neurons and deletion of $AMPK\alpha1$ in all tissue types, body weight and food intake were measured in

$\alpha1KORIPCre\alpha2KO$ mice. 8-week old male $\alpha1KORIPCre\alpha2KO$ mice had a normal body weight in comparison to control mice (Figure 3.11). 24-hr food intake and feeding behaviour after a 16-hr fast were also indistinguishable between $\alpha1KORIPCre\alpha2KO$ and control mice (Figures 3.12, 3.13). Because it has already been shown that $AMPK\alpha1$-global-null mice (Viollet et al., 2003a) and $RIPCre\alpha2KO$ mice have normal peripheral insulin sensitivity, determined by insulin tolerance test, insulin sensitivity was not determined in $\alpha1KORIPCre\alpha2KO$ mice.
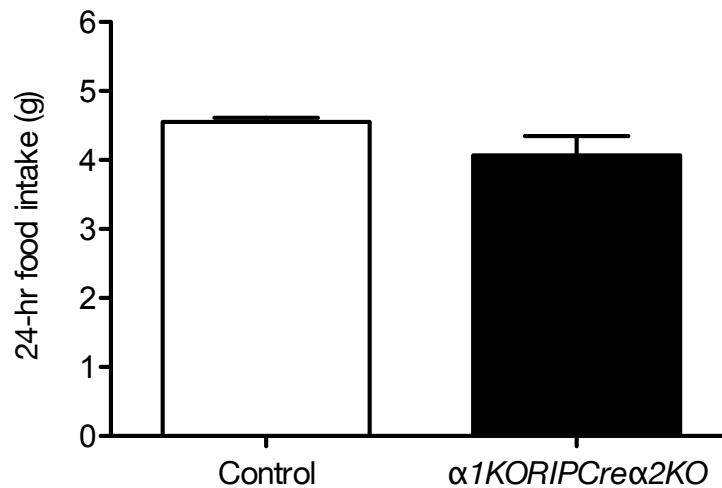
Figure 3.12: 24-hr food intake in $\alpha1KORIPCre\alpha2KO$ and control mice. 16-week old male mice used (n = 4 vs 4). Data shown are mean $\pm$ SEM.

3.6 Glucose homeostasis in $\alpha1KORIPCre\alpha2KO$ mice

3.6.1 Fasted glucose and insulin

Blood glucose concentrations of fasted and post-glucose injected $\alpha1KORIPCre\alpha2KO$ and control mice were measured to investigate glucose handling and its clearance.
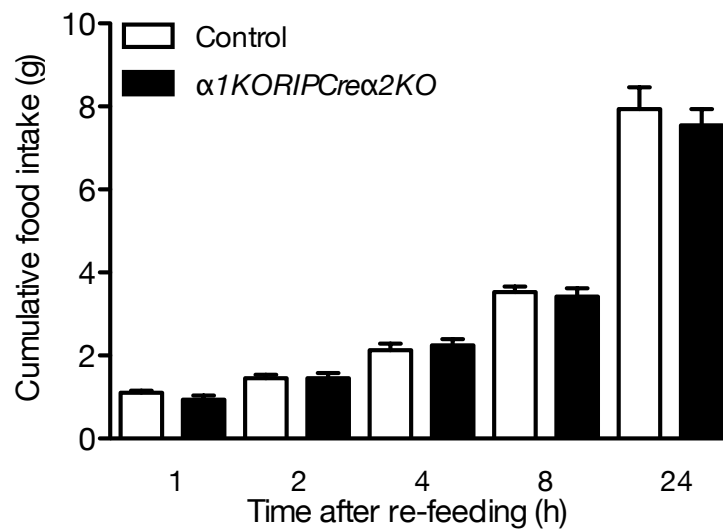
Figure 3.13: Feeding behaviour over a 24-hr period after a 16-hr fast in *α1KORIPCreα2KO* and control mice. 20-week old male mice used (n = 5 vs 5). Data shown are mean ± SEM.
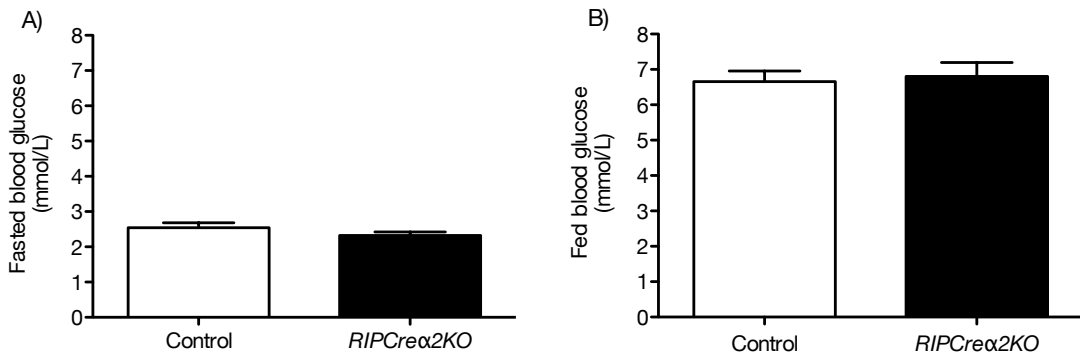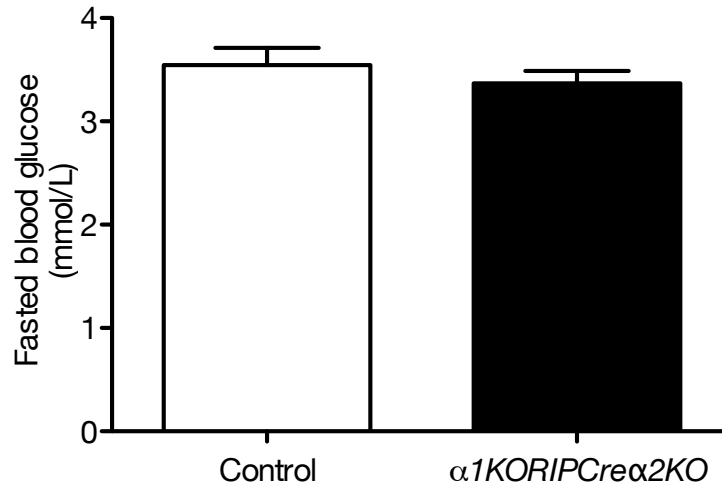
Figure 3.14: Fasted blood glucose levels in $\alpha 1KORIPCre\alpha 2KO$ and control mice. Blood glucose levels after a 24-hr fast in 5-week old (n = 9 vs 12). Bloods were collected from tail bleeds. Data shown are mean $\pm$ SEM.

Fasted blood glucose levels in male $\alpha 1KORIPCre\alpha 2KO$ mice were normal in comparison to control mice at 5-weeks of age (Figure 3.14). This means that the mice are able to correctly regulate their blood glucose concentration at fasted state. The fasted plasma insulin levels were also normal when measured in 10-week old male $\alpha 1KORIPCre\alpha 2KO$ and control mice (Figure 3.15).

3.6.2 Glucose tolerance

A glucose tolerance test was performed on the male $\alpha 1KORIPCre\alpha 2KO$ mice and their littermate controls at 5-weeks of age. At 5-weeks of age, a clear and significant difference in glucose tolerance between the $\alpha 1KORIPCre\alpha 2KO$ and control mice was measured (Figure 3.16). The data shows that the $\alpha 1KORIPCre\alpha 2KO$ mice have a clear defect in their glucose handling.
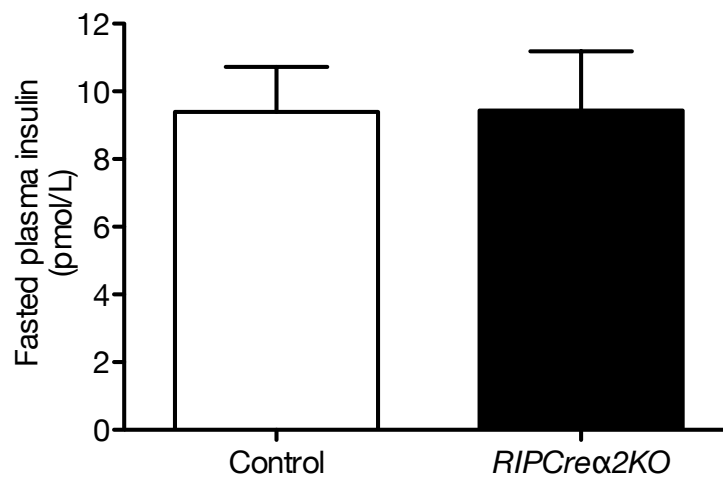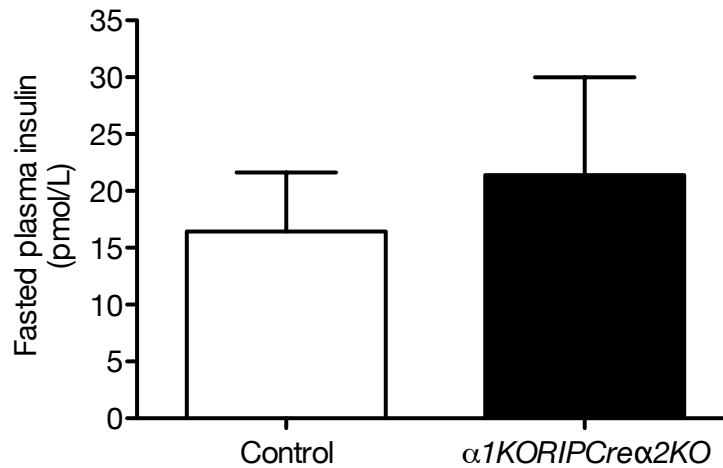
Figure 3.15: Fasted plasma insulin levels in $\alpha 1KORIPCre\alpha 2KO$ and control mice. Plasma insulin levels after a 24-hr fast in 10-week old male mice (n = 9 vs 12). Bloods were collected from tail bleeds and plasma insulin levels were measured with Rat/Mouse Insulin Elisa Kit. Data shown are mean $\pm$ SEM.
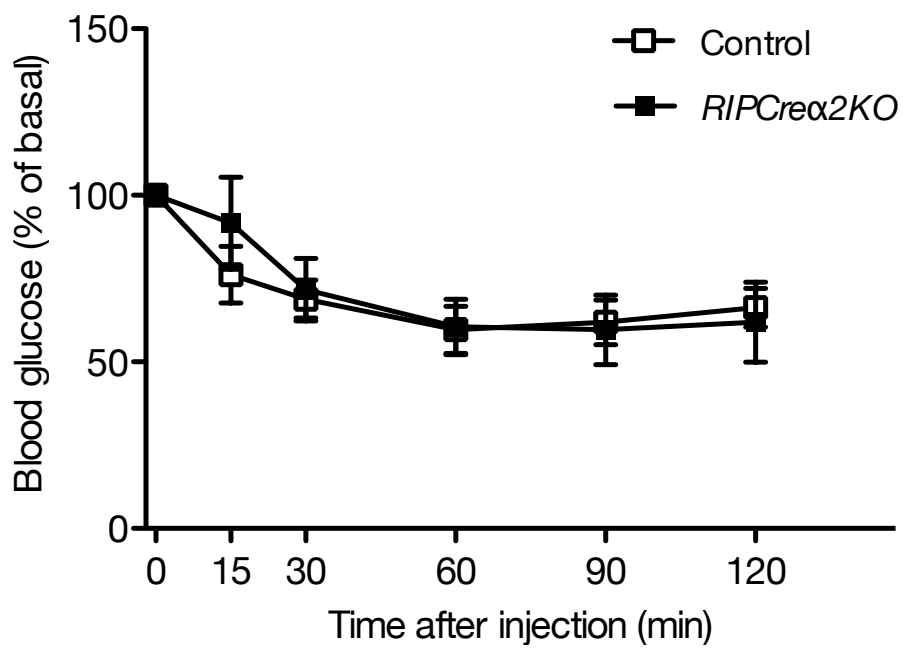
3.6.3 Glucose-stimulated insulin secretion *in vivo*

To detect any insulin secretory defects in $\alpha 1KORIPCre\alpha 2KO$ mice, a glucose-stimulated insulin secretion test was performed. This revealed that even though fasted insulin levels were indistinguishable from the control values, at 10-weeks of age the $\alpha 1KORIPCre\alpha 2KO$ mice exhibited significantly impaired insulin secretory function in response to a glucose challenge (Figure 3.17).

These results clearly demonstrate that $\alpha 1KORIPCre\alpha 2KO$ mice exhibit significant glucose intolerance, which is due to a severe defect in glucose-stimulated insulin secretory function. The impaired glucose homeostasis in $\alpha 1KORIPCre\alpha 2KO$ mice occurred at an earlier age and was more severe than in $RIPCre\alpha 2KO$ mice.

In summary, investigation of glucose homeostasis in $\alpha 1KORIPCre\alpha 2KO$ mice shows that the KO mice have normal fasted blood glucose levels. However, they have highly impaired glucose tolerance. Even though their fasted plasma insulin levels are normal in comparison to control mice, glucose-stimulated insulin secretory behaviour is significantly impaired which explains the marked glucose
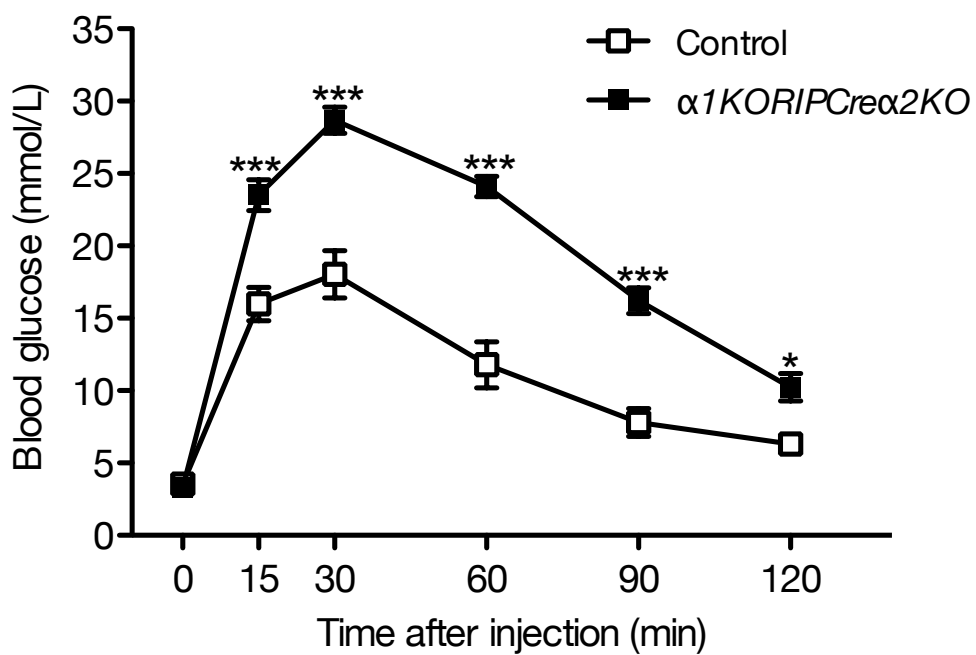
Figure 3.16: Glucose tolerance in *α1KORIPCreα2KO* and control mice. Blood glucose concentrations were measured from tail bleeds at indicated times after an i.p. injection of 20 % D-glucose (2 g/kg). 5-week old male mice (n= 8 vs 8) were used. Data shown are mean ± SEM, *P <0.05 and ***P<0.001.
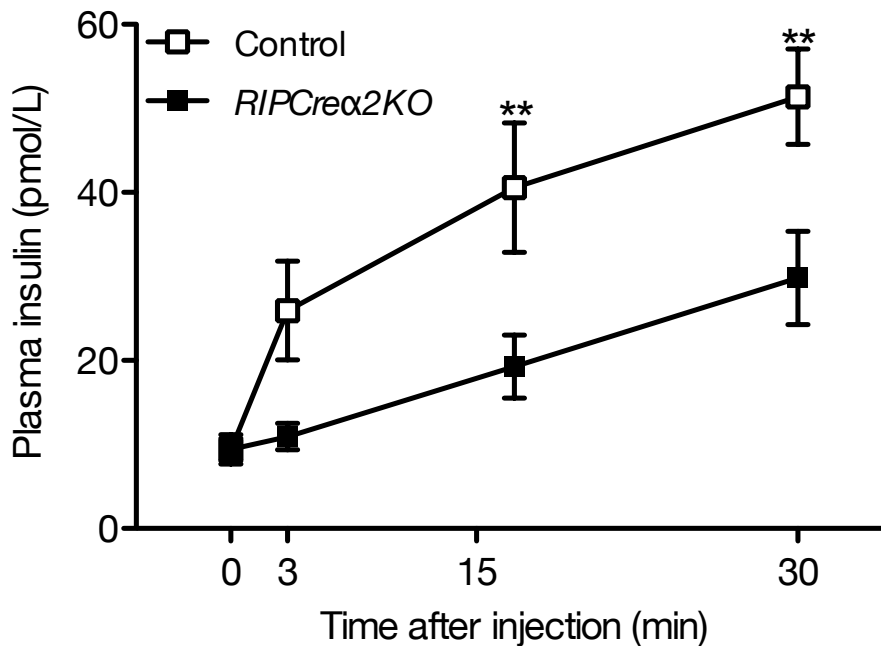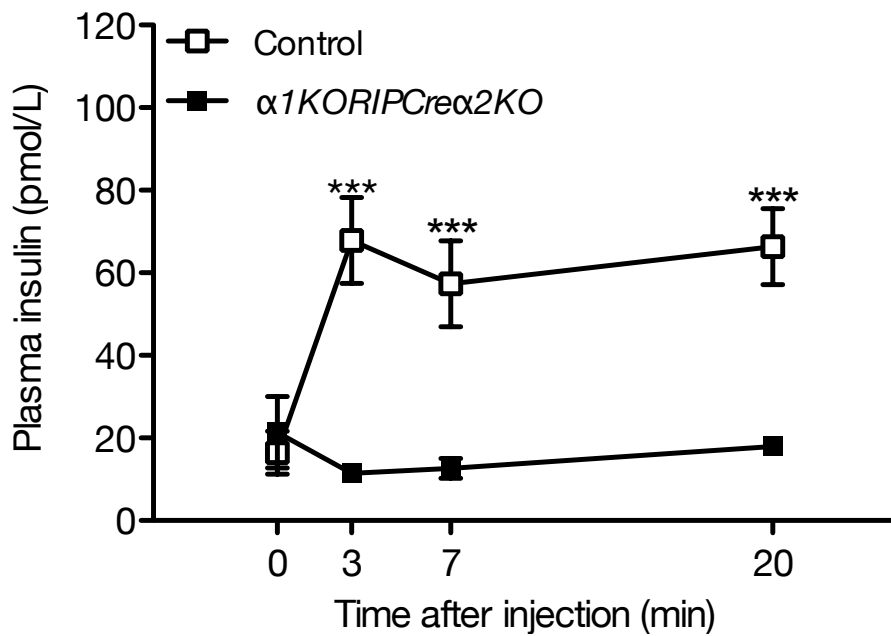
Figure 3.17: *In vivo* glucose-stimulated insulin secretion (GSIS) in *α1KORIPCreα2KO* and control mice. Bloods were collected from tail bleeds at indicated times after an i.p. injection of 20 % D-glucose (2 g/kg) and plasma insulin levels were measured with Rat/Mouse Insulin Elisa Kit. 10-week old male mice were used (n= 6 vs 6). Data shown are mean ± SEM, ***P<0.001.

intolerance in $\alpha 1KORIPCre\alpha 2KO$ mice.

3.7   Summary

The results presented in this chapter demonstrate that both the $RIPCre\alpha 2KO$ and $\alpha 1KORIPCre\alpha 2KO$ are suitable models for investigation of AMPK function in pancreatic beta cells. RIPCre mediated deletion of $AMPK\alpha 2$ was confirmed in islets and hypothalamus but not in other tissues. $AMPK\alpha 2$ mRNA and protein levels were significantly reduced in the islets of $RIPCre\alpha 2KO$ mice. Even though $AMPK\alpha 2$ is also deleted in a population of hypothalamic neurons in these mice, and additionally $AMPK\alpha 1$ is deleted globally in all tissues of the $\alpha 1KORIPCre\alpha 2KO$ mice, these models do not demonstrate any significant defects in hypothalamic function such as alteration in body weight or food intake that could affect the assessment of whole-body glucose homeostasis and *in vivo* glucose-stimulated insulin secretion. Insulin sensitivity in peripheral tissues was also normal in these mice, further confirming that insulin resistance or increased peripheral insulin sensitivity does not influence glucose homeostasis and insulin secretion from the beta cells.

Fasted blood glucose and plasma insulin levels were normal in both transgenic AMPK KO lines. Mice with a deletion of $AMPK\alpha 2$ in beta cells developed mild glucose intolerance by 3 months of age, as assessed by glucose tolerance testing. This phenotype was exacerbated when both catalytic subunits $AMPK\alpha 2$ and $AMPK\alpha 1$ were deleted. $\alpha 1KORIPCre\alpha 2KO$ mice exhibited a marked glucose intolerance which is apparent already at 5-weeks of age. Assessment of glucose-stimulated insulin secretion (GSIS) *in vivo* in $RIPCre\alpha 2KO$ mice demonstrated that the mice had a defective GSIS as insulin secretion in response to glucose was significantly reduced. Again a more marked defect in GSIS was seen in $\alpha 1KORIPCre\alpha 2KO$ mice as the insulin secretion in response to glucose was not increased above basal insulin levels. Because the fasted blood glucose and plasma insulin levels were normal, but upon glucose stimulation defect in glucose handling and insulin secretion was observed, these results give an indication that AMPK might be involved specifically in beta cell glucose sensing and regulation of insulin secretion in response to glucose stimulation. In conclusion, these results

demonstrate that AMPK is important for maintaining functional whole-body glucose homeostasis and glucose-stimulated insulin secretion. Defective GSIS could result in alteration in beta cell mass and defect in intrinsic beta cell function such as insulin secretion. These aspects are examined further in Chapter 4.

Chapter 4

AMPK regulated beta cell function *in vitro*

4.1 Introduction

[1]In Chapter 3 data were presented that showed that mice with a deletion of the *AMPKα2* catalytic subunit in beta cells developed mild glucose intolerance by three months of age caused by decreased glucose-stimulated insulin secretion. This phenotype was exacerbated when both the catalytic isoforms (*α1* and *α2*) were deleted in beta cells. Mice with no functional AMPK catalytic subunit in beta cells had a marked glucose intolerance, and glucose-stimulated insulin secretion was reduced to basal insulin secretion levels. Even though these mice also had a deletion of *AMPKα2* in a population of hypothalamic neurons, no significant hypothalamic phenotype was observed in these animals. The mice also had normal insulin sensitivity. In this chapter, the role of AMPK in regulation of beta cell function *in vitro* is discussed. Results from the whole-animal physiology suggest that the observed decrease in glucose-stimulated insulin secretion could be caused by alterations in beta cell mass, or by functional defect within the beta cells. The studies in this chapter examine beta cell mass and islet mor-

---

[1]This chapter, and the previous one, were published in Biochemical Journal (Beall et al., 2010) where the author of this PhD thesis (KP) and C. Beall share the first authorship. See Appendix C- Publications. Some of the published data, produced by C. Beall has been included in this chapter with the permission of C. Beall.

phology together with an examination of islet glucose-stimulated insulin secretion capacity *in vitro*. To further determine the reasons for defective insulin secretion, gene expression analysis of key beta cell genes involved in glucose sensing and metabolism was conducted, and islet reactive oxygen species (ROS) production and expression of anti-oxidant enzymes were also measured. Electrophysiological characterisation of control and *RIPCreα2KO* and *α1KORIPCreα2KO* beta cell were done by C. Beall, and the summary of the results are included in this chapter.

4.2 Beta cell morphology

Pancreatic sections from *RIPCreα2KO* and control mice were stained with insulin and glucagon antibodies to assess any alterations in islet structure and beta cell mass. Beta cell mass was determined by morphology in *RIPCreα2KO* and control pancreases, and no significant difference was measured between the genotypes (Figure 4.1). The whole pancreatic mass was also unaltered (Figure 4.1). Qualitative comparison of pancreas sections also showed no structural differences between *RIPCreα2KO* and control mice 4.2. Hence, it can be concluded that the defect in insulin secretion is not caused by alterations in pancreatic or beta cell mass, or islet organisation.

4.3 Analysis of glucose-stimulated insulin secretion *in vitro*

Normal beta cell mass seen in *RIPCreα2KO* mice suggested that impaired glucose-stimulated insulin secretion (GSIS) observed *in vivo*, is caused by functional rather than anatomical defects. Hence, islets were isolated from *RIPCreα2KO* and *α1KORIPCreα2KO* mice and islet GSIS was examined *in vitro* (*ex vivo*), thus avoiding possible inter-tissue interaction such as increased sympathetic nervous activity that can affect islet insulin secretion.

Over a 10-fold increase over basal secretion (2 mmol/L glucose) was measured in control islets in response to a stimulatory glucose (20 mmol/L) concentration.
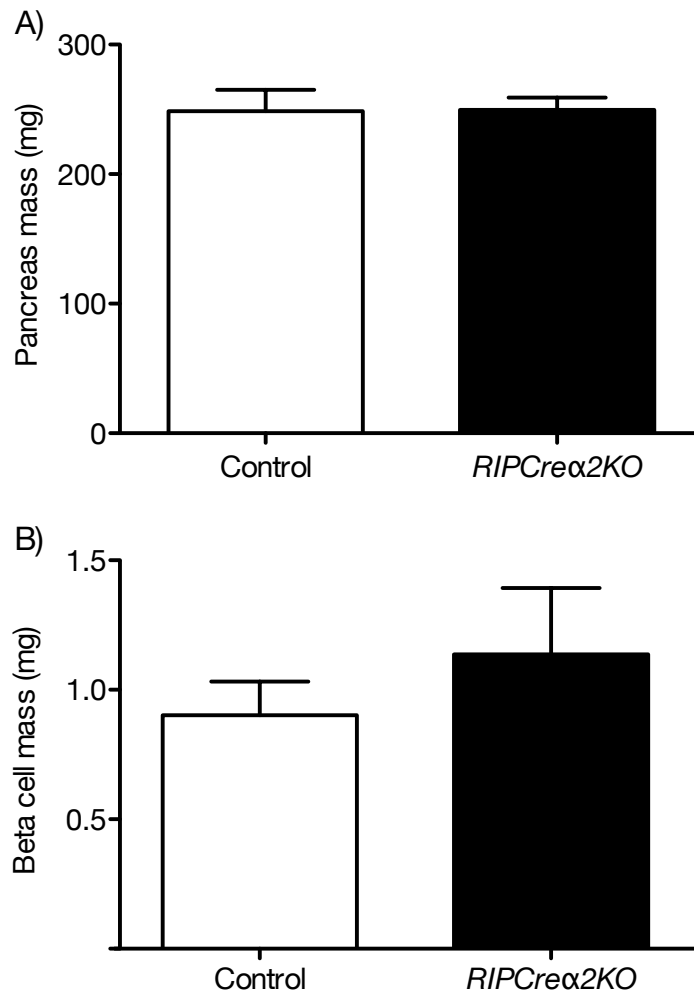
Figure 4.1: Pancreatic and beta cell mass in *RIPCreα2KO* and control mice. Pancreas mass (mg) (A) and beta cell mass (mg) (B) in 10-week old male mice (n = 4 vs 4). Data shown is mean ± SEM.

Control **RIPCreα2KO**
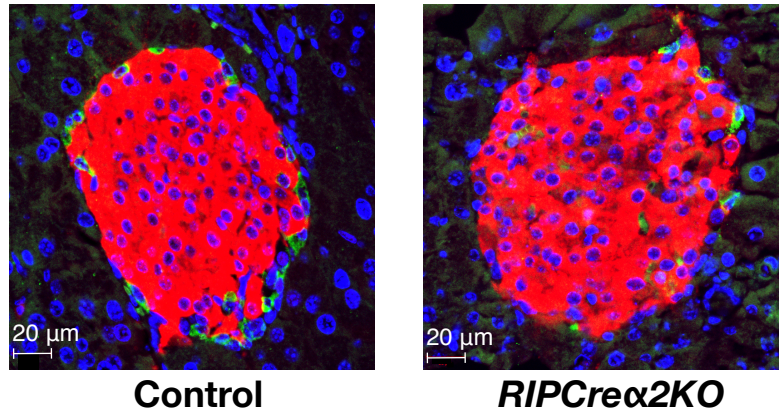
Figure 4.2: Pancreatic sections from *RIPCreα2KO* and control mice. 10-week male mice were used. Sections co-stained with insulin (red), glucagon (green) and DAPI (blue).

In *RIPCreα2KO* and *α1KORIPCreα2KO* islets there was a significant increase in insulin secretion in response to low glucose when compared to insulin secretion from control islets, i.e. an increased basal insulin secretion. However, the increase in insulin secretion over the basal secretion was reduced around 50 % in *RIPCreα2KO* islets (Figure 4.3) and around 90 % in *α1KORIPCreα2KO* islet (Figure 4.4).

In conclusion, *RIPCreα2KO* and *α1KORIPCreα2KO* islets showed a significant increase in insulin secretion at basal (2 mmol/L) glucose concentration. At stimulatory (20 mmol/L) glucose concentration, *RIPCreα2KO* and *α1KORIPCreα2KO* islets showed a significant reduction in insulin secretion. These results suggest that impaired glucose-stimulated insulin secretion is due to an intrinsic beta cell defect within the islets of *RIPCreα2KO* and *α1KORIPCreα2KO* mice. These results indicate that expression of AMPK in beta cells is important for normal glucose-stimulated insulin secretion.

4.4 Glucose sensing in AMPK deficient beta cells

Impaired GSIS could be caused by a defect in beta cell electrical activity. Normal beta cells are electrically active at >10 mmol/L glucose concentration, char-
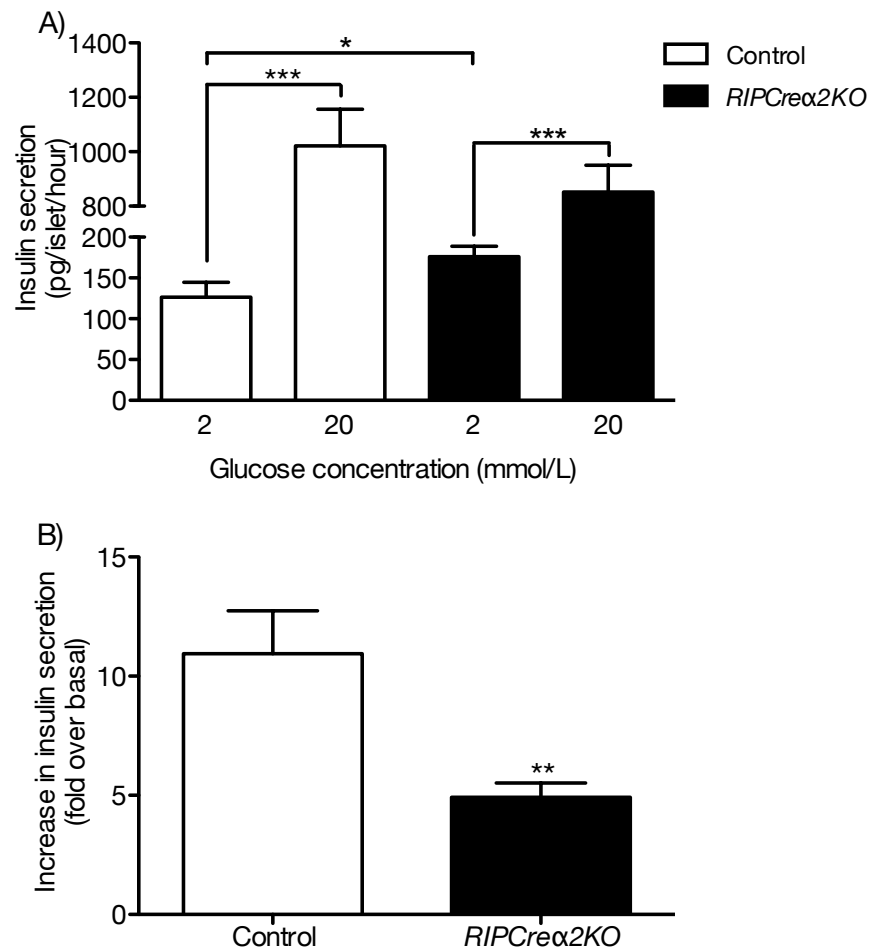
Figure 4.3: *In vitro* glucose-stimulated insulin secretion in *RIPCreα2KO* and control islets. Groups of 5 islets were incubated either in 2 or 20 mmol/L glucose for 1 hour and the amount of insulin secreted (as pg/islet/hour) was measured (A). (B) represent the same data as a fold increase in insulin secretion over basal secretion. Islets were isolated from 6 mice per genotype. 16-week old male mice were used. Data shown are mean $\pm$ SEM, *P<0.05, **P<0.01 and ***P<0.001.
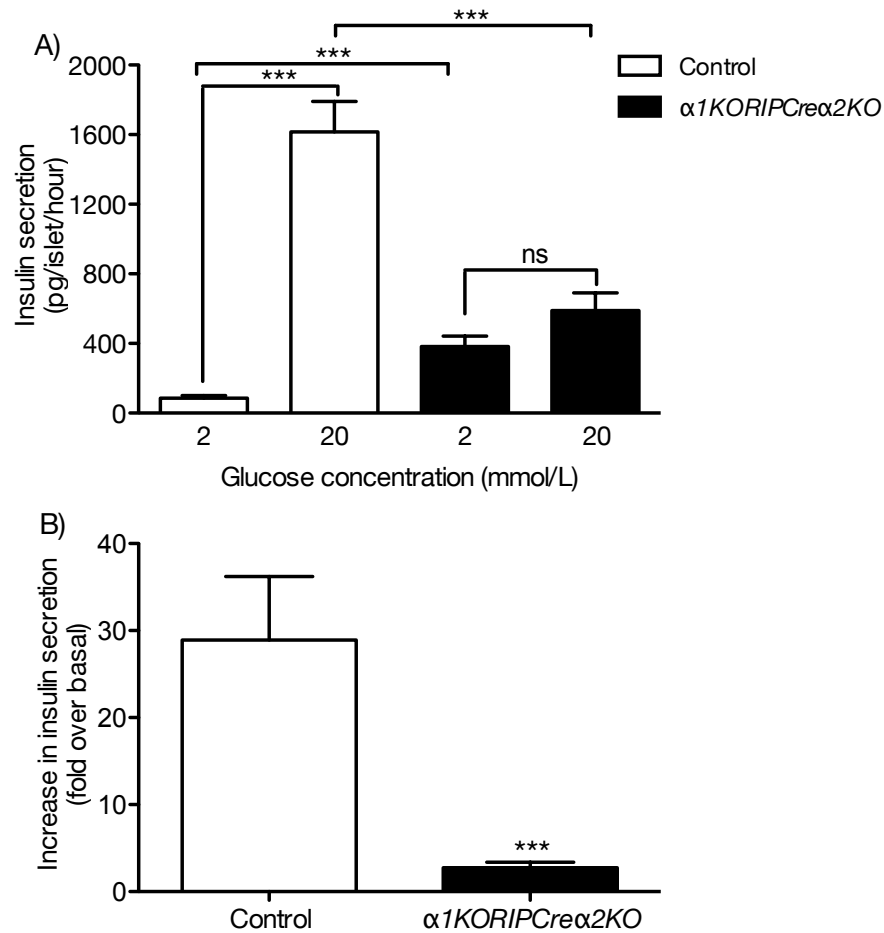
Figure 4.4: *In vitro* glucose-stimulated insulin secretion in *α1KORIPCreα2KO* and control islets. Groups of 5 islets were incubated either in 2 or 20 mmol/L glucose for 1 hour and the amount of insulin secreted (as pg/islet/hour) was measured (A). (B) represent the same data as a fold increase in insulin secretion over basal secretion. Islets were isolated from 6 mice per genotype. 16-week old male mice were used. Data shown are mean $\pm$ SEM, ***$P<0.001$.

acterised by calcium action potential firing, reflected by plasma membrane depolarisation (Rorsman, 1997). When the glucose concentration is reduced to 2 mmol/L, beta cells become electrically silent, characterised by a loss of action potentials and hyperpolarisation of the plasma membrane. *RIPCreα2KO* and *α1KORIPCreα2KO* beta cells failed to become electrically silent when glucose concentration was reduced from 10 to 2 mmol/L glucose, with continuous action potential firing and depolarisation of the plasma membrane even at low glucose concentration[1] (Figure 4.5). This suggests that the *RIPCreα2KO* and *α1KORIPCreα2KO* beta cells are unable to sense glucose properly. The continuous electrical activity at low glucose concentration could also explain the increased insulin secretion observed at low glucose concentration.

4.4.1   Gene expression analysis of Glut2 and hexokinases in *RIPCreα2KO* islets

Loss of hypoglycaemic sensing could be caused by altered expression levels of the GLUT2 glucose transporter, or the beta cell glucose sensor glucokinase.To determine whether the expression of genes, involved in glucose transport and glucose sensing, is altered in *RIPCreα2KO* islets, *Glut2* and *Glucokinase* mRNA levels were measured using qRT-PCR (Figure 4.6). GLUT2 is the predominant glucose transporter in beta cells. Glucokinase is a high Km hexokinase (hexokinase IV), regarded as a beta cell glucose sensor as it phosphorylates glucose and initiates glycolysis. However, no changes in *Glut2* or *Glucokinase* mRNA expression levels were detected.

Three low Km hexokinases are also expressed in beta cells, although at very low levels. Hence mRNA levels of *Hexokinases I, II* and *III* were measured to see whether altered glucose sensing could be due to changes in the low Km hexokinase levels. However, no change in mRNA expression was detected (Figure 4.7).

---

[1]This experiment was conducted by C. Beall at University of Dundee in isolated islets from mice that I generated.
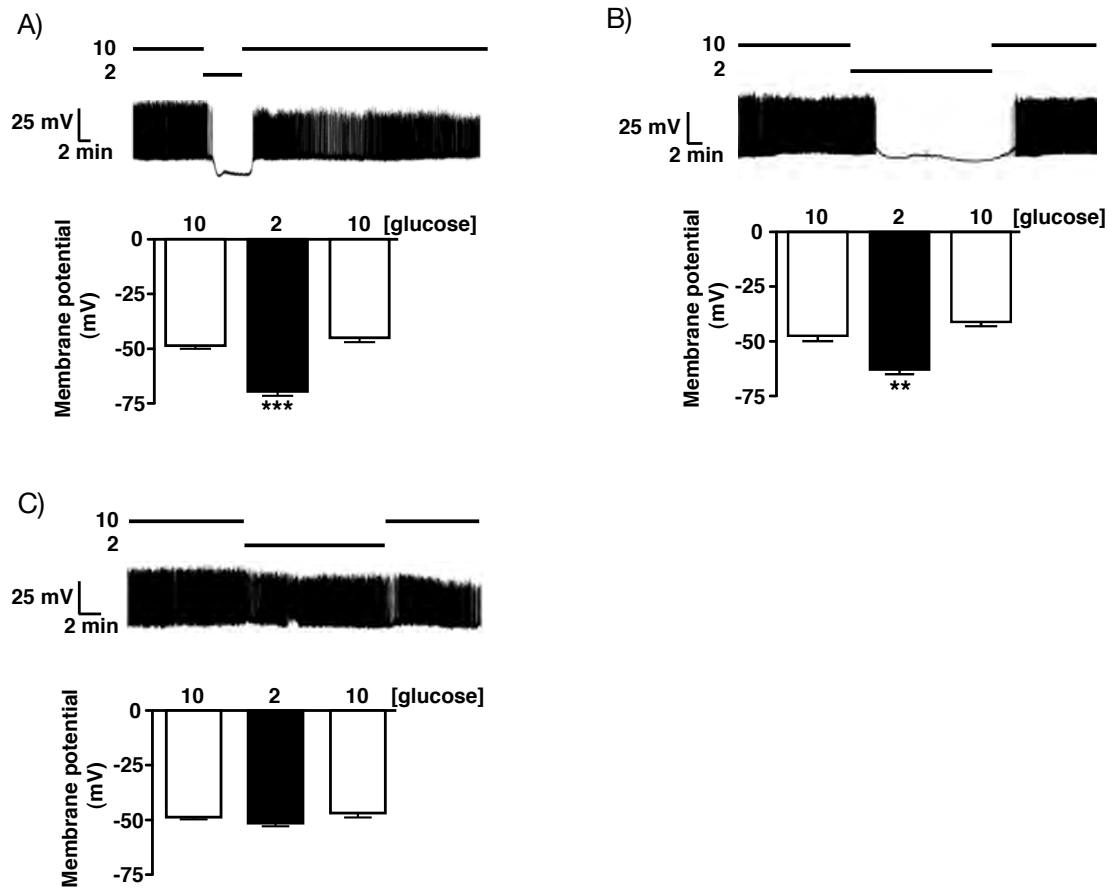
Figure 4.5: Loss of hypoglycaemic sensing in isolated beta cells from *RIPCreα2KO* mice. WT (A) and RIPCre (B) mouse cultured beta cells respond to the reduction of glucose from 10 to 2 mmol/L by hyperpolarisation and cessation of firing. (C) *RIPCreα2KO* beta cells are unresponsive to a reduction of glucose concentration from 10 to 2 mmol/L. The histograms in (A-C) are the mean values for membrane potential in beta cells exposed to 10, 2 and 10 mmol/L glucose for each condition. Values were derived from seven to 10 individual beta cell recordings per group and are shown as mean ± SEM, **P <0.01, ***P<0.001. 14-week old male mice were used. Figure from Beall et al. (2010), produced by C. Beall.
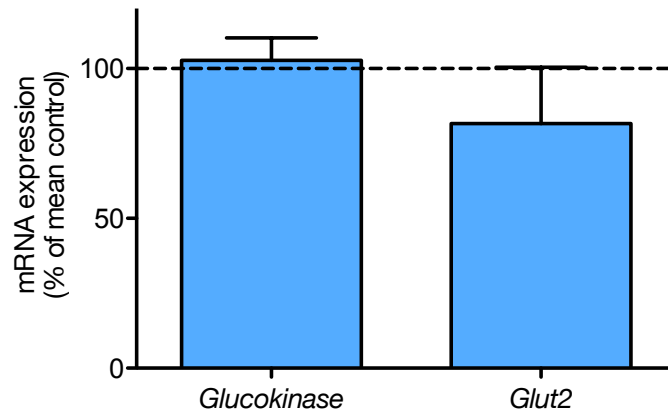
Figure 4.6: Expression levels of *Glut2* (solute carrier family 2 [facilitated glucose transporter], member 2 gene, Slc2a2) and *Glucokinase* in *RIPCreα2KO* and control islets. 20-week old male mice were used (n = 7-8). Data shown are mean ± SEM.
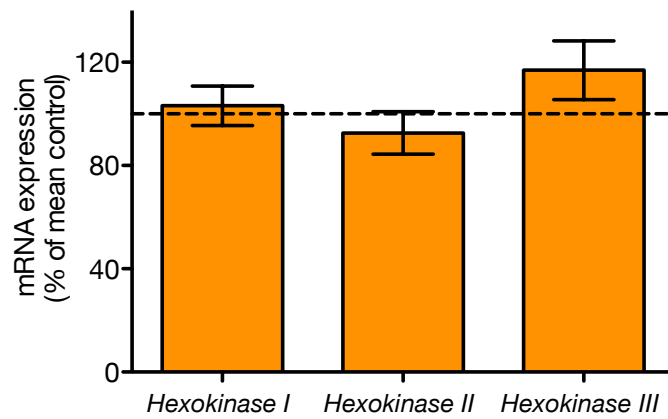
Figure 4.7: Expression of hexokinase isoforms (I-III) in *RIPCreα2KO* and control islets. 20-week old male mice were used (n = 7-8). Data shown are mean ± SEM.

4.5 Mitochondrial function in *RIPCreα2KO* islets

Because proper mitochondrial biogenesis is essential for functional beta cells, especially in terms of insulin secretion, mRNA expression levels of three genes, *Nrf1*, *Tfam* and *Pgc-1α*, involved in the regulation of mitochondrial biogenesis, respiration and mitochondrial DNA transcription were also measured (Scarpulla, 2008, 2002). However, the expression of these genes remained unchanged in *RIPCreα2KO* islets (Figure 4.8).
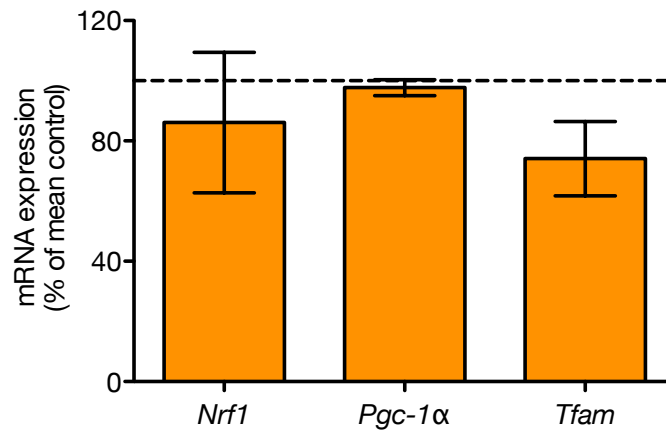
Figure 4.8: Expression of mitochondrial biogenesis regulating genes in *RIPCreα2KO* and control islets. *Nrf1* (Nuclear respiratory factor 1 gene), *Pgc-1α* (Peroxisome proliferator-activated receptor gamma coactivator-1 alpha gene), *Tfam* (Transcription factor A, mitochondrial gene). 20-week old male mice were used (n = 5-6). Data shown are mean ± SEM.

Previous studies have indicated a link between AMPK and UCP2 expression. For example, *UCP2* expression was reduced in the aortas of *AMPKAα2*-global-null mice, and decreased in response to AMPK activation (Xie et al., 2008). UCP2 has also been shown to affect islet GSIS, although whether it is involved in stimulating or inhibiting GSIS has remained unclear (Pi et al., 2009; Zhang et al., 2001). Therefore, mRNA expression of *Ucp2* was measured in *RIPCreα2KO* and control islets, and was found to be significantly downregulated (Figure 4.9). To confirm that reduction in *Ucp2* expression was not caused by reduced mitochon-

drial mass, mitochondrial mass was estimated by examining the expression of mitochondrial protein ATP synthase. No change in mitochondrial mass observed reflected by unchanged ATP synthase levels (Figure 4.10).
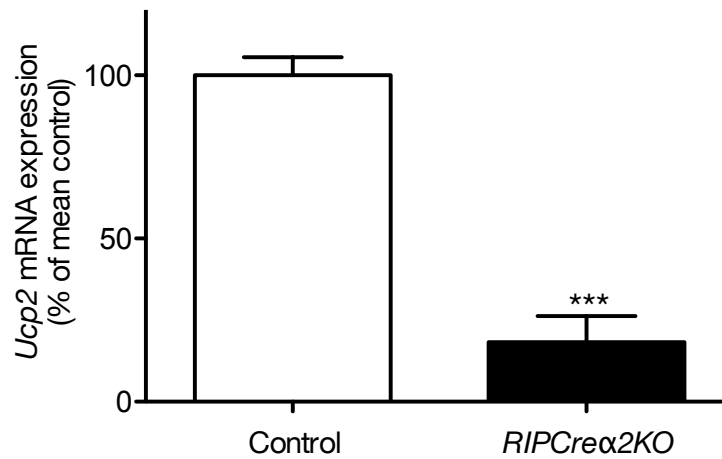
Figure 4.9: Gene expression levels of *Ucp2* (*Uncoupling protein 2*) gene in *RIPCreα2KO* and control islets. 20-week old male mice used (n = 5-6). Data shown is mean ± SEM, ***P<0.001.
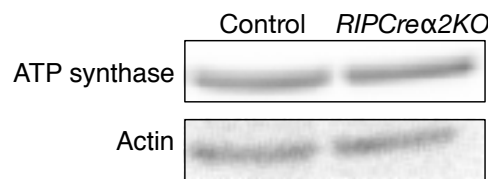
Figure 4.10: Immunoblot for ATP synthase from *RIPCreα2KO* and control islets.

4.5.1 Production of reactive oxygen species in *RIPCreα2KO* and *α1KORIPCreα2KO* islets

UCP2 is an important regulator of mitochondrial reactive oxygen species (ROS) production. Previous studies have shown that reduction of UCP2 in beta cells

can lead to increased ROS production and impaired GSIS (Joseph et al., 2002). Hence, H_2O_2 production (as an indicator of ROS generation) determined by CM-H_2DCFDA fluorescence was measured at 2 and 20 mmol/L glucose concentrations in control, *RIPCreα2KO* and *α1KORIPCreα2KO* islets (Figure 4.11). However, no differences in CM-H_2DCFDA fluorescence was detected.
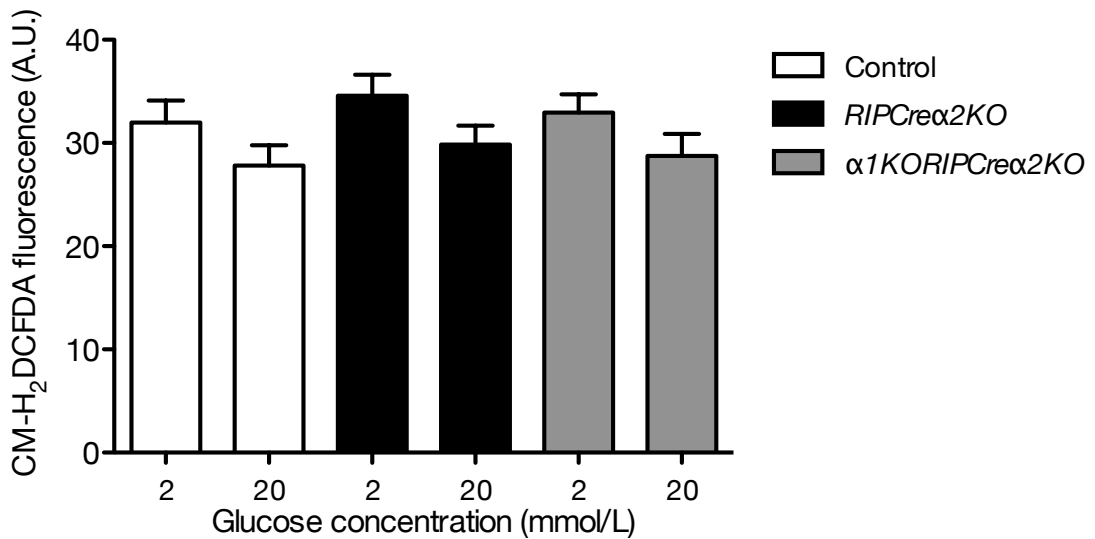
Figure 4.11: H_2O_2-derived fluorescence in *RIPCreα2KO*, *α1KORIPCreα2KO* and control islets at 2 and 20 mmol/L glucose concentration. Islets were isolated from 3 mice per genotype (n = 16-23 islets in each condition). Data shown are mean ± SEM.

To investigate whether increased anti-oxidant enzyme levels could have explained why ROS levels remained unchanged between control and *RIPCreα2KO* and *α1KORIPCreα2KO* islets, mRNA expression levels of *Gpx4*, *Hmox1* and *Sod2* were measured in *RIPCreα2KO* and control islets. However, no change in *Gpx4* and *Hmox1* expression levels were detected, and surprisingly, *Sod2* levels showed a minor reduction between *RIPCreα2KO* and control islets (Figure 4.12).
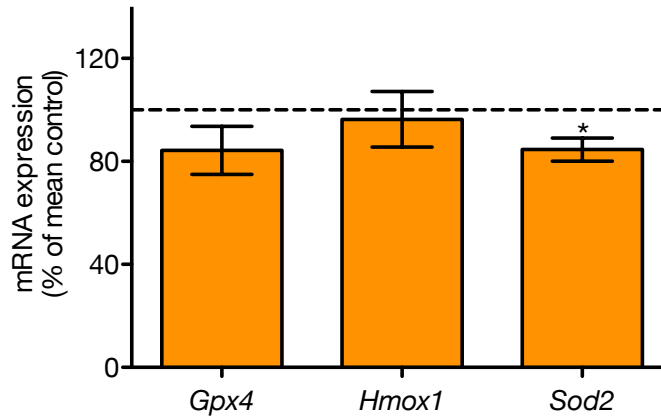
Figure 4.12: Expression of antioxidant enzymes in *RIPCreα2KO* and control islets. *Gpx4* (Glutathione peroxidase 4 gene), *Hmox1* (Heme oxygenase (decycling 1) gene), *Sod2* (Superoxide dismutase 2 gene). 20-week old male mice were used (n = 8-10). Data shown are mean $\pm$ SEM, *P<0.05.

4.6 K_{ATP}-channel function in *RIPCreα2KO* beta cells

As the *RIPCreα2KO* beta cells remained electrically active at low glucose concentration and insulin secretion was significantly elevated, it was postulated that the K_{ATP}-channels remain closed at low glucose (Beall et al., 2010). Loss of function mutations of K_{ATP}-channel subunits or reduced expression of K_{ATP}-channels on the plasma membrane have been shown to cause increased electrical activity and insulin secretion at low glucose (Ashcroft, 2005; Miki et al., 1998; Seghers et al., 2000). Previous studies have shown that deletion of *Sur1* leads to alterations in insulin secretion(Chan et al., 2004a). Hence, mRNA expression of *Sur1*, a subunit of the K_{ATP}-channel was measured. Surprisingly, expression of *Sur1* was significantly downregulated (Figure 4.13). Reduced *Sur1* expression levels could indicate an alteration in K_{ATP}-channel function or ATP-sensitivity, which could explain altered insulin secretion at basal, hypoglycaemic levels. However, voltage-clamped whole-cell currents in control and *RIPCreα2KO* beta cells at

various ATP concentrations were unaltered[1] (Figure 4.14). These results indicate that even though *Sur1* expression is reduced, the K_{ATP}-channels in *RIPCreα2KO* beta cells have a normal decreased channel conductivity in response to increased ATP concentration, and voltage-clamped currents are also normal.
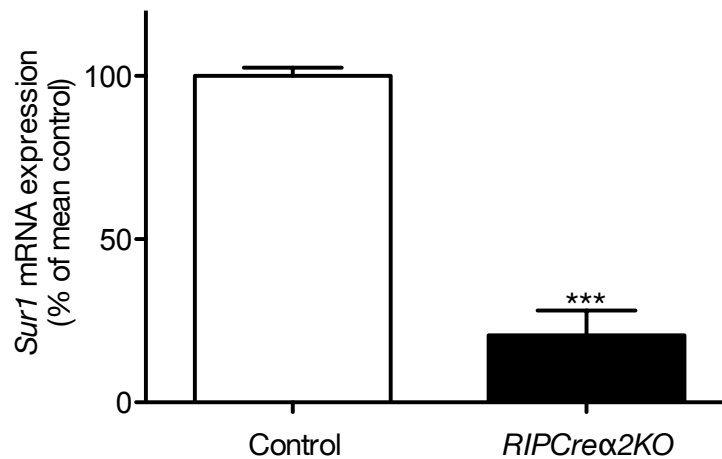
Figure 4.13: Gene expression level of K_{ATP}-channel subunit gene *Sur1* (Sulfonylurea receptor 1 gene) in *RIPCreα2KO* and control islets. 20-week old male mice used (n = 5-6). Data shown are mean $\pm$ SEM, ***P<0.001.

4.7   Summary

Deletion of AMPK catalytic subunits in beta cells caused glucose intolerance and impaired glucose-stimulated insulin secretion *in vivo*. Even though these animals had a normal hypothalamic function and normal peripheral insulin sensitivity, more detailed examination of AMPK deficient islets *in vitro* was necessary in order to obtain a better understanding of the role of AMPK in regulation of beta cell function.

Impaired GSIS could result from a change in beta cell mass or beta cell dysfunction. Recently, an AMPK upstream kinase, LKB1, has been implicated in

---

[1]This experiment was conducted by C. Beall at University of Dundee
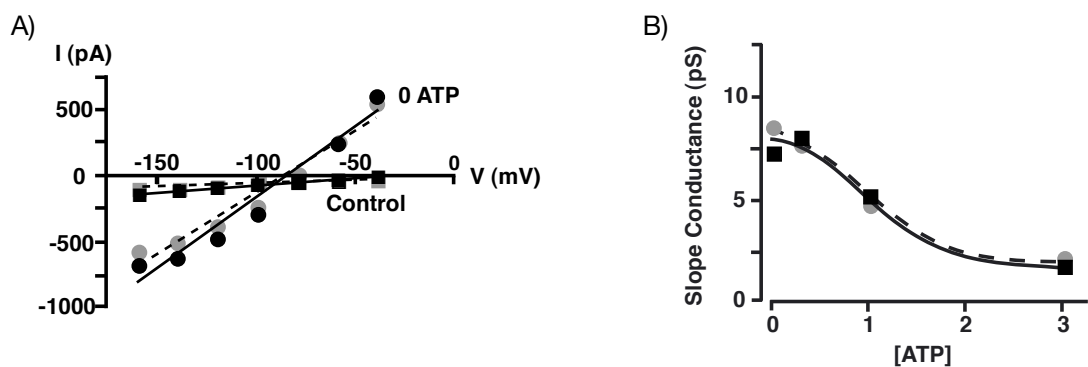
Figure 4.14: Loss of AMPKα2 does not alter beta cell K$_{ATP}$ current or ATP sensitivity. (A) Current-voltage relationship for voltage-clamped currents of RIPCre control (black symbols) and *RIPCreα2KO* (grey symbols) cultured beta cells. Mean currents were measured at various membrane potentials shortly after attaining whole-cell recording (i.e. prior to significant washout of cell ATP; filled squares) and 20 min later (following maximal washout of cellular ATP; filled circles. (B) Mean slope conductance values for current-voltage relationships as shown in (A) as a function of [ATP] (0, 0.5, 1.0 or 3.0 mM in the pipette solution). Lines of best fit (dose-response) are shown for RIPCre control (black filled squares) and *RIPCreα2KO* (grey filled circles) beta cells (n = 3-6). Figure from Beall et al. (2010), produced by C. Beall.

regulation of beta cell mass. Deletion of LKB1 in beta cells led to increased beta cell mass and cell proliferation, and change in cell polarity (Granot et al., 2009; Sun et al., 2010b). Therefore it could be possible that loss of AMPK in beta cells could also lead to changes in islet beta cell mass. However, no change in beta cell mass was observed in *RIPCreα2KO* mice. Because the beta cell mass was found to be normal, it was even more likely that impaired GSIS was due to an intrinsic beta cell defect.

In vitro GSIS was assessed in *RIPCreα2KO* and *α1KORIPCreα2KO* islets. The increase in insulin secretion over basal secretion level was significantly reduced in *RIPCreα2KO* and *α1KORIPCreα2KO* islets at 20 mmol/L glucose. These results further confirm that the impaired GSIS observed *in vivo* is due to an intrinsic beta cell defect in the *RIPCreα2KO* and *α1KORIPCreα2KO* mice. Interestingly, at a low glucose concentration both the AMPK single and double KO islets secreted significantly more insulin in response to 2 mmol/L glucose. This effect was more profound in the double KO islets. *In vitro* GSIS results suggest that AMPK could be involved in sensing low and high glucose concentrations and regulating insulin secretion correspondingly.

To further examine whether there could be a change in beta cell glucose sensing, electrical activity in control and *RIPCreα2KO* beta cells was measured by C. Beall. In *RIPCreα2KO* beta cells, plasma membrane was not hyperpolarised and action potentials could still be recorded when glucose concentration was reduced to 2 mmol/L. Continuous electrical activity at low glucose concentration could also explain the increased insulin secretion measured at basal glucose level.

Therefore AMPK seems to be involved in glucose sensing and regulation of insulin secretion. Loss of low glucose sensing could be caused by altered expression levels of glucose transporter *Glut2* and *Glucokinase* (hexokinase IV), which acts as a rate-limiting enzyme of the glycolysis. However, both *Glut2* and *Glucokinase* mRNA levels were normal in *RIPCreα2KO* islets in comparison to control islets. Expression levels of three low Km hexokinases (*Hexokinase I, II* and *III*) were also found normal in *RIPCreα2KO* islets.

Impaired mitochondrial function, including defect in key genes regulating mitochondrial biogenesis was assessed. However, mRNA expression of *Nrf1*, *Tfam* and *Pgc-1α* were all normal in *RIPCreα2KO* islets. Previous studies have indicated

that UCP2 might have a role in regulating beta cell glucose-stimulated insulin secretion. Furthermore, reduced *UCP2* expression has been reported in the aortas of *AMPKα2*-global-null mice, indicating a link between AMPK and UCP2 (Xie et al., 2008). Interestingly, mRNA expression of *Ucp2* in *RIPCreα2KO* islets was significantly reduced, and it was confirmed that the reduction was not caused by decreased mitochondrial mass but genuine reduction in *Ucp2* gene expression. Genetical knockdown of *Ucp2*, and inhibition of UCP2 activity by genipin has been shown to result in increased glucose-stimulated insulin secretion (Zhang et al., 2006). To further examine the relationship between reduced *Ucp2* expression in *RIPCreα2KO* islets, and increased electrical activity and insulin secretion at low glucose concentration, we showed (Beall et al., 2010) that treatment of wt beta cells with the UCP2 inhibitor genipin resulted in a similar electrophysiological phenotype that was observed in *RIPCreα2KO* beta cells with a failure to hyperpolarise the plasma membrane at low glucose concentration. These results suggest that loss of glucose sensing and increased insulin secretion at low glucose might result from UCP2-dependent mechanism.

Mitochondrial uncoupling proteins are linked to generation of reactive oxygen species (ROS). ROS generation has been linked to regulation of glucose-stimulated insulin secretion. Previous studies have shown that reduced UCP2 levels result in increased ROS production, which could stimulate insulin secretion from beta cells (Pi et al., 2010). Hence ROS production was measured in *RIPCreα2KO* and *α1KORIPCreα2KO* islets. However, no difference in ROS generation was measured between control and KO islets. Hence, the defective GSIS observed was not due to alterations in ROS generation.

The *RIPCreα2KO* beta cells failed to hyperpolarise the plasma membrane in response to hypoglycaemia and basal insulin secretion was elevated. Loss of function mutations of K$_{ATP}$-channel subunits or reduced expression of K$_{ATP}$-channels on the plasma membrane have been shown to cause increased electrical activity and insulin secretion at low glucose (Ashcroft, 2005; Miki et al., 1998; Seghers et al., 2000). Furthermore, deletion of the K$_{ATP}$-channel subunit *Sur1* has been shown to cause impaired islet insulin secretion (Seghers et al., 2000). Hence, *Sur1* mRNA expression levels were measured in *RIPCreα2KO* islets and found to be significantly reduced. This indicated that perhaps K$_{ATP}$-channels in the

RIPCreα2KO beta cells had a change in ATP-sensitivity or channel conductance. However, voltage-clamped currents assessed at various ATP concentrations, measured by C. Beall were unaltered in *RIPCreα2KO* beta cells. Hence, even though *Sur1* gene expression was reduced, no defect in ATP-sensitivity or channel conductance was found that could explain the increased electrical activity and insulin secretion at low glucose.

As a summary, deletion of *AMPKα2* and *AMPKα1* catalytic subunits in beta cells causes impaired glucose-stimulated insulin secretion. At a low glucose concentration, beta cells deficient in AMPK secrete significantly more insulin, but at a stimulatory glucose concentration the insulin secretion is reduced. Increased insulin secretion at low glucose it most likely caused by continuous electrical activity and maintenance of plasma membrane depolarisation at this concentration. Our results suggest that AMPK is required in beta cells for glucose sensing at low and stimulatory glucose concentration, and regulation of insulin secretion accordingly. It is possible that this regulation is dependent on the mitochondrial uncoupling protein UCP2 but the more detailed mechanisms remain yet to be determined.

Chapter 5

Physiological characterisation of *RIPCrep110αβKO* mice and determination of *in vitro* beta cell function

5.1 Introduction

Activation of tyrosine kinase receptors, such as insulin and IGF-1 receptors, leads to activation of phosphoinositide 3-kinase (PI3K) (Kozma and Thomas, 2002). Once activated, class IA PI3Ks phosphorylate membrane associated $PI(3,4)P_2$, which leads to generation of $PI(3,4)P_3$. PIP_3 mediates signals downstream from PI3K by functioning as a docking site and activator for multiple enzymes such as Pdk1, Akt and PKC (Cantley, 2002). Hence metabolic signalling from insulin and IGF-1 receptors are mediated via PI3K, and results in a regulation of a wide variety of different metabolic and cellular functions such as cell growth and survival, and in beta cells insulin secretion (Leibiger and Berggren, 2008).

Previous studies that have studied the class IA catalytic isoforms have highlighted a key role for catalytic isoforms in insulin signalling. Gene targeting and use of isoform specific inhibitors have shown that p110α isoform is a predominant class IA catalytic isoform that associates with IRS-1/2 complexes and mediates signals

downstream from the insulin receptor (Foukas et al., 2006; Guillermet-Guibert et al., 2008; Hooshmand-Rad et al., 2000). On the contrary, we have shown a dominant role for p110β in POMC and AgRP neurons in the regulation of whole-body energy homeostasis and hypothalamic insulin- and leptin-receptor signalling (Al-Qassab et al., 2009).

The role of PI3K in pancreatic beta cells has been investigated using non-specific inhibitors of PI3K catalytic subunits (Aspinwall et al., 2000; Kubota et al., 2004). However, no research exists that directly examines the role of both p110α and p110β subunits in pancreatic beta cell function *in vivo* and *in vitro*. Hence we have generated mice that express kinase dead p110α and p110β subunits (simultaneously) in pancreatic beta cells under rat insulin promoter (RIP) cre-recombinase. The aim was to investigate the whole-body glucose homeostasis in these mice as well as to look at the *in vitro* mechanism that results in dysfunctional PI3K signalling in pancreatic beta cells.

5.2 Analysis of deletion

5.2.1 Efficacy of *p110*α and *p110*β deletion

Both *p110*α and *p110*β floxed alleles are designed to create a kinase dead catalytic subunit upon cre-mediated recombination without changing the stoichiometry between the p110 catalytic and p85 regulatory subunit (Graupera et al., 2008; Guillermet-Guibert et al., 2008). Hence transcription and translation of both the subunits should remain normal despite manipulation of kinase activity loop regions within the subunit genes. In order to confirm that transcription of *p110*α and *p110*β catalytic subunits and *p85* regulatory subunit are unchanged, their islet and hypothalamic[1] mRNA levels in *RIPCrep110*$\alpha\beta$*KO* and control mice were measured by real time quantitative PCR (qRT-PCR). No change in *p110*α, *p110*β or *p85* islet mRNA levels were detected (Figure 5.1).

Significant reduction in the PI3K lipid kinase activity was confirmed in the *RIPCrep110*$\alpha\beta$*KO* islets in comparison to controls, demonstrating that RIPCre

---

[1]Experiment and figure by H. Al-Qassab at UCL
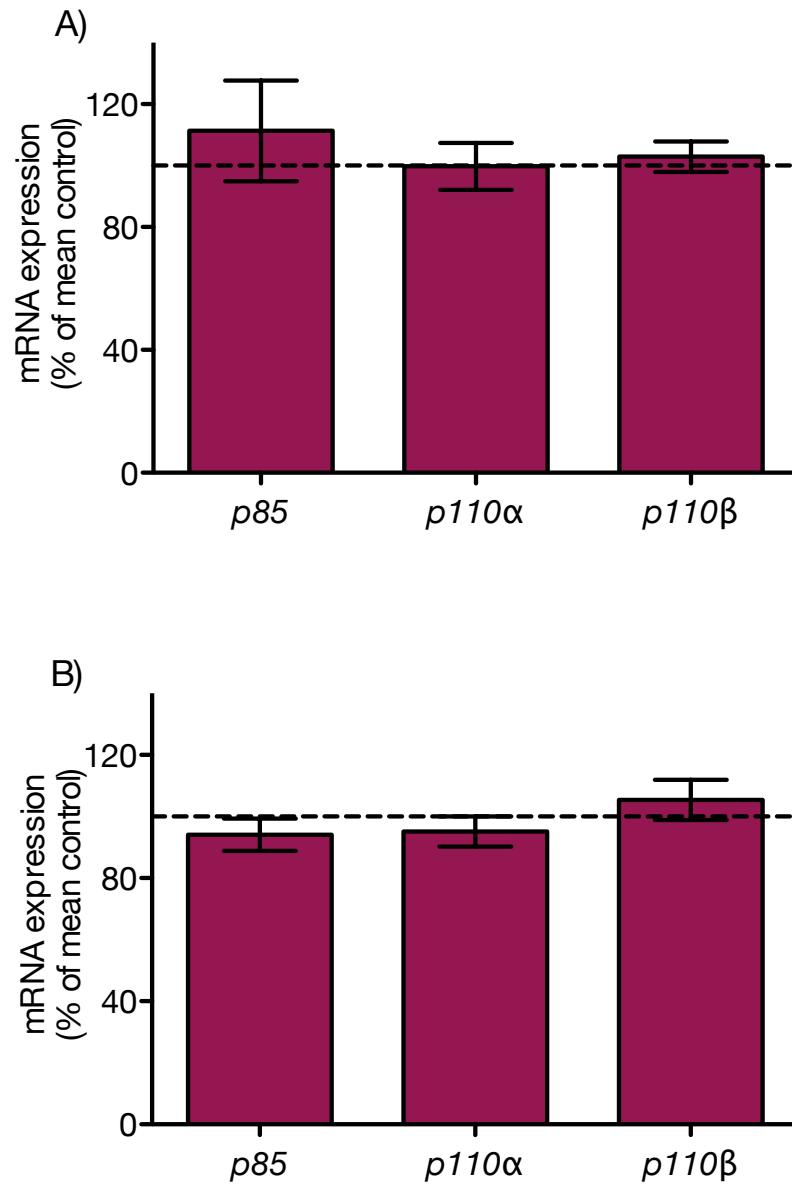
Figure 5.1: Expression of catalytic (*p110α* and *p110β*) and regulatory (*p85*) subunits of PI3K in *RIPCrep110αβKO* and control islets (A) and hypothalami (B). 16-week old male mice were used (n = 8 vs 6). Data shown are mean $\pm$ SEM.

mediated recombination of floxed *p110α* and *p110β* alleles is successful[1] (Figure 5.2). *RIPCrep110αβKO* islet protein lysates were treated with isoform selective inhibitors (PIK75 against p110α and TGX221 against p110β) and relative PI3K activity was measured. This suggested that in the *RIPCrep110αβKO* islets, some of the PI3K p110α specific kinase activity still remained after RIPCre mediated recombination and disruption of p110α. However, no further reduction in p110β specific kinase activity was detected.
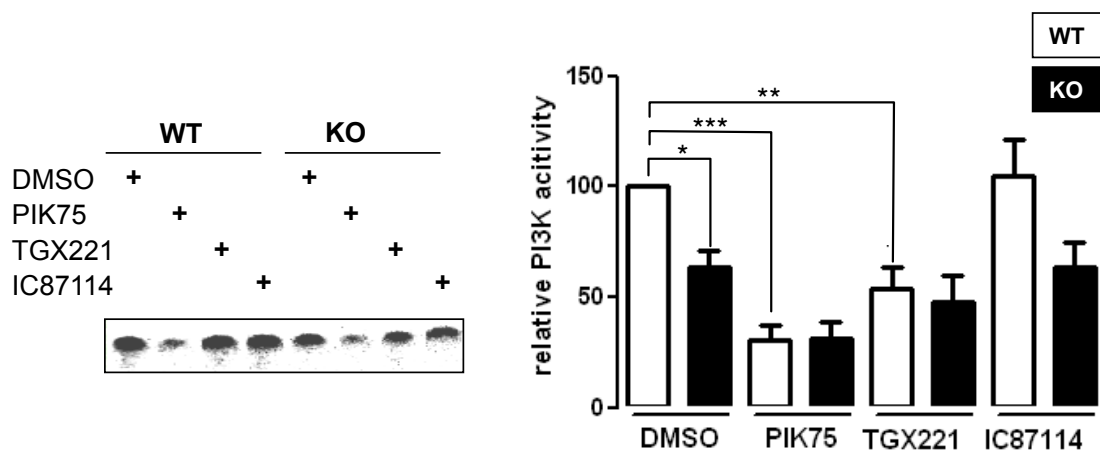
Figure 5.2: Lipid kinase activity in *RIPCrep110αβKO* and control islets. Total class IA activity was immunoprecipitated with p85 antibody from control or *RIPCrep110αβKO* islets. PI3K activity was then assayed in the presence of 100 nM of the indicated inhibitor or DMSO. PIK75 inhibits the p110α isoform, TGX221 inhibits the p110β isoform and IC87114 inhibits the p110δ isoform. A representative TLC profile as well as quantification of PI3K assays performed from independent determinations are shown (n=10 and 11 for KO and WT mice, respectively); Results are expressed relative to the activity in the presence of DMSO and presented as mean ± SEM, *P<0.05, **P<0.01 and ***P<0.001. Figure produced by C. Chaussade.

5.3 Glucose homeostasis in *RIPCre110αβKO* mice

Blood glucose concentrations of fasted, random fed and post-glucose injected *RIPCrep110αβKO* and control mice were measured to investigate glucose handling in these animals. *In vivo* glucose-stimulated insulin secretion was performed to assess insulin secretory function of pancreatic beta cells. Fasted and fed plasma insulin levels were measured and insulin tolerance tests performed to investigate insulin sensitivity in *RIPCrep110αβKO* mice.

5.3.1 Fasted/fed glucose

Fasted blood glucose levels were significantly increased in 12-week old *RIPCrep110αβKO* male mice (Figure 5.3). This indicates that the *RIPCrep110αβKO* mice are unable to handle glucose levels properly in fasting conditions. Random fed blood glucose levels in 8-week old *RIPCrep110αβKO* male mice were also significantly elevated, suggesting that blood glucose levels are not controlled sufficiently after feeding and *RIPCrep110αβKO* mice might be glucose intolerant (Figure 5.3).

5.3.2 Glucose tolerance

Glucose tolerance tests were performed on the male *RIPCrep110αβKO* mice and their littermate controls at 6- and 12-weeks of age (Figure 5.4). At 6-weeks of age *RIPCrep110αβKO* mice were significantly less glucose tolerant than control mice. At 12-weeks of age *RIPCrep110αβKO* mice displayed marked glucose intolerance: even 2 hours after glucose challenge the mean blood glucose levels were 18.7 mmol/L compared to 6.5 mmol/L in control mice.

5.3.3 Insulin sensitivity

Insulin sensitivity was assessed in *RIPCrep110αβKO* and control mice. Fasted and fed plasma insulin levels were measured to establish whether *RIPCrep110αβKO* mice are hypo/hypersecreting insulin. Both the fasted and fed plasma insulin levels were found to be normal, indicating that the *RIPCrep110αβKO* mice are not
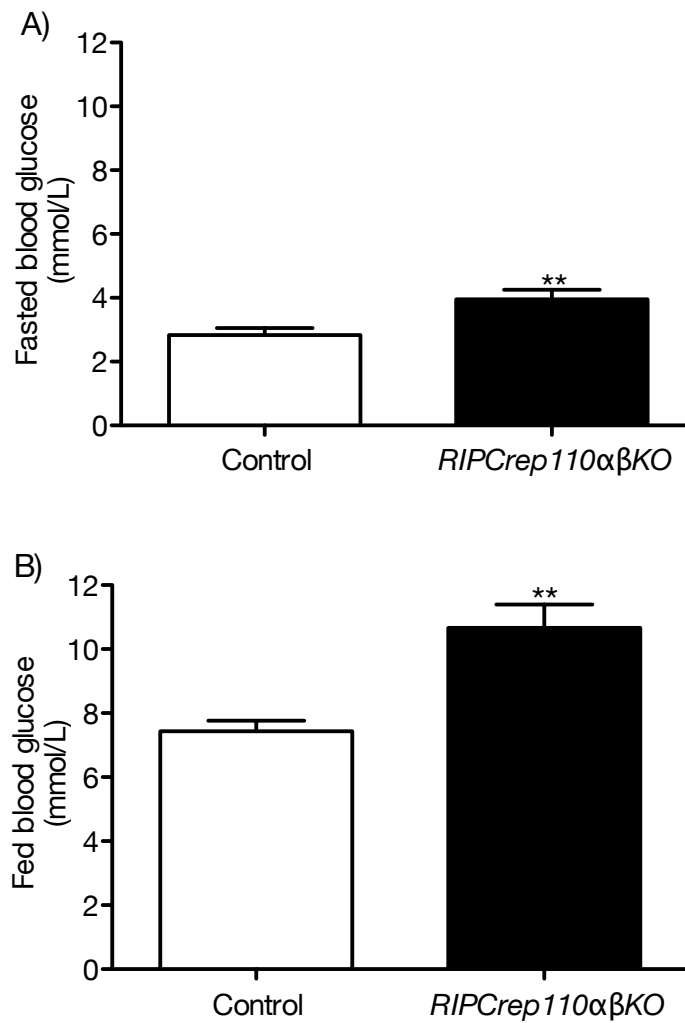
Figure 5.3: Fasted and fed blood glucose levels in *RIPCrep110αβKO* and control mice. (A) blood glucose levels after a 16-hr fast in 12-week old and (B) random fed blood glucose levels in 8-week old male mice (n = 8 vs 7). Bloods were collected from tail bleeds. Data shown are mean ± SEM, **P<0.01.
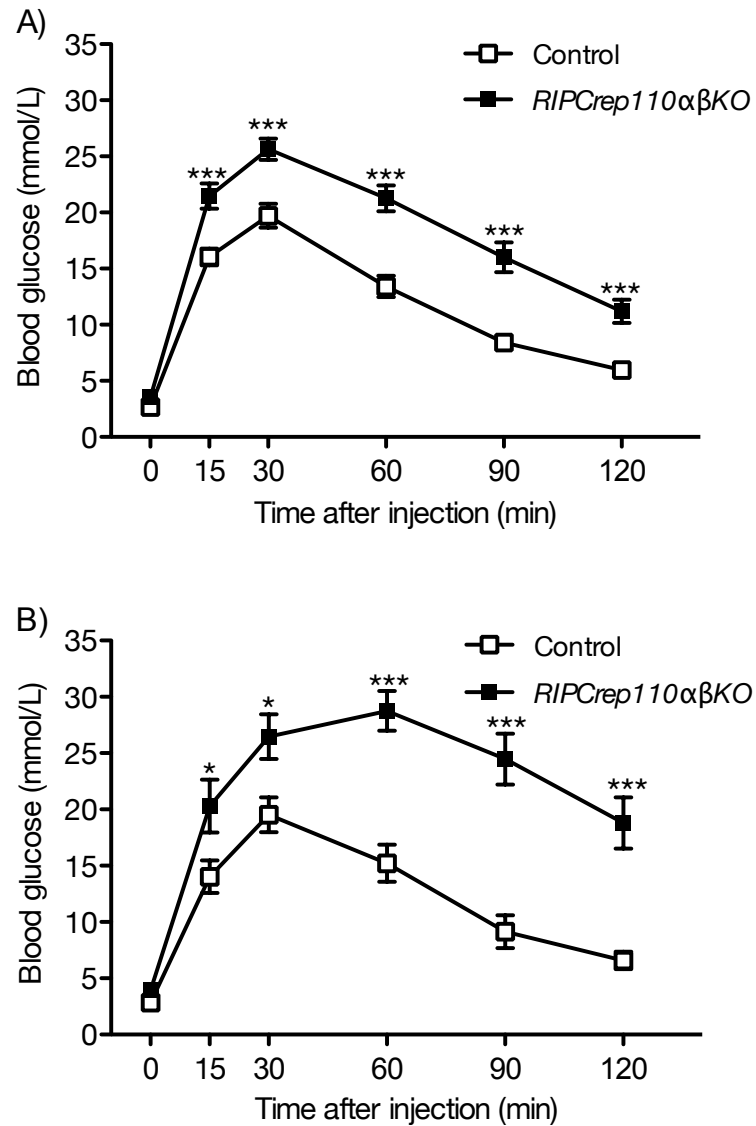
Figure 5.4: Glucose tolerance in *RIPCrep110αβKO* and control mice. Glucose tolerance test; blood glucose concentrations were measured from tail bleeds at indicated times after i.p. injection of 20 % D-glucose (2 g/kg); (A) 6-week old male mice (n= 21 vs 20) and (B) 12-week old male mice (n = 7 vs 8). Data shown are mean ± SEM, *P<0.05, **P<0.01 and ***P<0.001.

insulin resistant (Figure 5.5). To further confirm this, an insulin tolerance test was performed to measure insulin sensitivity of insulin target tissues. Glucose clearance in response to insulin was equivalent in *RIPCrep110αβKO*s compared to control animals (Figure 5.6). Together these results demonstrate normal insulin sensitivity in *RIPCrep110αβKO* mice.
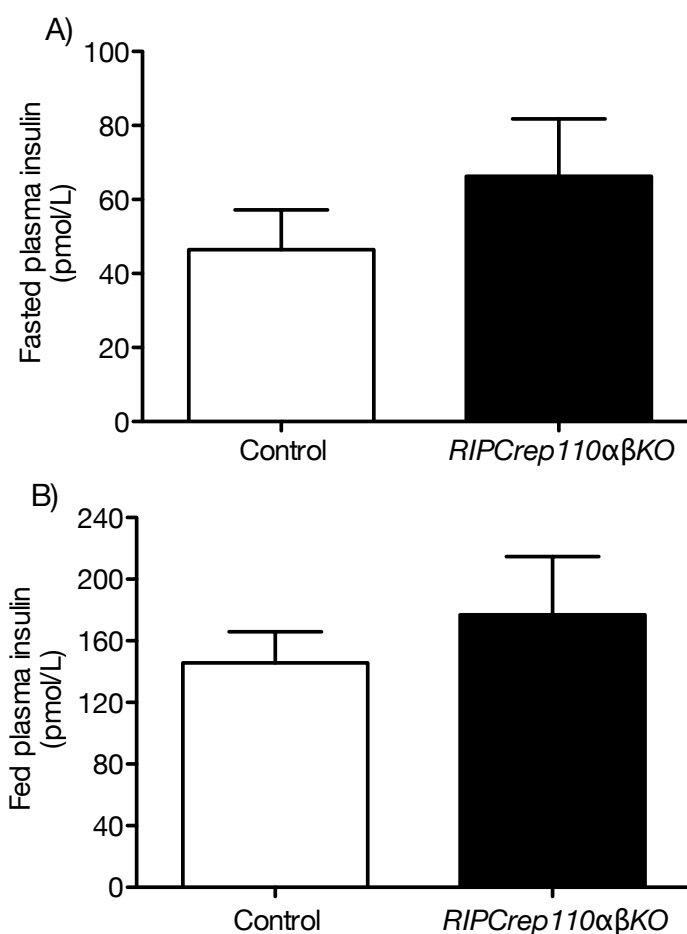
Figure 5.5: Fasted and fed plasma insulin levels in *RIPCre110αβKO* and control mice. A) Plasma insulin levels after a 16-hr fast in 12-week old and B) random fed plasma insulin levels in 8-week old male mice (n = 8 vs 7). Bloods were collected from tail bleeds and plasma insulin levels were measured with a Rat/Mouse Insulin Elisa Kit. Data shown are mean ± SEM.
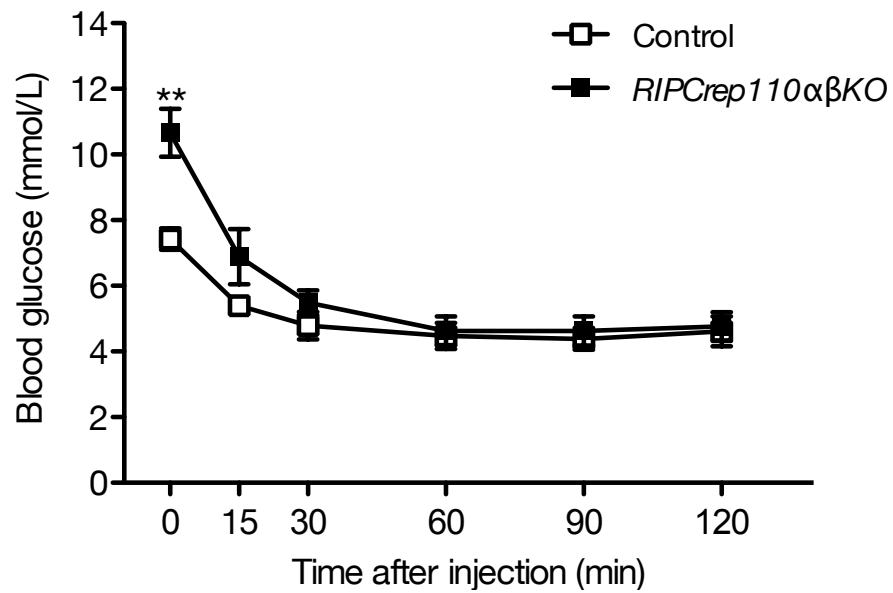
Figure 5.6: Insulin sensitivity in *RIPCrep110αβKO* and control mice. Blood glucose concentrations were measured from tail bleeds at indicated times after i.p. injection of insulin (0.75 mU/kg. Random fed, 8-week old male mice were used (n = 7 vs 8). Data shown are mean ± SEM, **P<0.01.

5.3.4   Glucose-stimulated insulin secretion *in vivo*

As the *RIPCrep110αβKO* did not show any signs of insulin resistance but were overly glucose intolerant it is likely that the impaired glucose tolerance is caused by defective glucose-stimulated insulin secretion from pancreatic beta cells. To detect any insulin secretory defects in *RIPCrep110αβKO* mice, a glucose-stimulated insulin secretion (GSIS) test was performed on 8-week old *RIPCrep110αβKO* and control mice. The test showed a significant difference between insulin secretion in response to glucose injection in *RIPCrep110αβKO* and control mice (Figure 5.7). This revealed that even though fasted insulin levels were equivalent to those measured in control mice, *RIPCre110αβKO* mice exhibited significantly impaired insulin secretory function in response to a glucose challenge. Both the first- and second phase of insulin secretion were significantly decreased in *RIPCrep110αβKO* mice, and the familiar secretion profile seen in control mice was almost completely lost in *RIPCrep110αβKO* mice.

5.4   Analysis of glucose-stimulated insulin secretion *in vitro*

RIPCrep110αβKO mice showed a clear defect in their insulin secretory function *in vivo*. However, because of the disruption in PI3K signalling in the hypothalamus, and in order to avoid any inter-tissue interaction, it was necessary to examine *RIPCrep110αβKO* islet function *in vitro* in order to confirm that the impaired glucose homeostasis phenotype observed *in vivo* was due to a defect specifically in islet GSIS. Islets isolated from *RIPCrep110αβKO* control mice were used to measure static glucose-stimulated insulin secretion (GSIS) *in vitro* (*ex vivo*) (Figure 5.8).

Control islets demonstrated a significant increase in insulin secretion between basal 2 mmol/L and stimulatory 20 mmol/L glucose concentration, as expected. *RIPCrep110αβKO* islets also showed a significant increase in insulin secretion between 2 mmol/L and 20 mmol/L glucose concentrations. However, the increase in insulin secretion between basal and stimulatory glucose concentrations in *RIPCrep110αβKO* islets was significantly less than in control islets.
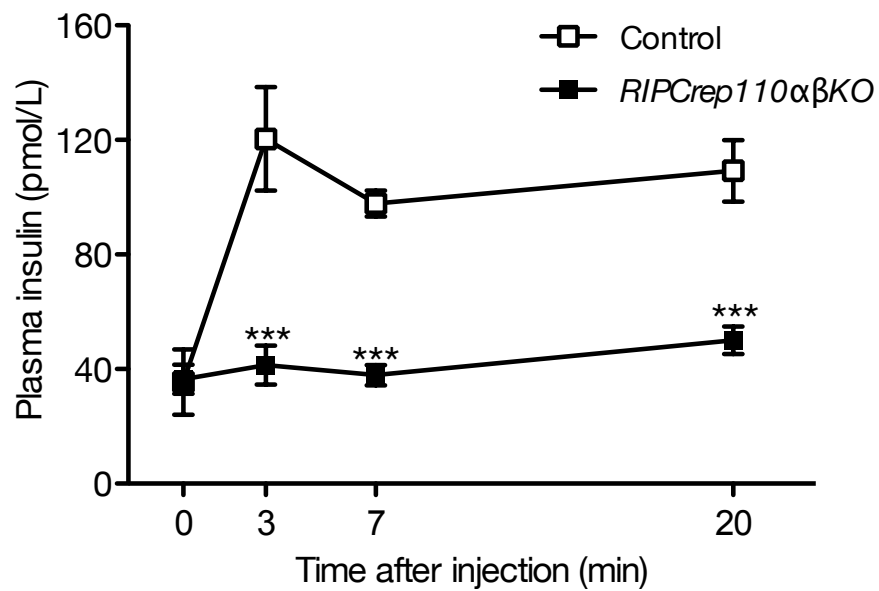
Figure 5.7: *In vivo* glucose-stimulated insulin secretion in *RIPCrep110αβKO* and control mice. Bloods were collected from tail bleeds at indicated times after i.p. injection of 20 % D-glucose (2 g/kg) and plasma insulin levels were measured with a Rat/Mouse Insulin Elisa Kit. 8-week old male mice used (n= 5 vs 6). Data shown are mean $\pm$ SEM, ***P<0.001.

At basal glucose concentration, insulin secretion was also significantly less in *RIPCrep110αβKO* islets than in control islets.
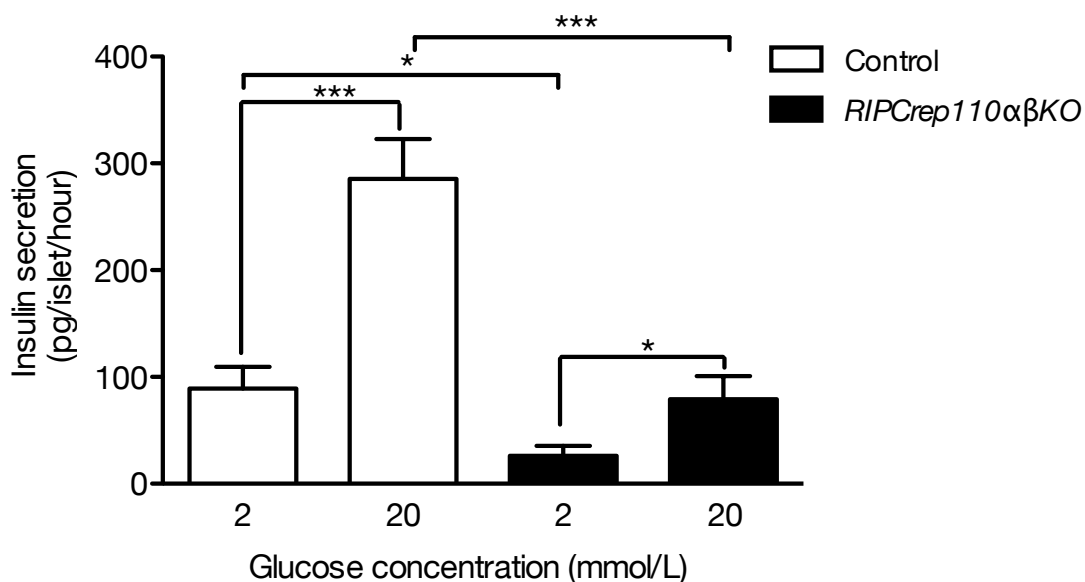
Figure 5.8: *In vitro* glucose-stimulated insulin secretion from *RIPCrep110αβKO* and control islets. Groups of 5 islets were incubated either in 2 or 20 mmol/L glucose for 1 hour and the amount of insulin secreted (as pg/islet/hour) was measured. Islets were isolated from 6 mice per genotype. 12-week old male mice were used. Data shown are mean ± SEM, *P<0.05 and ***P<0.001.

5.5 Beta cell morphology

The PI3K signalling pathway has been shown to be important for regulation of cell growth and survival. For example, deletion of the negative regulator of PI3K, PTEN, in mouse beta cells (*RIPCrePTENKO*) leads to increased beta cell proliferation, cell size and mass (Elghazi and Bernal-Mizrachi, 2009). On the other hand lack of IRS-2 in pancreatic beta cells (*PdxCreIRS-2KO*) decreases beta cell proliferation and leads to decreased beta cell mass and pancreatic insulin content (Cantley et al., 2007). Hence pancreatic and beta cell mass in *RIPCrep110αβKO*

and control mice were measured and islet density determined (Figures 5.9, 5.10). However, no alterations in pancreas or beta cell mass, or in islet density were found in *RIPCrep110αβKO* mice.
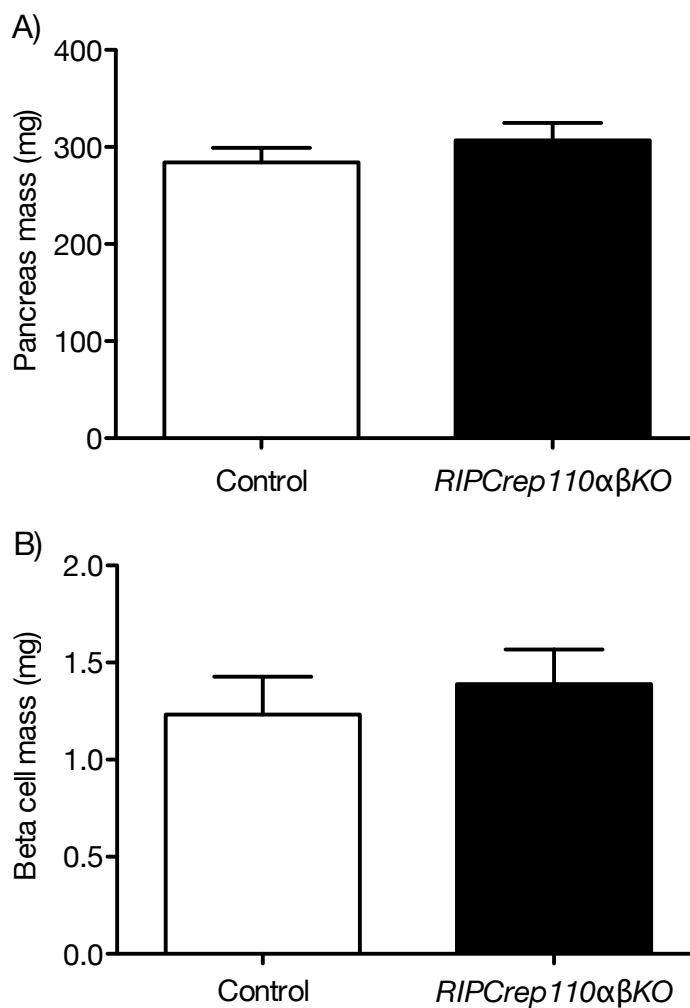
Figure 5.9: Pancreatic (A) and beta cell mass (B) in *RIPCrep110αβKO* and control mice. 12-week old male mice were used (A; n = 8 vs 7, B; n = 4 vs 4). Data shown are mean ± SEM.
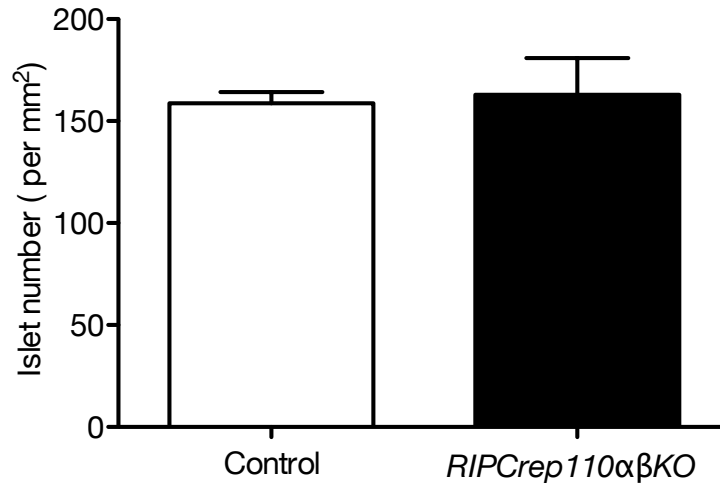
Figure 5.10: Islet density in *RIPCrep110αβKO* and control mice. Number of islets per mm^2 pancreas section. 12-week old male mice used. 12-week old male mice used (n = 4 vs 4). Data shown is mean ± SEM.

5.6 *RIPCre110αβKO* islet gene expression

Relative mRNA expression of genes involved in glucose uptake and PI3K signalling pathway were measured in *RIPCrep110αβKO* and control islets (Figure 5.11). Transcription of upstream and downstream molecules of the PI3K signalling cascade such as *Irs-1*, *Pten*, *Akt*, *FoxO1* and *Ins II* was normal. *Glut2* (i.e. *Slc2a2*) expression was also unaltered. Small increase in mRNA expression of *pyruvate dehydrogenase kinase 1* (*Pdk1*) was detected in *RIPCrep110αβKO* islets.
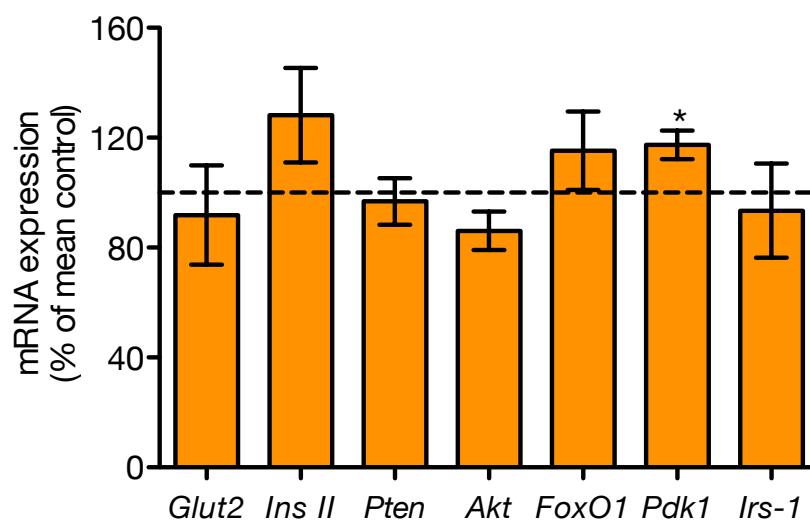
Figure 5.11: Expression of key beta cell genes in *RIPCrep110αβKO* and control islets. *Glut2* (*Slc2a2* (solute carrier family 2 [facilitated glucose transporter], member 2 gene), *Ins II* (Insulin II gene), *Pten* (Phosphatase and tensin homolog gene), *Akt* (Protein kinase B gene), *FoxO1* (Forkhead box O1 gene), *Pdk1* (Pyruvate dehydrogenase kinase, isoenzyme 1 gene), *Irs-1* (Insulin receptor substrate 1 gene). 16-week old male mice used (n = 8 vs 6). Data shown is mean $\pm$ SEM, *P<0.05.

5.7 Investigation of energy homeostasis in *RIPCrep110αβKO*

5.7.1 Body weight

As described above, the RIPCre transgene deletes in a small population of hypothalamic neurons. *RIPCreIRS-2KO* mice showed a marked hypothalamic phenotype such as increased body weight and body fat, and increased food intake (Choudhury et al., 2005). Hence it was important to characterise hypothalamic function in *RIPCrep110αβKO* mice as changes in hypothalamic activity was expected based on previous studies.

RIPCrep110αβKO mice had significantly increased body weight from 8-weeks of age onwards (Figure 5.12). This was observed both in male and female mice, however only male data are shown. All other experiments used for assessment of hypothalamic function were only performed in male mice in order to reduce animal usage (three Rs, Home Office Animal Act 1986).

5.7.2 Body length

When just visually inspecting *RIPCrep110αβKO* mice, they appeared bigger and longer (Figure 5.13). Measurement of naso-anal body length (cm) showed that *RIPCrep110αβKO* mice were significantly longer than control mice (Figure 5.14).

5.7.3 Body composition

Even though *RIPCrep110αβKO* mice were heavier, they did not just appear fatter than control mice but bulkier overall, which is usually a sign of a disrupted melanocortin signalling Butler (2006); Huszar et al. (1997). Hence a dual energy X-ray absorptiometry (DEXA) scan was performed which showed that *RIPCrep110αβKO* mice had significantly increased lean and fat tissue mass and about 28 % increase in body fat % (Figure 5.15). The mice also had significantly increased bone mineral density (g/cm^2) and bone mineral content (g) (Figure 5.15).
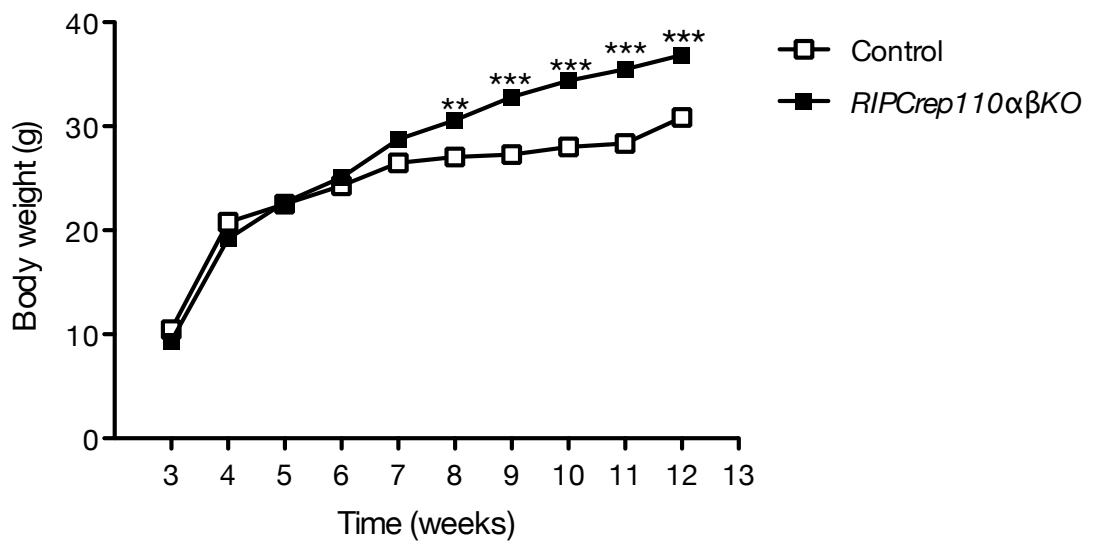
Figure 5.12: Body weight curve for male *RIPCrep110αβKO* and control mice. Data shown are mean ± SEM (n = 15-20 mice per genotype), **P<0.01 and ***P<0.001.
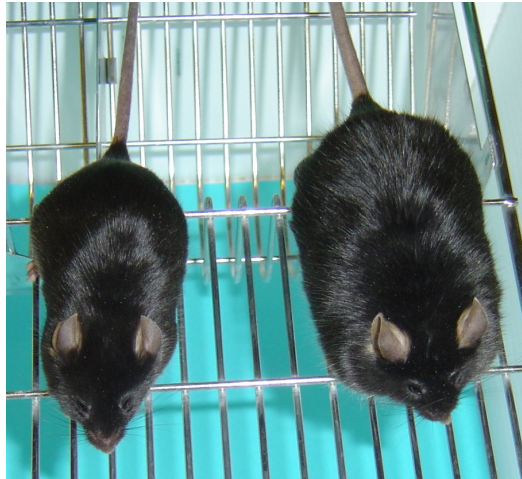
Figure 5.13: Photograph of male (A) and female (B) *RIPCre110αβKO* (right) and control (left) mice at 16 weeks and 12 months of age respectively.
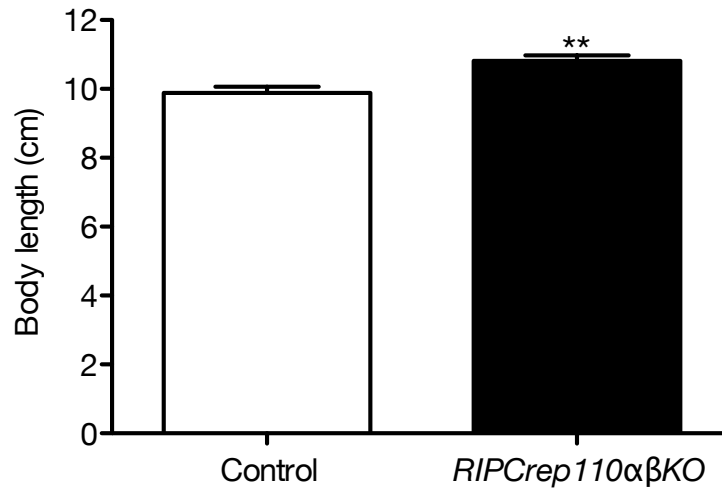
Figure 5.14: Naso-anal body length (cm) in *RIPCre110αβKO* and control mice. 10-month-old male mice used (n = 8 vs 7). Data shown are mean ± SEM, **P<0.01.

5.7.4 Expression of neuropeptides in *RIPCrep110αβKO*

Because of the hypothalamic expression of kinase dead p110α and p110β genes in RIPCre neurons of *RIPCrep110αβKO* mice, expression levels of key hypothalamic neuropeptides *AgRP*, *Npy* and *Pomc* were measured in the hypothalamus of *RIPCrep110αβKO* and control mice [1]. Both the mRNA expression of *AgRP* and *Pomc* were significantly reduced in the hypothalamus of *RIPCrep110αβKO* mice (Figure 5.16).

5.7.5 Fasted leptin

Circulating plasma leptin levels are usually proportional to body fat mass. Because *RIPCrep110αβKO* mice had increased body fat %, fasted plasma leptin levels (ng/ml) were measured, which showed that *RIPCrep110αβKO* mice had significantly increased fasted plasma leptin levels (Figure 5.17).

---

[1]Experiment and figure produced by H. Al-Qassab at UCL
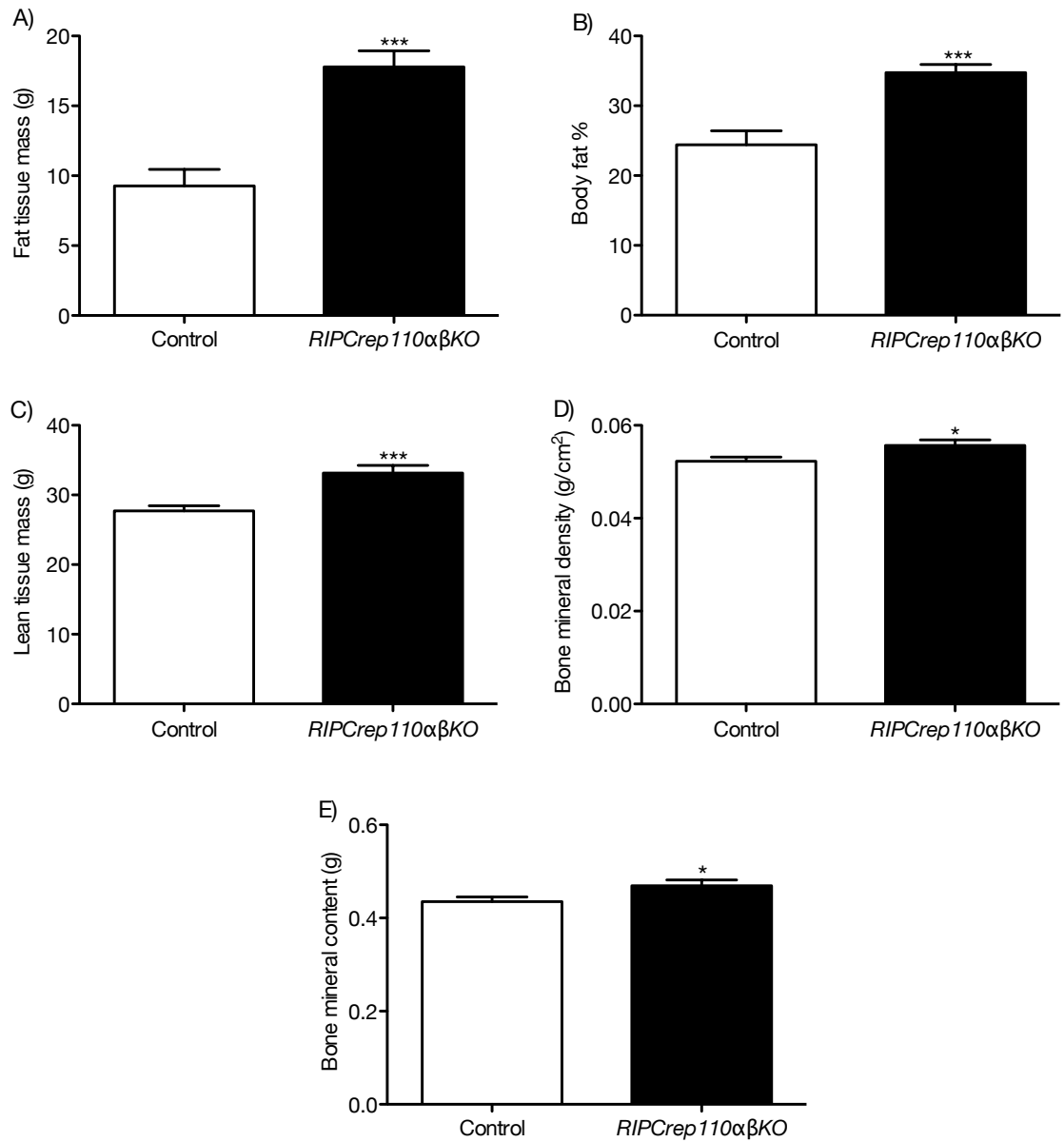
Figure 5.15: Body composition analysis by DEXA scan in *RIPCrep110αβKO* and control mice. (A) Fat tissue mass, (B) Body fat %, (C) Lean tissue mass (g), (D) Bone mineral density (g/cm^2) (g), (E) Bone mineral content (g). 10-month-old male mice used (n = 8 vs 7). Data shown are mean $\pm$ SEM, *P<0.05 and ***P<0.001.
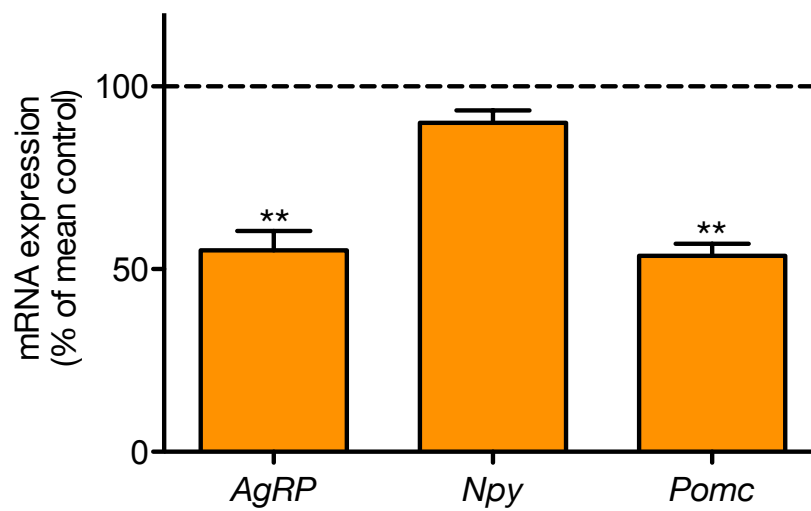
Figure 5.16: Expression of hypothalamic neuropeptides in *RIPCrep110αβKO* and control hypothalami. *AgRP* (Agouti-related peptide gene), *Npy* (neuropeptide Y gene) and *Pomc* (pro-opiomelanocortin gene). 16-week-old male mice used (n = 8 vs 8). Data shown are mean ± SEM, **P<0.01. Figure produced by H. Al-Qassab.
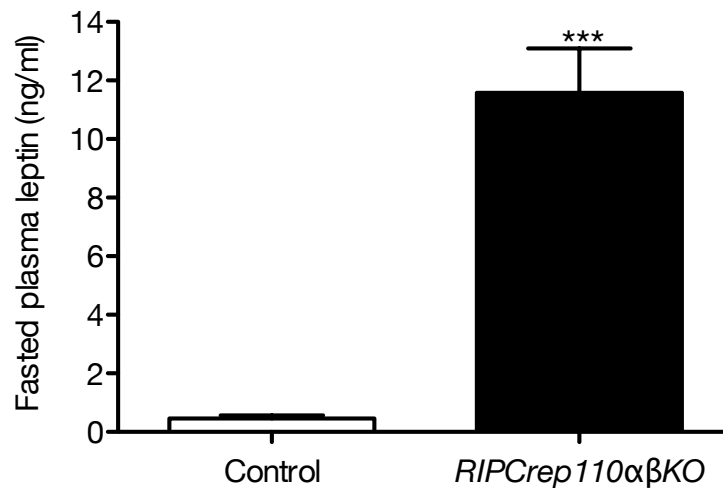
Figure 5.17: Plasma leptin levels after a 16-hr fast in *RIPCrep110αβKO* and control mice. 12-week old male mice were used (n = 8 vs 7). Blood was collected from tail bleeds and plasma leptin levels were measured with a Rat/Mouse Leptin Elisa Kit. Data shown are mean ± SEM with unpaired student t-test ***P<0.001.

5.7.6 Feeding behaviour

Because *RIPCrep110αβKO* mice were much heavier and had increased body fat it was obvious to investigate the feeding behaviour of *RIPCrep110αβKO* mice. Interestingly, 24-hr food intake and feeding behaviour for 24-hrs after a overnight fast were found to be normal in *RIPCrep110αβKO* mice in comparison to control mice (Figures 5.18, 5.19). There was significantly decreased food intake in *RIPCrep110αβKO* mice 8-hr after re-feeding. However, when considering the overall feeding behaviour over the 24-hr period it is quite safe to conclude that there are not any difference in feeding behaviour in response to an overnight fast.
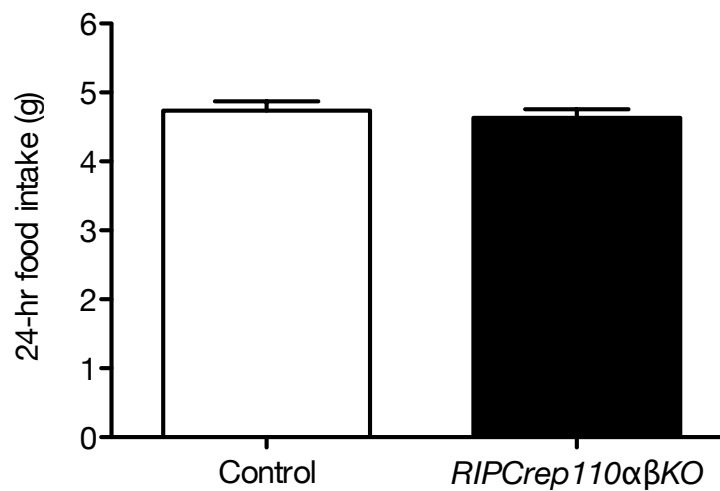
Figure 5.18: 24-hr food intake in *RIPCre110αβKO* and control mice. 12-week old male mice were used (n = 8 vs 7). Data shown are mean ± SEM.

5.7.7 Basal metabolic rate

Because *RIPCrep110αβKO* mice were shown to have a normal feeding behaviour their basal metabolic rate was measured in order to determine whether increased body weight was due to a slower basal metabolic rate. However, no difference was detected between *RIPCrep110αβKO* and control mice (Figure 5.20).
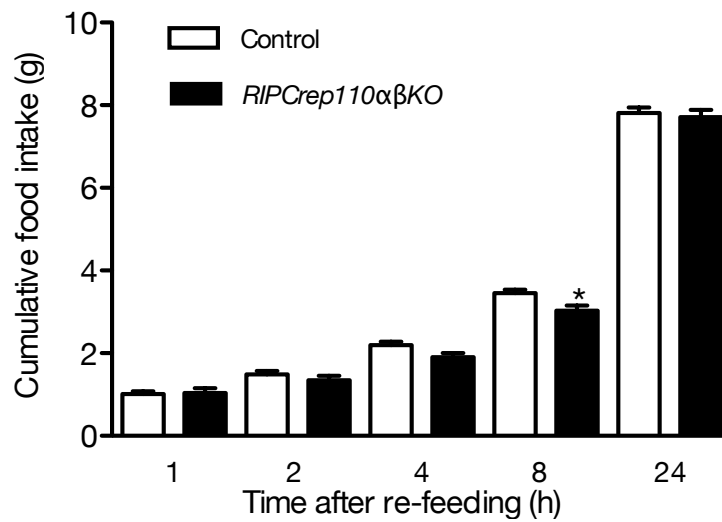
Figure 5.19: Feeding behaviour after a 16-hr fast in *RIPCrep110αβKO* and control mice. 16-week old male mice were used (n = 8 vs 7). Data shown are mean ± SEM, *P<0.05.
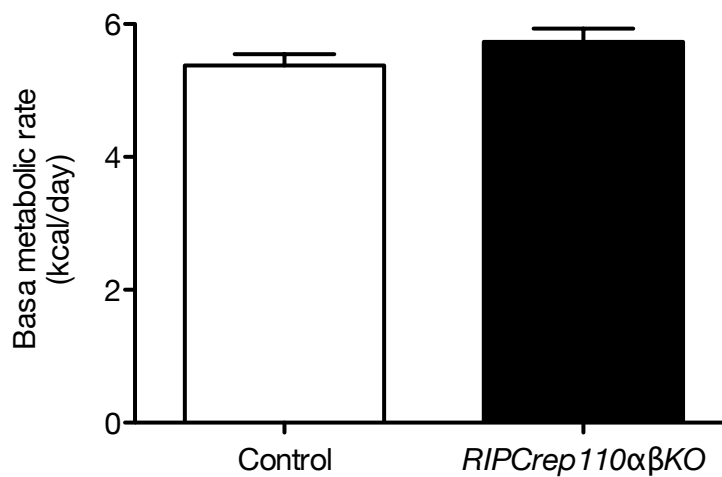
Figure 5.20: Basal metabolic rate in *RIPCrep110αβKO* and control mice. 16-week old male mice were used (n = 8 vs 7). Data shown are mean ± SEM.

5.7.8 Leptin sensitivity

Circulating plasma leptin levels are usually found to be increased in obesity (El-Haschimi et al., 2000). However, this does not mean that leptin could have a greater effect in suppressing appetite in obese subject. In fact, it is usually the opposite as obese subject are often found to be leptin resistant, meaning that leptin binding to leptin receptors does not activate the leptin receptor signalling cascade.

Hence, mice were treated with vehicle or leptin and their feeding behaviour in response to leptin treatment was investigated (Figure 5.21). As can be seen, both control and *RIPCrep110αβKO* mice lost body weight and had decreased food intake when treated with leptin in comparison to vehicle treatment. However, *RIPCrep110αβKO* mice ate significantly more when treated with leptin than control mice, even though the food intake was still less than when treated with vehicle. This indicates that there is some degree of leptin resistance in *RIPCrep110αβKO* mice but leptin still has a significant impact on reducing food intake in *RIPCrep110αβKO* mice.

5.7.9 MT-II sensitivity

Melanocortin signalling also has an important role in controlling feeding behaviour and adiposity. MT-II is a melanocortin receptor agonist that reduces food intake (Seeley et al., 2005). *RIPCrep110αβKO* and control mice were injected with MT-II or vehicle and their food intake was measured for a 24-hr period after an overnight fast. MT-II had a similar effect of reducing food intake in both *RIPCrep110αβKO* and control mice in comparison to vehicle (Figure 5.22). The effect of MT-II was greatest within the first 4 hr after re-feeding, when there was a significant reduction in food intake in *RIPCrep110αβKO* and control mice.
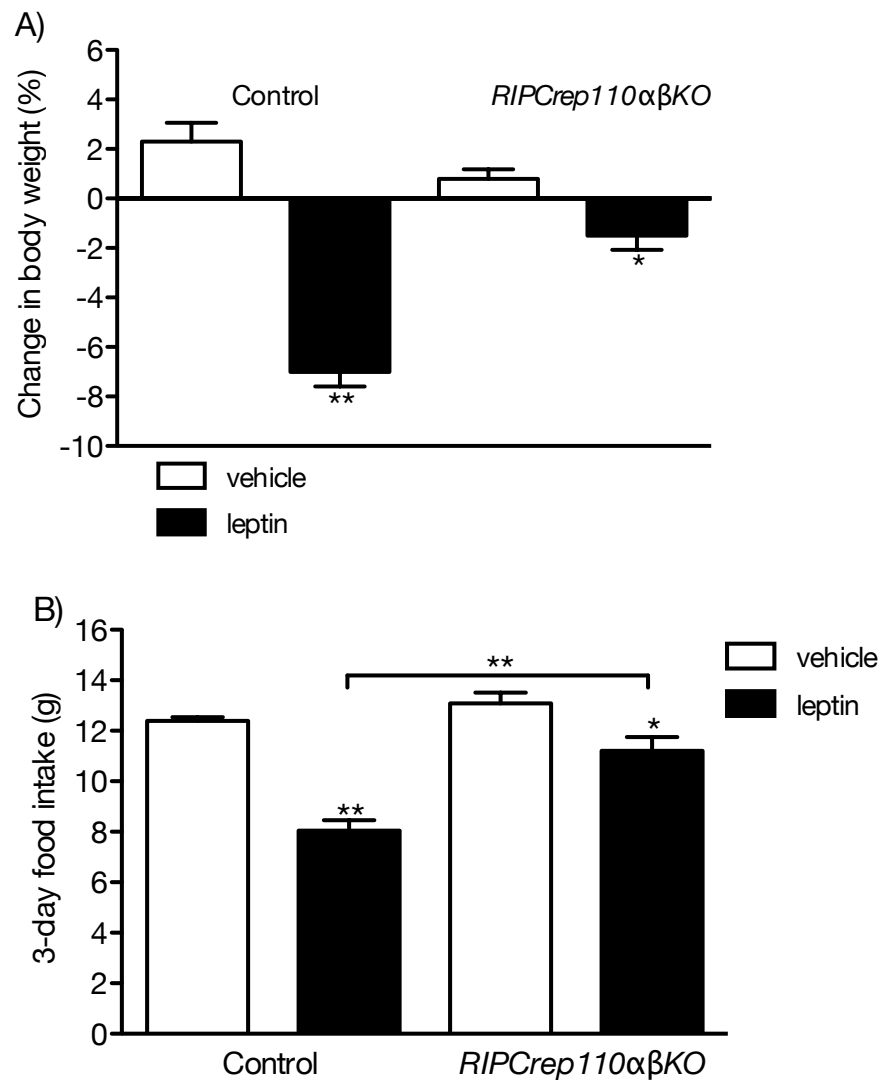
Figure 5.21: Leptin sensitivity in *RIPCrep110αβKO* and control mice. The response to 3 day i.p. administration of leptin (5 μg/g) upon (A) body weight and (B) food intake in 17-week old male mice (n = 8 vs 7). Data shown are mean $\pm$ SEM, *P<0.05 and **P<0.01.
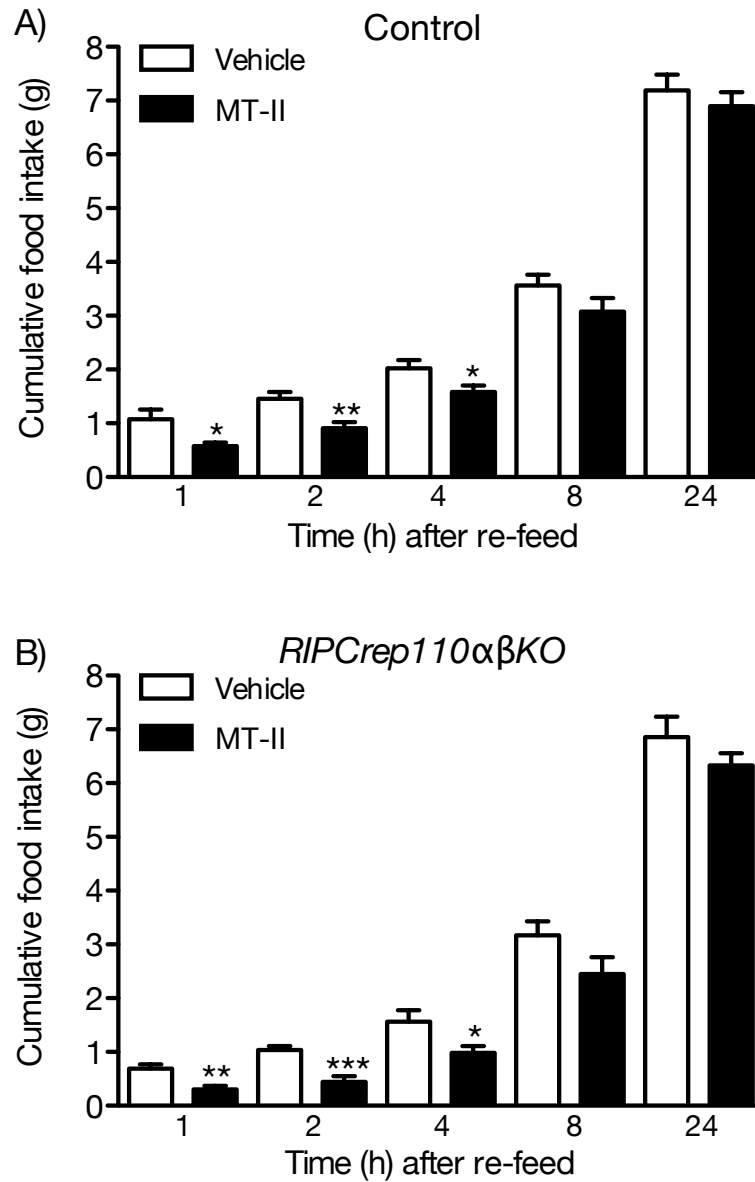
Figure 5.22: MT-II sensitivity in *RIPCrep110αβKO* (B) and control (A) mice. Cumulative food intake at the times indicated after an i.p. administration of vehicle or MT-II following an overnight fast (0.5 μg/g) in 15-week old male mice (n = 8 vs 7). Data shown are mean ± SEM, *P<0.05, **P<0.01 and ***P<0.001.

5.8 Summary

5.8.1 Analysis of deletion

RIPCre mediated recombination of floxed *p110α* and floxed *p110β* catalytic subunits of the PI3K was proven successful. Islet mRNA expression levels of *p110α*, *p110β* and *p85* were unchanged in *RIPCrep110αβKO* mice in comparison to control mice, confirming that recombination of the loxP sites does not change transcription of the catalytic or regulatory subunits, and the stoichiometry between the regulatory and catalytic subunits remains normal. Lipid kinase assay from *RIPCrep110αβKO* and control islets showed that kinase activity was significantly reduced in *RIPCrep110αβKO* islets. Hence, it can be concluded that *RIPCrep110αβKO* mouse is a sufficient model to study the role of PI3K catalytic isoforms p110α and p110β in pancreatic beta cells and their effect on whole-body glucose homeostasis. Because the Cre-recombinase expression is driven from the rat insulin promoter, *RIPCrep110αβKO* mouse can also give new insight to the role of PI3K signalling in the insulin expressing neurons of the hypothalamus.

5.8.2 Glucose homeostasis

Glucose homeostasis was severely impaired in *RIPCrep110αβKO* mice. The mice showed significant glucose intolerance at an early age, and by 12-weeks of age the mice had developed a clear diabetic phenotype characterised by fasting hyperglycaemia and marked glucose intolerance. Glucose clearance in response to exogenous insulin was normal, and fasted and fed plasma insulin levels were unchanged, indicating that impaired glucose homeostasis in *RIPCrep110αβKO* mice was not caused by insulin resistance. *In vivo* glucose-stimulated insulin secretion was markedly decreased, with a significant reduction in both the first- and second phase of insulin secretion, suggesting that glucose intolerance was caused by reduced insulin secretion.

5.8.3 Glucose-stimulated insulin secretion *in vitro*

Static incubation of *RIPCrep110αβKO* and control islets at basal (2 mmol/L) and stimulatory (20 mmol/L) glucose concentrations showed that *RIPCrep110αβKO* islets secrete significantly less insulin at both glucose concentrations. This also supports the *in vivo* findings, meaning that glucose intolerance and impaired insulin secretion is due to an intrinsic defect in insulin secretion in *RIPCrep110αβKO* islets.

5.8.4 Pancreas morphology and gene expression of PI3K signalling molecules in *RIPCre110αβKO* mice

Pancreas and beta cell mass, as well as islet density, were all normal in *RIPCrep110αβKO* mice. Gene expression of upstream and downstream signalling molecules of the PI3K signalling pathway were unaltered. However, mRNA expression of *pyruvate dehydrogenase kinase-1* (Pdk1) was increased $\approx$ 20 % in *RIPCrep110αβKO* in comparison to control islets.

5.8.5 Metabolic studies

Simultaneous disruption of p110α and p110β catalytic isoforms in RIPCre neurons of the hypothalamus alters energy homeostasis in *RIPCrep110αβKO* mice. In general, *RIPCrep110αβKO* mice are bigger in size and display increased body weight from 8-weeks onwards. *RIPCrep110αβKO* mice also have increased body fat % and increased skeletal and bone mass. Hypothalamic mRNA expression of *Pomc* and *AgRP* neuropeptides is also significantly reduced in *RIPCrep110αβKO* mice. However, they have a normal feeding behaviour, and their sensitivity to melanocortin receptor agonist MT-II is normal. Basal metabolic rate was also unchanged in these animals. Plasma leptin levels were significantly increased in the *RIPCrep110αβKO* mice, and even though intraperitoneal leptin administration resulted in reduced food intake, the reduction was significantly less than in control animals, indicating a mild leptin resistance in the *RIPCrep110αβKO* mice. Therefore it can be concluded that disruption of p110α and p110β signalling in RIPCre neurons causes abnormal energy homeostasis within the whole animal,

characterised by increased body mass, increased plasma leptin levels and mild leptin resistance.

5.8.6 Conclusion

Results in this chapter establish a vital role for PI3K in whole-body glucose homeostasis. To conclude, *RIPCrep110αβKO* mice are hyperglycaemic and develop severe glucose intolerance at young age. This is caused by impaired glucose-stimulated insulin secretion from pancreatic beta cells. Because beta cell mass and islet density are unchanged in these mice, it seems that the impaired insulin secretion from the *RIPCrep110αβKO* beta cells is caused by defects in yet unidentified downstream signalling cascades from PI3K that are involved in the regulation of insulin secretion, but not in cell growth. *RIPCrep110αβKO* also exhibit a significant hypothalamic phenotype that is seen as a general increase in body size and body fat %. The mice are also hyperleptinaemic and mildly leptin resistance, however, they have a normal feeding behaviour. Thus, results in this chapter also highlight a significant role for PI3K in RIPCre expressing neurons in the regulation of body growth and leptin receptor signalling.

Chapter 6

Discussion

6.1 The involvement of AMPK in pancreatic beta cells

AMPK has been the focus of intense investigation to determine its role in whole-body energy homeostasis. Much of the previous work has investigated the role of AMPK in distinct cells, tissues and organ systems to determine the specific role of AMPK in glucose homeostasis. In liver and skeletal muscle AMPK improves glucose homeostasis by stimulating glucose uptake and oxidation, and inhibiting hepatic gluconeogenesis (Fryer et al., 2002; Kurth-Kraczek et al., 1999; Lochhead et al., 2000; Merrill et al., 1997). AMPK is thought to be a target for a commonly prescribed anti-diabetic drug metformin which has been shown to activate AMPK (Fryer et al., 2002). It is believed that many of the beneficial effects, such as reduced blood glucose levels of metformin is achieved by activation of AMPK, although recent genetic evidence suggest that AMPK is not a sole effector of metformin (Foretz et al., 2010; Fryer et al., 2002; Hinke et al., 2007). Nevertheless, a direct activator (A-769662) of AMPK has been shown to have beneficial metabolic effects, for example improvement of plasma glucose and lipid levels in *ob/ob* mice (Cool et al., 2006a). Hence AMPK has an interesting role as a pharmacological target for treatment of T2DM. However, even though activation of AMPK in peripheral tissues has a positive impact on glucose homeostasis and on the treatment of T2DM, it is unclear whether its activation in pancreatic beta

cells has an adverse effect in terms of regulation of insulin secretion and glucose homeostasis.

AMPK functions as a cellular energy regulator and its activity is linked to changes in the cellular ATP/AMP ratio. Therefore it seems likely that AMPK could have a key role in the regulation of beta cell function and insulin secretion as these are dependent on changes in cellular adenosine nucleotide levels (Carling, 2004). The role of AMPK in pancreatic beta cells has been of great interest for several years. However, despite the numerous studies conducted over the years, no clear conclusion has been made yet and discrepancies between the studies exist, especially about the role of AMPK in the regulation of insulin secretion. The reasons explaining the discrepancies could be caused by the use of different beta cell lines (INS-1, MIN6) and use of different dominant negative forms of AMPK that might have different substrate specificities (Rutter and Leclerc, 2008).

Surprisingly, islets isolated from *AMPKα2*-global-null mice did not show any intrinsic beta cell defect in glucose- or arginine-stimulated insulin secretion despite glucose intolerance and decreased plasma insulin levels (Viollet et al., 2003a,b). As increased urine catecholamine levels were measured in these mice, it was argued that the impaired glucose handling and lower plasma insulin levels were due to alterations in the sympathetic nervous system (Viollet et al., 2003a,b). Even though this study did indicate that AMPKα2 is important for whole-body glucose homeostasis, it did not give specific insight into the role of AMPK in beta cells. Hence, I generated two transgenic mice lines: *RIPCreα2KO* and *α1KORIPCreα2KO*. The former lacks *AMPKα2* in beta cells and in a poorly defined population of RIPCre expressing hypothalamic neurons, and the latter is deficient in *AMPKα2* as the other created mouse line, but also has global deletion of *AMPKα1*.

6.2 Deletion of AMPK in beta cell - the impact on whole-body physiology

To achieve deletion of *AMPKα2* in beta cells, mice expressing a Cre-recombinase from Rat insulin promoter 2 (RIP) were crossed with mice carrying a loxP targeted *AMPKα2* gene. RIPCre, rather than PdxCre (Cre expression driven from the Pancreas duodenal homeobox 1 promoter) was used, as at the time when this study was started, the RIPCre provided the best deletion efficiency in the beta cells. For example a study by Cantley et al. (2009) reported RIPCre mediated deletion in 95 % of the beta cells and PdxCre mediated deletion only in 70 % of the beta cells. In addition, RIPCre deletes specifically in the beta cells, whereas PdxCre deletes also in the other endocrine cells as well as the epithelial cells of the pancreas (Dessimoz et al., 2005). RIPCre mediated gene deletion also occurs in a population of hypothalamic neurons located in the arcuate, lateral and ventromedial hypothalamus (Choudhury et al., 2005). Therefore a hypothalamic phenotype arising in RIPCre mice is always a possibility that has to be accounted for. However, deletion of *AMPKα2* in RIPCre neurons did not cause any significant hypothalamic energy homeostasis phenotype in *RIPCreα2KO* mice, as no alteration in body weight, food intake or expression of hypothalamic feeding peptides were observed. Similarly, normal body weight and food intake were recorded in the *α1KORIPCreα2KO* mice.

RIPCreα2KO mice display a defective glucose homeostasis with a mild, age-dependent deteriorating glucose intolerance caused by a marked defect in glucose-stimulated insulin secretion. Overall the whole body phenotype is mild in the *RIPCreα2KO* mice. This could be due to compensation by the AMPKα1 subunit, alternated regulation by the CNS or by trans-tissue compensation, with glucose disposal being impaired in other tissues. However, normal peripheral insulin sensitivity was measured in *RIPCreα2KO* mice. Hence, *α1KORIPCreα2KO* mice were generated to rule out any compensatory effect by AMPKα1.

As with the *RIPCreα2KO* no hypothalamic phenotype was observed in the *α1KORIPCreα2KO* mice as they also had a normal body weight and feeding behaviour. Deletion of both the AMPK catalytic subunits led to a significant

defect in glucose homeostasis. At 5 weeks of age, the $\alpha1KORIPCre\alpha2KO$ mice exhibited markedly impaired glucose intolerance, caused by a significant defect in glucose-stimulated insulin secretion (GSIS). The impaired GSIS showed that the $\alpha1KORIPCre\alpha2KO$ mice secreted significantly less insulin compared to the control mice in response to glucose, and the mice lacked the commonly distinguishable first- and second phases of insulin secretion. As the $AMPK\alpha1$-global-null mice did not have a defect in their glucose homeostasis (Viollet et al., 2003a,b), it can be concluded that the phenotype reported here is most likely due to the deletion of both the subunits specifically in beta cells. Hence from the *in vivo* data it can be concluded that AMPK participates in the regulation of glucose-stimulated insulin secretion and lack of AMPK in beta cells impairs GSIS, which leads to a defect in glucose homeostasis.

When I started to study the $RIPCre\alpha2KO$ and $\alpha1KORIPCre\alpha2KO$ mice, no other transgenic animal models of beta cell specific AMPK existed. However, as our study was in the process of being published, Sun et al. (2010a) reported a study of $\beta AMPKdKO$ mice (AMPKα1 and AMPKα2 deficiency in beta cells using RIPCre and $AMPK\alpha1$-global-null mice). Similarly to my study, Sun et al. (2010a) reported an impaired glucose homeostasis phenotype along with a reduced *in vivo* GSIS. This is consistent with the physiology reported in the $AMPK\alpha2$-global-null mice that had impaired glucose homeostasis and defective insulin secretion *in vivo* (Viollet et al., 2003a,b). Sun et al. (2010a) also reported a normal hypothalamic function in their $\beta AMPKdKO$ mice, further confirming that RIPCre is a suitable system to study AMPK function in beta cells at the whole-body physiological level.

6.3   Normal islet morphology in $RIPCre\alpha2KO$ mice

Defects in GSIS could reflect either a change in beta cell mass or morphology or a functional defect within the beta cells. LKB1, the upstream kinase on the LKB1/AMPK pathway has been implicated in the regulation of beta cell mass

and islet morphology. For example, deletion of LKB1 in adult mice using inducible PdxCre led to a 65 % increase in beta cell size, and a change in cell polarity resulting in altered intracellular organisation of the nucleus and cilia in relation to the capillary blood vessels (Granot et al., 2009). Another study by Sun et al. (2010b) using the *RIPCreLKB1KO* mice also showed significantly increased beta cell size, increased cell proliferation and change in cell polarity. The phosphorylation levels of the LKB1 downstream kinase AMPK were significantly reduced in both studies. AMPK has been shown to inhibit the mTOR signalling pathway, the major regulator of cell growth and protein synthesis (Gleason et al., 2007). Hence the increased beta cell size was thought to be caused by reduced AMPK activity and subsequently increased mTOR signalling, measured as increased phospho-rpS6 and decreased phospho-4E-BP1 levels (Granot et al., 2009; Sun et al., 2010b).

In contrast to the LKB1 KO mice, I found no defect in beta cell mass or islet organisation in the *RIPCreα2KO* mice suggesting that this did not contribute in to the beta cell defect. In a separate study by Sun et al. (2010a) using the *βAMPKdKO* mice, beta cell mass was also found to be normal. However rather confusingly, Sun et al. (2010a) reported increased beta cell proliferation but decreased beta cell and islet size in *βAMPKdKO* mice. In contrast to the beta cell specific LKB1 KO studies, this was not accounted for altered mTOR signalling as the phosphorylation of rpS6 was unchanged (Sun et al., 2010a).

6.4 Lack of AMPK in beta cells impairs *in vitro* GSIS

Normal beta cell mass in *RIPCreα2KO* mice suggests a functional defect in terms of glucose sensing and insulin secretion in response to glucose. At basal (2 mmol/L) glucose concentration, islets isolated from the *RIPCreα2KO* and *α1KORIPCreα2KO* mice secreted significantly more insulin in comparison to control islets. This may suggest that AMPK has a role in beta cells sensing hypoglycaemia, as it is important to suppress insulin release. These data are also

consistent with the studies, in which beta cells or islets expressing a DN form of AMPK have increased insulin secretion in response to low glucose (da Silva Xavier et al., 2000; Leclerc et al., 2004). It has also been shown that in the ventromedial hypothalamus (VMH), AMPK has a key regulatory role in response to hypoglycaemia, when it will activate mechanisms that restore glucose concentration back to normal levels (Mccrimmon et al., 2007).

In contrast to my findings, islets isolated from the $AMPK\alpha2$-global-null mice did not show any significant difference in insulin secretion at low glucose concentration (Viollet et al., 2003a,b). Furthermore, Sun et al. (2010a) reported no alteration in insulin secretion in response to low glucose in $\beta AMPKdKO$ islets. However, if the GSIS data from the $AMPK\alpha2$-global-null islets is examined carefully, a clear trend towards increased insulin secretion at low glucose can be seen. Nonetheless, in both of the previous studies, the lowest glucose concentration used to stimulate insulin secretion was 3 mmol/L, rather than 2 mmol/L that I have used. Perhaps 1 mmol/L difference in glucose concentration is an important factor in this context. Because such a low glucose level is not normally achieved at whole-body physiological level, unless using a hypoglycaemic clamp, we cannot detect increased insulin secretion in fasted $RIPCre\alpha2KO$ and $\alpha1KORIPCre\alpha2KO$ mice. Also, the presence of other nutrients and compensatory mechanisms *in vivo* can provide other means for stimulating insulin release.

At a high (20 mmol/L) glucose concentration $RIPCre\alpha2KO$ and $\alpha1KORIPCre\alpha2KO$ islets secreted significantly less insulin in comparison to control islets. When the insulin secretion at high glucose was presented as pg/islet/hour in $RIPCre\alpha2KO$ islets, only a trend towards decreased insulin secretion was seen. However, in the $\alpha1KORIPCre\alpha2KO$ islets a significant decrease in insulin secretion was measured as pg/islet/hour. When the insulin secretion at high glucose was represented as an increment fold change over the basal insulin secretion, over a 10-fold increase in insulin secretion was measured in control islets. In the $RIPCre\alpha2KO$ and $\alpha1KORIPCre\alpha2KO$ islets, the fold change is significantly less in comparison to control islets. This means that the increment in insulin secretion that normally occurs, is significantly downregulated. The regulation of insulin secretion in beta cells is a dynamic process that is controlled at many different levels. It is dependent on acute changes in metabolic coupling pathways, allosteric activation

156

of enzymes regulating the insulin secretory pathway and regulation of gene expression. However, these changes only occur when the fold change in insulin secretion is above a certain threshold. In the case of AMPK KO beta cells, the cells are used to the constantly higher insulin levels. In response to high glucose concentration, there might be an initial small increase in insulin secretion, but if the increase is not high enough, the changes in metabolic coupling pathways and gene expression to further stimulate insulin release do not occur.

Completely opposite to my results, a separate study by Sun et al. (2010a) who also used the AMPK KO islets ($\beta2AMPKdKO$) reported an enhanced insulin secretion in response to high glucose (16.7 mmol/L), even though the $\beta2AMPKdKO$ mice that were used in their study exhibited a similar physiological phenotype to my mice with glucose intolerance and reduced *in vivo* GSIS. Hence, it is rather surprising that the findings by Sun et al. (2010a) showed increased insulin secretion at high glucose concentration in $\beta AMPKdKO$ islets. However, it is possible that the expression of data as percentage of total insulin secretion is not a suitable way to represent the data. In addition, islets from heterozygous mice were used as controls rather than wt mice (Sun et al., 2010a). Furthermore, when the insulin secretion in response to 10 mmol/L glucose was measured in the $AMPK\alpha2$-global-null islets, no significant difference was measured, although if the data are examined carefully, a trend towards reduced insulin secretion can be seen (Viollet et al., 2003b).

In conclusion, my results show that the *in vitro* GSIS confirms that both the $RIPCre\alpha2KO$ and $\alpha1KORIPCre\alpha2KO$ mice have an intrinsic beta cell defect, which results in an increased basal glucose-stimulated insulin secretion. At a high, stimulatory glucose concentration the $RIPCre\alpha2KO$ and $\alpha1KORIPCre\alpha2KO$ islets are unable to increase their insulin secretion and meet the fold change required by the normal beta cells. It seems clear that the role of AMPK in beta cells is to control insulin secretion in response to glucose but it is not involved in the regulation of beta cell mass. In order to understand the mechanisms how AMPK regulates GSIS in beta cells, we examined parts of the classical beta cell stimulus-secretion coupling pathway which can be divided into three different parts which are discussed further in this chapter: glucose sensing, mitochondrial metabolism and function and K_{ATP}-channel activity.

6.5 Loss of AMPK alters beta cell glucose sensing

When glucose is reduced from 10 to 2 mmol/L beta cells become electrically silenced with a reduction in action potential which is reflected in by hyperpolarisation of the plasma membrane (Beall et al., 2010). However, in *RIPCreα2KO* beta cells, there was no electrical silencing at low glucose with a continuous electrical firing of action potentials and failure to hyperpolarise the plasma membrane, as no change in membrane potential was observed [1]. This is the most likely explanation as to why the KO islets continue to secrete insulin at low glucose. These results suggest that the deletion of AMPK in beta cells affects the ability of the cells to sense glucose. Similarly in hypothalamic POMC neurons, plasma membrane hyperpolarisation in response to hypoglycaemia was prevented in *POMCCreAMPKα2KO* neurons (Claret et al., 2007). This is why proximal elements of the mechanisms involved in glucose sensing were analysed by measuring mRNA levels of glucose transporter *Glut2* and the rate limiting enzyme of the glycolysis, *Glucokinase* (i.e. Hexokinae IV). However, islet mRNA levels of *Glut2* and *Glucokinase* were normal in *RIPCreα2KO* islets in comparison to control islet expression. Furthermore, mRNA expression of low Km *hexokinases* (*I-III*) was also normal.

6.6 Mitochondrial gene expression analysis in *RIPCreα2KO* islets

Because AMPK is a cellular energy sensor whose activity is dependent on changes in cellular phosphorylated adenosine nucleotides, largely generated in the mitochondria, expression of key genes involved in the regulation of mitochondrial biogenesis was measured as their expression and activity might be affected by the deletion of AMPK. Nuclear respiratory factor-1 (Nrf1) is a transcription

---

[1]Experiments discussed in this section where conducted by C. Beall at University of Dundee using mice generated by me

factor that regulates the expression of respiratory proteins and mitochondrial transcription and replication (Bergeron et al., 2001). It has been shown previously that increased AMPK activity in skeletal muscle stimulated Nrf1 function, which led to increased mitochondrial biogenesis (Bergeron et al., 2001). Apart from Nrf1, AMPK has also been shown to to stimulate the activation of peroxisome proliferator-activated receptor γ coactivator 1-α (Pgc-1α) and mitochondrial transcription factor A (Tfam) (Irrcher et al., 2003). For example, Tfam controls mitochondrial function by regulation of mtDNA copy number and transcription (Wiederkehr and Wollheim, 2006). Pgc-1α on the other hand is a transcriptional co-activator that regulates the expression of genes that code for mitochondrial proteins of the respiratory chain (Wredenberg et al., 2006). However, normal mRNA expression levels of *Nrf1*, *Tfam* and *Pgc-1α* were measured in *RIPCreα2KO* islets.

6.6.1 The impact of reduced *Ucp2* expression in AMPK deficient beta cells

Beta cell GSIS is dependent on mitochondrial ATP production that can be regulated by mitochondrial uncoupling proteins (Produit-Zengaffinen et al., 2007). Mitochondrial uncoupling protein 2 (UCP2) uncouples mitochondrial oxidative phosphorylation by promotion of proton leakage from the mitochondrial inter-membrane space back to the matrix (Bordone et al., 2006; Chan et al., 2004b). The uncoupling dissipates the proton motive force generated across the membrane that is used in the conversion of ADP to ATP, leading to a reduction in the production of ATP (Chan et al., 2004b). Thus, UCP2 negatively regulates the production of ATP (Affourtit and Brand, 2008). Previous studies have indicated a link between AMPK and UCP2 expression. A study by Xie et al. (2008) showed that immunohistochemical staining of *AMPKAα2*-global-null mouse aortas had reduced *UCP2* expression levels, accompanied by increased superoxide anion levels. On the contrary activation of AMPK by AICAR, or overexpression of CA-AMPK was shown to increase *Ucp2* mRNA and protein levels in human umbilical vein endothelial cells and protect them from high glucose induced su-

peroxide anion levels (Xie et al., 2008). Similarly, overexpression of *AMPKα2* in mouse liver, increased *UCP2* expression (Foretz et al., 2005). As UCP2 has also been shown to affect islet GSIS, mRNA expression of *Ucp2* was measured in *RIPCreα2KO* and control islets. As a matter of fact, the *Ucp2* mRNA levels were found to be significantly decreased, supporting the earlier studies indicating that reduced AMPK expression leads to reduced UCP2 expression and *vice versa*. In order to confirm that reduction in *Ucp2* mRNA levels was not a result of reduced mitochondrial mass, mitochondrial protein ATP synthase levels were measured to estimate mitochondrial mass. However, no difference in ATP synthase levels were detected indicating that there was no difference in mitochondrial mass and reduced *UCP2* mRNA levels represent a true change at a transcriptional level.

A partial inhibition of Ucp2 using antisense oligonucleotide to Ucp2 in islets led to increased GSIS (Souza et al., 2007). Similarly a study by Zhang et al. (2001) demonstrated that mice deficient in *Ucp2* on a mixed B6/129 background had higher plasma insulin and reduced blood glucose levels. In addition, the UCP2 deficient islet exhibited higher ATP content and increased GSIS (Zhang et al., 2001). A study by Pi et al. (2009) also found similar increased GSIS on islets isolated from UCP2 deficient mice on the same genetic background. However, when the *Ucp2*-global-null mice were crossed back into inbred strains (B6, 129, A/J, JAX B6), by the eight backcross, a decreased GSIS in the *Ucp2* deficient islets was measured (Pi et al., 2009). No significant hyperglycaemia and hypoinsulinemia was present in the backcrossed *Ucp2*-global-null mice Pi et al. (2009). As previous findings have demonstrated that UCP2 facilitates the regulation of GSIS, they support my data as I have shown that *Ucp2* mRNA expression is reduced in *RIPCreα2KO* islets, together with impaired GSIS. However, whether UCP2 acts as a negative or positive regulator of GSIS remain inconclusive. If Ucp2 deficiency stimulated insulin secretion, it could explain why I see increased basal insulin secretion in *RIPCreα2KO* and *α1KORIPCreα2KO* islets. However, it would not explain why insulin secretion is reduced in response to high glucose. On the other hand, if Ucp2 reduction leads to decrease in GSIS, it would explain, why in the *RIPCreα2KO* and *α1KORIPCreα2KO* islets, high glucose induced insulin secretion is reduced.

Chronic exposure of islets to high glucose has been shown to increase basal in-

sulin secretion but to decrease GSIS. Treatment with a UCP2 inhibitor, genipin, rescues islets from high glucose induced suppression of GSIS (Zhang et al., 2006). Chronic exposure of Ucp2 deficient islets to high glucose did not suppress GSIS, and no change in GSIS was observed upon genipin treatment, suggesting that genipin alters GSIS via UCP2 dependent manner (Zhang et al., 2006). Furthermore, treatment of wt beta cells and POMC neurons with genipin caused a phenotype similar to that seen in *RIPCreα2KO* beta cells and *POMCCreα2KO* neurons, with a failure to hyperpolarise the plasma membrane at low glucose, suggesting that the low *UCP2* expression measured in the *RIPCreα2KO* islets may contribute to the electrophysiological phenotype observed in *RIPCreα2KO* islets (Beall et al., 2010). In conclusion, my data, as well as previous studies, suggest that UCP2 is involved in the regulation of GSIS in beta cells (Affourtit and Brand, 2008).

6.7 Lack of AMPK does not alter the generation of ROS

Some studies have suggested that beta cell reactive oxygen species (ROS) production contributes to glucose sensing behaviour and regulation of insulin secretion. For example in islets isolated from Zucker rat lean controls (ZLC), high glucose induced a significant increase in O_2^- generation (Bindokas et al., 2003). Similarly, glucose induced increase in H_2O_2 production in mouse islets and INS-1 cells has been reported (Pi et al., 2007a). Furthermore, it was demonstrated that insulin secretion can be stimulated by H_2O_2, derived from glucose metabolism (Pi et al., 2007a). However, decrease in GSIS was measured in mouse islets and INS-1 cell upon exposure to oxidative stressors (Pi et al., 2007a).

As already mentioned above, AMPK and UCP2 activity might play an important role in the control of mitochondrial ROS production (Cai et al., 2007). Lack of UCP2 in beta cells is thought to increase ROS production and impair GSIS in islets. ROS production was also increased in macrophages of UCP2 deficient mice (Pi et al., 2010). Therefore H_2O_2 production, indicative of ROS gener-

ation was measured in control, *RIPCreα2KO* and *α1KORIPCreα2KO* islets. However, no change in H_2O_2 production was detected in *RIPCreα2KO* and *α1KORIPCreα2KO* islets in comparison to control islets at 2 or 20 mmol/L glucose, as assessed by CM-H_2DCFDA fluorescence.

Expression levels of antioxidant enzymes in beta cells are low is comparison to other cell and tissue types (Pi et al., 2010). However, expression of endogenous antioxidant enzymes might be upregulated, when cellular exposure to oxidative stress increases. This has been reported to be an indicative of an increased adaptive response to oxidative stress and potentially impair GSIS (Pi et al., 2007b, 2010). Yet, no increase in mRNA levels of anti-oxidant enzymes, *Gpx4* and *Hmox1* was detected, and rather unexpectedly *Sod2* mRNA expression was mildly reduced in *RIPCreα2KO* islets. Therefore it seems that reduced *Ucp2* mRNA levels measured in *RIPCreα2KO* islets do not affect ROS production or result in compensatory alterations in expression of anti-oxidant defence mechanisms. It can also suggest that it is unlikely that impaired GSIS is not caused by changes in beta cell oxidative stress in *RIPCreα2KO*.

6.8 Normal K_{ATP}-channel activity in AMPK deficient beta cells

The plasma membrane K_{ATP}-channels couple the production of ATP to beta cell electrical activity which leads to stimulation of insulin secretion. Both the number of open channels (not bound by ATP) as well as the number of channels present at the plasma membrane affect the following electrical activity and stimulation of insulin secretion (Lim et al., 2009). As the *RIPCreα2KO* beta cells remained electrically active at low glucose concentration and insulin secretion was significantly elevated, it was postulated that the K_{ATP}-channels remain closed at low glucose (Beall et al., 2010). Loss-of-function mutations of K_{ATP}-channel subunits or reduced expression of K_{ATP}-channels on the plasma membrane have been shown to cause increased electrical activity and insulin secretion at low glucose (Ashcroft, 2005; Miki et al., 1998; Seghers et al., 2000). Hence, *Sur1* mRNA expression

levels were measured in *RIPCreα2KO* and control islets. The *Sur1* expression levels were found to be reduced, suggesting that reduced *Sur1* expression might lead to altered K_{ATP}-channel activity and defective GSIS.

A study by Lim et al. (2009) showed that AMPK regulates the trafficking of insulin granule vehicles and Kir6.2 subunits of the K_{ATP}-channel in response to low energy status. AMPK activation in response to glucose deprivation was shown to increase the number of K_{ATP}-channels on the plasma membrane and the channel activity. Islets from Sur1 KO mice have shown that a deletion of *Sur1* caused impaired docking and fusion of insulin granules, which lead to decreased insulin exocytosis (Kikuta et al., 2005). However, Sun et al. (2010a) reported increased number of docked insulin granules in AMPK KO beta cells.

Perhaps AMPK is needed as a positive regulator of *Sur1* expression, and deletion of AMPK downregulates *Sur1* gene expression, thus affecting the insulin secretion. AMPK might also directly phosphorylate SUR1 subunit that may be important for a functional K_{ATP}-channel (Wang et al., 2005). To determine whether deletion of AMPK leads to altered ATP-sensitivity or current activity of K_{ATP}-channels, whole-cell recordings were made with different ATP concentrations in the electrode solution [1]. Similar voltage clamped currents were measured before and after washout of cellular ATP in wt and KO beta cells. No change in ATP dependent reduction in channel conductance was measured between wt and KO cells. Hence it can be concluded that deletion of AMPK in beta cells did not alter K_{ATP}-channel ATP sensitivity and current activity. Furthermore, diazoxide, which is a pharmacological agent that opens K_{ATP}-channels even at high, stimulatory glucose concentrations, was able to normally hyperpolarise the *RIPCreα2KO* beta cells (Henquin, 2009). In contrast, the AMPK double KO islets studied by Sun et al. (2010a) were reported to have increased K_{ATP}-channel sensitivity to ATP at low glucose. However, glucose induced K_{ATP}-channel closure and increased intracellular calcium levels remained normal (Sun et al., 2010a).

---

[1]Experiments discussed in this section where conducted by C. Beall at University of Dundee

6.9 Conclusion

Thus it can be concluded that AMPK is involved in glucose sensing and regulation of insulin secretion from the beta cells, and the insulin secretory response is tightly coupled to changes in glucose concentration. When glucose levels are low, such as in a fasted state, the probable role for AMPK is to inhibit insulin secretion. Failure to do so could lead to severe hypoglycaemia in the worst case. I have shown that lack of AMPK in beta cells led to increased insulin secretion at basal glucose levels. However, an increase in insulin secretion in response to a stimulatory glucose concentration was significantly impaired, demonstrated *in vivo* and in static incubation of isolated islets. Consequently, the impaired GSIS resulted in the development of glucose intolerance. Even though the basal insulin secretion was enhanced, the AMPK KO islets showed significantly decreased fold change in insulin secretion over basal secretion. Insulin secretion is a dynamic process that is dependent on acute changes in metabolic coupling pathways such as glycolysis and mitochondrial ATP generation via oxidative phosphorylation, activation of enzymes regulating the insulin secretory pathway, such as positive and negative phosphorylation of kinesin-I that drives the insulin granule movement along microtubules, and regulation of gene expression such as insulin gene transcription (Leibiger et al., 1998; McDonald et al., 2009; Wiederkehr and Wollheim, 2006).

At basal levels, the metabolic secretion coupling is probably elevated as the basal insulin secretion is enhanced. However, when the glucose concentration increases, there is a bigger demand for increased rate of glucose metabolism, coupled to insulin secretion. It has been shown previously that suppression of insulin secretion by pharmacological activation of K_{ATP}-channels improves glucose tolerance and beta cell function by providing the cells a period of rest from insulin secretion (Wajchenberg, 2007). Perhaps continuous electrical activity at low glucose and increased basal insulin secretion desensitises AMPK KO beta cells as the basal metabolic secretion coupling is probably constantly elevated. Therefore, when there is a demand to increase glucose metabolism and insulin secretion, the AMPK KO beta cells fail to detect this or are unable to respond.

As a summary, lack of AMPK in beta cells causes impaired glucose home-

ostasis and insulin secretion. The AMPK KO beta cells continue to fire action potentials at low glucose, failing to hyperpolarise the plasma membrane. This leads to increased insulin secretion at low glucose. The same electrophysiological effect is seen when wt beta cells are treated with the UCP2 inhibitor genipin. As *UCP2* mRNA levels are reduced in *RIPCreα2KO* mice, the results suggest a key role for beta cell AMPK in sensing low glucose levels and suppressing insulin secretion possibly via a UCP2 dependent mechanism. Therefore lack of AMPK may result in disconnection of the normal response to nutrient deprivation whereby AMPK and UCP2 would act to lower insulin secretion at low glucose and maintain secretion at high glucose levels. In conclusion, the work presented in this thesis highlights a key role for AMPK in beta cells in glucose sensing and whole-body glucose homeostasis

6.10   Future studies

Future work should focus on finding the link between UCP2 and AMPK that results in the defective insulin secretion. First of all, it should be important to confirm that reduced *Ucp2* mRNA levels correlate with reduced protein levels. Reduced *UCP2* levels should lead to increased mitochondrial respiration and increased production of cellular ATP. Hence if ATP levels are increased, this should lead to increased insulin secretion. Therefore, future work should put more emphasis on studying mitochondrial function in AMPK KO beta cells. Islet ATP levels, mitochondrial membrane potential and oxygen consumption could be measured in *RIPCreα2KO* and *α1KORIPCreα2KO* beta cells. This could potentially explain the enhanced insulin secretion at basal glucose concentration, and whether or not the mitochondrial oxidative phosphorylation is reduced in response to stimulatory glucose concentration.

6.11 The role of PI3K in pancreatic beta cells

6.12 Importance of study

Phosphatidylinositol 3-kinase (PI3K) mediates signals downstream from insulin and IGF-1 receptors, which is important for the regulation and maintenance of cellular processes including cell proliferation and growth, survival and cellular metabolism (Taniguchi et al., 2006). The PI3K pathway has been implicated in many human cancers, and it has a significant impact on the regulation of cancer growth, motility, survival and metabolism (Cantley, 2002; Courtney et al., 2010). In many cases the development of cancer results from the constant activation of the PI3K pathway, caused by somatic mutations in several genes that encode for PI3K regulatory and catalytic subunits (Courtney et al., 2010). Over the years, several PI3K inhibitors have been developed to be used in the treatment against various cancers, many of which are under early clinical trials (Courtney et al., 2010). Deficiency in PI3K, or upstream or downstream signalling molecules of PI3K, has been shown to be detrimental for energy- and glucose homeostasis at cellular and whole-body physiological level (Hirsch et al., 2007). Therefore, it is important to understand what are the potential long-term effects of the use of PI3K inhibitors in the treatment of cancer. For example, PI3K catalytic subunit *p110α*-global-null and *p110β*-global-null mice die in utero, implicating the importance of the isoforms for the whole-body physiology and development (Vanhaesebroeck et al., 2005). Heterozygous p110α knock-in mice that have a 50 % reduction in p110α kinase activity, but preserved stoichiometry between the catalytic and regulatory subunits were insulin resistant, glucose intolerant, hyperinsulinaemic and hyperphagic, however no islet phenotype was reported (Foukas et al., 2006). They also had reduced somatic growth and increased adiposity (Foukas et al., 2006). Kinase dead p110β mice had a mild hyperglycaemia and insulin resistance, accompanied by islet hyperplasia and increased insulin secretion (Ciraolo et al., 2008).

Even though the role of class IA PI3Ks in peripheral tissues is well studied, the role of PI3K in pancreatic beta cells has remained inconclusive. The insulin

receptor/IGF-1 signalling is usually dominated by one of the p110α or p110β catalytic isoforms, depending on tissue type (p110α in peripheral tissues and p110β in hypothalamic neurons) (Al-Qassab et al., 2009; Foukas et al., 2006; Sopasakis et al., 2010). In general it is thought that p110α is the main mediator of the insulin signalling pathway, but p110β is required for long-term support and PIP$_3$ production (Ciraolo et al., 2008). However, whether this is also true in beta cells, remains unknown. No transgenic mouse models of p110α or p110β catalytic subunits exist that would have studied their role in pancreatic beta cells.

The work in this thesis focuses on the combined role of p110α and p110β catalytic subunits in pancreatic beta cells and hypothalamic RIPCre neurons, and their impact on whole-body energy- and glucose homeostasis. *RIPCrep110$\alpha\beta$KO* mice were created by employing the cre-loxP system to target the kinase domains of the isoforms, which results in kinase dead subunits, without changing the stoichiometry between the catalytic and regulatory subunits. Cre-recombinase is expressed from rat insulin promoter (RIP) which works in the pancreatic beta cells and in RIPCre expressing hypothalamic neurons (Choudhury et al., 2005; Ray et al., 1999). Hence, when the impact of kinase inactivation was studied at the physiological level, both glucose homeostasis and hypothalamic function were investigated.

6.12.1   Efficiency of kinase inactivation

Gene expression levels of *p110α*, *p110β* and *p85*, measured by qRT-PCR, were not changed in *RIPCrep110$\alpha\beta$KO* islets confirming that stoichiometry of the catalytic and regulatory subunits remains intact upon RIP-Cre mediated recombination of floxed *p110α* and *p110β* kinase domains. However, the lipid kinase activity was significantly reduced in the *RIPCrep110$\alpha\beta$KO* islets, demonstrating that the *RIPCrep110$\alpha\beta$KO* islets have a reduced ability to phosphorylate cellular PI(3,4)P$_2$ to produce PI(3,4,5)P$_3$[1]. However, the kinase activity was only reduced $\approx$35 %, which might be due to the kinase activity being measured from whole islet preparations, which also contain other islet cell types such as alpha and delta cells, therefore the kinase activity, which will be unaffected in non-beta cell cells,

---

[1]Experiment conducted by C. Chaussade at Queen Mary, University of London

will affect the final kinase activity measured.

6.12.2   Glucose homeostasis in *RIPCrep110αβKO* mice

Impaired whole-body glucose homeostasis in *RIPCrep110αβKO* mice is consistent with other beta cell transgenic mouse models of the insulin receptor/IGF-1 receptor signalling pathway (Taniguchi et al., 2006; Vanhaesebroeck et al., 2005). Both upstream and downstream signalling molecules of PI3K have been shown to have a pivotal role in the regulation of normal glucose homeostasis (Hirsch et al., 2007).

The diminished glucose homeostasis in *RIPCrep110αβKO* mice was manifested by fasted and fed hyperglycaemia and marked glucose intolerance, present already at an early age (5 weeks). Surprisingly, fasted and fed plasma insulin levels remained unaltered. Similarly to my results, mice with a deletion of insulin receptor (IR)(*RIPCreIRKO*) or IGF-1 receptor (*RIPCreIgf-1KO*) in beta cells also developed progressive glucose intolerance but fasted plasma insulin levels were only mildly increased (Kulkarni et al., 1999; Xuan et al., 2002). A significant glucose intolerance was also reported in beta cell specific (RIPCre and PdxCre) IRS-2 KO mice (Cantley et al., 2007; Choudhury et al., 2005; Kubota et al., 2004; Lin et al., 2004a). Whilst Lin et al. (2004a) and Choudhury et al. (2005) reported increased fasted plasma insulin levels in *RIPCreIRS-2KO* mice, no changes in the insulin levels were reported by Kubota et al. (2004) in their *RIPCreIRS-2KO* mice, and Cantley et al. (2007) in *PdxCreIRS-2KO*. Furthermore, deletion of *Pdk1* (in beta cells (RIPCre) or expression of kinase-dead Akt1 (RIPCre) led to impaired glucose homeostasis, although fasted insulin levels remained unchanged (Bernal-Mizrachi et al., 2004; Hashimoto et al., 2006). On the other hand, deletion of PTEN, a negative regulator of PI3K, in beta cells (*RIPCrePTENKO*) led to improved glucose tolerance and reduced blood glucose and plasma insulin levels as expected (Nguyen et al., 2006). Peripheral insulin sensitivity, assessed by insulin tolerance test was normal, which demonstrated that the *RIPCrep110αβKO* mice were able to correctly respond to peripheral insulin stimulus observed as reduced blood glucose levels. This also means that the glucose intolerance is not caused by peripheral insulin resistance, suggesting a

defective insulin secretion from pancreatic beta cells. *In vivo* glucose-stimulated insulin secretion (GSIS) demonstrated a loss of first phase and reduced second phase of insulin secretion. Hence, these results suggest that the impaired glucose homeostasis in *RIPCrep110αβKO* mice is caused by impaired insulin secretion in response to a glucose, which results in hyperglycaemia and inability to handle glucose properly in response to glucose load. Similarly, impaired GSIS was reported in the beta cell insulin - and IGF-1 receptor KO and IRS-2 KO mice (Cantley et al., 2007; Kubota et al., 2004; Kulkarni et al., 1999; Xuan et al., 2002). In the *RIPCrePTENKO* mice, GSIS remained normal, although a trend towards increased GSIS was noted (Nguyen et al., 2006). Expression of kd-Akt in beta cells also led to a significant reduction in GSIS (Bernal-Mizrachi et al., 2004). No GSIS data was reported in the *RIPCrePdk1KO* mice (Hashimoto et al., 2006). Therefore it can be concluded that insulin- and IGF-1 receptor signalling via PI3K in pancreatic beta cells is required for proper *in vivo* GSIS and maintenance of whole-body glucose homeostasis.

6.12.3   Islet physiology in *RIPCrep110αβKO* mice

Even though the *in vivo* GSIS was reduced, it is not entirely clear whether it results from an intrinsic beta cell defect or reduced beta cell mass or altered islet morphology. Additionally, altered CNS function could also affect the pancreatic beta cell function. Hence, *in vitro* GSIS in *RIPCrep110αβKO* mice islets was investigated. This showed that insulin secretion in response to low (2 mmol/L) and high (20 mmol/L) glucose concentration was significantly reduced, suggesting that the glucose intolerance and impaired GSIS *in vivo*, were caused by intrinsic beta cell defect. Similarly to my findings, insulin secretion in response to low and high glucose concentrations in islets isolated from *RIPCreIGF-1KO*, *PdxCreIRS-2KO* and *RIPCrekd-Akt* mice was significantly reduced (Bernal-Mizrachi et al., 2004; Cantley et al., 2007; Kulkarni et al., 2002). In contrast, static incubation of islets isolated from control and *RIPCreIRS-2KO* mice demonstrated increased insulin secretion in response to 11.1 mmol/L glucose (Kubota et al., 2004). Quite expectedly, perfusion of *RIPCrePTENKO* pancreases demonstrated preserved glucose-stimulated insulin secretion (Nguyen et al., 2006).

Most of the previous PI3K studies in beta cells have used the non-selective PI3K inhibitors wortmannin and LY-294002, which are likely to inhibit other kinases such as mTOR (Aspinwall et al., 2000; Puri, 2006). Therefore, any conclusions from these studies should be considered with caution. However, the general consensus is that PI3K catalytic isoforms might be involved in regulating insulin secretion but whether they are needed to inhibit or stimulate insulin secretion has remained inconclusive.

It is well established, that insulin stimulates the upregulation of insulin gene transcription via activation of class IA PI3K (Barker et al., 2002). This was demonstrated by Leibiger et al. (2001) who showed that treatment of beta cells with the PI3K inhibitors wortmannin and LY-294002 inhibited insulin stimulated insulin gene transcription (Leibiger et al., 2001, 1998). The positive insulin autocrine effect on beta cells to stimulate insulin release has been demonstrated to be dependent on IRS-1 and PI3K (Aspinwall et al., 2000). Stimulation of beta cells with insulin leads to increase in intracellular calcium, released from the endoplasmic reticulum (ER) stores, and stimulation of insulin secretion. However, both the insulin stimulated intracellular calcium release and insulin secretion were abolished in IRS-1 KO beta cells or treatment with wt beta cells with the PI3K inhibitor wortmannin (Aspinwall et al., 2000). Similarly, thiazolidinediones such as rosiglitazone (RSG) and BLX-1002 that belong to a group of anti-hyperglycaemic drugs that have been shown to enhance high-glucose stimulated insulin secretion. However, the enhanced insulin secretion by RSG and BLX-1002 was abolished with a treatment with the PI3K inhibitor LY-294002 or wortmannin (Yang et al., 2001a; Zhang et al., 2009). On the contrary, (Khan et al., 2001) showed that insulin stimulated beta cell K_{ATP}-channel activity which led to hyperpolarisation of the plasma membrane and reduction in intracellular calcium levels. However, this effect was blocked by treatment of beta cells with wortmannin, demonstrating that insulin hyperpolarises the plasma membrane via activation of PI3K (Khan et al., 2001). Furthermore, a study by Kubota et al. (2004) showed that insulin secretion in response to 11.1 mmol/L glucose was significantly higher when wt islets were treated with the PI3K inhibitor LY-294002 in comparison to untreated islets. Similarly, treatment of islets isolated from *RIPCreIRS-2KO* islets showed higher insulin secretion in response to high glucose when treated with LY-294002

than untreated (Kubota et al., 2004).

Arginine also stimulates insulin release by promoting plasma membrane depolarisation and increase in intracellular calcium. Interestinly, arginine-stimulated insulin secretion was also impaired in the IGF-1 receptor KO but not in the IR KO mice (Kulkarni et al., 1999; Xuan et al., 2002). A study by Aspinwall et al. (2000) has suggested that insulin can stimulate insulin secretion through PI3K by promoting calcium release from the intracellular stores. Hence, it might be possible that IGF-1 receptor acts via PI3K to stimulate insulin secretion.

Insulin receptor/PI3K mediated signalling in pancreatic beta cells have been considered to be important for the maintenance of beta cell mass. Reduced beta cell mass can also result in reduced insulin secretion. Beta cell specific deletion of *IRS-2* and *Pdk1* for instance have resulted in decreased beta cell mass and insulin secretion, whereas deletion of *PTEN* has shown to increase beta cell mass (Cantley et al., 2007; Choudhury et al., 2005; Kubota et al., 2004; Lin et al., 2004a; Nguyen et al., 2006). Even thought Akt is one of the main modulators in regulating cell growth and proliferation, transgenic mouse models of Akt have shown inconclusive results. Expression of constitutively active Akt1 in beta cells increased both beta cell size and number (Bernal-Mizrachi et al., 2004; Tuttle et al., 2001). On the contrary, expression of dominant-negative form of Akt1 in beta cells, in which Akt activity was reduced by 80 % did not show decreased beta cell mass (Elghazi et al., 2007). The results reported in this thesis demonstrate that inactivation of both the p110α and p110β kinase function in beta cells does not affect the beta cell mass or islet density. In contrast, the heterozygous kinase dead p110α and kinase dead p110β mice displayed islet hyperplasia and hyperinsulinaemia (Foukas et al., 2006). However, it is likely that increased islet mass is compensatory mechanism for peripheral insulin resistance present in these mice. In addition, if inactivation of either p110α or p110β isoforms can still lead to increased islet mass, it is possible that PI3K is not required for the maintenance of beta cell mass.

Gene expression analysis of some of the key beta cell genes such as *Glut2*, *insulin*, *Irs-1* and *Akt*, did not show any significant changes in mRNA expression levels, apart from a small increase in expression of *pyruvate dehydrogenase kinase 1* (Pdk1). Pdk1 is a negative regulator of pyruvate dehydrogenase (PDH),

which is phosphorylated and inactivated by PDK1. PDH decarboxylates pyruvate to acetyl-CoA before it can enter the mitochondrial TCA cycle. Both PDH as well as pyruvate carboxylase (PC), which carboxylates pyruvate to oxaloacetate, are important mediators of metabolic flux to the TCA cycle (whan Kim et al., 2006). Recent studies have identified PDK1 as a potential regulator of GSIS in pancreatic beta cells. Knock-down of PDK1 in clonal beta cells lead to increased PDH activity, increased mitochondrial metabolic flux and oxidative phosphorylation coupled to ATP production, which enhanced GSIS *in vitro* (Krus et al., 2010).

6.12.4 Energy homeostasis in *RIPCrep110αβKO* mice

Investigation of whole-body energy homeostasis in *RIPCrep110αβKO* mice suggests that inactivation of p110α and p110β isoforms in hypothalamic insulin expressing neurons (RIP) does not affect feeding behaviour or basal metabolic rate, although mild leptin resistance seems to occur, possibly due to increased plasma leptin levels. In contrast, increased food intake was observed in *RIPCreIRS-2KO* mice reported by three independent studies (Choudhury et al., 2005; Kubota et al., 2004; Lin et al., 2004b). Similar to my results, all three studies also reported increased plasma leptin levels (Choudhury et al., 2005; Kubota et al., 2004; Lin et al., 2004b) and mild leptin resistance was also observed by Choudhury et al. (2005); Kubota et al. (2004).

Body composition is markedly altered in *RIPCrep110αβKO* mice, demonstrated by increased body weight, lean body mass, bone mineral content and significant adiposity. The naso-anal body length was also significantly increased. Similarly to the *RIPCrep110αβKO* mice, increased body weight and adiposity were reported in *RIPCreIRS-2KO* mice (Choudhury et al., 2005; Kubota et al., 2004; Lin et al., 2004b) and increased somatic growth was reported by (Choudhury et al., 2005; Lin et al., 2004b). Heterozygous p110α knock-in mice also displayed increased adiposity and hyperleptinaemia but the body size was reduced due to reduced lean body mass (Foukas et al., 2006). In contrast, *RIPCrePTENKO* mice, in which PI3K signalling is enhanced, exhibited reduced body growth (Choi et al., 2008).

Both insulin and melanocortin receptor agonist MT-II, but not leptin, depolarise RIPCre neurons (Choudhury et al., 2005). Interestingly both *Pomc* and *AgRP* mRNA expression levels were significantly decreased in the hypothalami of *RIPCrep110αβKO* mice. As *Pomc* mRNA expression levels were also decreased in *RIPCreIRS-2KO* mice it is possible that impaired melanocortin signalling might be responsible for the altered energy homeostasis in the emphRIPCrep110αβKO mice (Choudhury et al., 2005; Lin et al., 2004b). Even though *Pomc* mRNA levels were not reported in *RIPCrePTENKO* mice, it is possible that disruption of insulin receptor signalling pathway leads to impaired melanocortin signalling, which is involved in the regulation of body growth and size (Ellacott and Cone, 2006). Therefore, results reported in this thesis as well as earlier studies suggest that insulin/IGF-1 signalling mediated via IRS-2 and PI3K in RIPCre expressing neurons has a key role in the regulation of body growth and size.

6.12.5 Summary

Overall, results reported in this thesis imply that p110α and p110β isoforms are required for normal glucose-stimulated insulin secretion from pancreatic beta cells. However, they are not involved in the regulation of normal beta cell mass, islet density and morphology. As these studies are less complete, further experiments are required to understand the underlying cause for defective GSIS, and involvement of PI3K in the regulation of insulin secretion.

Because the kinase activity of both the p110α and p110β are abolished in this study, it is not possible to distinguish whether the isoforms are involved in regulating different pathways in the beta cells, as it has been shown in other tissue types. In hypothalamic POMC and AgRP neurons, p110β was shown to be the dominating isoform, whereas in peripheral tissues p110α has the dominant role, although the p110β activity is still required, especially in the long term insulin receptor signalling (Al-Qassab et al., 2009). Previous studies have also shown that in tissues, where p110α has a dominant role in insulin receptor signalling, p110β, in addition to p110γ, mediates signals downstream of G-protein coupled receptors (GPCR) (Guillermet-Guibert et al., 2008; MacDonald et al., 2004). However, in

this study, it was more important to establish the general role for PI3K in beta cells, rather than trying to distinguish isoform specific differences.

6.12.6   Future studies

Previous studies that have also shown that IRS-1/2 and PI3K regulate insulin secretion, have suggested that one potential mechanism would involve regulation of calcium release from intracellular calcium stores (Cantley et al., 2007). Therefore, it would be interesting to study calcium signalling in *RIPCrep110αβKO* islets, or wt islets, treated with isoform specific inhibitors. Arginine-stimulated insulin secretion is thought to act via direct stimulation of plasma membrane depolarisation and increase in intracellular calcium. Beta cell specific IGF-1 receptor, but not insulin receptor KO mice exhibited impaired arginine-stimulated insulin secretion. Therefore, an arginine-stimulated insulin secretion *in vitro* should be performed (Xuan et al., 2002).

As mentioned above, p110β has been shown to mediate signals additionally downstream of GPCR (Graupera et al., 2008). Whether this is true in beta cells could suggest an alternative role for p110β in beta cells in mediating insulin secretion. Deletion of p110γ isoform, which couples signals downstream only from GPCR, in beta cells lead to impaired GSIS (MacDonald et al., 2004). For example GLP-1 receptor is a GPCR that stimulates insulin secretion, although it is still dependent of glucose (Ahrén, 2009). Hence, using p110α and p110β inhibitors and measuring insulin secretion in response to a GLP-1 receptor agonist exendin-4, could potentially indicate whether p110β is coupled to GPCR signalling in beta cells and whether GPCR signalling is one potential mechanism in the regulation of insulin secretion.

In conclusion, *RIPCrep110αβKO* mice develop impaired glucose homeostasis associated with marked hyperglycaemia and glucose intolerance due to intrinsic beta cell defect in glucose-stimulated insulin secretion. Due to impaired p110α and p110β activity additionally in hypothalamic RIPCre expressing neurons, *RIPCrep110αβKO* mice display increased somatic growth and adiposity. These findings suggest a key role for PI3K in regulation of insulin secretion in pancreatic beta cells and regulation of body growth in RIPCre expressing hy-

pothalamic neurons.

Appendix A - Solutions

Tissue extraction buffer

- 50 mmol/L Tris pH 8.0

- 100 mmol/L EDTA

- 100 mmol/L NaCl

- 1 % SDS

TAE buffer

- 40 mmol/L Tris acetate pH 8.3

- 1 mmol/L EDTA

Leptin reconstitution (1.85 mg/ml stock)

- 1.5 ml of 15 mmol/L HCL (add first)

- 1.2 ml of 7.5 mmol/L NaOH (add slowly avoiding precipitation)

2X KRB stock solution

- 136 mmol/L NaCl

- 4.7 mmol/L KCl

- 1.2 mmol/L KH_2PO_4

- 5 mmol/L NaHCO$_3$

- 1.2 mmol/L MgSO$_4$ (7H$_2$O)

Quenching buffer (1X KRB) pH 7.4

- 2X KRB stock

- 10 mmol/L Hepes

- 1 mmol/L CaCl2

- 2 mmol/L D-glucose

- ddH$_2$O

After pH, supplement with 100 units/ml penicillin + 100 μg/ml streptomycin. Take an aliquot for Liberase solution and filter. Supplement the rest of the solution with either newborn calf serum (NCS, Gibco 16010-159), if islets are used for *in vitro* culture or with bovine serum albumin (BSA, Sigma A7906), if islets are used for DNA/RNA/protein extraction. Filter solution after supplementing with NCS or before supplementing with BSA.

Pancreatic digestion solution

Use the 1X KRB solution (pH 7.4) with penicillin/streptomycin and filter the solution. Prepare 0.225 mg/ml Liberase solution from 2.5 mg/ml Liberase stock solution (Liberase TL Research Grade, Roche 05 401 020 001). Keep cold.

Overnight culture medium

- RPM1 1640 GlutaMAX + 25 mM Hepes (Gibco 72400-021)

- 10 % Fetal bovine serum (FBS) (Gibco 10270-106)

- 100 units/ml penicillin + 100 μg/ml streptomycin (Gibco 15070-063)

Secretion buffer

1X KRB solution (as described earlier) supplemented with 0.5 % BSA and either with 2 mmol/L or 20 mmol/L glucose concentration.

Bouins fixative

- 71.43 % picric acid (saturated aqueous)

- 23.8 % formalin (40 % aqueous formaldehyde)

- 4.76 % glacial acetic acid

Ripa lysis buffer

- 1X Ripa buffer (Sigma R0278)

- Cocktail protease inhibitor tablet (1/4 tablet in 5 ml of Ripa buffer)

- 1 mmol/L PMSF (phenyl-methyl-sulfonyl fluoride)

2x Laemmli buffer

- 50 mmol/L Tris-HCL (pH 6.8)

- 2 % SDS

- 0.1 % Bromophenol blue

- 10 % glycerol

- 5 % β-mercapthoethanol

SDS-polyacrylamide gel

12 % Separating gel

- 0.375 mol/L Tris-HCL, pH 8.8

- 12 % acrylamide

- 0.1 % SDS

- 0.1 % ammonium persulfate

- 0.04 % TEMED (Tetramethylethylenediamine)

5 % Stacking gel

- 0.125 mol/L Tris, pH 6.8

- 5 % acrylamide

- 0.1% SDS

- 0.1 % ammonium persulfate

- 0.1 % TEMED (Tetramethylethylenediamine)

Tris-glycine-SDS running buffer

- 25 mmol/L Trizma base (Sigma)

- 192 mmol/L glycine

- 0.1 % SDS

Tris-glycine transfer buffer

- 25 mmol/L Trizma base (Sigma)

- 192 mmol/L glycine

- 20 % methanol

- 0.1 % SDS

1X TBST washing buffer

- 20 mmol/L Tris-HCL (pH 7.6)

- 137 mmol/L NaCl

- 0.1 % Tween20

Blocking solution

- 1X TBST washing buffer

- 5 % non-fat dried milk

Appendix B - Abbreviations

4EBP1	Eukaryotic translation initiation factor 4E binding protein-1
ABCC8	ATP-binding cassette, sub-family C, member 8
ACC	Acetyl-CoA carboxylase
ADP	Adenosine diphosphate
AGC	cAMP-dependent, cGMP-dependent and protein kinase C
AgRP	Agouti-related peptide
AICAR	5-aminoimidazole-4-carboxamide-1-β-D-ribofuranoside
AMP	Adenosine monophosphate
AMPK	AMP-activated protein kinase
ANOVA	Analysis of variance
ANT	Adenine nucleotide transferase
ARC	Arcuate nucleus
AS160	Rab-GTPase-activating protein
ATP	Adenosine trisphosphate
Bp	Base pair
BSA	Bovine serum albumin
CA	Constitutively active
Ca^{2+}	Calcium ion
CaMKK	Ca^{2+}/calmodulin-dependent protein kinase kinase
cAMP	cyclic adenosine monophoshate
CART	cocaine-amphetamine-regulated-transcript
CBS	Cystathione beta-synthase
CCD	Charged coupled device
CDKAL1	CDK5 regulatory subunit associated protein 1-like 1
CDKN2B	Cyclin-dependent kinase inhibitor 2B
cDNA	complementary deoxyribonucleic acid
Cl^-	Chloride ion
CM-H_2DCFDA	5-(and 6)-chloromethyl-2,7-dicholorodihydrofluorescein diacetate acetylester

CNS	Central nervous system
CoA	Coenzyme A
CPT1	Carnitine-palmitoyl-CoA-acyltransferase 1
Cre	Cre-recombinase
CREB	Cyclic AMP response element binding protein
DAPI	$4',’6$-diamidino-2-phenylindole
DEXA	Dual-energy X-ray absorptiometry
DMSO	Dimethyl sulfoxide
DN	Dominant negative
DNA	Deoxyribonucleic acid
dNTP	Deoxynucletide trisphoshate
EDTA	Ethylenediaminetetraacetic acid
EGF	Epidermal growth factor
EIF4E	Eukaryotic translation initiation factor 4E
ELISA	Enzyme-linked immunosorbent assay
ER	Endoplasmic reticulum
Erk	Extracellular signal-regulated kinase
$FADH_2$	Flavin adenine dinucleotide (reduced form)
FBS	Fetal bovine serum
FITC	Fluorescein isothiocyanate
FoxO	Forkhead box, sub-group O
G6Pase	Glucose-6-phosphatase
GAPDH	Glyceraldehyde-3-phosphate dehydrogenase
GIP	Gastric inhibitory polypeptide
GK	Glucokinase
GLP-1	Glucagon-like peptide-1
GLUT	Glucose transporter
GPCR	G-protein coupled receptor
GPX4	Glutathione peroxidase 4
Grb2	Growth factor receptor-bound protein 2
GS	Glycogen synthase
GSIS	Glucose-stimulated insulin secretion
GSK3	Glycogen synthase kinase-3
GTT	Glucose tolerance test
GWAS	Genome-wide association study
H_2O_2	Hydrogen peroxide
HCL	Hydrochloric acid
HEPES	4-(2-hydroxyethyl)-1-piperazineethanesulfonic acid
HHEX	Hematopoietically expressed homeobox

HI	Hyperinsulinism
HK	Hexokinase
HMOX1	Heme oxygenase (decycling) 1
HNF-4	Hepatic nuclear factor-4
HPRT	Hypoxanthine-guanine phosphoribosyltransferase
HRP	Horseradish peroxidase
i.p.	Intraperitoneal
IGF-1	Insulin-like growth factor 1
IGF2BP2	Insulin-like growth factor 2 mRNA binding protein 2
IL	Interleukin
INS-1	Insulinoma cell line
Ins2	Insulin 2
IP3	Inositol trisphosphate
IR	Insulin receptor
IRS-1	Insulin receptor substrate 1
IRS-2	Insulin receptor substrate 2
ITT	Insulin tolerance test
JNK	c-Jun N-terminal kinase
K^+	Potassium ion
K_{ATP}	ATP sensitive potassium channel
KCNJ11	Potassium inwardly-rectifying channel, subfamily J, member 11
Kd	Kinase dead
KIF5B	Kinesin family member 5 B
KO	Knock-out
KRB	Krebs-ringer buffer
L-PK	Liver type pyruvate kinase
LKB1	Liver kinase B1
MAPK	Mitogen-activated protein kinase
MEF	Mouse embryonic fibroblast
MODY	Maturity onset diabetes of young
mRNA	Messenger ribonucleic acid
MT-II	Melanotan-II
MTNR1B	Melatonin receptor 1B
mTOR	Mammalian target of rapamycin
NAD	Nicotinamide adenine dinucleotide
NAHD	Nicotinamide adenine dinucleotide (reduced form)
NCS	Newborn calf serum
ND	Neonatal diabetes

NF-κB	Nuclear factor kappa beta
NHS	National Health Service
NPY	Neuropeptide Y
Nrf1	Nuclear respiratory factor 1
PC	Pyruvate carboxylase
PCR	Polymerase chain reaction
PDH	Pyruvate dehydrogenase
Pdk1	Phosphatidylinositol dependent kinase 1
PDK1	Pyruvate dehydrogenase kinase, isoenzyme 1
Pdx1	Pancreatic and duodenal homeobox 1 promoter
PEPCK	Phosphoenolpyruvate carboxykinase
PGC-1α	Peroxisome proliferator-activated receptor-gamma coactivator 1alpha
PH	Plextrin homology
PHHI	Persistent hyperinsulinaemic hypoglycaemia of infancy
PI3K	Phosphoinositide 3-kinase
PIP$_2$	Phosphatidyl inositol 3,4-bisphosphate
PIP$_3$	Phosphatidyl inositol 3,4,5-trisphosphate
PKA	Protein kinase A
PKB/Akt	Protein kinase B
PKC	Protein kinase C
PLC-γ	Phospholipase C-gamma
POMC	Pro-opiomelanocortin
PP	Pancreatic polypeptide
PPARG	Peroxisome proliferator-activated receptor gamma
PPI	Pre-proinsulin
PTB	Phosphotyrosine-binding
PtdIns	Phosphatidyl inositol
PTEN	Phosphatase and tensin homolog
qPCR	Quantitative polymerase chain reaction
RIP	Rat insulin promoter
RNA	Ribonucleic acid
ROS	Reactive oxygen species
RPM	Revolutions per minute
RSG	Rosiglitazone
RT-PCR	Reverse transcription-polymerase chain reaction
S6K	S6 kinase
SDS	Sodium dodecyl sulfate
SEM	Standard error of the mean

SgK	Serine/threonine-protein kinase
SH2	Src-homology-2-domain
SIRT1	Sirtuin 1
Slc2a2	Solute carrier family 2 (facilitated glucose transporter) member 2
SLC30A8	Solute carrier family 30 (zinc transporter), member 8
SNAP-25	Synaptosomal-associated protein, 25kDa
SNARE	Soluble NSF (N-ethylmaleimide-sensitive factor) attachment protein receptor
SOD	Superoxide dismutase
SOS	Son-of-sevenless
SUR1	Sulfonylurea receptor subunit 1
T2DM	Type 2 diabetes mellitus
TAE	Tris-acetate-EDTA
TBST	Tris-buffered saline Tween20
TCA	Tricarboxylic acid
TCF7L2	Transcription factor 7-like 2
TEMED	Tetramethylethylenediamine
Tfam	Transcription factor A, mitochondrial
Thr	Threonine
TNF-α	Tumour necrosis factor-alpha
TORC2	Transducer of regulated cyclic AMP response element binding protein activity 2
Tris	Tris(hydroxymethyl)aminoethane
TRITC	Tetramethyl rhodamine iso-thiocyanate
TSC2	Tuberous sclerosis protein 2
UCP2	Uncoupling protein 2
UV	Ultraviolet
VAMP	Vesicle-associated membrane protein
VEGF	Vascular epidermal growth factor
ZMP	5-aminoimidazole-4-carboxamide ribonucleoside

Appendix C - Publications

The following publication has arisen as a result of the work described in Chapter 3 and 4 and is included at the back of this thesis:

Craig Beall, **Kaisa Piipari** et al. (2010). "Loss of AMP-activated protein kinase $\alpha2$ subunit in mouse β-cells impairs glucose-stimulated insulin secretion and inhibits their sensitivity to hypoglycaemia." Biochemical Journal. **429**, 323-333.

References

Accili, D, Drago, J, et al. Early neonatal death in mice homozygous for a null allele of the insulin receptor gene. *Nature Genetics*, 12, 1996. 35

Accili, D. and Arden, K.C. FoxOs at the crossroads of cellular metabolism, differentiation, and transformation. *Cell*, 117(4):421–6, 2004. 39

Affourtit, C. and Brand, M. On the role of uncoupling protein-2 in pancreatic beta cells. *Biochimica et Biophysica Acta (BBA)-Bioenergetics*, 2008. URL `http://linkinghub.elsevier.com/retrieve/pii/S0005272808000674`. 11, 45, 159, 161

Agency, E. Europe-wide suspension of marketing authorisation for Avandia (rosiglitazone). *European Medicines Agency Press Report*, pp. 1–2, 2010. 33

Ahrén, B. Islet G protein-coupled receptors as potential targets for treatment of type 2 diabetes. *Nat Rev Drug Discov*, 8(5):369–85, 2009. doi:10.1038/nrd2782. 174

Al-Qassab, H., Smith, M.A., Irvine, E.E., Guillermet-Guibert, J., et al. Dominant role of the p110beta isoform of PI3K over p110alpha in energy homeostasis regulation by POMC and AgRP neurons. *Cell Metab*, 10(5):343–54, 2009. doi:10.1016/j.cmet.2009.09.008. URL `http://linkinghub.elsevier.com/retrieve/pii/S1550-4131(09)00296-4`. 37, 50, 54, 58, 68, 122, 167, 173

Albright, A. What Is Public Health Practice Telling Us about Diabetes? *Journal*

of the American Dietetic Association, 108(4):S12–S18, 2008. doi:10.1016/j. jada.2008.01.023. 1

Andreelli, F., Foretz, M., Knauf, C., Cani, P.D., et al. Liver adenosine monophosphate-activated kinase-alpha2 catalytic subunit is a key target for the control of hepatic glucose production by adiponectin and leptin but not insulin. *Endocrinology*, 147(5):2432–41, 2006. doi:10.1210/en.2005-0898. URL `http://endo.endojournals.org/cgi/content/full/147/5/2432`. 31

Araki, E., Lipes, M.A., Patti, M.E., Brüning, J.C., et al. Alternative pathway of insulin signalling in mice with targeted disruption of the IRS-1 gene. *Nature*, 372(6502):186–90, 1994. doi:10.1038/372186a0. URL `http://www.ncbi.nlm.nih.gov/entrez/query.fcgi?db=pubmed&cmd=Retrieve&dopt=AbstractPlus&list_uids=7526222`. 35

Ashcroft, F.M. ATP-sensitive potassium channelopathies: focus on insulin secretion. *The Journal of clinical investigation*, 115(8):2047–58, 2005. doi:10. 1172/JCI25495. URL `http://www.ncbi.nlm.nih.gov/entrez/query.fcgi?db=pubmed&cmd=Retrieve&dopt=AbstractPlus&list_uids=16075046`. 5, 11, 115, 119, 162

Aspinwall, C., Qian, W., Roper, M., Kulkarni, R., et al. Roles of insulin receptor substrate-1, phosphatidylinositol 3-kinase, and release of intracellular Ca2+ stores in insulin-stimulated insulin secretion in -cells. *Journal of Biological Chemistry*, 275(29):22331, 2000. 2, 34, 54, 122, 170, 171

Assmann, A., Ueki, K., Winnay, J.N., Kadowaki, T., et al. Glucose effects on beta-cell growth and survival require activation of insulin receptors and insulin receptor substrate 2. *Molecular and Cellular Biology*, 29(11):3219–28, 2009. doi:10.1128/MCB.01489-08. 35

Barker, C.J., Leibiger, I.B., Leibiger, B., and Berggren, P.O. Phosphorylated inositol compounds in beta -cell stimulus-response coupling. *Am J Physiol Endocrinol Metab*, 283(6):E1113–22, 2002. doi:10.1152/ajpendo.00088.2002. 37, 170

Beall, C., Piipari, K., Al-Qassab, H., Smith, M., et al. Loss of AMP-activated protein kinase 2 subunit in mouse ß-cells impairs glucose-stimulated insulin secretion and inhibits their sensitivity to hypoglycaemia. *biochemj.org*, 2010. URL `http://www.biochemj.org/bj/imps/pdf/BJ20100231.pdf`. 8, 83, 103, 110, 115, 117, 119, 158, 161, 162

Bergeron, R., Ren, J.M., Cadman, K.S., Moore, I.K., et al. Chronic activation of AMP kinase results in NRF-1 activation and mitochondrial biogenesis. *Am J Physiol Endocrinol Metab*, 281(6):E1340–6, 2001. 159

Bernal-Mizrachi, E., Fatrai, S., Johnson, J.D., Ohsugi, M., et al. Defective insulin secretion and increased susceptibility to experimental diabetes are induced by reduced Akt activity in pancreatic islet beta cells. *The Journal of clinical investigation*, 114(7):928–36, 2004. doi:10.1172/JCI20016. 39, 55, 168, 169, 171

Bindokas, V.P., Kuznetsov, A., Sreenan, S., Polonsky, K.S., et al. Visualizing superoxide production in normal and diabetic rat islets of Langerhans. *J Biol Chem*, 278(11):9796–801, 2003. doi:10.1074/jbc.M206913200. 161

Bjørbaek, C. and Kahn, B.B. Leptin signaling in the central nervous system and the periphery. *Recent Progress In Hormone Research*, 59:305–31, 2004. 19, 31

Bordone, L., Motta, M., Picard, F., and Robinson..., A. Correction: Sirt1 Regulates Insulin Secretion by Repressing UCP2 in Pancreatic ß Cells. *PLoS . . .*, 2006. URL `http://www.ncbi.nlm.nih.gov/pmc/articles/PMC1569658/`. 159

Burdakov, D., Luckman, S.M., and Verkhratsky, A. Glucose-sensing neurons of the hypothalamus. *Philos Trans R Soc Lond, B, Biol Sci*, 360(1464):2227–35, 2005. doi:10.1098/rstb.2005.1763. 19

Butler, A. The melanocortin system and energy balance. *Peptides*, 2006. URL `http://linkinghub.elsevier.com/retrieve/pii/S0196978105004407`. 136

Butler, A.E., Janson, J., Bonner-Weir, S., Ritzel, R., et al. Beta-cell deficit and increased beta-cell apoptosis in humans with type 2 diabetes. *Dia-*

betes, 52(1):102–10, 2003. URL `http://diabetes.diabetesjournals.org/cgi/content/full/52/1/102`. 15

Cabrera, O., Berman, D.M., Kenyon, N.S., Ricordi, C., et al. The unique cytoarchitecture of human pancreatic islets has implications for islet cell function. *Proc Natl Acad Sci USA*, 103(7):2334–9, 2006. doi:10.1073/pnas.0510790103. 3

Cai, Y., Martens, G.A., Hinke, S.A., Heimberg, H., et al. Increased oxygen radical formation and mitochondrial dysfunction mediate beta cell apoptosis under conditions of AMP-activated protein kinase stimulation. *Free Radic Biol Med*, 42(1):64–78, 2007. doi:10.1016/j.freeradbiomed.2006.09.018. URL `http://www.sciencedirect.com/science?_ob=ArticleURL&_udi=B6T38-4M0B2HX-1&_user=125795&_rdoc=1&_fmt=&_orig=search&_sort=d&view=c&_acct=C000010182&_version=1&_urlVersion=0&_userid=125795&md5=f17632ca63d432c6cc0382c2c0873641`. 25, 161

Cantley, J., Choudhury, A.I., Asare-Anane, H., Selman, C., et al. Pancreatic deletion of insulin receptor substrate 2 reduces beta and alpha cell mass and impairs glucose homeostasis in mice. *Diabetologia*, 50(6):1248–56, 2007. doi:10.1007/s00125-007-0637-9. URL `http://www.springerlink.com/content/y036p1g3q7427487/`. 35, 36, 55, 132, 168, 169, 171, 174

Cantley, J., Selman, C., Shukla, D., Abramov, A.Y., et al. Deletion of the von Hippel-Lindau gene in pancreatic beta cells impairs glucose homeostasis in mice. *The Journal of clinical investigation*, 119(1):125–35, 2009. doi:10.1172/JCI26934. 153

Cantley, L. The phosphoinositide 3-kinase pathway. *Science*, 2002. URL `http://www.sciencemag.org/cgi/content/abstract/296/5573/1655`. 121, 166

Cantó, C., Gerhart-Hines, Z., Feige, J.N., Lagouge, M., et al. AMPK regulates energy expenditure by modulating NAD+ metabolism and SIRT1 activity. *Nature*, 458(7241):1056–1060, 2009. doi:10.1038/nature07813. URL `http://dx.doi.org/10.1038/nature07813`. 30, 33

Carling, D. The AMP-activated protein kinase cascade – a unifying system for energy control. *Trends in Biochemical Sciences*, 29(1):18–24, 2004. doi:10.1016/j.tibs.2003.11.005. 21, 22, 152

Carling, D., Sanders, M.J., and Woods, A. The regulation of AMP-activated protein kinase by upstream kinases. *Int J Obes Relat Metab Disord*, 32:S55–S59, 2008. doi:10.1038/ijo.2008.124. 20

Chan, C., Saleh, M., Koshkin, V., and Wheeler, M. Uncoupling protein 2 and islet function. *Diabetes*, 2004a. URL `http://diabetes.diabetesjournals.org/cgi/content/abstract/53/suppl_1/S136`. 115

Chan, C.B. and Kashemsant, N. Regulation of insulin secretion by uncoupling protein. *Biochem Soc Trans*, 34(Pt 5):802–5, 2006. doi:10.1042/BST0340802. URL `http://www.biochemsoctrans.org/bst/034/0802/bst0340802.htm`. 10

Chan, C.B., Saleh, M.C., Koshkin, V., and Wheeler, M.B. Uncoupling protein 2 and islet function. *Diabetes*, 53 Suppl 1:S136–42, 2004b. 159

Chang, T., Chen, W., Yang, C., Lu, P., et al. Serine-385 phosphorylation of inwardly rectifying K(+) channel subunit (Kir6.2) by AMP-dependent protein kinase plays a key role in rosiglitazone-induced closure of the K(ATP) channel and insulin secretion in rats. *Diabetologia*, 2009. doi:10.1007/s00125-009-1337-4. URL `http://www.springerlink.com/content/j1133u5768v41h83/`. 33

Chang-Chen, K.J., Mullur, R., and Bernal-Mizrachi, E. -cell failure as a complication of diabetes. *Rev Endocr Metab Disord*, p. 15, 2008. doi:10.1007/s11154-008-9101-5. 3, 15, 16

Cheung, P.C., Salt, I.P., Davies, S.P., Hardie, D.G., et al. Characterization of AMP-activated protein kinase gamma-subunit isoforms and their role in AMP binding. *Biochem J*, 346 Pt 3:659–69, 2000. URL `http://www.biochemj.org/bj/346/0659/bj3460659.htm`. 21

Choi, D., Nguyen, K.T.T., Wang, L., Schroer, S.A., et al. Partial deletion of Pten in the hypothalamus leads to growth defects that cannot be rescued by exogenous growth hormone. *Endocrinology*, 149(9):4382–6, 2008. doi: 10.1210/en.2007-1761. URL `http://endo.endojournals.org/cgi/content/full/149/9/4382`. 172

Choudhury, A.I., Heffron, H., Smith, M.A., Al-Qassab, H., et al. The role of insulin receptor substrate 2 in hypothalamic and beta cell function. *The Journal of clinical investigation*, 115(4):940–50, 2005. doi:10.1172/JCI24445. URL `http://www.jci.org/articles/view/24445`. 35, 36, 84, 136, 153, 167, 168, 171, 172, 173

Ciraolo, E., Iezzi, M., Marone, R., Marengo, S., et al. Phosphoinositide 3-kinase p110beta activity: key role in metabolism and mammary gland cancer but not development. *Science signaling*, 1(36):ra3, 2008. doi:10.1126/scisignal.1161577. URL `http://www.ncbi.nlm.nih.gov/entrez/query.fcgi?db=pubmed&cmd=Retrieve&dopt=AbstractPlus&list_uids=18780892`. 47, 166, 167

Claret, M., Smith, M., Batterham, R., Selman, C., et al. AMPK is essential for energy homeostasis regulation and glucose sensing by POMC and AgRP neurons. *The Journal of clinical investigation*, 117(8), 2007. doi:10.1172/JCI31516. URL `http://www.pubmedcentral.nih.gov/articlerender.fcgi?tool=pubmed&pubmedid=17671657`. 32, 158

Cool, B., Zinker, B., Chiou, W., Kifle, L., et al. Identification and characterization of a small molecule AMPK activator that treats key components of type 2 diabetes and the metabolic syndrome. *Cell metabolism*, 2006a. URL `http://linkinghub.elsevier.com/retrieve/pii/S1550413106001604`. 151

Cool, B., Zinker, B., Chiou, W., Kifle, L., et al. Identification and characterization of a small molecule AMPK activator that treats key components of type 2 diabetes and the metabolic syndrome. *Cell Metab*, 3(6):403–16, 2006b. doi:10.1016/j.cmet.2006.05.005. URL `http://linkinghub.elsevier.com/retrieve/pii/S1550-4131(06)00160-4`. 29, 31

Corton, J.M., Gillespie, J.G., and Hardie, D.G. Role of the AMP-activated protein kinase in the cellular stress response. *Curr Biol*, 4(4):315–24, 1994. URL `http://www.sciencedirect.com/science?_ob=ArticleURL&_udi= B6VRT-4DFBN8S-2X&_user=125795&_rdoc=1&_fmt=&_orig=search&_sort= d&view=c&_acct=C000010182&_version=1&_urlVersion=0&_userid= 125795&md5=2ec04dfd592629e7cd0680bac8c243a8`. 20

Corton, J.M., Gillespie, J.G., Hawley, S.A., and Hardie, D.G. 5-aminoimidazole-4-carboxamide ribonucleoside. A specific method for activating AMP-activated protein kinase in intact cells? *Eur J Biochem*, 229(2):558–65, 1995. 20, 21, 23

Courtney, K.D., Corcoran, R.B., and Engelman, J.A. The PI3K pathway as drug target in human cancer. *J Clin Oncol*, 28(6):1075–83, 2010. doi:10.1200/JCO. 2009.25.3641. 166

Creveaux, M., Domin, J., Berggren, P., and Leibiger, I. Insulin-feedback via PI3K-C2 alpha activated PKB alpha/Akt1 is required for glucose-stimulated insulin secretion. *The FASEB Journal*, 2010. URL `http://www.fasebj.org/ cgi/content/abstract/24/6/1824`. 40

Crute, B.E., Seefeld, K., Gamble, J., Kemp, B.E., et al. Functional domains of the alpha1 catalytic subunit of the AMP-activated protein kinase. *J Biol Chem*, 273(52):35347–54, 1998. URL `http://www.jbc.org/cgi/content/full/273/ 52/35347`. 21

da Silva Xavier, G., Leclerc, I., Salt, I.P., Doiron, B., et al. Role of AMP-activated protein kinase in the regulation by glucose of islet beta cell gene expression. *Proc Natl Acad Sci USA*, 97(8):4023–8, 2000. URL `http://www.pnas.org/ content/97/8/4023.long`. 25, 156

D'Autréaux, B. and Toledano, M. ROS as signalling molecules: mechanisms that generate specificity in ROS homeostasis. *Nat Rev Mol Cell Biol*, 8(10):813–824, 2007. 9

de Koning, E.J.P., Bonner-Weir, S., and Rabelink, T.J. Preservation of beta-cell function by targeting beta-cell mass. *Trends Pharmacol Sci*, 29(4):218–27, 2008. doi:10.1016/j.tips.2008.02.001. URL

```
http://www.sciencedirect.com/science?_ob=ArticleURL&_udi=
B6T1K-4S3P83F-1&_user=125795&_rdoc=1&_fmt=&_orig=search&_sort=
d&view=c&_acct=C000010182&_version=1&_urlVersion=0&_userid=
125795&md5=6a2ff640afdad3a2f758149d66f0aeef. 15
```

DeFronzo, R. Pathogenesis of type 2 diabetes mellitus. *Medical Clinics of North America*, 88(4):787–836, 2004. 1, 3, 15, 29, 50, 51

Deshmukh, A.S., Treebak, J.T., Long, Y.C., Viollet, B., et al. Role of adenosine 5'-monophosphate-activated protein kinase subunits in skeletal muscle Mammalian target of rapamycin signaling. *Mol Endocrinol*, 22(5):1105–12, 2008. doi:10.1210/me.2007-0448. URL `http://mend.endojournals.org/cgi/content/full/22/5/1105`. 30

Dessimoz, J., Bonnard, C., Huelsken, J., and Grapin-Botton, A. Pancreas-specific deletion of beta-catenin reveals Wnt-dependent and Wnt-independent functions during development. *Curr Biol*, 15(18):1677–83, 2005. doi:10.1016/j.cub.2005.08.037. 153

Donovan, C.M. and Bohland, M. Hypoglycemic Detection at the Portal Vein: Absent in Humans or Yet to Be Elucidated? *Diabetes*, 58(1):21–23, 2009. doi:10.2337/db08-1437. 19

Duchen, M.R. Roles of mitochondria in health and disease. *Diabetes*, 53 Suppl 1:S96–102, 2004. 5, 9, 10

Ebelt, H., Peschke, D., Brömme, H.J., Mörke, W., et al. Influence of melatonin on free radical-induced changes in rat pancreatic beta-cells in vitro. *J Pineal Res*, 28(2):65–72, 2000. 10

Eizirik, D.L., Cardozo, A.K., and Cnop, M. The role for endoplasmic reticulum stress in diabetes mellitus. *Endocr Rev*, 29(1):42–61, 2008. doi:10.1210/er.2007-0015. URL `http://edrv.endojournals.org/cgi/content/full/29/1/42`. 16

El-Haschimi, K., Pierroz, D.D., Hileman, S.M., Bjørbaek, C., et al. Two defects contribute to hypothalamic leptin resistance in mice with diet-induced

obesity. *The Journal of clinical investigation*, 105(12):1827–32, 2000. doi: 10.1172/JCI9842. 145

Elghazi, L., Rachdi, L., Weiss, A., Cras-Méneur, C., et al. Regulation of -cell mass and function by the Akt/protein kinase B signalling pathway. *Diabetes, Obesity and Metabolism*, 9(s2):147–157, 2007. 38, 171

Elghazi, L. and Bernal-Mizrachi, E. Akt and PTEN: beta-cell mass and pancreas plasticity. *Trends Endocrinol Metab*, 20(5):243–51, 2009. doi:10.1016/j.tem. 2009.03.002. 39, 132

Eliasson, L. SUR1 Regulates PKA-independent cAMP-induced Granule Priming in Mouse Pancreatic B-cells. *The Journal of General Physiology*, 121(3):181– 197, 2003. doi:10.1085/jgp.20028707. 13

Ellacott, K. and Cone, R. The role of the central melanocortin system in the regulation of food intake and energy homeostasis: lessons from mouse models. *Philosophical Transactions of the Royal Society B: Biological Sciences*, 361(1471):1265, 2006. 173

Elmquist, J.K., Coppari, R., Balthasar, N., Ichinose, M., et al. Identifying hypothalamic pathways controlling food intake, body weight, and glucose homeostasis. *J Comp Neurol*, 493(1):63–71, 2005. doi:10.1002/cne.20786. 18

Foretz, M., Hébrard, S., Leclerc, J., and Zarrinpashneh, E. Metformin inhibits hepatic gluconeogenesis in mice independently of the LKB1/AMPK pathway via a decrease in hepatic energy state. *ncbi.nlm.nih.gov*, 2010. URL `http://www.ncbi.nlm.nih.gov/pmc/articles/PMC2898585/`. 33, 151

Foretz, M., Ancellin, N., Andreelli, F., Saintillan, Y., et al. Short-term overexpression of a constitutively active form of AMP-activated protein kinase in the liver leads to mild hypoglycemia and fatty liver. *Diabetes*, 54(5):1331–9, 2005. URL `http://diabetes.diabetesjournals.org/cgi/content/full/54/5/1331`. 31, 160

Foukas, LC, Claret, M., Pearce, W., et al. Critical role for the p110alpha phosphoinositide-3-OH kinase in growth and metabolic regulation. *Nature*,

441, 2006. URL `http://www.google.com/search?client=safari&rls=` `en-us&q=Critical+role+for+the+p110alpha+phosphoinositide-3-OH+` `kinase+in+growth+and+metabolic+regulation.&ie=UTF-8&oe=UTF-8`. 47, 49, 54, 122, 166, 167, 171, 172

Foukas, L. and Okkenhaug, K. Gene-targeting reveals physiological roles and complex regulation of the phosphoinositide 3-kinases. *Archives of biochemistry and biophysics*, 2003. URL `http://linkinghub.elsevier.com/retrieve/` `pii/S0003986103001772`. 44, 47

Fryer, L.G.D., Parbu-Patel, A., and Carling, D. The Anti-diabetic drugs rosiglitazone and metformin stimulate AMP-activated protein kinase through distinct signaling pathways. *J Biol Chem*, 277(28):25226–32, 2002. doi:10.1074/jbc. M202489200. URL `http://www.jbc.org/cgi/content/full/277/28/25226`. 83, 151

Geering, B., Cutillas, P., and Vanhaesebroeck, B. Regulation of class IA PI3Ks: is there a role for monomeric PI3K subunits? *Biochem Soc Trans*, 35(2):5, 2007. URL `http://www.biochemsoctrans.org/bst/035/0199/bst0350199.` `htm`. 44

Gleason, C.E., Lu, D., Witters, L.A., Newgard, C.B., et al. The role of AMPK and mTOR in nutrient sensing in pancreatic beta-cells. *J Biol Chem*, 282(14):10341–51, 2007. doi:10.1074/jbc.M610631200. 30, 155

Gloyn, A. The search for type 2 diabetes genes. *Ageing Research Reviews*, 2003. URL `http://linkinghub.elsevier.com/retrieve/pii/` `S1568163702000612`. 1, 2, 8

Gloyn, A.L., Tribble, N.D., van de Bunt, M., Barrett, A., et al. Glucokinase (GCK) and other susceptibility genes for beta-cell dysfunction: the candidate approach. *Biochem Soc Trans*, 36(Pt 3):306–11, 2008. doi:10.1042/ BST0360306. 8

Granot, Z., Swisa, A., Magenheim, J., Stolovich-Rain, M., et al. LKB1 regulates pancreatic beta cell size, polarity, and function. *Cell metabolism*, 10(4):296– 308, 2009. doi:10.1016/j.cmet.2009.08.010. 29, 118, 155

Graupera, M., Guillermet-Guibert, J., Foukas, L.C., Phng, L.K., et al. Angiogenesis selectively requires the p110alpha isoform of PI3K to control endothelial cell migration. *Nature*, 453(7195):662–6, 2008. doi:10.1038/nature06892. 47, 49, 58, 122, 174

Guerra, S.D., Lupi, R., Marselli, L., and Masini, M. Functional and molecular defects of pancreatic islets in human type 2 diabetes. *Diabetes*, 2005. URL `http://diabetes.diabetesjournals.org/content/54/3/727.full`. 7

Guillermet-Guibert, J., Bjorklof, K., Salpekar, A., Gonella, C., et al. The p110 isoform of phosphoinositide 3-kinase signals downstream of G protein-coupled receptors and is functionally redundant with p110. *Proceedings of the National Academy of Sciences*, 105(24):8292, 2008. 49, 58, 122, 173

Hardie, D.G. and Carling, D. The AMP-activated protein kinase–fuel gauge of the mammalian cell? *Eur J Biochem*, 246(2):259–73, 1997. 21, 30

Hashimoto, N., Kido, Y., Uchida, T., Asahara, S.I., et al. Ablation of PDK1 in pancreatic cells induces diabetes as a result of loss of cell mass. *Nature Genetics*, 38(5):589–593, 2006. doi:10.1038/ng1774. 38, 55, 168, 169

Hawley, S.A., Davison, M., Woods, A., Davies, S.P., et al. Characterization of the AMP-activated protein kinase kinase from rat liver and identification of threonine 172 as the major site at which it phosphorylates AMP-activated protein kinase. *J Biol Chem*, 271(44):27879–87, 1996. URL `http://www.jbc.org/cgi/content/full/271/44/27879`. 21

Heinrichs, S.C. Mouse feeding behavior: ethology, regulatory mechanisms and utility for mutant phenotyping. *Behav Brain Res*, 125(1-2):81–8, 2001. 87

Henquin, J. Regulation of insulin secretion: a matter of phase control and amplitude modulation. *Diabetologia*, 2009. doi:10.1007/s00125-009-1314-y. URL `http://www.springerlink.com/content/fx7301t6511q534u/`. 12, 163

Henquin, J.C. Triggering and amplifying pathways of regulation of insulin secretion by glucose. *Diabetes*, 49(11):1751–60, 2000. 12

Henquin, J.C., Ravier, M.A., Nenquin, M., Jonas, J.C., et al. Hierarchy of the beta-cell signals controlling insulin secretion. *Eur J Clin Invest*, 33(9):742–50, 2003. 11

Herman, M.A. and Kahn, B.B. Glucose transport and sensing in the maintenance of glucose homeostasis and metabolic harmony. *The Journal of clinical investigation*, 116(7):1767–75, 2006. doi:10.1172/JCI29027. URL `http://www.jci.org/articles/view/29027`. 5, 7, 8

Hinke, S.A., Martens, G.A., Cai, Y., Finsi, J., et al. Methyl succinate antagonises biguanide-induced AMPK-activation and death of pancreatic beta-cells through restoration of mitochondrial electron transfer. *Br J Pharmacol*, 150(8):1031–43, 2007. doi:10.1038/sj.bjp.0707189. URL `http://www3.interscience.wiley.com/journal/121665134/abstract?CRETRY=1&SRETRY=0`. 26, 33, 151

Hiriart, M. and Aguilar-Bryan, L. Channel regulation of glucose sensing in the pancreatic beta-cell. *Am J Physiol Endocrinol Metab*, 295(6):E1298–306, 2008. doi:10.1152/ajpendo.90493.2008. URL `http://ajpendo.physiology.org/cgi/content/full/295/6/E1298`. 5, 7

Hirsch, E., Costa, C., and Ciraolo, E. Phosphoinositide 3-kinases as a common platform for multi-hormone signaling. *J Endocrinol*, 194(2):243–56, 2007. doi:10.1677/JOE-07-0097. 38, 40, 41, 42, 43, 52, 166, 168

Hohmeier, H.E. and Newgard, C.B. Cell lines derived from pancreatic islets. *Mol Cell Endocrinol*, 228(1-2):121–8, 2004. doi:10.1016/j.mce.2004.04.017. URL `http://www.sciencedirect.com/science?_ob=ArticleURL&_udi=B6T3G-4CTN9CN-2&_user=125795&_rdoc=1&_fmt=&_orig=search&_sort=d&view=c&_acct=C000010182&_version=1&_urlVersion=0&_userid=125795&md5=869c541f5315ef81322f1942d4aafc70`. 23

Holmes, B.F., Kurth-Kraczek, E.J., and Winder, W.W. Chronic activation of 5'-AMP-activated protein kinase increases GLUT-4, hexokinase, and glycogen in muscle. *J Appl Physiol*, 87(5):1990–5, 1999. URL `http://jap.physiology.org/cgi/content/full/87/5/1990`. 21, 30

Hooshmand-Rad, R., Hájková, L., Klint, P., Karlsson, R., et al. The PI 3-kinase isoforms p110(alpha) and p110(beta) have differential roles in PDGF- and insulin-mediated signaling. *J Cell Sci*, 113 Pt 2:207–14, 2000. 49, 122

Horikoshi, M., Hara, K., Ohashi, J., Miyake, K., et al. A polymorphism in the AMPKalpha2 subunit gene is associated with insulin resistance and type 2 diabetes in the Japanese population. *Diabetes*, 55(4):919–23, 2006. 15

Hui, H., Nourparvar, A., Zhao, X., and Perfetti, R. Glucagon-like peptide-1 inhibits apoptosis of insulin-secreting cells via a cyclic 5'-adenosine monophosphate-dependent protein kinase A- and a phosphatidylinositol 3-kinase-dependent pathway. *Endocrinology*, 144(4):1444–55, 2003. 38

Huszar, D., Lynch, C.A., Fairchild-Huntress, V., Dunmore, J.H., et al. Targeted disruption of the melanocortin-4 receptor results in obesity in mice. *Cell*, 88(1):131–41, 1997. 136

Iancu, C.V., Mukund, S., Fromm, H.J., and Honzatko, R.B. R-state AMP complex reveals initial steps of the quaternary transition of fructose-1,6-bisphosphatase. *J Biol Chem*, 280(20):19737–45, 2005. doi:10.1074/jbc. M501011200. URL `http://www.jbc.org/cgi/content/full/280/20/19737`. 23

Inoki, K., Zhu, T., and Guan, K.L. TSC2 mediates cellular energy response to control cell growth and survival. *Cell*, 115(5):577–90, 2003. URL `http://linkinghub.elsevier.com/retrieve/pii/S0092867403009292`. 26

Irrcher, I., Adhihetty, P.J., Sheehan, T., Joseph, A.M., et al. PPARgamma coactivator-1alpha expression during thyroid hormone- and contractile activity-induced mitochondrial adaptations. *Am J Physiol, Cell Physiol*, 284(6):C1669–77, 2003. doi:10.1152/ajpcell.00409.2002. 159

Jambal, P., Masterson, S., Nesterova, A., Bouchard, R., et al. Cytokine-mediated Down-regulation of the Transcription Factor cAMP-response Element-binding Protein in Pancreatic -Cells. *Journal of Biological Chemistry*, 278(25):23055, 2003. 26

Jia, S., Liu, Z., Zhang, S., Liu, P., et al. Essential roles of PI(3)K-p110beta in cell growth, metabolism and tumorigenesis. *Nature*, 454(7205):776–9, 2008. doi: 10.1038/nature07091. URL `http://www.nature.com/doifinder/10.1038/nature07091`. 47

Jørgensen, S.B., Nielsen, J.N., Birk, J.B., Olsen, G.S., et al. The alpha2-5'AMP-activated protein kinase is a site 2 glycogen synthase kinase in skeletal muscle and is responsive to glucose loading. *Diabetes*, 53(12):3074–81, 2004. URL `http://diabetes.diabetesjournals.org/cgi/content/full/53/12/3074`. 31, 57, 94

Joseph, J.W., Koshkin, V., Zhang, C.Y., Wang, J., et al. Uncoupling protein 2 knockout mice have enhanced insulin secretory capacity after a high-fat diet. *Diabetes*, 51(11):3211–9, 2002. URL `http://diabetes.diabetesjournals.org/cgi/content/full/51/11/3211`. 114

Joshi, RL, Lamothe, B, et al. Targeted disruption of the insulin receptor gene in the mouse results in neonatal lethality. *EMBO J*, 15, 1996. URL `http://www.google.com/search?client=safari&rls=en-us&q=Targeted+disruption+of+the+insulin+receptor+gene+in+the+mouse+results+in+neonatal+lethality.&ie=UTF-8&oe=UTF-8`. 35

Kahn, B. Facilitative Glucose Transporters: Regulatory Mechanisms and Dysregulation in Diabetes. *The Journal of clinical investigation*, 89:8, 1992. 7

Kahn, B., Alquier, T., Carling, D., and Hardie, D. AMP-activated protein kinase: ancient energy gauge provides clues to modern understanding of metabolism. *Cell Metab*, 2005. URL `http://linkinghub.elsevier.com/retrieve/pii/S1550413104000099`. 24

Kefas, B.A., Heimberg, H., Vaulont, S., Meisse, D., et al. AICA-riboside induces apoptosis of pancreatic beta cells through stimulation of AMP-activated protein kinase. *Diabetologia*, 46(2):250–4, 2003. doi:10.1007/s00125-002-1030-3. URL `http://www.springerlink.com/content/jqk3xuapjb78lnnc/`. 26

Kefas, B.A., Cai, Y., Kerckhofs, K., Ling, Z., et al. Metformin-induced stimulation of AMP-activated protein kinase in beta-cells impairs

their glucose responsiveness and can lead to apoptosis. *Biochem Pharmacol*, 68(3):409–16, 2004. doi:10.1016/j.bcp.2004.04.003. URL `http://www.sciencedirect.com/science?_ob=ArticleURL&_udi=` `B6T4P-4CJ49TC-3&_user=125795&_rdoc=1&_fmt=&_orig=search&_sort=` `d&view=c&_acct=C000010182&_version=1&_urlVersion=0&_userid=` `125795&md5=46f5918b52832a4ab581cf1562c673de.` 26

Kelly, M., Gauthier, M.S., Saha, A.K., and Ruderman, N.B. Activation of AMP-activated protein kinase by interleukin-6 in rat skeletal muscle: association with changes in cAMP, energy state, and endogenous fuel mobilization. *Diabetes*, 58(9):1953–60, 2009. doi:10.2337/db08-1293. 29

Khan, F.A., Goforth, P.B., Zhang, M., and Satin, L.S. Insulin activates ATP-sensitive K(+) channels in pancreatic beta-cells through a phosphatidylinositol 3-kinase-dependent pathway. *Diabetes*, 50(10):2192–8, 2001. 34, 54, 170

Kikuta, T., Oharaimaizumi, M., Nakazaki, M., Nishiwaki, C., et al. Docking and fusion of insulin secretory granules in SUR1 knock out mouse B-cells observed by total internal reflection fluorescence microscopy. *FEBS Lett*, 579(7):1602–1606, 2005. doi:10.1016/j.febslet.2005.01.074. 163

Kim, J.W., Cho, J.H., Ko, S.H., Park, H.S., et al. Transcriptional mechanism of suppression of insulin gene expression by AMP-activated protein kinase activator 5-amino-4-imidazolecarboxamide riboside (AICAR) in beta-cells. *Biochem Biophys Res Commun*, 365(4):614–20, 2008. doi:10.1016/j.bbrc.2007.11.041. URL `http://www.sciencedirect.com/science?_ob=ArticleURL&_udi=` `B6WBK-4R5X0HY-1&_user=125795&_rdoc=1&_fmt=&_orig=search&_sort=` `d&view=c&_acct=C000010182&_version=1&_urlVersion=0&_userid=` `125795&md5=1f5cf72754a045be9b2f3b1f97debb6d.` 25

Kim, M. and Lee, K. Role of hypothalamic 5-AMP-activated protein kinase in the regulation of food intake and energy homeostasis. *Journal of molecular medicine*, 2005. URL `http://www.springerlink.com/index/` `v66k7m34n613372n.pdf.` 19

Kitamura, T., Nakae, J., Kitamura, Y., Kido, Y., et al. The forkhead transcription factor Foxo1 links insulin signaling to Pdx1 regulation of pancreatic beta cell growth. *The Journal of clinical investigation*, 110(12):1839–47, 2002. doi:10.1172/JCI16857. 39, 40

Klingenberg, M. The ADP and ATP transport in mitochondria and its carrier. *Biochimica et Biophysica Acta (BBA)-Biomembranes*, 1778(10):1978–2021, 2008. 5

Knight, ZA, Gonzalez, B., Feldman, M., et al. A pharmacological map of the PI3-K family defines a role for p110alpha in insulin signaling. *Cell*, 125, 2006. URL http://www.google.com/search?client=safari&rls=en-us&q=A+pharmacological+map+of+the+PI3-K+family+defines+a+role+for+p110alpha+in+insulin+signaling.&ie=UTF-8&oe=UTF-8. 49

Kola, B. Role of AMP-activated protein kinase in the control of appetite. *J Neuroendocrinol*, 20(7):942–51, 2008. doi:10.1111/j.1365-2826.2008.01745.x. 20

Kozma, S.C. and Thomas, G. Regulation of cell size in growth, development and human disease: PI3K, PKB and S6K. *Bioessays*, 24(1):65–71, 2002. doi:10.1002/bies.10031. 121

Krus, U., Kotova, O., Spégel, P., Hallgard, E., et al. Pyruvate dehydrogenase kinase 1 controls mitochondrial metabolism and insulin secretion in INS-1 832/13 clonal beta- cells. *The Biochemical journal*, 2010. doi:10.1042/BJ20100142. 172

Kubota, N., Terauchi, Y., Tobe, K., Yano, W., et al. Insulin receptor substrate 2 plays a crucial role in beta cells and the hypothalamus. *The Journal of clinical investigation*, 114(7):917–27, 2004. doi:10.1172/JCI21484. 122, 168, 169, 170, 171, 172

Kulkarni, R.N. Receptors for insulin and insulin-like growth factor-1 and insulin receptor substrate-1 mediate pathways that regulate islet function. *Biochem Soc Trans*, 30(2):1–6, 2002. 35

Kulkarni, R.N., Brüning, J.C., Winnay, J.N., Postic, C., et al. Tissue-specific knockout of the insulin receptor in pancreatic beta cells creates an insulin

secretory defect similar to that in type 2 diabetes. *Cell*, 96(3):329–39, 1999. 35, 168, 169, 171

Kulkarni, R., Holzenberger, M., Shih, D., Ozcan, U., et al. -cell–specific deletion of the Igf1 receptor leads to hyperinsulinemia and glucose intolerance but does not alter -cell mass. *Nature Genetics*, 31(1):111–115, 2002. 169

Kurth-Kraczek, E.J., Hirshman, M.F., Goodyear, L.J., and Winder, W.W. 5' AMP-activated protein kinase activation causes GLUT4 translocation in skeletal muscle. *Diabetes*, 48(8):1667–71, 1999. URL `http://diabetes.diabetesjournals.org/cgi/reprint/48/8/1667`. 20, 21, 30, 151

Kuzuya, T., Nakagawa, S., Satoh, J., Kanazawa, Y., et al. Report of the Committee on the classification and diagnostic criteria of diabetes mellitus. *Diabetes Research and Clinical Practice*, 55(1):65–85, 2002. URL `http://linkinghub.elsevier.com/retrieve/pii/S0168822701003655`. 1

Laemmli, U.K. Cleavage of structural proteins during the assembly of the head of bacteriophage T4. *Nature*, 227(5259):680–5, 1970. 76

Lage, R., Dieguez, C., Vidalpuig, A., and Lopez, M. AMPK: a metabolic gauge regulating whole-body energy homeostasis. *Trends in Molecular Medicine*, 14(12):539–549, 2008. doi:10.1016/j.molmed.2008.09.007. 31

Leclerc, I., Lenzner, C., Gourdon, L., Vaulont, S., et al. Hepatocyte nuclear factor-4alpha involved in type 1 maturity-onset diabetes of the young is a novel target of AMP-activated protein kinase. *Diabetes*, 50(7):1515–21, 2001. URL `http://diabetes.diabetesjournals.org/cgi/content/full/50/7/1515`. 25

Leclerc, I. and Rutter, G.A. AMP-activated protein kinase: a new beta-cell glucose sensor?: Regulation by amino acids and calcium ions. *Diabetes*, 53 Suppl 3:S67–74, 2004. URL `http://diabetes.diabetesjournals.org/cgi/content/full/53/suppl_3/S67`. 3, 27

Leclerc, I., Woltersdorf, W.W., Xavier, G.D.S., Rowe, R.L., et al. Metformin, but not leptin, regulates AMP-activated protein kinase in pancreatic islets:

impact on glucose-stimulated insulin secretion. *Am J Physiol Endocrinol Metab*, 286(6):E1023–31, 2004. doi:10.1152/ajpendo.00532.2003. URL `http://ajpendo.physiology.org/cgi/content/full/286/6/E1023`. 26, 33, 156

Lee, W.J., Kim, M., Park, H.S., Kim, H.S., et al. AMPK activation increases fatty acid oxidation in skeletal muscle by activating PPARalpha and PGC-1. *Biochem Biophys Res Commun*, 340(1):291–5, 2006. doi:10.1016/j.bbrc.2005.12.011. 30

Leibiger, B., Leibiger, I.B., Moede, T., Kemper, S., et al. Selective insulin signaling through A and B insulin receptors regulates transcription of insulin and glucokinase genes in pancreatic beta cells. *Mol Cell*, 7(3):559–70, 2001. 170

Leibiger, B., Moede, T., Uhles, S., Berggren, P., et al. Short-term regulation of insulin gene transcription. *Biochem Soc Trans*, 30:312–317, 2002. 35

Leibiger, I.B., Leibiger, B., Moede, T., and Berggren, P.O. Exocytosis of insulin promotes insulin gene transcription via the insulin receptor/PI-3 kinase/p70 s6 kinase and CaM kinase pathways. *Mol Cell*, 1(6):933–8, 1998. 164, 170

Leibiger, I.B. and Berggren, P.O. Insulin signaling in the pancreatic beta-cell. *Annu Rev Nutr*, 28:233–51, 2008. doi:10.1146/annurev.nutr.28.061807.155530. 3, 35, 50, 51, 121

Lim, A., Park, S., Sohn, J., Jeon, J., et al. Glucose Deprivation Regulates KATP Channel Trafficking via AMP-Activated Protein Kinase in Pancreatic -Cells. *Diabetes*, 2009. URL `http://diabetes.diabetesjournals.org/content/58/12/2813.full`. 162, 163

Lin, X., Taguchi, A., Park, S., Kushner, J.A., et al. Dysregulation of insulin receptor substrate 2 in beta cells and brain causes obesity and diabetes. *The Journal of clinical investigation*, 114(7):908–16, 2004a. doi:10.1172/JCI22217. 168, 171

Lin, X., Taguchi, A., Park, S., Kushner, J.A., et al. Dysregulation of insulin receptor substrate 2 in beta cells and brain causes obesity and diabetes. *The*

Journal of clinical investigation, 114(7):908–16, 2004b. doi:10.1172/JCI22217. 172, 173

Lochhead, P.A., Salt, I.P., Walker, K.S., Hardie, D.G., et al. 5-aminoimidazole-4-carboxamide riboside mimics the effects of insulin on the expression of the 2 key gluconeogenic genes PEPCK and glucose-6-phosphatase. *Diabetes*, 49(6):896–903, 2000. URL `http://diabetes.diabetesjournals.org/cgi/reprint/49/6/896`. 21, 151

MacDonald, P.E., Joseph, J.W., Yau, D., Diao, J., et al. Impaired glucose-stimulated insulin secretion, enhanced intraperitoneal insulin tolerance, and increased beta-cell mass in mice lacking the p110gamma isoform of phosphoinositide 3-kinase. *Endocrinology*, 145(9):4078–83, 2004. doi:10.1210/en.2004-0028. 47, 173, 174

Macdonald, P.E., Joseph, J.W., and Rorsman, P. Glucose-sensing mechanisms in pancreatic beta-cells. *Philos Trans R Soc Lond, B, Biol Sci*, 360(1464):2211–25, 2005. doi:10.1098/rstb.2005.1762. 11, 12, 13

Maechler, P. and Wollheim, C.B. Mitochondrial function in normal and diabetic beta-cells. *Nature*, 414(6865):807–12, 2001. doi:10.1038/414807a. 3, 9, 10, 13

Martinez, S.C., Cras-Méneur, C., Bernal-Mizrachi, E., and Permutt, M.A. Glucose regulates Foxo1 through insulin receptor signaling in the pancreatic islet beta-cell. *Diabetes*, 55(6):1581–91, 2006. doi:10.2337/db05-0678. 40

Marty, N., Dallaporta, M., and Thorens, B. Brain glucose sensing, counterregulation, and energy homeostasis. *Physiology (Bethesda, Md.)*, 22:241, 2007. 2, 18, 19

Matschinsky, F., Liang, Y., Kesavan, P., Wang, L., et al. Glucokinase as pancreatic beta cell glucose sensor and diabetes gene. *The Journal of clinical investigation*, 92(5):2092–8, 1993. doi:10.1172/JCI116809. 8

McCarthy, M. and Zeggini, E. Genome-wide association studies in type 2 diabetes. *Current diabetes reports*, 9(2):164–171, 2009. 2

Mccrimmon, R.J., Shaw, M., Fan, X., Cheng, H., et al. Key Role for AMP-Activated Protein Kinase in the Ventromedial Hypothalamus in Regulating Counterregulatory Hormone Responses to Acute Hypoglycemia. *Diabetes*, 57(2):444–450, 2007. doi:10.2337/db07-0837. 156

McDonald, A., Fogarty, S., Leclerc, I., Hill, E.V., et al. Control of insulin granule dynamics by AMPK dependent KLC1 phosphorylation. *Islets*, 1(3):198–209, 2009. doi:10.4161/isl.1.3.9608. 164

McTaggart, J.S., Clark, R.H., and Ashcroft, F.M. The role of the KATP channel in glucose homeostasis in health and disease: more than meets the islet. *The Journal of physiology*, 2010. doi:10.1113/jphysiol.2010.191767. 11, 12

Merrill, G.F., Kurth, E.J., Hardie, D.G., and Winder, W.W. AICA riboside increases AMP-activated protein kinase, fatty acid oxidation, and glucose uptake in rat muscle. *Am J Physiol*, 273(6 Pt 1):E1107–12, 1997. URL `http://ajpendo.physiology.org/cgi/content/full/273/6/E1107`. 20, 30, 151

Miki, T., Nagashima, K., Tashiro, F., Kotake, K., et al. Defective insulin secretion and enhanced insulin action in KATP channel-deficient mice. *Proc Natl Acad Sci USA*, 95(18):10402–6, 1998. 11, 115, 119, 162

Milicevic, Z., Raz, I., Beattie, S.D., Campaigne, B.N., et al. Natural history of cardiovascular disease in patients with diabetes: role of hyperglycemia. *Diabetes Care*, 31 Suppl 2:S155–60, 2008. doi:10.2337/dc08-s240. URL `http://care.diabetesjournals.org/cgi/content/full/31/Supplement_2/S155`. 1

Mobbs, C.V., Kow, L.M., and Yang, X.J. Brain glucose-sensing mechanisms: ubiquitous silencing by aglycemia vs. hypothalamic neuroendocrine responses. *Am J Physiol Endocrinol Metab*, 281(4):E649–54, 2001. 18

Molina, A.J.A., Wikstrom, J.D., Stiles, L., Las, G., et al. Mitochondrial networking protects beta-cells from nutrient-induced apoptosis. *Diabetes*, 58(10):2303–15, 2009. doi:10.2337/db07-1781. 9, 39

Morris, D.L., Cho, K.W., Zhou, Y., and Rui, L. SH2B1 enhances insulin sensitivity by both stimulating the insulin receptor and inhibiting tyrosine dephosphorylation of insulin receptor substrate proteins. *Diabetes*, 58(9):2039–47, 2009. doi:10.2337/db08-1388. 51

Nguyen, K.T.T., Tajmir, P., Lin, C.H., Liadis, N., et al. Essential role of Pten in body size determination and pancreatic beta-cell homeostasis in vivo. *Mol Cell Biol*, 26(12):4511–8, 2006. doi:10.1128/MCB.00238-06. 168, 169, 171

Obici, S. Molecular targets for obesity therapy in the brain. *Endocrinology*, 150(6):2512, 2009. 19, 32

Okamoto, M., Ohara-Imaizumi, M., Kubota, N., Hashimoto, S., et al. Adiponectin induces insulin secretion in vitro and in vivo at a low glucose concentration. *Diabetologia*, 51(5):827–835, 2008. doi:10.1007/s00125-008-0944-9. 19, 31

Pan, D.A. and Hardie, D.G. A homologue of AMP-activated protein kinase in Drosophila melanogaster is sensitive to AMP and is activated by ATP depletion. *Biochem J*, 367(Pt 1):179–86, 2002. doi:10.1042/BJ20020703. URL `http://www.biochemj.org/bj/367/0179/bj3670179.htm`. 21

Parton, L., Ye, C., Coppari, R., Enriori, P., et al. Glucose sensing by POMC neurons regulates glucose homeostasis and is impaired in obesity. *Nature*, 2007. URL `http://www.nature.com/nature/journal/vaop/ncurrent/full/nature06098.html`. 19

Pi, J., Bai, Y., Daniel, K., Liu, D., et al. Persistent Oxidative Stress Due to Absence of Uncoupling Protein 2 Associated with Impaired Pancreatic beta-Cell Function. *Endocrinology*, 2009. URL `http://endo.endojournals.org/cgi/content/abstract/150/7/3040`. 112, 160

Pi, J., Bai, Y., Zhang, Q., Wong, V., et al. Reactive oxygen species as a signal in glucose-stimulated insulin secretion. *Diabetes*, 2007a. URL `http://diabetes.diabetesjournals.org/content/56/7/1783.short`. 161

Pi, J., Bai, Y., Zhang, Q., Wong, V., et al. Reactive oxygen species as a signal in glucose-stimulated insulin secretion. *Diabetes*, 56(7):1783–91, 2007b. doi: 10.2337/db06-1601. 9, 162

Pi, J., Zhang, Q., Fu, J., Woods, C.G., et al. ROS signaling, oxidative stress and Nrf2 in pancreatic beta-cell function. *Toxicol Appl Pharmacol*, 244(1):77–83, 2010. doi:10.1016/j.taap.2009.05.025. URL `http://www.sciencedirect.com/ science?_ob=ArticleURL&_udi=B6WXH-4WGK6JX-1&_user=10&_coverDate= 04rch&_sort=d&_docanchor=&view=c&_acct=C000050221&_version= 1&_urlVersion=0&_userid=10&md5=19af5d665553c19f433443fcfa634a28`. 9, 10, 119, 161, 162

Postic, C., Shiota, M., Niswender, K.D., Jetton, T.L., et al. Dual roles for glucokinase in glucose homeostasis as determined by liver and pancreatic beta cell-specific gene knock-outs using Cre recombinase. *J Biol Chem*, 274(1):305–15, 1999. URL `http://www.jbc.org/cgi/content/full/274/1/305`. 56

Prentki, M. New insights into pancreatic beta-cell metabolic signaling in insulin secretion. *Eur J Endocrinol*, 134(3):272–86, 1996. URL `http://www. eje-online.org/cgi/reprint/134/3/272`. 6

Prentki, M., Tornheim, K., and Corkey, B.E. Signal transduction mechanisms in nutrient-induced insulin secretion. *Diabetologia*, 40 Suppl 2:S32–41, 1997. URL `http://www.springerlink.com/content/100410/`. 6

Produit-Zengaffinen, N., Davis-Lameloise, N., Perreten, H., Bécard, D., et al. Increasing uncoupling protein-2 in pancreatic beta cells does not alter glucose-induced insulin secretion but decreases production of reactive oxygen species. *Diabetologia*, 50(1):84–93, 2007. doi:10.1007/s00125-006-0499-6. URL `http: //www.springerlink.com/content/481h8233147x30t7/`. 11, 159

Puri, K. Therapeutic Potential of Phosphoinositide 3-Kinase-Selective Small Molecule Inhibitors. *Current Enzyme Inhibition*, 2006. URL `http://www.ingentaconnect.com/content/ben/cei/2006/00000002/ 00000002/art00004`. 170

Ravnskjaer, K., Boergesen, M., Dalgaard, L.T., and Mandrup, S. Glucose-induced repression of PPARalpha gene expression in pancreatic beta-cells involves PP2A activation and AMPK inactivation. *J Mol Endocrinol*, 36(2):289–99, 2006. doi:10.1677/jme.1.01965. URL `http://jme.endocrinology-journals.org/cgi/content/full/36/2/289`. 25

Ray, M.K., Fagan, S.P., Moldovan, S., DeMayo, F.J., et al. Beta cell-specific ablation of target gene using Cre-loxP system in transgenic mice. *J Surg Res*, 84(2):199–203, 1999. doi:10.1006/jsre.1999.5642. 167

Reasner, C.A. Reducing cardiovascular complications of type 2 diabetes by targeting multiple risk factors. *J Cardiovasc Pharmacol*, 52(2):136–44, 2008. doi:10.1097/FJC.0b013e31817ffe5a. 1

Remedi, M.S. and Nichols, C.G. Hyperinsulinism and diabetes: genetic dissection of beta cell metabolism-excitation coupling in mice. *Cell Metabolism*, 10(6):442–53, 2009. doi:10.1016/j.cmet.2009.10.011. 8

Reznick, R.M., Zong, H., Li, J., Morino, K., et al. Aging-associated reductions in AMP-activated protein kinase activity and mitochondrial biogenesis. *Cell Metab*, 5(2):151–6, 2007. doi:10.1016/j.cmet.2007.01.008. URL `http://linkinghub.elsevier.com/retrieve/pii/S1550-4131(07)00009-5`. 21

Riboulet-Chavey, A., Diraison, F., Siew, L.K., Wong, F.S., et al. Inhibition of AMP-activated protein kinase protects pancreatic beta-cells from cytokine-mediated apoptosis and CD8+ T-cell-induced cytotoxicity. *Diabetes*, 57(2):415–23, 2008. doi:10.2337/db07-0993. URL `http://diabetes.diabetesjournals.org/cgi/content/full/57/2/415`. 25, 26

Richter, E.A. and Ruderman, N.B. AMPK and the biochemistry of exercise: implications for human health and disease. *Biochem J*, 418(2):261–75, 2009. doi:10.1042/BJ20082055. URL `http://www.biochemj.org/bj/418/0261/bj4180261.htm`. 21

Ridderstråle, M. and Groop, L. Genetic dissection of type 2 diabetes. *Mol Cell Endocrinol*, 297(1-2):10–7, 2009. doi:10.1016/j.mce.2008.10.002.

URL `http://www.sciencedirect.com/science?_ob=ArticleURL&_udi=B6T3G-4TPX0R4-1&_user=125795&_rdoc=1&_fmt=&_orig=search&_sort=d&view=c&_acct=C000010182&_version=1&_urlVersion=0&_userid=125795&md5=6e80b209c6ec2ec7f626c286feea4caf`. 2

Robertson, R.P., Harmon, J., Tran, P.O.T., and Poitout, V. Beta-cell glucose toxicity, lipotoxicity, and chronic oxidative stress in type 2 diabetes. *Diabetes*, 53 Suppl 1:S119–24, 2004. 16

Robertson, R.P. and Harmon, J.S. Diabetes, glucose toxicity, and oxidative stress: A case of double jeopardy for the pancreatic islet beta cell. *Free Radic Biol Med*, 41(2):177–84, 2006. doi:10.1016/j.freeradbiomed.2005.04.030. URL `http://www.sciencedirect.com/science?_ob=ArticleURL&_udi=B6T38-4JW7V6V-2&_user=125795&_rdoc=1&_fmt=&_orig=search&_sort=d&view=c&_acct=C000010182&_version=1&_urlVersion=0&_userid=125795&md5=2427e20ca7ae128bceae19c8f1da5398`. 15, 16

Rorsman, P. The pancreatic beta-cell as a fuel sensor: an electrophysiologist's viewpoint. *Diabetologia*, 40(5):487–95, 1997. 11, 12, 109

Rorsman, P. and Renström, E. Insulin granule dynamics in pancreatic beta cells. *Diabetologia*, 46(8):1029–45, 2003. doi:10.1007/s00125-003-1153-1. URL `http://www.springerlink.com/content/em9pv38nan1lpe2e/`. 12

Rung, J., Cauchi, S., Albrechtsen, A., Shen, L., et al. Genetic variant near IRS1 is associated with type 2 diabetes, insulin resistance and hyperinsulinemia. *Nature Genetics*, pp. 1–8, 2009. doi:10.1038/ng.443. URL `http://dx.doi.org/10.1038/ng.443`. 2

Rutter, G. and Leclerc, I. The AMP-regulated kinase family: Enigmatic targets for diabetes therapy. *Mol Cell Endocrinol*, p. 9, 2008. doi:10.1016/j.mce.2008.05.020. 33, 152

Scarpulla, R.C. Transcriptional Paradigms in Mammalian Mitochondrial Biogenesis and Function. *Physiological Reviews*, 88(2):611–638, 2008. doi:10.1152/physrev.00025.2007. 112

Scarpulla, R.C. Nuclear activators and coactivators in mammalian mitochondrial biogenesis. *Biochim Biophys Acta*, 1576(1-2):1–14, 2002. 112

Schuit, F., Huypens, P., Heimberg, H., and Pipeleers, D. Glucose sensing in pancreatic -cells. *Diabetes*, 2001. URL `http://diabetes.diabetesjournals.org/content/50/1/1.full`. 7

Seeley, R.J., Burklow, M.L., Wilmer, K.A., Matthews, C.C., et al. The effect of the melanocortin agonist, MT-II, on the defended level of body adiposity. *Endocrinology*, 146(9):3732–8, 2005. doi:10.1210/en.2004-1663. 145

Seeley, R. and Tschop, M. How diabetes went to our heads. *Nature Medicine*, 12(1):47–49, 2006. 18

Seghers, V, Nakazaki, M, et al. Sur1 knockout mice. A model for K(ATP) channel-independent regulation of insulin secretion. *Journal of Biological Chemistry*, 275, 2000. URL `http://www.google.com/search?client=safari&rls=en-us&q=Sur1+knockout+mice.+A+model+for+K(ATP)+channel-independent+regulation+of+insulin+secretion.&ie=UTF-8&oe=UTF-8`. 11, 115, 119, 162

Seo, S., Ju, S., Chung, H., Lee, D., et al. Acute Effects of Glucagon-Like Peptide-1 on Hypothalamic Neuropeptide and AMP Activated Kinase Expression in Fasted Rats. *Endocrine Journal*, p. 11, 2008. doi:10.1507/endocrj.K08E-091. URL `http://www.jstage.jst.go.jp/article/endocrj/advpub/0/advpub_0805020133/_article`. 18

Sesti, G., Cardellini, M., Marini, M.A., Frontoni, S., et al. A common polymorphism in the promoter of UCP2 contributes to the variation in insulin secretion in glucose-tolerant subjects. *Diabetes*, 52(5):1280–3, 2003. URL `http://diabetes.diabetesjournals.org/cgi/content/full/52/5/1280`. 10

Shackelford, D.B. and Shaw, R.J. The LKB1–AMPK pathway: metabolism and growth control in tumour suppression. *Nat Rev Cancer*, 9(8):563–575, 2009. doi:10.1038/nrc2676. URL `http://dx.doi.org/10.1038/nrc2676`. 20

Shepherd, P.R. and Kahn, B. Glucose Transporters and Insulin Action. *The New England Journal of Medicine*, 22:10, 2000. 7

Shepherd, P.R., Withers, D.J., and Siddle, K. Phosphoinositide 3-kinase: the key switch mechanism in insulin signalling. *Biochem J*, 333 (Pt 3):471–90, 1998. URL `http://www.biochemj.org/bj/333/0471/bj3330471.htm`. 42, 43

Sladek, R., Rocheleau, G., Rung, J., Dina, C., et al. A genome-wide association study identifies novel risk loci for type 2 diabetes. *Nature*, 445(7130):881–5, 2007. doi:10.1038/nature05616. URL `http://www.nature.com/nature/journal/v445/n7130/abs/nature05616.html`. 2

Soldatos, G. and Cooper, M. Diabetic nephropathy: important pathophysiologic mechanisms. *Diabetes Research and Clinical Practice*, 82:S75–S79, 2008. 1

Sopasakis, V.R., Liu, P., Suzuki, R., Kondo, T., et al. Specific Roles of the p110α Isoform of Phosphatidylinsositol 3-Kinase in Hepatic Insulin Signaling and Metabolic Regulation. *Cell Metabolism*, 11(3):220–230, 2010. doi:10.1016/j.cmet.2010.02.002. URL `http://dx.doi.org/10.1016/j.cmet.2010.02.002`. 167

Souza, C.D., Araujo, E., Stoppiglia, L., and Pauli..., J. Inhibition of UCP2 expression reverses diet-induced diabetes mellitus by effects on both insulin secretion and action. *The FASEB Journal*, 2007. URL `http://www.fasebj.org/cgi/content/abstract/21/4/1153`. 160

Stancáková, A., Kuulasmaa, T., Paananen, J., Jackson, A.U., et al. Association of 18 confirmed susceptibility loci for type 2 diabetes with indices of insulin release, proinsulin conversion, and insulin sensitivity in 5,327 nondiabetic Finnish men. *Diabetes*, 58(9):2129–36, 2009. doi:10.2337/db09-0117. 2

Straub, S.G. and Sharp, G.W.G. Glucose-stimulated signaling pathways in biphasic insulin secretion. *Diabetes/Metabolism Research and Reviews*, 18(6):451–463, 2002. doi:10.1002/(ISSN)1520-7560. 5

Sun, G., Tarasov, A.I., Mcginty, J., Mcdonald, A., et al. Ablation of AMP-activated protein kinase alpha1 and alpha2 from mouse pancreatic beta

cells and RIP2.Cre neurons suppresses insulin release in vivo. *Diabetologia*, 53(5):924–36, 2010a. doi:10.1007/s00125-010-1692-1. 154, 155, 156, 157, 163

Sun, G., Tarasov, A.I., McGinty, J.A., French, P.M., et al. LKB1 deletion with the RIP2.Cre transgene modifies pancreatic beta-cell morphology and enhances insulin secretion in vivo. *Am J Physiol Endocrinol Metab*, 298(6):E1261–73, 2010b. doi:10.1152/ajpendo.00100.2010. 29, 118, 155

Tamemoto, H., Kadowaki, T., Tobe, K., Yagi, T., et al. Insulin resistance and growth retardation in mice lacking insulin receptor substrate-1. *Nature*, 372(6502):182–6, 1994. doi:10.1038/372182a0. 35

Taniguchi, C.M., Emanuelli, B., and Kahn, C.R. Critical nodes in signalling pathways: insights into insulin action. *Nat Rev Mol Cell Biol*, 7(2):85–96, 2006. doi:10.1038/nrm1837. 38, 39, 42, 43, 44, 50, 51, 52, 166, 168

Tarasov, A., Dusonchet, J., and Ashcroft, F. Metabolic regulation of the pancreatic beta-cell ATP-sensitive K+ channel: a pas de deux. *Diabetes*, 53 Suppl 3:S113–22, 2004. 3

Tengholm, A. and Gylfe, E. Oscillatory control of insulin secretion. *Mol Cell Endocrinol*, 297(1-2):58–72, 2009. doi:10.1016/j.mce.2008.07.009. 5

Terauchi, Y., Tsuji, Y., Satoh, S., Minoura, H., et al. Increased insulin sensitivity and hypoglycaemia in mice lacking the p85 alpha subunit of phosphoinositide 3-kinase. *Nature Genetics*, 21(2):230–5, 1999. doi:10.1038/6023. 45

Thorens, B. GLUT2 in pancreatic and extra-pancreatic gluco-detection. *Mol Membr Biol*, 18(4):265–273, 2001. 7

Thorens, B. Glucose sensing and the pathogenesis of obesity and type 2 diabetes. *International journal of obesity*, 2008. URL `http://www.nature.com/ijo/journal/v32/n6s/full/ijo2008208a.html`. 3, 8

Tuttle, R.L., Gill, N.S., Pugh, W., Lee, J.P., et al. Regulation of pancreatic beta-cell growth and survival by the serine/threonine protein kinase Akt1/PKBalpha. *Nat Med*, 7(10):1133–7, 2001. doi:10.1038/nm1001-1133. 39, 55, 171

Vanhaesebroeck, B. and Alessi, D.R. The PI3K-PDK1 connection: more than just a road to PKB. *Biochem J*, 346 Pt 3:561–76, 2000. 40

Vanhaesebroeck, B., Ali, K., Bilancio, A., Geering, B., et al. Signalling by PI3K isoforms: insights from gene-targeted mice. *Trends Biochem Sci*, 30(4):194–204, 2005. doi:10.1016/j.tibs.2005.02.008. 42, 44, 45, 46, 47, 48, 166, 168

Viollet, B., Andreelli, F., Jørgensen, S.B., Perrin, C., et al. Physiological role of AMP-activated protein kinase (AMPK): insights from knockout mouse models. *Biochem Soc Trans*, 31(Pt 1):216–9, 2003a. doi:10.1042/. 32, 94, 95, 152, 154, 156

Viollet, B., Andreelli, F., Jørgensen, S.B., Perrin, C., et al. The AMP-activated protein kinase alpha2 catalytic subunit controls whole-body insulin sensitivity. *The Journal of clinical investigation*, 111(1):91–8, 2003b. doi: 10.1172/JCI16567. 32, 152, 154, 156, 157

Viollet, B., Lantier, L., Devin-Leclerc, J., Hebrard, S., et al. Targeting the AMPK pathway for the treatment of Type 2 diabetes. *Front Biosci*, 14:3380–400, 2009. 20, 33

Vos, A.D., Heimberg, H., Quartier, E., Huypens, P., et al. Human and rat beta cells differ in glucose transporter but not in glucokinase gene expression. *The Journal of clinical investigation*, 96(5):2489–95, 1995. doi:10.1172/JCI118308. 5

Wajchenberg, B. beta-Cell Failure in Diabetes and Preservation by Clinical Treatment. *Endocrine reviews*, 2007. URL `http://edrv.endojournals.org/cgi/content/abstract/28/2/187`. 164

Wang, C.Z., Wang, Y., Di, A., Magnuson, M.A., et al. 5-amino-imidazole carboxamide riboside acutely potentiates glucose-stimulated insulin secretion from mouse pancreatic islets by KATP channel-dependent and -independent pathways. *Biochem Biophys Res Commun*, 330(4):1073–9, 2005. doi:10.1016/j.bbrc.2005.03.093. URL `http://www.sciencedirect.com/science?_ob=ArticleURL&_udi=`
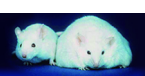
B6WBK-4FSCJS9-B&_user=125795&_rdoc=1&_fmt=&_orig=search&_sort=
d&view=c&_acct=C000010182&_version=1&_urlVersion=0&_userid=
125795&md5=ce15c5ea81c1b3f618512f9548290a62. 163

Weir, G.C. and Bonner-Weir, S. Five stages of evolving beta-cell dysfunction during progression to diabetes. *Diabetes*, 53 Suppl 3:S16–21, 2004. 15, 16

whan Kim, J., Tchernyshyov, I., Semenza, G.L., and Dang, C.V. HIF-1-mediated expression of pyruvate dehydrogenase kinase: a metabolic switch required for cellular adaptation to hypoxia. *Cell Metab*, 3(3):177–85, 2006. doi:10.1016/j. cmet.2006.02.002. 172

WHO. Definition and diagnosis of diabetes mellitus and intermediate hyperglycemia. *Report of a WHO/IDF consultation*, p. 50, 2006. 1

Wiederkehr, A. and Wollheim, C.B. Minireview: implication of mitochondria in insulin secretion and action. *Endocrinology*, 147(6):2643–9, 2006. doi:10.1210/ en.2006-0057. 159, 164

Withers, D.J., Gutierrez, J.S., Towery, H., Burks, D.J., et al. Disruption of IRS-2 causes type 2 diabetes in mice. *Nature*, 391(6670):900–4, 1998. doi: 10.1038/36116. 35

Wollheim, C.B. and Maechler, P. Beta-cell mitochondria and insulin secretion: messenger role of nucleotides and metabolites. *Diabetes*, 51 Suppl 1:S37–42, 2002. 3, 8

Woods, A., Cheung, P.C., Smith, F.C., Davison, M.D., et al. Characterization of AMP-activated protein kinase beta and gamma subunits. Assembly of the heterotrimeric complex in vitro. *J Biol Chem*, 271(17):10282–90, 1996. 21

Woods, S., Benoit, S., and Clegg, D. The brain-gut-islet connection. *Diabetes*, 2006. URL http://diabetes.diabetesjournals.org/cgi/content/ abstract/55/Supplement_2/S114. 18

Wredenberg, A., Freyer, C., Sandström, M.E., Katz, A., et al. Respiratory chain dysfunction in skeletal muscle does not cause insulin resistance. *Biochem Biophys Res Commun*, 350(1):202–7, 2006. doi:10.1016/j.bbrc.2006.09.029. 159

Xavier, G.D.S., Leclerc, I., Varadi, A., Tsuboi, T., et al. Role for AMP-activated protein kinase in glucose-stimulated insulin secretion and preproinsulin gene expression. *Biochem J*, 371(Pt 3):761–74, 2003. doi:10.1042/BJ20021812. URL `http://www.biochemj.org/bj/371/0761/bj3710761.htm`. 21, 25

Xiao, B., Heath, R., Saiu, P., Leiper, F.C., et al. Structural basis for AMP binding to mammalian AMP-activated protein kinase. *Nature*, 449(7161):496–500, 2007. doi:10.1038/nature06161. 21

Xie, Z., Zhang, J., Wu, J., Viollet, B., et al. Upregulation of mitochondrial uncoupling protein-2 by the AMP-activated protein kinase in endothelial cells attenuates oxidative stress in diabetes. *Diabetes*, 57(12):3222–30, 2008. doi:10.2337/db08-0610. 112, 119, 159, 160

Xuan, S., Kitamura, T., Nakae, J., Politi, K., et al. Defective insulin secretion in pancreatic beta cells lacking type 1 IGF receptor. *The Journal of clinical investigation*, 110(7):1011–9, 2002. doi:10.1172/JCI15276. 168, 169, 171, 174

Xue, B. and Kahn, B.B. AMPK integrates nutrient and hormonal signals to regulate food intake and energy balance through effects in the hypothalamus and peripheral tissues. *J Physiol*, 574(Pt 1):73–83, 2006. doi:10.1113/jphysiol.2006. 113217. URL `http://jp.physoc.org/cgi/content/full/574/1/73`. 19, 20, 29, 31, 32

Yamagata, K., Furuta, H., Oda, N., Kaisaki, P.J., et al. Mutations in the hepatocyte nuclear factor-4alpha gene in maturity-onset diabetes of the young (MODY1). *Nature*, 384(6608):458–60, 1996. doi:10.1038/384458a0. URL `http://www.nature.com/nature/journal/v384/n6608/abs/384458a0.html`. 25

Yang, C., Chang, T.J., Chang, J.C., Liu, M.W., et al. Rosiglitazone (BRL 49653) enhances insulin secretory response via phosphatidylinositol 3-kinase pathway. *Diabetes*, 50(11):2598–602, 2001a. 37, 170

Yang, W., Hong, Y.H., Shen, X.Q., Frankowski, C., et al. Regulation of transcription by AMP-activated protein kinase: phosphorylation of p300 blocks its interaction with nuclear receptors. *J Biol Chem*, 276(42):38341–4, 2001b. doi:10.1074/jbc.C100316200. 25

Zhang, C., Baffy, G., Perret, P., Krauss, S., et al. Uncoupling Protein-2 Negatively Regulates Insulin Secretion and Is a Major Link between Obesity,[beta] Cell Dysfunction, and Type 2 Diabetes. *Cell*, 2001. URL `http://linkinghub.elsevier.com/retrieve/pii/S0092867401003786`. 10, 11, 16, 112, 160

Zhang, C.Y., Parton, L.E., Ye, C.P., Krauss, S., et al. Genipin inhibits UCP2-mediated proton leak and acutely reverses obesity- and high glucose-induced beta cell dysfunction in isolated pancreatic islets. *Cell Metab*, 3(6):417–27, 2006. doi:10.1016/j.cmet.2006.04.010. 11, 119, 161

Zhang, F., Dey, D., Bränström, R., Forsberg, L., et al. BLX-1002, a novel thiazolidinedione with no PPAR affinity, stimulates AMP-activated protein kinase activity, raises cytosolic Ca2+, and enhances glucose-stimulated insulin secretion in a PI3K-dependent manner. *Am J Physiol, Cell Physiol*, 296(2):C346–54, 2009. doi:10.1152/ajpcell.00444.2008. 37, 170

Zheng, D., MacLean, P.S., Pohnert, S.C., Knight, J.B., et al. Regulation of muscle GLUT-4 transcription by AMP-activated protein kinase. *J Appl Physiol*, 91(3):1073–83, 2001. 21, 30

Loss of AMP-activated protein kinase α2 subunit in mouse β-cells impairs glucose-stimulated insulin secretion and inhibits their sensitivity to hypoglycaemia

Craig BEALL*[1], Kaisa PIIPARI†[1], Hind AL-QASSAB†, Mark A. SMITH†*, Nadeene PARKER‡, David CARLING§, Benoit VIOLLET||, Dominic J. WITHERS†[2] and Michael L. J. ASHFORD*[2]

*Biomedical Research Institute, Ninewells Hospital and Medical School, University of Dundee, Dundee DD1 9SY, Scotland, U.K., †Metabolic Signalling Group, MRC Clinical Sciences Centre, Imperial College London, London W12 0NN, U.K., ‡Department of Cell and Developmental Biology, University College London, London WC1 6BT, U.K. §Cellular Stress Group, MRC Clinical Sciences Centre, Imperial College London, London W12 0NN, U.K., and ||INSERM U567, CNRS, UMR 8104, Institut Cochin, Université Paris Descartes, Paris, France

AMPK (AMP-activated protein kinase) signalling plays a key role in whole-body energy homoeostasis, although its precise role in pancreatic β-cell function remains unclear. In the present stusy, we therefore investigated whether AMPK plays a critical function in β-cell glucose sensing and is required for the maintenance of normal glucose homoeostasis. Mice lacking AMPKα2 in β-cells and a population of hypothalamic neurons (*RIPCreα2KO* mice) and *RIPCreα2KO* mice lacking AMPKα1 (*α1KORIPCreα2KO*) globally were assessed for whole-body glucose homoeostasis and insulin secretion. Isolated pancreatic islets from these mice were assessed for glucose-stimulated insulin secretion and gene expression changes. Cultured β-cells were examined electrophysiologically for their electrical responsivenss to hypoglycaemia. *RIPCreα2KO* mice exhibited glucose intolerance and impaired GSIS (glucose-stimulated insulin secretion) and this was exacerbated in *α1KORIPCreα2KO* mice. Reduced glucose concentrations failed to completely suppress insulin secretion in islets from *RIPCreα2KO* and *α1KORIPCreα2KO* mice, and conversely GSIS was impaired. β-Cells lacking AMPKα2 or expressing a kinase-dead AMPKα2 failed to hyperpolarize in response to low glucose, although K_{ATP} (ATP-sensitive potassium) channel function was intact. We could detect no alteration of GLUT2 (glucose transporter 2), glucose uptake or glucokinase that could explain this glucose insensitivity. UCP2 (uncoupling protein 2) expression was reduced in *RIPCreα2KO* islets and the UCP2 inhibitor genipin suppressed low-glucose-mediated wild-type mouse β-cell hyperpolarization, mimicking the effect of AMPKα2 loss. These results show that AMPKα2 activity is necessary to maintain normal pancreatic β-cell glucose sensing, possibly by maintaining high β-cell levels of UCP2.

Key words: AMP-activated protein kinase (AMPK), ATP-sensitive potassium channel (K_{ATP}), β-cell, glucokinase, pancreas, uncoupling protein 2 (UCP2).

INTRODUCTION

Raised plasma glucose increases the amount of glucose taken up by pancreatic β-cells predominantly through the glucose transporter, GLUT2 [1]. This increase in glucose metabolism occurs over the physiological range of glucose concentrations by the action of the rate-limiting enzyme GK (glucokinase). The raised β-cell metabolic flux increases the ratio of cellular [ATP]/[ADP], which closes K_{ATP} (ATP-sensitive potassium) channels, leading to membrane depolarization, opening of voltage-gated calcium channels, raised intracellular calcium and insulin secretion [2]. Thus temporal fluctuations of blood glucose levels are directly linked to variations in insulin secretion by the concerted activity of these key pancreatic β-cell proteins. Therefore these proteins are essential for pancreatic β-cells to mount an initial rapid insulin secretory response, which is followed by a slower K_{ATP}-independent release of insulin. There is strong evidence that dysfunctional pancreatic β-cells are central to the development of Type 2 diabetes [3,4]. A progressive increase in basal insulin secretion (during fasting) along with

a much reduced or absent first-phase of GSIS (glucose-stimulated insulin secretion) are considered early and common defects in Type 2 diabetes. Indeed, the loss or reduction of β-cell secretory responsiveness to glucose, when imposed on a background of peripheral insulin resistance, is likely to precipitate early-impaired glucose tolerance leading rapidly to Type 2 diabetes.

Oral anti-diabetic drug treatment has evolved in recent years to encompass the widespread use of metformin as a first-line drug for treatment of Type 2 diabetes [5]. Current evidence suggests that metformin reduces blood glucose levels by decreasing liver gluconeogenesis and increasing peripheral glucose uptake. The mechanisms by which metformin performs these actions have been linked to increased insulin action and the activation of AMPK (AMP-activated protein kinase). Consequently, AMPK has attracted considerable attention as a potential target for the treatment of Type 2 diabetes [6].

AMPK acts as a cellular integration node for various nutrient and hormone signals, and subsequent changes in AMPK activity regulates multiple metabolic pathways of glucose metabolism [7]. Thus there may be an expectation for AMPK to be

Biochemical Journal

critically involved in the regulation of insulin secretion by glucose. Indeed, diminished AMPK activity has been reported in islets from Type 2 diabetic patients [8]. However, the precise role of AMPK in the regulation of insulin secretion from β-cells is presently unclear and controversial. Activation of AMPK by AICAR (5-aminoimidazole-4-carboxamide-1-β-D-ribofuranoside), metformin or overexpression of a constitutively active form of AMPK reduces GSIS in rodent and human islets [9–12]. In contrast, overexpression of a dominant-negative form of AMPK is reported to increase insulin release at low glucose concentrations [10]. However, others have failed to replicate these findings [13,14], generating uncertainty over the role of AMPK in insulin secretion. Therefore to define the role of AMPK in β-cell function, we generated mice deficient in AMPKα2 (with or without global deletion of AMPKα1) in β-cells and examined the relationship between AMPK activity and the mechanisms thought to mediate normal glucose sensing.

MATERIALS AND METHODS

Animals

Floxed *AMPKα2* allele RIPCre mice (The Jackson Laboratory) were crossed to generate compound heterozygote mice. Double-heterozygote mice were crossed with *AMPKα2$^{+/fl}$* mice to obtain WT (wild-type), flox$^{+/+}$, *Cre* and Creflox$^{+/+}$. Mice lacking AMPKα2 in *RIPCre*-expressing cells were designated *RIPCreα2KO* mice. *RIPCreα2KO* and *AMPKα1KO* mice were crossed to generate mice lacking AMPKα1 globally (*α1KO*) and AMPKα2 in RIPCre-expressing cells (*α1KORIPCreα2KO* mice). All mice were maintained on a 12-h light/12-h dark cycle with free access to water and standard mouse chow (4% fat, RM1; Special Diet Services) and housed in pathogen-free barrier facilities. All procedures were in accordance with the UK Home Office Animal Procedures Act of 1986 and approved by the University of Dundee and University College London Animal Ethics Committees. All mice were studied with appropriate littermate controls. Genotyping of mice was performed by PCR amplification of tail DNA as described previously [15,16].

Physiological measurements

Body weight and feeding measurements, and tolerance tests were performed as described previously [15,17]. Blood glucose and plasma insulin levels were determined using mouse ELISAs (Linco Research).

Gene expression studies

Quantitative PCR was performed as described previously [15,16]. Expression levels of *AMPKα2, Gck* (glucokinase gene), *HMOX1* (haem oxygenase 1), *GPX4* (glutathione peroxidase 4), *NPY* (neuropeptide Y), *Nrf1* (nuclear respiratory factor 1), *Pgc1α* (peroxisome proliferator-activated receptor γ coactivator 1-α), *POMC* (pro-opiomelanocortin), *Slc2a2* [solute carrier family 2 (facilitated glucose transporter) member 2; previously known as *Glut2*], *SOD2* (superoxide dismutase 2), *SUR1* (sulfonylurea receptor 1), *Tfam* (transcription factor A, mitochondrial) and *UCP2* (uncoupling protein 2) were normalized to *GAPDH* (glyceraldehyde-3-phosphate dehydrogenase) or *HPRT* (hypoxanthine phosphoribosyltransferase 1) and data were analysed using the $2^{-\Delta Ct}$ method [15].
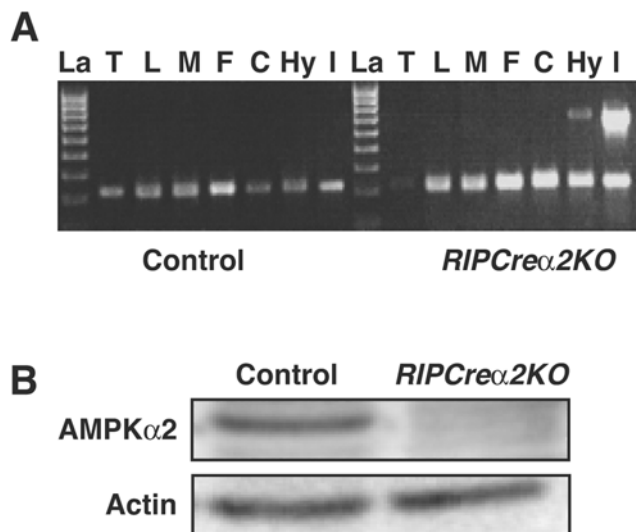

Figure 1   Reduction in islet and hypothalamic AMPKα2 in *RIPCreα2KO* mice

(**A**) Detection of the deletion of the *AMPKα2* allele in *RIPCreα2KO* mice. DNA was extracted from different tissues (T, tail; L, liver; M, skeletal muscle; F, fat; C, cerebral cortex; Hy, hypothalamus; I, islets of Langerhans) and recombination of the floxed *AMPKα2* allele was detected by PCR. The presence of the 750 bp band indicates deletion of *AMPKα2*. Recombination was only detected in islets of Langerhans and the hypothalamus from *RIPCreα2KO* mice. A PCR with *IL2* (interleukin-2) as an internal control shows the presence of DNA template in all of the samples. La, DNA ladder. (**B**) Representative immunoblot for AMPKα2 from control and *RIPCre2αKO* islets.

Western blot analysis

Islet and hypothalamic lysates were prepared as described previously [15–17] and immunoblots probed with polyclonal antibodies against ATP synthase (Abcam), AMPKα2 (supplied by David Carling) and β-actin (Cell Signalling), with ECL (enhanced chemiluminescence; Amersham Biosciences) detection.

Pancreas morphometry

Antibodies used were mouse anti-insulin (I-2018; Sigma–Aldrich), rabbit anti-glucagon (ab9379; Abcam), chicken anti-mouse Alexa Fluor® 594 and chicken anti-rabbit Alexa Fluor® 488 (both Molecular Probes/Invitrogen). Confocal images were captured using a Carl Zeiss LSM 700 laser scanning microscope with 20× air objective.

Islets and CRI-G1 (Cambridge rat insulinoma-G1) experiments

Mouse pancreatic islet isolation, islet insulin secretion studies and β-cell culture were performed as described previously [16,18]. Treatments of CRI-G1 cells with Compound C (Calbiochem), AICAR (Toronto Research Chemicals) and A-769662 were carried out in normal saline $\pm$ 10 mM glucose. Hexokinase activity in CRI-G1 cells was measured as described previously [19]. Cell lysates were prepared for immunoblotting and analysis as described previously [20]. For glucose uptake, the fluorescent glucose analogue 2-NBDG (Molecular Probes) was applied at 100 μM in the presence of glucose $\pm$ AICAR and $\pm$ Compound C, and imaged as described previuosly [21]. In control experiments, CRI-G1 cells took-up 2-NBDG in a linear manner for >1 h. For immunostaining, CRI-G1 cells were washed and immediately fixed after treatments and then permeabilized with 0.5% Triton X-100 in PBS. Non-specific-binding was blocked with 10% (w/v) BSA and primary antibodies against GLUT2 and GK
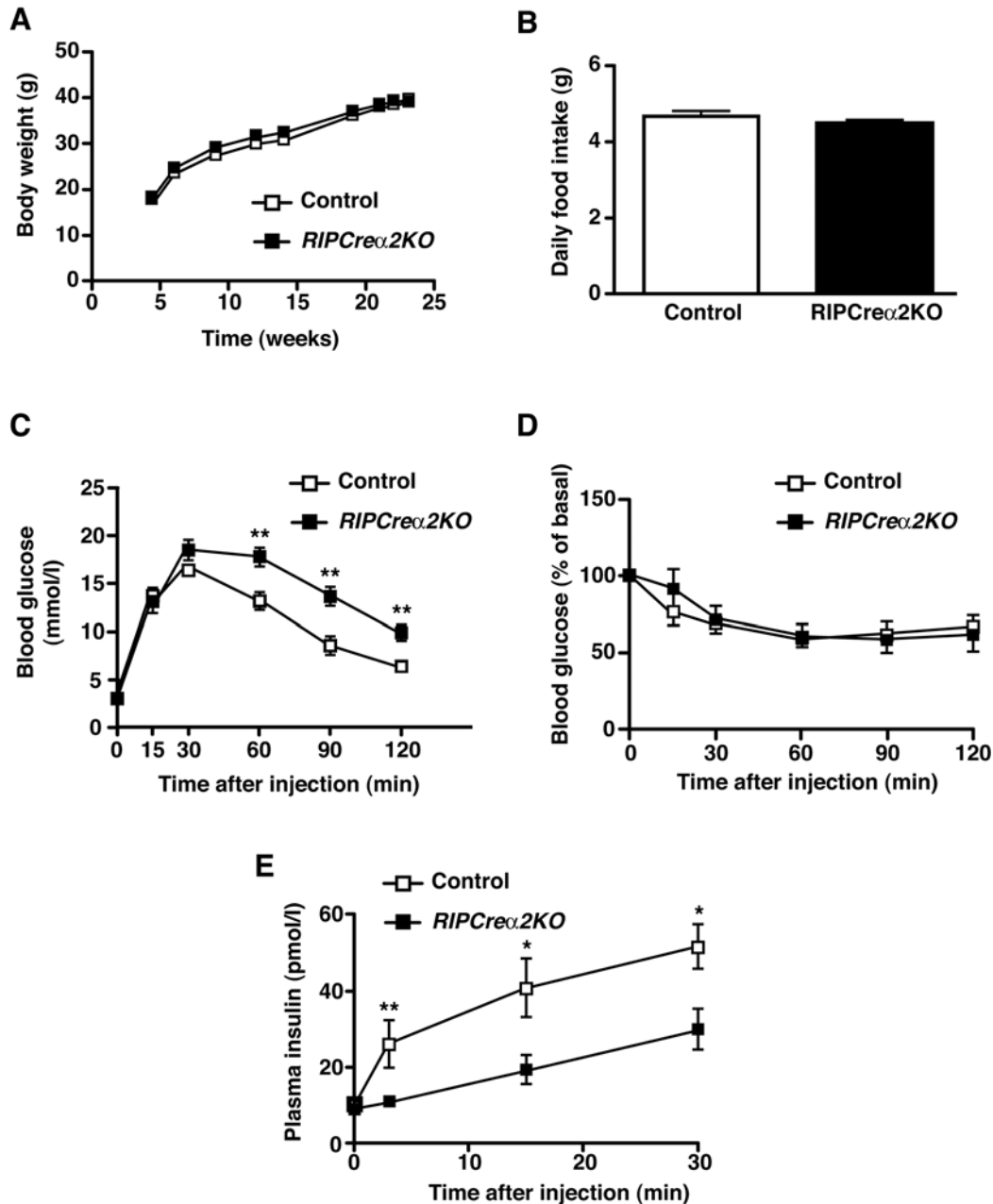
Figure 2   Glucose homoeostasis in *RIPCreα2KO* mice

(**A**) Weight curves of male control and *RIPCreα2KO* mice on a chow diet ($n = 5$–8). (**B**) Daily food intake of *RIPCreα2KO* and control mice ($n = 7$–9). (**C**) Intraperitoneal glucose tolerance test performed on 16-week-old male *RIPCreα2KO* (■) and control (□) mice ($n = 8$). (**D**) Insulin tolerance test performed on 20-week-old male *RIPCReα2KO* (■) and control (□) mice ($n = 7$). (**E**) Plasma insulin levels before and after intraperitoneal injection of glucose (2 g/kg of body weight) in 10-week-old male *RIPCreα2KO* (■) and control (□) mice ($n = 6$–7). Values are means ± S.E.M. $*P < 0.05$, $**P < 0.01$.

(Santa Cruz Biotechnology) were applied at a 1:1000 dilution for 1 h. For visualization, either Alexa Fluor® 488 (Molecular Probes) or Cy3 (indocarbocyanine; Jackson ImmunoResearch)-conjugated secondary antibodies were used according to the manufacturers' instructions. CRI-G1 cell nucleotide determination was performed as described previously [9]. H_2O_2 levels in individual islets were measured by epifluorescent microscopy using the fluorescent probe CM-H_2DCFDA [5-(and-6)-chloromethyl-2′,7′-dichlorodihydrofluorescein diacetate, acetyl ester] at a concentration of 1 μM, with a 60 min preloading time.

Electrophysiological studies

Mouse cultured β-cells were super-fused at room temperature (22–25 °C) with normal saline [135 mM NaCl, 5 mM KCl, 1 mM $MgCl_2$, 1 mM $CaCl_2$, 10 mM Hepes and 10 mM glucose (pH 7.4)]. Whole-cell recordings were made using borosilicate glass pipettes (5–10 MΩ) containing 140 mM KCl, 10 mM EGTA, 5 mM $MgCl_2$, 3.8 mM $CaCl_2$ and 10 mM Hepes (pH 7.2) ± ATP at 3.0 mM, 1.0 mM, 0.1 mM and 0 mM. For voltage-clamp recordings the membrane potential was held at −70 mV and 20 mV steps of 200 ms duration, with 20 ms

between pulses, applied (voltage range from -160 to -40 mV). Voltage-clamp data were analysed using pCLAMP 8.2 software. Perforated patch recordings were achieved by addition of 25–50 μg/ml amphotericin B (Sigma–Aldrich) to the pipette solution. Series resistance was <30 MΩ for all recordings. Following a minimum of 10 min of stable recording, the extracellular glucose concentration was altered or drugs applied by bath superfusion.

Statistics

Data are presented as means $\pm$ S.E.M. All statistics were performed using GraphPad (Prism 5) software. Paired or Wilcoxon signed-rank sum test and unpaired t tests were performed. P values $\leqslant 0.05$ were considered statistically significant.

RESULTS

Deletion of AMPKα2 in the pancreas and a subset of hypothalamic neurons does not affect body weight or food intake, but impairs glucose homoeostasis and GSIS in mice

Mice expressing *Cre* under the control of the rat insulin II promoter and mice with a floxed allele of *AMPKα2* were crossed to generate mice lacking AMPKα2 in pancreatic β-cells and a small population [15] of hypothalamic neurons (*RIPCreα2KO* mice). We detected recombination of the floxed *AMPKα2* allele in islets and hypothalamus from *RIPCreα2KO* mice and protein expression of AMPKα2 was significantly reduced in islets (Figures 1A and 1B). No significant change in *NPY* or *POMC* mRNA was detected in fasted *RIPCreα2KO* mice (Supplementary Figure S1A at http://www.BiochemJ.org/bj/429/bj4290323add.htm). Furthermore, *RIPCreα2KO* mice exhibited normal body weight and unchanged daily food intake compared with littermate controls (Figures 2A and 2B), suggesting no significant hypothalamic phenotype. *RIPCreα2KO* mice displayed normal fasted and fed blood glucose levels, and fasted plasma insulin as compared with control mice (Supplementary Figures S1B–S1D). *RIPCreα2KO* mice displayed mild glucose intolerance compared with littermate controls (Figure 2C), but no reduction in peripheral insulin sensitivity (Figure 2D). However, *in vivo* GSIS was depressed in *RIPCreα2KO* mice (Figure 2E), potentially explaining their mild glucose intolerance. To address the possibility of compensatory up-regulation of AMPKα1 expression in cells deleted for AMPKα2, we used mice with global deletion of *AMPKα1* (*α1KO*), which exhibit a normal metabolic phenotype [22] and *α1KORIPCreα2KO* mice (lacking AMPKα2 in pancreatic β-cells and some hypothalamic neurons and AMPKα1 in all tissues). The *α1KORIPCreα2KO* mice exhibited normal body weight (results not shown) and food intake compared with controls (Figure 3A), again indicating no hypothalamic disturbance. However, the *α1KORIPCreα2KO* mice displayed profound impairment of glucose tolerance and *in vivo* GSIS was markedly depressed in *α1KORIPCreα2KO* mice compared with controls (Figures 3B and 3C).

AMPK-deleted islets *in vitro* exhibit increased insulin release at basal glucose and decreased GSIS

Because AMPKα2 was also deleted in some hypothalamic neurons, we were concerned that altered autonomic activity to peripheral organs, as described for the global *AMPKα2KO* mouse [22], was influencing β-cell function. We therefore undertook further *in vitro* analysis of β-cell function using *RIPCreα2KO* and *α1KORIPCreα2KO* isolated islets. Static incubation of *RIPCreα2KO* islets showed enhanced insulin secretion under
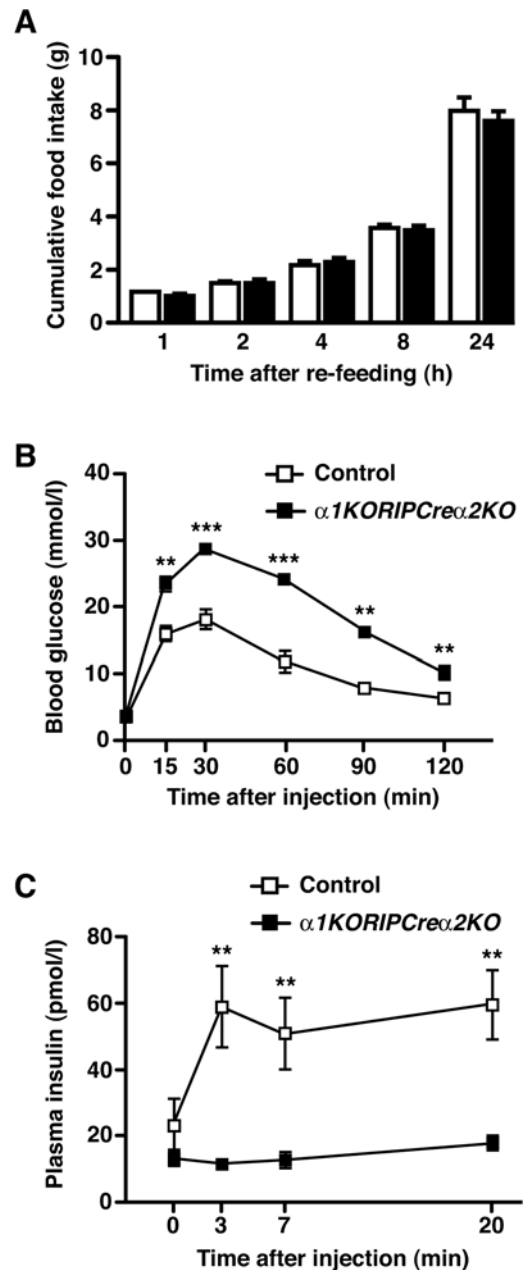
Figure 3   Mice lacking AMPKα1 globally and AMPKα2 in β-cells and a population of hypothalamic neurons exhibit glucose intolerance and defective GSIS

(**A**) Cumulative 24-h food intake in 20-week-old male control (open bars) and α1KORIPCreα2KO (solid bars) mice in response to an overnight fast ($n = 5$). (**B**) Intraperitoneal glucose tolerance test performed on 5-week-old male α1KORIPCreα2KO (■) and control (□) mice ($n = 8$–11). (**C**) Plasma insulin levels before and after intraperitoneal injection of glucose (2 g/kg of body weight) in 10-week-old male α1KORIPCreα2KO (■) and control (□) mice ($n = 6$–7). Values are means $\pm$ S.E.M. **$P < 0.01$, ***$P < 0.001$.

basal (2 mM) glucose conditions compared with control islets, whereas GSIS (glucose raised to 20 mM) displayed a non-significant trend towards decreased secretion (Figure 4A). Furthermore, insulin secretion from α1KORIPCreα2KO islets at 2 mM glucose was enhanced and GSIS significantly impaired compared with control animals (Figure 4B). The increased basal insulin secretion is consistent with that reported previously with adenoviral overexpression of a dominant-negative form of AMPK
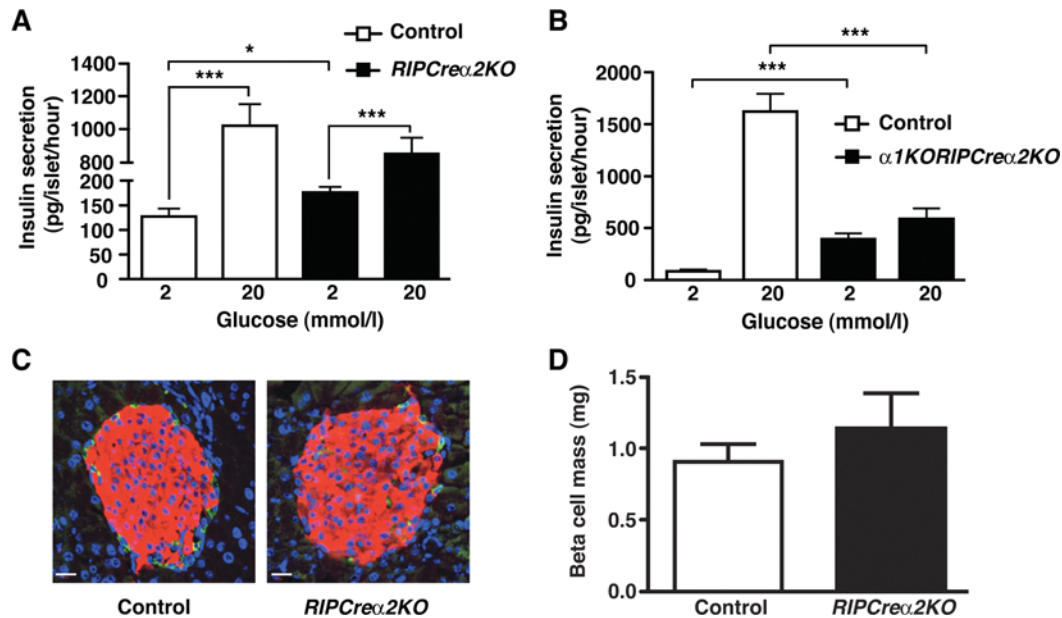
Figure 4   Defective GSIS in isolated islets from mice lacking AMPK catalytic α subunits

(**A**) Insulin secretion from isolated control (open bars) and *RIPCreα2KO* (solid bars) islets in static cultures in response to 2 and 20 mM glucose. (**B**) Insulin secretion from isolated control (open bars) and *α1KORIPCreα2KO* (solid bars) islets in static cultures in response to 2 and 20 mM glucose. (**C**) Pancreatic sections from control and *α1KORIPCreα2KO* islets, from 10-week-old male mice, co-stained for insulin (red), glucagon (green) and DAPI (4′,6-diamidino-2-phenylindole; blue). (**D**) Mean β-cell mass in islets of control and *α1KORIPCreα2KO* mice (n = 4). Values are means ± S.E.M. *P < 0.05, ***P < 0.001.

in β-cells [10]. Taken together, these findings indicate that appropriate expression of AMPK α subunits is required for normal glucose sensing and GSIS in pancreatic β-cells.

Deletion of AMPKα2 does not alter β-cell mass

Recent studies show that loss of LKB1, an AMPK kinase, increases β-cell size and enhances insulin secretion [23,24]. Therefore we undertook islet morphometric analysis in *RIPCreα2KO* and control mice to exclude increased β-cell mass as a contributing factor. Absolute β-cell mass was unaltered in *RIPCreα2KO* mice compared with control animals (Figures 4C and 4D), which indicated that altered β-cell function underlies the changes observed in basal insulin secretion and GSIS.

AMPKα2 is required for low-glucose-induced hyperpolarization of pancreatic β-cells

We next examined whether the high basal insulin secretion was associated with altered β-cell electrical responsiveness to glucose. Perforated patch recordings from single cultured isolated β-cells showed that control (WT and *RIPCre*) β-cells responded to low glucose (10 mM to 2 mM) by membrane potential hyperpolarization causing cessation of action potential firing, actions reversed on returning to 10 mM glucose (Figures 5A and 5B). In contrast, the majority (19 out of 24) of β-cells from *RIPCreα2KO* islets displayed no hyperpolarizing response to low glucose, maintaining an unchanged membrane potential in 2 mM and 10 mM glucose (Figure 5C). The remaining five cells responded normally to hypoglycaemia (results not shown), consistent with lack of deletion of the floxed allele in all β-cells [15].

One potential issue with this type of genetic manipulation is that developmental compensation for loss of the target gene may occur and modify the observed phenotype. In an attempt to preclude this possibility, we treated WT mouse cultured β-cells with adenovirus containing GFP (green fluorescent protein) as a control or a kinase-dead mutant form of AMPKα2, which acts as a dominant-negative towards native AMPK (DNAMPKα2). Control viral infected β-cells were electrically active and responded, reversibly, to low glucose by hyperpolarization and inhibition of action potential firing (Figure 6A), identical with control β-cells. Cells treated with DNAMPKα2 adenovirus were also electrically active in 10 mM glucose and, on reduction to 2 mM glucose, a significant proportion of the infected cells (n = 11/33) displayed no response to hypoglycaemic challenge (Figure 6B), with the remainder behaving as controls. The low proportion of β-cells unresponsive to hypoglycaemia is probably related to infection efficiency, as obvious GFP expression was observed in <50% of β-cells. Attempts to increase the MOI (multiplicity of infection) to achieve higher expression of DNAMPKα2 resulted in cell toxicity. The non-responsive *RIPCreα2KO* and DNAMPKα2 β-cells were demonstrated to be capable of hyperpolarization by their responsiveness to the K$_{ATP}$ activator, diazoxide, as compared with control β-cells (Figure 6C).

Isolated islets from *α1KORIPCreα2KO* mice also displayed significantly higher insulin secretion at 2 mM glucose in comparison with control mice. Thus to confirm the role of AMPKα2 in regulating β-cell sensitivity to hypoglycaemia, we made recordings from β-cells of *α1KO* and *α1KORIPCreα2KO* mice. All *α1KO* β-cells displayed normal responses to hypoglycaemic challenge, with rapid hyperpolarization and cessation of firing, actions reversed on re-addition of 10 mM glucose (Figure 6D). In contrast, the majority (7 out of 11) of *α1KORIPCreα2KO* β-cells displayed little or no sensitivity to hypoglycaemic challenge (Figure 6E), with the remaining cells responding like controls (results not shown), as described for *RIPCreα2KO* β-cells. Taken together, these findings suggest that AMPKα2 contributes to the normal glucose sensing behaviour of pancreatic β-cells.
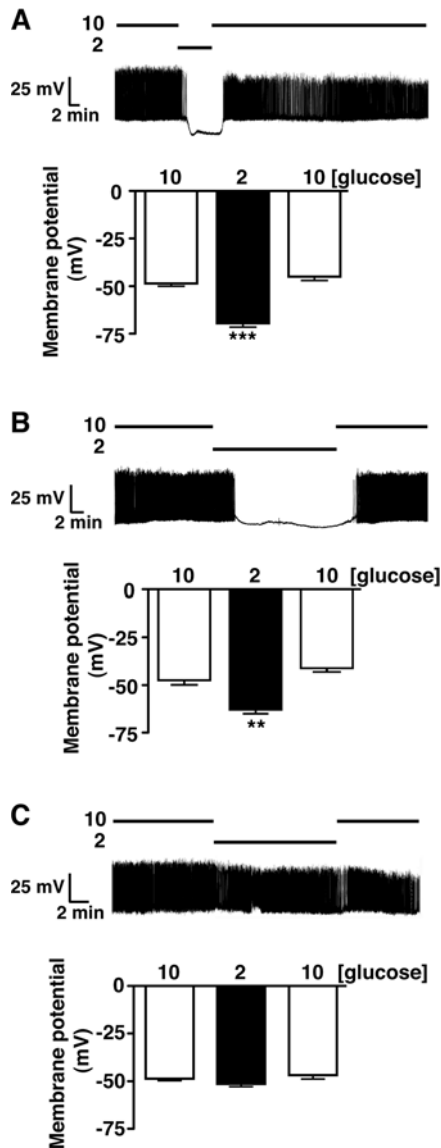
Figure 5   Loss of hypoglycaemic sensing in isolated β-cells from RIPCreα2KO mice

WT (**A**) and RIPCre (**B**) mouse cultured β-cells respond, reversibly, to the reduction of glucose from 10 to 2 mM by hyperpolarization and cessation of firing. (**C**) RIPCreα2KO β-cells are unresponsive to a reduction of glucose concentration from 10 to 2 mM. The histograms in (**A**–**C**) are the mean values for membrane potential in β-cells exposed to 10, 2 and 10 mM glucose for each condition. Values were derived from seven to 19 individual β-cell recordings per group and are shown as means ± S.E.M. **$P < 0.01$, ***$P < 0.001$.

Altered AMPK levels or activity do not modify ATP levels, glucose uptake or GK activity

Changing AMPK activity may regulate the expression, localization or activity of GK and GLUT2 [25–28]. Therefore we explored whether altered AMPK activity modified glucose uptake or metabolism in β-cells, using RIPCreα2KO islets and a rat β-cell line. Although AMPKα2 mRNA was significantly reduced in RIPCreα2KO compared with control islets, levels of GLUT2 or GK mRNA were unchanged (Figure 7A and Supplementary Figure S2D at http://www.BiochemJ.org/bj/429/bj4290323add.htm). Additionally, there was no change in the levels of mRNA for the low-K_m hexokinase isoforms (HK I–III) in RIPCreα2KO islets compared with control islets (Supplementary Figures

S2A–S2C). The CRI-G1 cell line was used to examine the actions of AMPK activity modification because it demonstrated significant GK expression and an innate hypersensitivity to glucose, whereby reducing glucose from 10 mM to 2 mM did not affect cell membrane potential or firing frequency, although lower glucose (<1 mM) levels caused hyperpolarization and inhibition of firing (Supplementary Figures S3A and S3B at http://www.BiochemJ.org/bj/429/bj4290323add.htm). CRI-G1 cells exhibited unchanged GLUT2 or GK protein expression, GK localization (results not shown) and glucose uptake (Supplementary Figure S3C) following stimulation or inhibition of AMPK activity with AICAR (1 mM) or compound C (40 μM) respectively. We next considered the possibility that AMPKα2 acts as a negative regulator of GK activity. GK is the primary glucose sensor of β-cells [29] and pharmacological activation of β-cell GK with GKA50 increases insulin secretion at 2 mM glucose [30], mimicking the RIPCreα2KO β-cell phenotype. Indeed, exposure of WT β-cells to 100 nM GKA50 prevented hyperpolarization and inhibition of electrical activity by hypoglycaemic challenge (Figure 7B). Furthermore, CRI-G1 cells displayed a glucose concentration-dependent increase in GK activity (Figure 7C), significantly higher than for INS-1 cells (CRI-G1 cells, ∼90–100 milli-units/mg of protein; INS-1 cells, 8–10 milli-units/mg of protein at 100 mM glucose [31]). This is consistent with CRI-G1 insensitivity to low glucose as high GK activity should raise cellular ATP and maintain K_{ATP} in the closed state, analogous to activating GK mutations, which are also characterized by hypersecretion of insulin at basal glucose levels [32]. Our initial studies appeared to corroborate this hypothesis, as AICAR (1 mM) caused significant inhibition (∼30%) of GK activity in CRI-G1 cells, at glucose concentrations above 0.5 mM, and compound C prevented this effect (Figures 7C and 7D). Although an attractive explanation for modification of glucose sensing by AMPK, the inhibition of GK activity was not replicated when AMPK activity was stimulated with the direct AMPK activator [33], A-769662 (Figure 7E). Additionally, the [ATP]/[ADP] ratio of CRI-G1 cells following stimulation or inhibition of AMPK was unaffected (Figure 7F).

RIPCreα2KO islets also displayed unaltered mitochondrial mass reflected by unchanged levels of ATP synthase (Figure 7G) and mRNA levels of transcription factors involved in mitochondrial energy metabolism, PGC1α, Tfam and Nrf were unaltered (Figure 7A). In contrast, the mRNA level for the K_{ATP} channel subunit, SUR1 (Figure 7A) was reduced, raising the possibility that altered K_{ATP} current levels or ATP sensitivity may underlie the lack of responsiveness to hypoglycaemia by AMPKα2 deletion. However, the maximal K_{ATP} current and ATP-sensitivity (Figures 8A and 8B) were unaltered between RIPCreα2KO and RIPCre control β-cells. Overall, we could not identify any alteration to glucose uptake, coupling of glucose metabolism to mitochondrial ATP production or deficiency in K_{ATP} channel function, which would explain the hypersecretion of insulin at low glucose or the reduction in GSIS in AMPKα2-deficient β-cells.

Islets lacking AMPKα2 have reduced UCP2, and UCP2 inhibition causes glucose insensitivity of β-cells

Increased UCP2 activity has been reported to impair GSIS in islets [34,35]. Conversely, UCP2 reduction increases GSIS [36,37], and pharmacological inhibition of UCP2 with genipin stimulates insulin secretion [38]. UCP2 mRNA was markedly suppressed in RIPCreα2KO islets (Figure 7A). Furthermore, exposure of WT β-cells to genipin prevented the hyperpolarization associated with hypoglycaemic challenge (Figure 8C), but did not influence
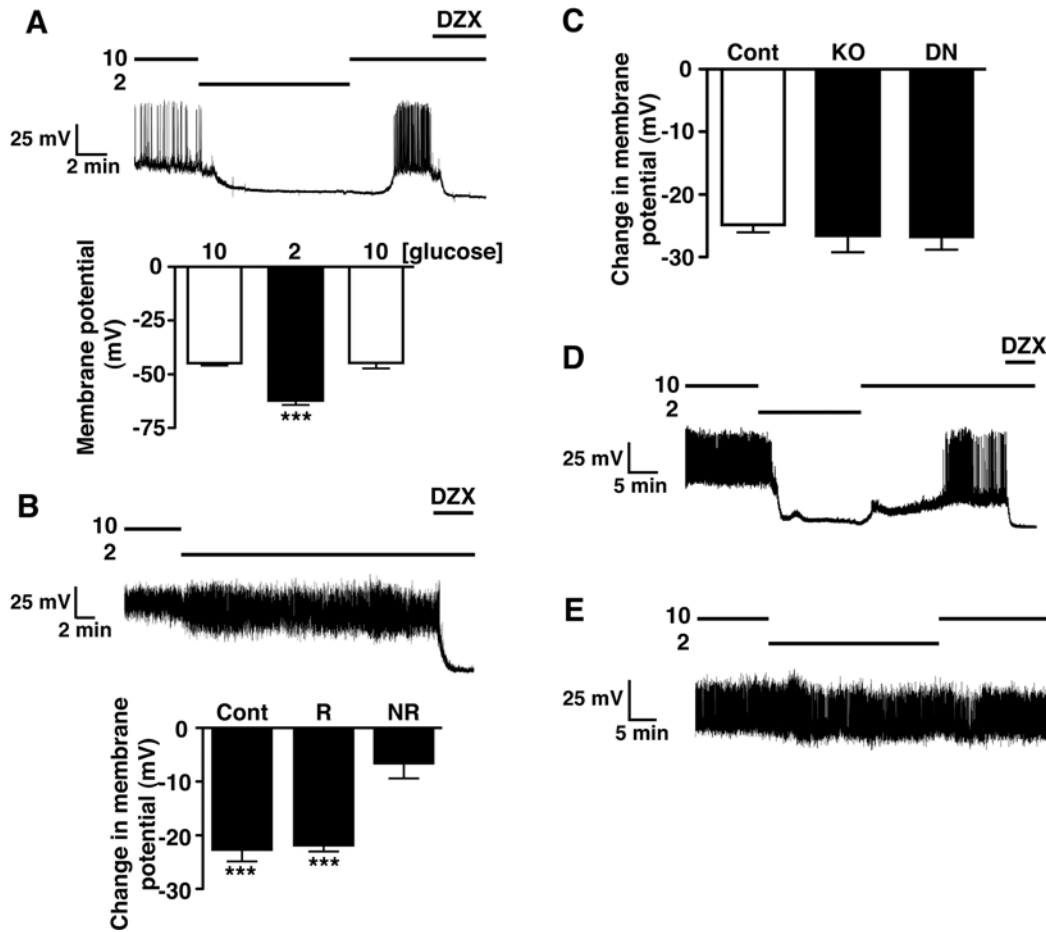
Figure 6   Loss of hypoglycaemic sensing in isolated β-cells lacking AMPK activity

(**A**) WT mouse cultured β-cells treated with GFP adenovirus display a normal reversible response to reduction of glucose from 10 to 2 mM. (**B**) WT mouse cultured β-cells treated with DNAMPKα2 adenovirus exhibit loss of electrical responsiveness to hypoglycaemia. The histograms are the mean values for the change in membrane potential associated with reduction in glucose from 10 to 2 mM in responding (R, $n = 22$) and non-responding (NR, $n = 11$) β-cells, in comparison with control (WT) β-cells (Cont, $n = 7$). (**C**) Mean change in membrane potential of control ($n = 12$), RIPCreα2KO (KO, $n = 11$) and glucose-unresponsive DNAMPKα2-treated (DN, $n = 11$) β-cells in response to application of diazoxide (250 μM). (**D**) α1KO mouse β-cells respond normally to reduction of glucose from 10 to 2 mM, showing typical hyperpolarization and inhibition of action potential activity. (**E**) α1KORIPCreα2KO β-cells are unresponsive, electrically, to hypoglycaemic challenge. Values are means $\pm$ S.E.M. ***$P < 0.001$. DZX, diazoxide.

the response of the cells to diazoxide (ΔV control $= -19.6 \pm 1.3$ mV; $n = 5$; ΔV genipin -19.0 ± 3.7 mV; $n = 6$). Although genipin has been reported to have a variety of activities, at the concentration used in the present study it is considered to act relatively specifically [38]. In addition, genipin excites mouse arcuate POMC neurons by closure of K_{ATP} channels only when UCP2 is present in the neurons [39]. Consistent with our β-cell data, hyperpolarization of POMC neurons in response to reduced glucose is also ablated in *AMPKα2KO* POMC neurons [17] and is reversibly occluded by genipin in WT mouse POMC neurons (Supplementary Figure S4 at http://www.BiochemJ.org/bj/429/bj4290323add.htm). However, UCP2 reduction itself, would be predicted to increase GSIS, whereas the loss of AMPKα2 in β-cells resulted in diminished GSIS. Thus we sought an alternative explanation. UCP2 activity plays a key role in the control of mitochondrial-driven ROS (reactive oxygen species) production [40] and a lack or reduction of UCP2 in β-cells increases ROS and impairs GSIS from islets [41]. However, we detected no increase in H_2O_2 production in WT, *RIPCreα2KO* or *α1KORIPCreα2KO* islets at 2 or 20 mM glucose, by CM-H_2DCFDA-derived fluorescence (Figure 8D). Furthermore, we did not detect any increase in mRNA level for

antioxidant enzymes in *RIPCreα2KO* islets (Figure 8E), indicative of an increased innate adaptive response to oxidative stress, which has also been reported to impair GSIS [41].

DISCUSSION

A previous study has shown that global *AMPKα2KO* mice demonstrate impaired glucose homoeostasis, which was ascribed to increased catecholamine secretion [22]. In contrast, we show that *RIPCreα2KO* and *α1KORIPCreα2KO* mice exhibit impaired glucose tolerance associated with dysfunctional GSIS *in vivo* and in isolated islets. Electrophysiological examination of AMPKα2-depleted isolated β-cells showed that the normal inhibitory electrical response to low glucose was ablated in the majority of these cells compared with control β-cells, in accordance with the observed enhanced basal insulin secretion. This outcome indicates that the K_{ATP} channels of AMPKα2-depleted β-cells, in contrast with control β-cells, remain closed under hypoglycaemic conditions. Elevated electrical activity and increased insulin release at low-glucose concentrations have been reported for β-cells with reduced levels of functional K_{ATP} channels in the
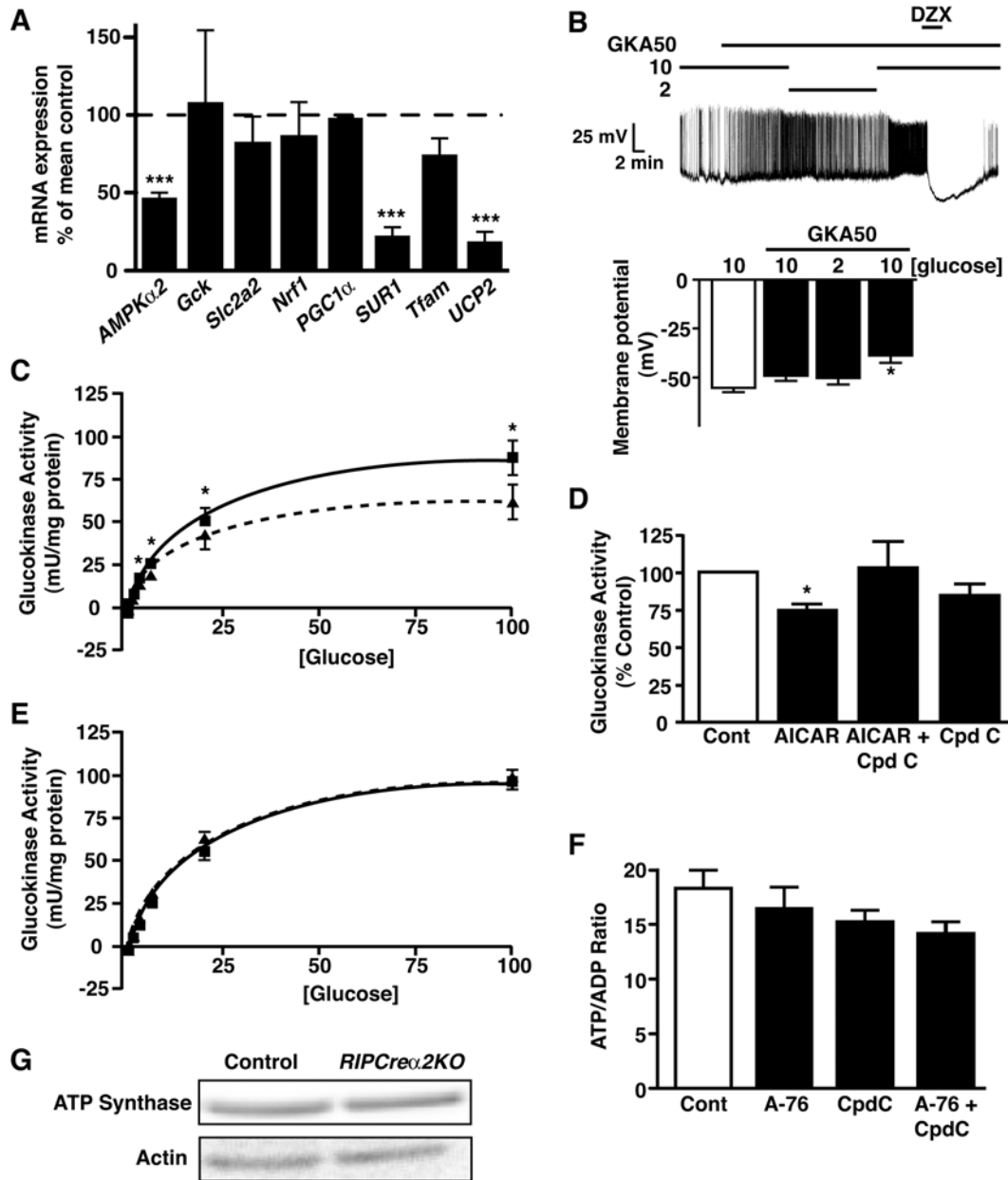
Figure 7   AMPK activity does not correlate with altered GK activity, nucleotide ratios or mitochondrial mass

(**A**) Relative islet mRNA expression, from 20-week-old male control and RIPCreα2KO mice, of AMPKα2, Gck, Slc2a2, Nrf1, PGC1a, SUR1, Tfam and UCP2 ($n = 6$). (**B**) WT mouse cultured β-cells treated with 100 nM GKA50 fail to respond electrically to hypoglycaemic challenge, but respond normally to diazoxide (250 μM; DZX). Histograms are the mean values for membrane potential in β-cells exposed to 10 mM glucose alone, and 10, 2 and 10 mM glucose in the presence of GKA. (**C**) Activity of GK in CRI-G1 β-cells as a function of glucose concentration in the absence (■) and presence (▲) of AICAR (1 mM). The curved lines (Control, solid; AICAR, broken) represent lines of best fit to the data points ($n = 5$–8 determinations per point). (**D**) GK activity, expressed relative to control conditions (6 mM glucose), in CRI-G1 β-cells exposed to 1 mM AICAR $\pm$ 40 μM Compound C in 6 mM glucose ($n = 5$–8 determinations for each condition). (**E**) Activity of GK in CRI-G1 β-cells as a function of glucose concentration in the absence (■) and presence (▲) of A-769662 (10 μM). The curved lines (Control, solid; A-769662, broken) represent lines of best fit to the data points ($n = 6$ determinations per point). (**F**) Mean values for the [ATP]/[ADP] ratio of CRI-G1 β-cells in control conditions and treated with 10 μM A-769662 $\pm$ 40 μM Compound C ($n = 3$–6 determinations for each condition). (**G**) Representative immunoblot of ATP synthase from control and RIPCre2αKO islets. A-76, A-769662; cont, control; Cpdc, compound C.

plasma membrane [42,43], or which have loss of function mutations in one of the K_{ATP} channel subunits, $K_{IR}6.2$ or SUR1 [44]. It has also been suggested that AMPK can modify β-cell K_{ATP} activity by phosphorylation of $K_{IR}6.2$ [45] or altered plasma membrane channel numbers [46]. However, this is unlikely to explain AMPKα2KO β-cell electrical insensitivity to hypoglycaemia because the cells display normal hyperpolarizing responses to diazoxide and exhibit an unaltered maximal K_{ATP} current compared with control cells. An alternative explanation is

that lack of AMPKα2 activity decreases K_{ATP} current by increased channel ATP sensitivity causing maintained K_{ATP} closure in the face of reduced cell ATP levels during the hypoglycaemic challenge. However, we could detect no difference in the ATP-sensitivity of K_{ATP} comparing AMPKα2-null and control β-cells.

Reduced expression of GLUT2 in rodents and humans correlates with β-cell glucose insensitivity [8,47]. However, as we could detect no evidence to link altered AMPK levels or activity to a change in GLUT2 mRNA or protein levels or to glucose
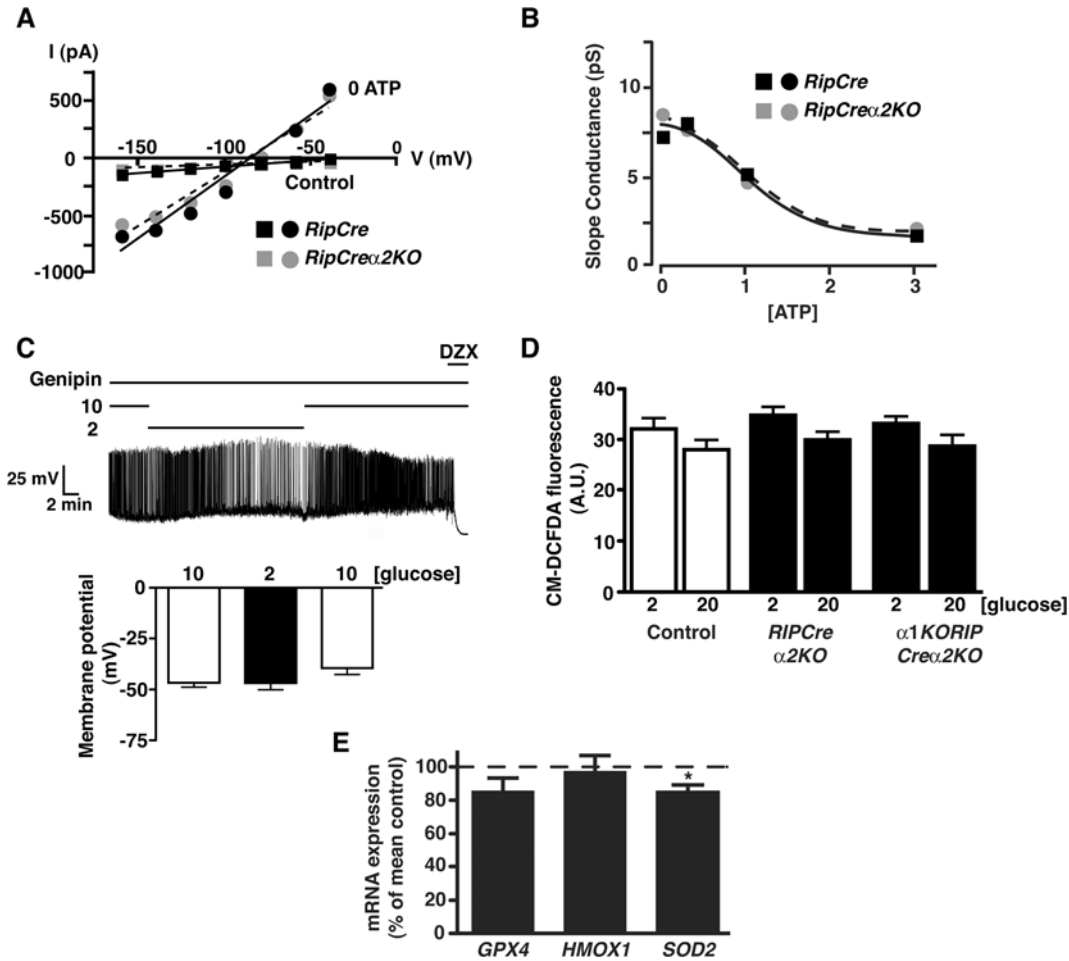
Figure 8   Loss of AMPKα2 does not alter β-cell K_ATP current or ATP-sensitivity or islet ROS response

(**A**) Representative current–voltage relationships for voltage-clamped currents of *RIPCre* control (black symbols) and a *RIPCreα2KO* (grey symbols) cultured β-cells. Mean currents were measured at various membrane potentials shortly after attaining whole-cell recording (i.e. prior to significant washout of cell ATP; filled squares) and 20 min later (following maximal washout of cellular ATP; filled circles). (**B**) Mean slope conductance values for current–voltage relationships as shown in (**A**), as a function of [ATP] (0, 0.5, 1.0 or 3.0 mM in the pipette solution). Lines of best fit (dose–response) are shown for *RIPCre* control (black filled squares) and *RIPCreα2KO* (grey filled circles) β-cells ($n = 3$–6). (**C**) WT β-cells exposed to genipin (100 nM) are electrically unresponsive to the reduction of glucose from 10 mM to 2 mM. Note that 250 μM diazoxide (DZX) hyperpolarizes the cell in the presence of genipin. Histograms are the mean values for membrane potential for β-cells, in the presence of genipin exposed to 10, 2 and 10 mM glucose respectively ($n = 6$). (**D**) H_2O_2-derived fluorescence in isolated islets of control, *RIPCreα2KO* and *α1KORIPCreα2KO* mice ($n = 16$–23 islets each) at 2 and 20 mM glucose. A. U., arbitray units. (**E**) Expression of antioxidant enzymes in isolated islets of *RIPCreα2KO* mice, normalized to the levels expressed in control WT mice ($n = 8$–10). *$P < 0.05$.

uptake, this component of β-cell glucose sensing is unlikely to be responsible for the defective control of insulin secretion described in the present study. Deletion of the upstream AMPK regulator LKB1 results in improved glucose tolerance, β-cell hypertrophy, higher insulin content and increased secretion *in vivo* and *in vitro* [23,24]. These results have been interpreted as LKB1, by increasing AMPK activity, acting to restrain insulin secretion. However, we observe no change in β-cell mass, and GSIS in AMPKα2-deleted islets is impaired not enhanced, indicating that AMPKα2 β-cell deletion is unlikely to be associated with reduced LKB1 activity. Our results also indicate that the outcome of LKB1 deletion in β-cells described in these reports may not be due simply to altered AMPK activity.

GK plays a central role in the control of GSIS because it allows glucose phosphorylation at physiological glucose concentrations. Inactivating mutations of GK result in reduced insulin secretion and Type 2 diabetes, whereas GK-activating mutations cause insulin hypersecretion and hypoglycaemia [48]. Thus high GK activity should result in high levels of ATP at low-glucose

concentrations and keep K_ATP channels closed. Indeed, stimulation of GK with GKA50 in control β-cells resulted in the loss of electrical sensitivity to low glucose. In support of this notion, CRI-G1 cells have reduced sensitivity to hypoglycaemic challenge and express high GK activity. Furthermore, stimulation of AMPK activity with AICAR significantly reduced GK activity, which was prevented by co-application of the AMPK inhibitor compound C. Although these results encouraged the view that loss of AMPKα2 up-regulated GK activity in β-cells, this effect was not replicated using the direct AMPK activator A-769662. In addition, we could detect no change in the levels of low-K_m hexokinases in AMPKα2-deleted islets, abrogating an induction of one or more of these hexokinases as a potential loss-of-function mediator. Taken together with the lack of change in bulk [ATP]/[ADP] ratio in CRI-G1 cells, we think it unlikely that modification of GK activity explains the insensitivity of β-cell electrical activity to low glucose in AMPKα2-deficient cells.

β-cells have a relatively modest endogenous antioxidant defence system and are very susceptible to toxicity induced

by ROS [49]. Increased respiratory energy production raises mitochondrial electron transport, which drives the generation of ROS. To counter this, pancreatic β-cells exhibit high UCP2 levels and activity, which uncouples respiratory energy production, reduces the mitochondrial membrane potential and attenuates ROS production [37]. UCP2 may be a crucial component of β-cell function as inappropriately high UCP2 levels (e.g. associated with chronic hyperglycaemia or obesity) or UCP2 overexpression causes β-cell dysfunction by lowering ATP levels and reducing GSIS [36]. Conversely, knockdown of UCP2 in islets or global UCP2-deficient mice exhibit raised islet ATP levels and increased insulin secretion [34]. Our finding that AMPKα2 deletion reduces UCP2 mRNA levels in islets might therefore have led to the prediction that insulin secretion would be increased. Clearly, this was not the case when GSIS was examined *in vivo* or *in vitro* in *RIPCreα2KO* and *α1KORIPCreα2KO* mice. Indeed, in isolated islets although basal insulin secretion in the presence of low glucose was enhanced, GSIS was either relatively unaffected (*RIPCreα2KO* mice) or significantly reduced (*α1KORIPCreα2KO* mice) compared with controls.

The finding that AMPKα2 deletion also ablates the K$_{ATP}$-mediated hyperpolarization associated with hypoglycaemia in hypothalamic POMC neurons [17] supports the notion that AMPKα2 deletion alters β-cell glucose sensing capability. Furthermore, K$_{ATP}$ activation by low glucose is occluded in both cell types by genipin, supporting the idea that UCP2 activity is a key component of hypoglycaemic sensing in these specialized cells. So how might we explain the reduced GSIS associated with loss of AMPKα2 and reduced UCP2 in β-cells? There is a growing body of evidence to indicate that β-cell ROS production contributes to glucose-sensing behaviour and the regulation of insulin secretion, either as a signal for insulin secretion or as a mediator of the adaptive antioxidant response [41]. However, the reduction of UCP2 in AMPKα2-deleted islets was not accompanied by any significant alteration in ROS levels at low- or high-glucose concentrations, and we could detect no evidence for an adaptive response causing raised levels of antioxidant enzymes.

The permanently depolarized nature of AMPKα2-null β-cells may be, at least partly, responsible for the overall reduction of GSIS and impaired glucose tolerance we observe in *RIPCreα2KO* mice. This notion arises from reports that suppression of insulin secretion by pharmacological opening of K$_{ATP}$ channels causing cell hyperpolarization and a period of rest for the insulin secretion process improves glucose tolerance and β-cell function in animal models of diabetes and preserves and improves human islet function [50]. Thus maintenance of AMPK activity may be an important component of β-cell protection against chronic overstimulation and loss of islet function.

In conclusion, loss of AMPKα2 appears to cause permanently dampened UCP2 levels in islets, which is associated with dysfunctional β-cell glucose sensing and diminished GSIS. Lack of AMPKα2 may therefore result in disconnection of the normal response to nutrient deprivation whereby raised AMPK activity and UCP2 levels would act to lower insulin secretion at low-glucose levels and maintain secretion at high-glucose levels. Thus we hypothesize that AMPK plays a key role in connecting nutrient fluctuations and UCP2 regulation with maintenance of GSIS in β-cells.

AUTHOR CONTRIBUTION

Craig Beall researched data, contributed to discussion and reviewed/edited manuscript. Kaisa Piipari researched data, contributed to discussion and reviewed/edited manuscript. Hind Al-Qassab, Mark Smith and Nadeene Parker researched data. David Carling provided materials and contributed to the discussion. Benoit Viollet provided materials. Dominic

REFERENCES

1 Thorens, B. (2001) GLUT2 in pancreatic and extra-pancreatic gluco-detection. Mol. Membr. Biol. **18**, 265–273

2 MacDonald, P. E., Joseph, J. W. and Rorsman, P. (2005) Glucose-sensing mechanisms in pancreatic β-cells. Philos. T. Roy. Soc. B **360**, 2211–2225

3 Marchetti, P., Dotta, F., Lauro, D. and Purrello, F. (2008) An overview of pancreatic β-cell defects in human type 2 diabetes: implications for treatment. Regul. Pept. **146**, 4–11

4 Khan, S. E., Hull, R. L. and Utzschneider, K. M. (2006) Mechanisms linking obesity to insulin resistance and type 2 diabetes. Nature **444**, 840–846

5 Bosi, E. (2009) Metformin: the gold standard in type 2 diabetes: what does the evidence tell us? Diabetes Obes. Metab. **11**, (Suppl. 2), 3–8

6 Viollet, B., Lantier, L., Devin-Leclerc, J., Hebrard, S., Amouyal, C., Mounier, R., Foretz, M. and Andreelli, F. (2009) Targeting the AMPK pathway for the treatment of Type 2 diabetes. Front. Biosci. **14**, 3380–3400

7 Xue, B. and Khan, B. B. (2006) AMPK integrates nutrient and hormonal signals to regulate food intake and energy balance through effects in the hypothalamus and peripheral tissues. J. Physiol. **574**, 73–83

8 Del Guerra, S., Lupi, R., Marselli, L., Masini, M., Bugliani, M., Sbrana, S., Pollera, M., Boggi, U., Mosca, F., Del Prato, S. and Marchetti, P. (2005) Functional and molecular defects of pancreatic islets in human type 2 diabetes. Diabetes **54**, 727–735

9 Salt, I. P., Johnson, G., Ashcroft, S. J. H. and Hardie, D. G. (1998) AMP-activated protein kinase is activated by low glucose in cell lines derived from pancreatic β-cells, and may regulate insulin secretion. Biochem. J. **335**, 533–539

10 da Silva Xavier, G., Leclerc, I., Varadi, A., Tsuboi, T., Moule, S. K. and Rutter, G. A. (2003) Role for AMP-activated protein kinase in glucose-stimulated insulin secretion and preproinsulin gene expression. Biochem. J. **371**, 761–774

11 Leclerc, I., Woltersdorf, W. W., da Silva Xavier, G., Rowe, R. L., Cross, S. E., Korbutt, G. S., Rajotte, R. V., Smith, R. and Rutter, G. A. (2004) Metformin, but not leptin, regulates AMP-activated protein kinase in pancreatic islets: impact on glucose-stimulated insulin secretion. Am. J. Physiol. Endocrinol. Metab. **286**, E1023–E1031

12 Richards, S. K., Parton, L. E., Leclerc, I., Rutter, G. A. and Smith, R. M. (2005) Over-expression of AMP-activated protein kinase impairs pancreatic β-cell function *in vivo*. J. Endocrinol. **187**, 225–235

13 Wang, C-Z., Wang, Y., Di, A., Magnuson, M. A., Ye, H., Roe, M. W., Nelson, D. J., Bell, G. I. and Phillipson, L. H. (2005) 5-Amino-imidazole carboxamide riboside acutely potentiates glucose-stimulated insulin secretion from mouse pancreatic islets by KATP channel-dependent and -independent pathways. Biochem. Biophy. Res. Commun. **330**, 1073–1079

14 Gleason, C. E., Lu, D., Witters, L. A., Newgard, C. B. and Birnbaum, M. J. (2007) The role of AMPK and mTOR in nutrient sensing in pancreatic β-cells. J. Biol. Chem. **282**, 10341–10351

15 Choudhury, A. I., Heffron, H., Smith, M. A., Al-Quassab, H., Xu, A. W., Selman, C., Simmgen, M., Clements, M., Claret, M., MacColl, G. et al. (2005) The role of insulin receptor substrate 2 in hypothalamic and β-cell function. J. Clin. Invest. **115**, 940–950

16 Cantley, J., Selman, C., Shukla, D., Abramov, A. Y., Forstreuter, F., Esteban, M. A., Claret, M., Lingard, S. J., Clements, M., Harten, S. K. et al. (2009) Deletion of the von Hippel-Lindau gene in pancreatic β-cells impairs glucose homeostasis in mice. J. Clin. Invest. **119**, 125–135

17 Claret, M., Smith, M. A., Batterham, R. L., Selman, C., Choudhury, A. I., Fryer, L. G., Clements, M., Al-Quassab, H., Heffron, H., Xu, A. W. et al. (2007) AMPK is essential for energy homeostasis regulation and glucose sensing by POMC and AgRP neurons. J. Clin. Invest. **117**, 2325–2336

18 Ning, K., Miller, L. C., Laidlaw, H. A., Burgess, L. A., Perera, N. M., Downes, C. P., Leslie, N. R. and Ashford, M. L. (2006) A novel leptin signalling pathway via PTEN inhibition in hypothalamic cell lines and pancreatic β-cells. EMBO J. **25**, 2377–2387

19 Meakin, P. J., Fowler, M. J., Rathbone, A. J., Allen, L. M., Ransom, B. R., Ray, D. E. and Brown, A. M. (2007) Fructose metabolism in the adult mouse optic nerve, a central white matter tract. J. Cereb. Blood Flow Metab. **27**, 86–99

20 Mirshamsi, S., Laidlaw, H. A., Ning, K., Anderson, E., Burgess, L. A., Gray, A., Sutherland, C. and Ashford, M. L. (2004) Leptin and insulin stimulation of signalling pathways in arcuate nucleus neurones: PI 3-kinase dependent actin reorganization and K_{ATP} channel activation. BMC Neurosci. **5**, 54

21 Yamada, K., Nakata, M., Horimoto, N., Saito, M., Matsuoka, H. and Inagaki, N. (2000) Measurement of glucose uptake and intracellular calcium concentration in single, living pancreatic β-cells. J. Biol. Chem. **275**, 22278–22283

22 Viollet, B., Andreelli, F., Jørgensen, S. B., Perrin, C., Flamez, D., Mu, J., Wojtaszewski, J. F., Schuit, F. C., Birnbaum, M., Richter, E. et al. (2003) Physiological role of AMP-activated protein kinase (AMPK): insights from knockout mouse models. Biochem. Soc. Trans. **31**, 216–219

23 Fu, A., Ng, A. C-H., Depatie, C., Wijesekara, N., He, Y., Wang, G. S., Bardeesy, N., Scott, F. W., Touyz, F. W., Wheeler, M. B. and Screaton, R. A. (2009) Loss of Lkb1 in adult β-cells increases β-cell mass and enhances glucose tolerance in mice. Cell Metab. **10**, 285–295

24 Granot, Z., Swisa, A., Magenheim, J., Stolovich-Rain, M., Fujimoto, W., Manduchi, E., Miki, T., Lennerz, J. K., Stoeckert, Jr, C. J., Meyuhas, O. et al. (2009) LKB1 regulates pancreatic β-cell size, polarity and function. Cell Metab. **10**, 296–308

25 Vincent, M. F., Bontemps, F. and Van den Berghe, G. (1992) Inhibition of glycolysis by 5-amino-4-imidazolecarboxamide riboside in isolated rat hepatocytes. Biochem. J. **281**, 267–272

26 Walker, J., Jijon, H. B., Diaz, H., Salehi, P., Churchill, T. and Madsen, K. L. (2005) 5-aminoimidazole-4-carboxamine riboside (AICAR) enhances GLUT2-dependent jejunal glucose transport: a possible role for AMPK. Biochem. J. **385**, 485–491

27 Mukhtar, M. H., Payne, V. A., Arden, C., Harbottle, A., Khan, S., Lange, A. J. and Agius, L. (2008) Inhibition of glucokinase translocation by AMP-activated protein kinase is associated with phosphorylation of both GKRP and 6-phosphofructo-2-kinase/fructose-2,6-bisphosphatase. Am. J. Physiol. Regul. Integr. Comp. Physiol. **294**, R766–R774

28 Zhang, X., Sun, N., Wang, L., Guo, H., Guan, Q., Cui, B., Tian, L., Gao, L. and Zhao, J. (2009) AMP-activated protein kinase and pancreatic/duodenal homeobox-1 involved in insulin secretion under high leucine exposure in rat insulinoma β-cells. J. Cell. Mol. Med. **13**, 758–770

29 Matschinsky, F. M. (2002) Regulation of pancreatic β-cell glucokinase: from basics to therapeutics. Diabetes **51**, S394–S404

30 Johnson, D., Shepherd, R. M., Gill, D., Gorman, T., Smith, D. M. and Dunne, M. J. (2007) Glucose-dependent modulation of insulin secretion and intracellular calcium ions by GKA50, a glucokinase activator. Diabetes **56**, 1694–1702

31 Wang, H. and Iynedijian, P. B. (1997) Modulation of glucose responsiveness of insulinoma β-cells by graded overexpression of glucokinase. Proc. Natl. Acad. Sci. U.S.A. **94**, 4372–4377

32 Gloyn, A. L. (2003) Glucokinase (GCK) mutations in hyper- and hypoglycemia: maturity-onset diabetes of the young, permanent neonatal diabetes, and hyperinsulinemia of infancy. Hum. Mutat. **22**, 353–362

33 Cool, B., Zinker, B., Chiou, W., Kifle, L., Cao, N., Perham, M., Dickinson, R., Adler, A., Gagne, G., Iyengar, R. et al. (2006) Identification and characterization of a small molecule AMPK activator that treats key components of type 2 diabetes and the metabolic syndrome. Cell Metab. **3**, 403–416

34 Zhang, C.-Y., Baffy, G., Perret, P., Krauss, S., Peroni, O., Grujic, D., Hagen, T., Vidal-Puig, A. J., Boss, O., Kim, Y. B. et al. (2001) Uncoupling protein-2 negatively regulates insulin secretion and is a major link between obesity, β-cell dysfunction and type 2 diabetes. Cell **105**, 745–755

35 Chan, C. B., De Leo, D., Joseph, J. W., McQuaid, T. S., Ha, X. F., Xu, F., Tsushima, R. G., Pennefather, P. S., Salapatek, A. M. and Wheeler, M. B. (2001) Increased uncoupling protein-2 levels in β-cells are associated with impaired glucose-stimulated insulin secretion: mechanisms of action. Diabetes **50**, 1302–1310

36 Krauss, S., Zhang, C-Y., Scorrano, L., Dalgaard, L. T., St-Pierre, J., Grey, S. T. and Lowell, B. B. (2003) Superoxide-mediated activation of uncoupling protein 2 causes pancreatic β-cell dysfunction. J. Clin. Invest. **112**, 1831–1842

37 Affourtit, C. and Brand, M. D. (2008) On the role of uncoupling protein-2 in pancreatic β-cells. Biochim. Biophys. Acta **1777**, 973–979

38 Zhang, C.-Y., Parton, L. E., Ye, C. P., Krauss, S., Shen, R., Lin, C. T., Porco, Jr, J. A. and Lowell, B. B. (2006) Genipin inhibits UCP2-mediated proton leak and acutely reverses obesity- and high glucose-induced β-cell dysfunction in isolated pancreatic islets. Cell Metab. **3**, 417–427

39 Parton, L. E., Ye, C. P., Coppari, R., Enriori, P. J., Choi, B., Zhang, C. Y., Xu, C., Vianna, C. R., Balthasar, N., Lee, C. E. et al. (2007) Glucose sensing by POMC neurons regulates glucose homeostasis and is impaired in obesity. Nature **449**, 228–232

40 Brand, M. D., Affourtit, C., Esteves, T. C., Green, K., Lambert, A. J., Miwa, S., Pakay, J. L. and Parker, N. (2004) Mitochondrial superoxide: production, biological effects, and activation of uncoupling proteins. Free Radical Biol. Med. **37**, 755–767

41 Pi, J., Zhang, Q., Fu, J., Woods, C. G., Hou, Y., Corkey, B. E., Collins, S. and Andersen, M. E. (2010) ROS signalling, oxidative stress and Nrf2 in pancreatic β-cell function. Toxicol. Appl. Pharmacol. **244**, 77–83

42 Miki, T., Nagashima, K., Tashiro, F., Kotake, K., Yoshitomi, H., Tamamoto, A., Gonoi, T., Iwanaga, T., Miyazaki, J. and Seino, S. (1998) Defective insulin secretion and enhanced insulin action in KATP channel-deficient mice. Proc. Natl. Acad. Sci. U.S.A. **95**, 10402–10406

43 Seghers, V., Nakazaki, M., DeMayo, F., Aguilar-Bryan, L. and Bryan, J. (2000) Sur1 knockout mice. A model for K(ATP) channel-independent regulation of insulin secretion. J. Biol. Chem. **275**, 9270–9277

44 Ashcroft, F. M. (2005) ATP-sensitive potassium channelopathies: focus on insulin secretion. J. Clin. Invest. **115**, 2047–2058

45 Chang, T. J., Chen, W. P., Yang, C., Lu, P. H., Liang, Y. C., Su, M. J., Lee, S. C. and Chuang, L. M. (2009) Serine-385 phosphorylation of inwardly rectifying K^+ channel subunit (Kir6.2) by AMP-dependent protein kinase plays a key role in rosiglitazone-induced closure of the K_{ATP} channel and insulin secretion in rats. Diabetologia **52**, 1112–1121

46 Lim, A., Park, S. H., Sohn, J. W., Jeon, J. H., Park, J. H., Song, D. K., Lee, S. H. and Ho, W. K. (2009) Glucose deprivation regulated K_{ATP} channel trafficking via AMP-activated protein kinase in pancreatic β-cells. Diabetes **58**, 2813–2819

47 Ostenson, C. G. and Efendic, S. (2007) Islet gene expression and function in type 2 diabetes; studies in the Goto-Kakizaki rat and humans. Diabetes Obes. Metab. **9**, 180–186

48 Gloyn, A. L., Tribble, N. D., van de Bunt, M., Barrett, A. and Johnson, P. R. (2008) Glucokinase (GCK) and other susceptibility genes for β-cell dysfunction: the candidate approach. Biochem. Soc. Trans. **36**, 306–311

49 Robertson, R. P. (2006) Oxidative stress and impaired insulin secretion in type 2 diabetes. Curr. Opin. Pharmacol. **6**, 615–619

50 Wajchenberg, B. L. (2007) β-Cell failure in diabetes and preservation by clinical treatment. Endocr. Rev. **28**, 187–218

online data

SUPPLEMENTARY ONLINE DATA

Loss of AMP-activated protein kinase α2 subunit in mouse β-cells impairs glucose-stimulated insulin secretion and inhibits their sensitivity to hypoglycaemia

Craig BEALL*[1], Kaisa PIIPARI†[1], Hind AL-QASSAB†, Mark A. SMITH†*, Nadeene PARKER‡, David CARLING§, Benoit VIOLLET||, Dominic J. WITHERS†[2] and Michael L. J. ASHFORD*[2]

*Biomedical Research Institute, Ninewells Hospital and Medical School, University of Dundee, Dundee DD1 9SY, Scotland, U.K., †Metabolic Signalling Group, MRC Clinical Sciences Centre, Imperial College London, London W12 0NN, U.K., ‡Department of Cell and Developmental Biology, University College London, London WC1 6BT, U.K., §Cellular Stress Group, MRC Clinical Sciences Centre, Imperial College London, London W12 0NN, U.K., and ||INSERM U567, CNRS, UMR 8104, Institut Cochin, Université Paris Descartes, Paris, France
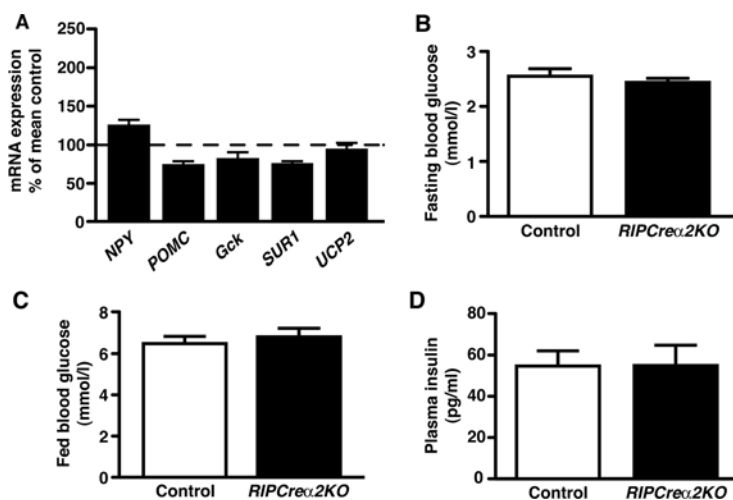

Figure S1   Hypothalamic mRNA expression profile and glucose homoeostasis parameters in *RIPCreα2KO* mice

(**A**) Expression of mRNA in the hypothalamus of *RIPCreα2KO* mice, relative to control WT mice ($n = 5$). Fasting (**B**) and fed (**C**) blood glucose levels in control ($n = 8$) and *RIPCreα2KO* 16- and 20-week-old male mice respectively ($n = 8$). (**D**) Fasted plasma insulin levels in control ($n = 9$) and *RIPCreα2KO* 10-week-old male mice ($n = 7$).

,

---

[1] These authors contributed equally to the present study
[2] Correspondence may be addressed to either of these authors (email m.l.j.ashford@dundee.ac.uk or d.withers@imperial.ac.uk).
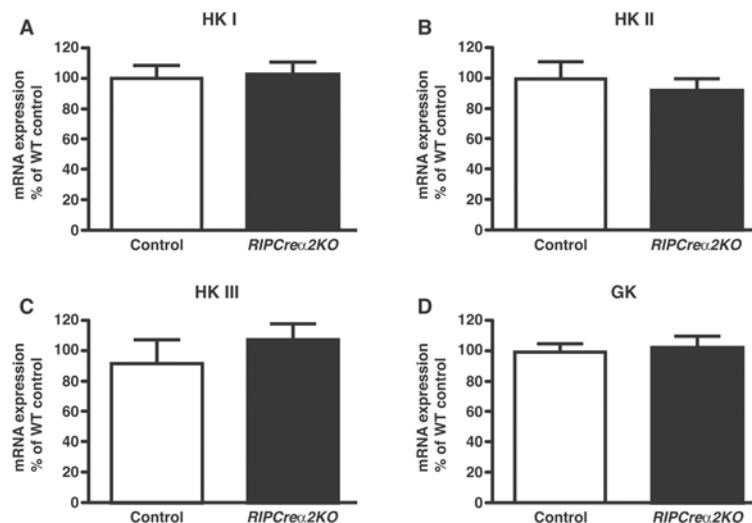
Figure S2   Expression of mRNA in islets of *RIPCreα2KO* mice, relative to control (*RIPCre*) islets for (A) HK I, (B) HK II, (C) HK III, and (D) GK

Values are means$\pm$S.E.M. for $n = 7$–9 determinations for each. The probes used were: Hexokinase I, Mm01145241_m1; Hexokinase II, Mm00443395_m1; and Hexokinase III, Mm01341937_m1.
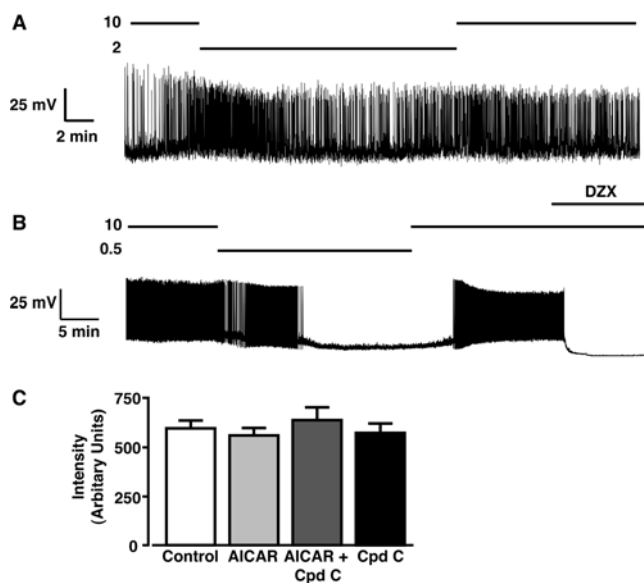

Figure S3   CRI-G1 β-cells exhibit glucose-sensing behaviour, and AMPK manipulation does not influence glucose uptake

Representative perforated patch recordings from CRI-G1 β-cells, showing (**A**) the lack of electrical response to reduction of glucose from 10 mmol/l to 2 mmol/l and (**B**) the hyperpolarization and inhibition of firing on reduction of glucose from 10 mmol/l to 0.1 mmol/l. Note that the application of 250 μmol/l diazoxide (DZX) hyperpolarizes the β-cell in the presence of 10 mmol/l glucose. (**C**) Glucose uptake, as measured by 2-NBDG uptake, in CRI-G1 β-cells is unaltered by treatment of cells (1 h) with 1 mmol/l AICAR $\pm$40 μmol/l compound C (CpdC) ($n = 44$, from six separate experiments).
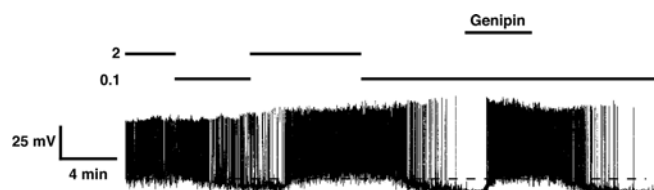

Figure S4   Representative perforated patch recording from a POMC arcuate nucleus neuron

Reducing glucose from 2 mM to 0.1 mM reversibly hyperpolarizes and reduces firing frequency, but this effect is reversibly occluded by the presence of 20 μM genipin. The broken line in the trace represents 0 mV.